รายงานวิจัยฉบับสมบูรณ์

การศึกษาการตอบสนองทางภูมิคุ้มกันต่อแอนติเจนจำลองของเชื้อ Mycobacterium tuberculosis เพื่อสรรหาโครงสร้างแอนติเจนที่เหมาะสม สำหรับใช้ในการผลิตวัคซีนต้านวัณโรค และวัคซีน Adjuvant

โดย

ศิวรัตน์ บุณยรัตกลิน และคณะ

15 พฤษภาคม 2553

สัญญาเลขที่ MRG5180240

รายงานวิจัยฉบับสมบูรณ์

การศึกษาการตอบสนองทางภูมิคุ้มกันต่อแอนติเจนจำลองของเชื้อ Mycobacterium tuberculosis เพื่อสรรหาโครงสร้างแอนติเจนที่เหมาะสม สำหรับใช้ในการผลิตวัคซีนต้านวัณโรค และวัคซีน Adjuvant

ศิวรัตน์ บุณยรัตกลิน และคณะ

ภาควิชาวิศวกรรมและเทคโนโลยีเคมีชีวภาพ
สถาบันเทคโนโลยีนานาชาติสิรินธร วิทยาเขตธรรมศาสตร์รังสิต
99 หมู่ 18 ถนนพหลโยธิน กม.41 ต.คลองหนึ่ง อ.คลองหลวง
จ. ปทุมธานี 12120
โทรศัพท์ (0) 2986-9009 ext. 2305 โทรสาร (0) 2986-9009 ext. 2301
e-mail: siwarutt.siit@gmail.com

สนับสนุนโดยสำนักงานกองทุนสนับสนุนการวิจัย

Abstract (บทคัดย่อ)

Project Code : MRG5180240

Project Title : การศึกษาการตอบสนองทางภูมิคุ้มกันต่อแอนติเจนจำลองของเชื้อ Mycobacterium tuberculosis เพื่อสรรหาโครงสร้างแอนติเจนที่เหมาะสมสำหรับใช้ในการผลิตวัคซีนต้านวัณโรค

Investigator : ศิวรัตน์ บุณยรัตกลิน
ภาควิชาวิศวกรรมและเทคโนโลยีเคมีชีวภาพ
สถาบันเทคโนโลยีนานาชาติสิรินธร วิทยาเขตธรรมศาสตร์รังสิต
99 หมู่ 18 ถนนพหลโยธิน กม.41 ต.คลองหนึ่ง อ.คลองหลวง
จ. ปทุมธานี 12120ชื่อนักวิจัย และสถาบัน

E-mail Address : siwarutt.siit@gmail.com

Project Period : 2 years

Keywords : TB, oligosaccharides, glycosylation, carbohydrate microarray, PIM

Abstract: The emergence of multidrug-resistant tuberculosis as well as the increasing failure of the BCG vaccine to protect humans against TB have prompted investigations into alternative approaches to combat these problems by exploring novel bacterial drug targets and vaccines. Phosphatidylinositol mannosides (PIMs) are biologically important glycoconjugates and represent common essential precursors of more complex mycobacterial cell wall glycolipids including lipomannan (LM), lipoarabinomannan (LAM), and mannan capped lipoarabinomannan (ManLAM). Synthetic PIMs constitute important biochemical tools to elucidate their biosynthesis, reveal their interactions with host cells, and investigate their function as potential antigens and/or adjuvants for vaccine development. Here, we report the efficient synthesis of all PIMs including phosphatidylinositol (PI) and phosphatidylinositol mono- to hexa-mannoside (PIM_1 to PIM_6). The robust and practical synthetic protocols were developed by utilizing bicyclic and tricyclic orthoesters as well as mannosyl phosphates as glycosylating agents. Rapid and scalable syntheses of mannoside building blocks involved orthoesters as key intermediates and glycosylations of mannosyl phosphates reliably resulted in excellent yields and selectivity. Each synthetic PIM was equipped with a thiol-linker for immobilization on surfaces and carrier proteins for biological and immunological studies. The synthetic compounds were immobilized on a glass slide microarray and were recognized by the dendritic cell specific intercellular adhesion molecule-grabbing non-

integrin (DC-SIGN) receptor in a specific manner. Immunization experiments in Balb/c mice with the synthetic PIMs coupled to the model antigen keyhole-limpet hemocyanin (KLH) highlight the potential of synthetic PIMs to serve as immune stimulators.

บทคัดย่อ (Executive Summary):

การปรากฏของเชื้อวัณโรคดื้อยาหลายชนิด (multidrug-resistant tuberculosis) และปัญหาเกี่ยวกับวัคซีนบีซีจีที่ใช้ป้องกันวัณโรคได้ทำให้เกิดการเสาะหาทางเลือกใหม่ในการต่อต้านโรคนี้โดยการค้นหาเป้าหมายยาและวัคซีนจากแบคทีเรียตัวใหม่ phosphatidylinositol mannosides (PIMs) เป็น glycoconjugate ที่สำคัญทางชีววิทยา และเป็นส่วนประกอบหลักที่สำคัญของส่วนประกอบของ glycolipid ที่ผิวของเชื้อในตระกูล Mycobacteria ที่ซับซ้อนมากขึ้น ซึ่งประกอบด้วย lipomannan (LM) lipoarabiomannan (LAM) และ mannan capped lipoarabiomannan (manLAM) สารประกอบ PIM ที่ได้จากการสังเคราะห์เป็นเครื่องมือทางชีวเคมีที่สำคัญที่ใช้อธิบายชีวสังเคราะห์ของโมเลกุลที่อยู่ในกลุ่มนี้ นอกจากนี้ยังใช้เพื่อแสดงอันตรกิริยาระหว่าง PIM กับเซลล์เจ้าบ้าน และเพื่อสังเกตกลไกของ PIM ในการเป็นแอนติเจนและ/หรือ adjuvant ที่มีประสิทธิภาพในการพัฒนาวัคซีน ผู้วิจัยได้รายงานการสังเคราะห์ที่มีประสิทธิภาพของสารประกอบ PIM ทั้งหมด ซึ่งประกอบด้วย phosphatidylinositol (PI) และ phosphatidylinositol mono- to hexa-mannosides (PIM_1 to PIM_6) วิธีการสังเคราะห์ที่มีประสิทธิภาพถูกพัฒนาเพื่อใช้ bicyclic และ tricyclic orthoester รวมทั้ง mannosyl phosphate เป็น glycosylating agent สารประกอบ PIM ที่สังเคราะห์ได้แต่ละตัวถูกเชื่อมต่อกับ thiol-linker สำหรับตรึงอยู่บนพื้นผิวและโปรตีนนำพาเพื่อการศึกษาทางชีววิทยาและระบบภูมิคุ้มกัน สารประกอบ PIM ถูกตรึงอยู่บน microarray สไลด์ เพื่อสังเกตความแตกต่างในการเชื่อมกับ dendritic cell specific intracellular adhesion molecule-grabbing nonintegrin (DC-SIGN) receptor สารประกอบ PIM สามารถใช้เป็นสารกระตุ้นระบบภูมิคุ้มกันในการทดลองในหนู C57BL/6 เมื่อต่อเข้ากับ model antigen keyhole limpet hemocyanin (KLH)

เนื้อหางานวิจัย

วัตถุประสงค์:

1. To develop fast, reliable and practical synthetic methods to efficiently synthesize chemically defined phosphatidylinositol mannoside (PIM) glycans from Mycobacterium tuberculosis.
2. To evaluate the synthetic phosphatidylinositol mannoside (PIM) glycans for their immunological properties.

Introduction

Tuberculosis (TB) is a complex disease and a major cause of mortality world-wide.[1-3] Despite the development of new treatments, TB remains a global health concern.[4, 5] Annually, there are more than seven million new cases and two million deaths caused by TB.[6] Coinfection with HIV leads to an exacerbation of the disease[4] and contributes to higher mortality in HIV patients.[6, 7] Programs to combat TB in many countries have failed to eradicate TB,[8] partly due to the spread of multidrug-resistant TB[9] and the low efficacy of the BCG vaccine. Therefore, the exploration of novel drug targets and vaccines against *Mycobacterium tuberculosis* (*Mtb*), the main causative pathogen of TB, is essential.

Among pathogenic bacteria, *Mtb* causes more deaths in humans than any other pathogen.[6, 10, 11] Approximately one third of the world population has already been infected by *Mtb*.[4] *Mtb* is an intracellular pathogen that has evolved to persist efficiently in infected macrophages.[4, 8, 12] The composition of the *Mtb* cell wall is important for the interaction with host cells during the initial steps of the infection. Later, cell wall components play a crucial role in modulating the pro-inflammatory response by macrophages and also serve as a protective barrier to prevent anti-tuberculosis agents from permeating inside. Consequently, the antibiotics used for the treatment of tuberculosis require long term administration.[5] Mortality in people living in developing countries is high since their access to these antibiotics is often limited.

The major components of the mycobacterial cell wall are the mycoyl arabinogalactan-peptidoglycan (mAGP) complex and interspersed glycolipids including ManLAM, LAM, LM, and PIMs. While the mAGP complex is covalently attached to the bacterial plasma membrane, the glycolipids are non-covalently attached through their phosphatidyl-*myo*-inositol (PI) anchor.[13-15] PIMs constitute the only conserved substructure of LM, LAM and ManLAM (Figure 1). The inositol residue of PI is mannosylated at the C-2 position to form PIM_1 and further at the C-6 position to form PIM_2, one of the two most abundant naturally occurring PIMs, along with PIM_6. Further α–1,6 mannosylations give rise to PIM_3 and PIM_4 – the common biosynthetic precursors for PIM_5, PIM_6 and the much larger LM structures. LAM is constituted by attachment of arabinans – the repeating units of α–1,5 arabinose terminated with a single β–1,2 arabinose– to unknown mannose units of LM. The non-reducing end arabinose in the arabinan moiety of LAM can be capped at the C-5 position with one or two α-mannose units to furnish ManLAM.

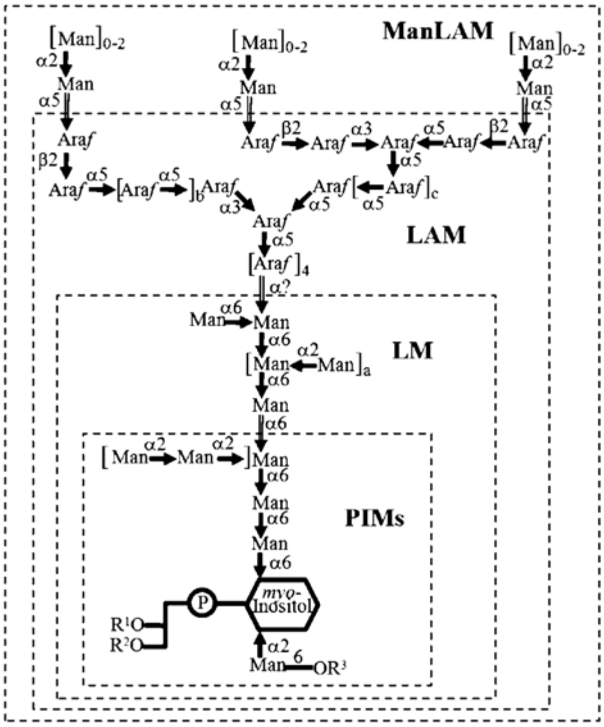

Figure 1. Structural features of PIMs, LM, LAM, and ManLAM of *Mycobacterium tuberculosis*. PIMs are the common precursors of more complex components of the mycobacterial cell wall including lipomannan (LM), lipoarabinomannan (LAM), and mannan capped lipoarabinomannan (ManLAM). (a, b, and c are varied; typically, R^2 is tuberculostearic acid, R^1 and R^3 are various fatty acids.)

Among the surface components involved in the *Mtb* interaction with host cells, PIMs play a crucial role in the modulation of the host immune response.[16-23] The functional importance of PIMs was emphasized by the finding that PIMs bind to receptors on both phagocytic[17, 24, 25] and nonphagocytic[12] mammalian cells. Recently, it has been shown that PIMs, but neither LAM nor ManLAM interact with the VLA-5 on $CD4^+$ T lymphocytes and induce its activation integrin.[22] These findings suggest that PIMs are not only secreted to the extracellular environment, but also exposed on the surface of *Mtb* to interact with host cells.

Although different functions have been ascribed to the PIMs, it remains to be determined whether and to which extent the different PIM substructures display biological activity. Furthermore, in order to be able to counteract with the problems of drug resistance and bacterial persistence, a better understanding of the mycobacterial cell wall biosynthesis is required. For this purpose, synthetic PIMs represent important biochemical tools since they can be used for elucidating biosynthetical pathways, revealing interactions with receptors on host cells and their potential as vaccine antigens or adjuvants.

Several synthetic PIMs containing fewer mannoside units have been synthesized employing various chemical methodologies.[26-33] In contrast to PIM_3 and PIM_4 that contain only $\alpha-1,6$ mannosidic linkages, PIM_5 and PIM_6 also have $\alpha-1,2$ mannosidic linkages that might contribute to different biological activities of these PIMs. In all studies reported so far synthetic PIMs did not contain linkers for immobilization. In order to use synthetic PIMs for biochemical studies, coupling them to appropriate supports (e.g. carrier proteins, beads, quantum dots, microarray or SPR surface) is necessary. Here, we report the efficient synthesis of all PIMs including phosphatidylinositol (**PI**) and **PIM$_1$** to **PIM$_6$** (Figure 2). The native diacylglycerol phosphate at the C-1 position of *myo*-inositol is replaced by a 6-thiohexyl phosphate residue. Thus, immobilization of the synthetic PIMs for biochemical studies is possible.

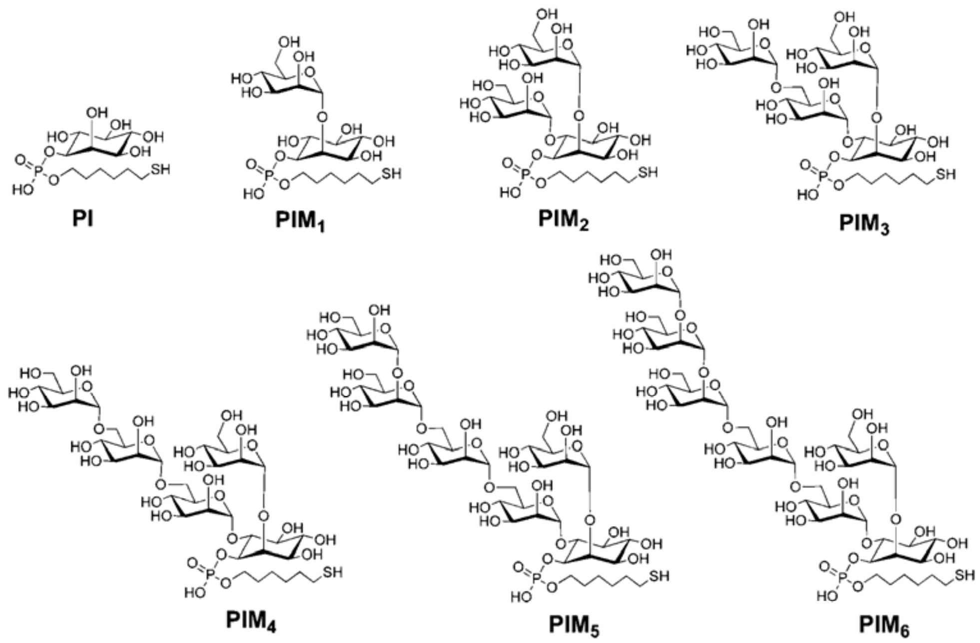

Figure 2. Structures of synthetic **PI** and **PIM$_1$** to **PIM$_6$**.

Results and Discussion

Retrosynthetic analysis. The overall structure of the synthetic PIM targets (Figure 2) can be attained by the convergent union of oligomannosides, D-*myo*-inositol containing pseudosaccharides, and a thiol-terminated phosphate linker (Scheme 1). The late-stage couplings between protected oligosaccharide fragments (**1**-**4**) and **8** allow for parallel syntheses of the intermediates for all target molecules. The key glycosylations in these syntheses are the couplings between mannosyl phosphate **1**, oligomannosyl trichloroacetimidates (**2**-**4**) and the common pseudotrisaccharide **8**. The two main carbohydrate moieties are coupled by these glycosylations, followed by protecting group manipulations. Subsequently, a phosphate diester linker is installed using an H-phosphonate followed by oxidation to P (V). Since the target molecules contain sulfur that is known to deactivate the Pd/C catalyst, the permanent benzyl protecting groups are globally removed under Birch reduction conditions.

The stereoselectivity of each glycosydic bond is ensured by neighboring C-2 acyl participating groups. In this study, we employed dibutyl phosphate ester as a leaving group for the monosaccharide mannose building blocks. This methodology proved advantages when compared to previous PIM syntheses. Moreover, the monosaccharide mannosyl phosphates used here can be readily prepared. In addition to the inositol building block only three mannose building blocks (**1**, **5**, and **10**) are needed.

Scheme 1. Retrosynthetic Analysis for the Assembly of Synthetic PIMs

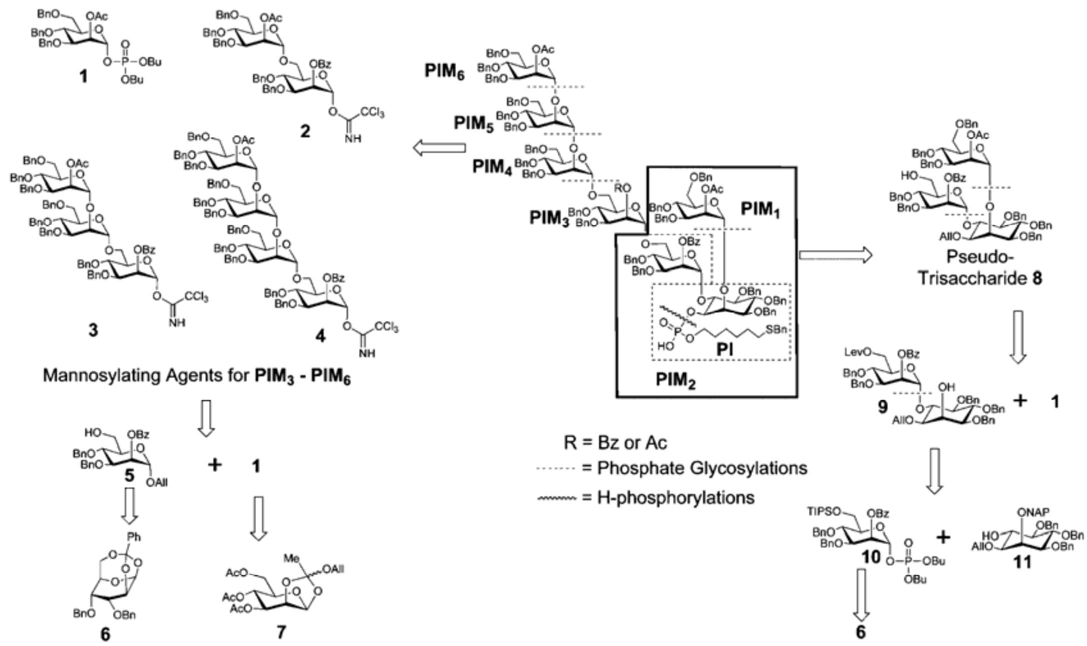

Syntheses of building blocks 1, 5, 10, and 11. Large amounts of mannosyl building blocks **1**, **5**, and **10** were rapidly and efficiently synthesized from mannose bicyclic and tricyclic orthoesters (**6**, **12**, Scheme 2).[34, 35] Starting from D-mannose, mannosyl phosphate **1** was prepared in six steps by dibutyl phosphoric acid opening of the bicyclic orthoester **7**. Mannosyl tricyclic orthoester **6** is readily available from D-mannose over six high yielding steps.[35] This process required only one purification at the last step and gave **6** in overall 70% yield. The versatile intermediate **6** was opened by allyl alcohol upon activation with $BF_3{\cdot}Et_2O$ to afford **5** in excellent yield. Treatment of orthoester **6** with dibutyl phosphate selectively opened the tricyclic orthoester to furnish glycosyl phosphate **13**, leaving the C-6 hydroxyl group unprotected. The installation of a triisopropylsilyl (TIPS) group was straightforward and furnished building block **10**.

Scheme 2. Efficient Multi-Gram Preparations of Mannose Building Blocks via Bicyclic and Tricyclic Orthoester Intermediates[a]

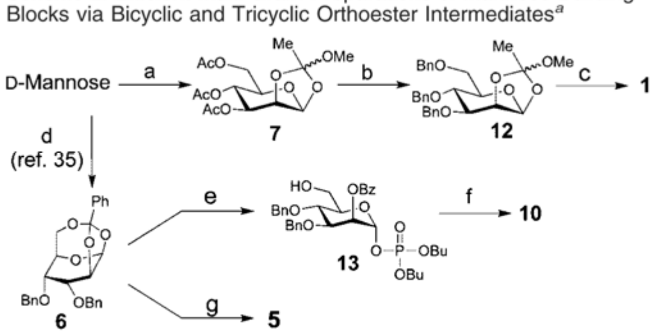

[a] Reagents and conditions: (a) i. Ac_2O, $HClO_4$ (cat.), ii. HBr/HOAc, iii. MeOH, Lutidine, 90%, three steps; (b) i. NaOMe/MeOH/THF, ii. NaH, BnBr, DMF, quant. two steps; (c) $HOP(O)(OBu)_2$, 4 Å MS 93%; (d) ref 35 - i. BzCl, Py, ii. HBr/HOAc, iii. AllOH, Lutidine, iv. NaOMe/MeOH/THF, reflux, v. CSA, MeCN, vi. NaH, BnBr, DMF, 70%, six steps; (e) $HOP(O)(OBu)_2$, 4 Å MS, 97%; (f) TIPSCl, NEt_3, DMAP, CH_2Cl_2, 91%; (g) AllOH, BF_3-Et_2O, CH_2Cl_2, 99%.

The previously reported synthetic route to the differentially protected *myo*-inositol by Fraser-Reid *et al.*[36] was modified (Scheme 3). The 1-*O*-methyl glucopyranose was quantitatively converted to **15** in three consecutive steps. A Parikh-Doering reaction oxidized the primary hydroxyl group in **15** to an aldehyde in quantitative yield. Using this oxidation, we avoided the complication involving the urea byproduct created when dicyclohexylcarbodiimide (DCC) was used as activator. The sulfate byproduct was readily removed by water extraction. The partially protected *myo*-inositol **16** was prepared from compound **15** in 40% yield over four consecutive steps. The allyl and NAP protecting groups were introduced at C1 and C2 of the D-*myo*-inositol respectively as previously described[37] to furnish **11**, ready for further decoration at the C6 hydroxyl group.

Scheme 3. Modified Synthesis of 1-*O*-Acetyl-3,4,5-tri-*O*-benzyl-*myo*-inositol (**16**)[a]

[a] Reagents and conditions: (a) i. Imidazole, TIPSCl, DMF 0 °C to rt, ii. NaH, BnBr, DMF, 0 °C to rt, iii. TBAF, THF, 99%, three steps; (b) i. SO_3−Py, DIPEA, DMSO, CH_2Cl_2, 0 °C to rt, ii. K_2CO_3, Ac_2O, MeCN, reflux, iii. $Hg(CF_3COO)_2$, Acetone/H_2O (4:1), rt, 1 h, then NaOAc (aq), NaCl (aq), 0 °C to rt, iv. $NaBH(CH_3COO)_3$, AcOH, MeCN, 0 °C to rt, 40%, four steps.

Assembly of *myo*-inositol containing pseudosaccharides. The *myo*-inositol containing pseudotrisaccharide **8** was assembled in a stepwise manner. Glycosylation of inositol **11** with mannosyl phosphate **10** that contained TIPS as a temporary protecting group on the C6 hydroxy was found to be optimal at -40 °C, in toluene, and promoted by a stoichiometric amount of TMSOTf (Scheme 4). Under these conditions the reaction gave a good yield with complete α selectivity. To sustain further glycosylations, the temporary TIPS protecting group was replaced by the levulinoyl (Lev) group. The presence of TIPS rather than Lev on the C6 hydroxyl group of **10** was found to be necessary in order to obtain high yield and selectivity during this first glycosylation.[37] Treatment of **19** with DDQ unmasked the C2 hydroxyl group on inositol to give **20** that served in turn as nucleophile for the next mannosylation.

Scheme 4. Assembly of *myo*-Inositol Containing Pseudotrisaccharide **8**[a]

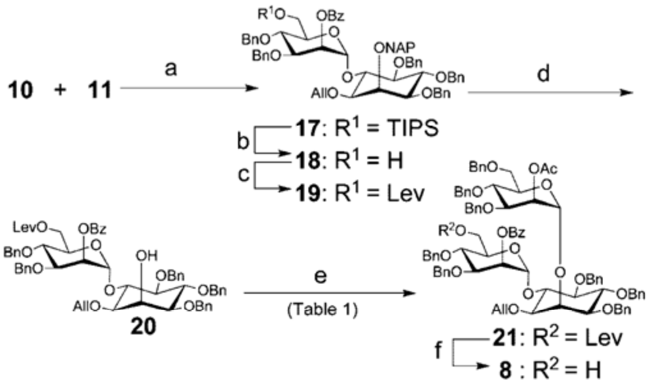

[a] Reagents and conditions: (a) TMSOTf, Toluene, −40 °C, 90%; (b) AcCl, MeOH, CH_2Cl_2, 0 °C, quant.; (c) LevOH, DIPC, DMAP, quant.; (d) DDQ, CH_2Cl_2, MeOH, 0 °C, 95%; (e) **1**, TBDMSOTf, Toluene, −40 °C, 95%, (see Table 1); (f) H_2NNH_3OAc, MeOH, rt, 89%.

The second mannosylation on the C2 hydroxyl group of pseudodisaccharide **20** was found to be nontrivial (Table 1). Activation by TMSOTf afforded the desired pseudodisaccharide **21** in just 15% yield (Table 1, Entry 1). The decomposition of **1** to its anomeric lactol counterpart was observed instead. Switching the promoter from TMSOTf to the milder activator TBDMSOTf dramatically improved the yield of the desired product (Table 1, Entry 2). This observation suggested that the difference in reactivity between highly activated **1** and less activated **20** constitute a mismatch. To optimize this glycosylation, the reactivity of **1** was reduced using TBDMSOTf as milder activator. Product **21** was obtained in excellent yield (95%) and selectivity by performing the glycosylation at 0 °C (Table 1, Entry 5). The α linkages in **21** were confirmed by 2D NMR. ^{1}H – ^{13}C coupled HSQC NMR revealed ^{1}H1 – ^{13}C1 coupling constants ($J_{C1,H1}$) of 178 Hz at the anomeric position of mannose 1 (on C2 inositol) and 182 Hz at the anomeric position of mannose 2 (on C6 inositol). $J_{C1,H1}$ of β mannosidic linkages are typically lower at around 159 Hz.[38]

Table 1. Effects of Promoter and Temperature on the Glycosylation of Glycosyl Phosphate **1** and *myo*-inositol Intermediate **20**

entry	promoter	temperature (°C)	yield (%)
1	TMSOTf	−40	15
2	TBDMSOTf	−40	27
3	TBDMSOTf	−10	57
4	TBDMSOTf	rt	55
5	**TBDMSOTf**	**0**	**95**

groups were introduced at C1 and C2 of the D-*myo*-inositol respectively as previously described[37] to furnish **11**, ready for further decoration at the C6 hydroxyl group.

Removal of the Lev group in **21** was achieved by treatment with hydrazine acetate and required careful monitoring. Longer reaction times resulted in the reduction of the allyl moiety to a propyl group was predominantly observed.

The partially protected inositol **16** was subjected to protecting group manipulations to furnish the inositol intermediates for **PI** and **PIM$_1$** (Scheme 5). Based on the difference in reactivity, the equatorial C6 hydroxyl group of the diol **22** was selectively acetylated to afford **23** as the intermediate for **PIM$_1$**. The **PI** intermediate **24** was obtained in parallel by benzylation of the common intermediate **22**.

Scheme 5. Protecting Group Manipulations on *myo*-Inositol **16** for PI Intermediate **23** and PIM$_1$ Intermediate **24**[a]

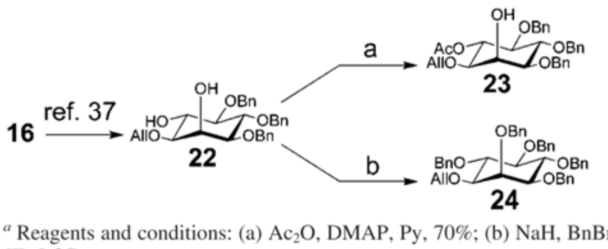

[a] Reagents and conditions: (a) Ac_2O, DMAP, Py, 70%; (b) NaH, BnBr, DMF, 0 °C to rt, quant.

Assembly of oligomannoside fragments. The oligomannoside trichloroacetimidates **2**, **3**, and **4** were assembled in a linear fashion (Scheme 6). All glycosylations employed mannosyl phosphate **1** and TMSOTf as activator. The α−1,6 glycosydic bond was readily formed at 0 ºC in quantitative yield. Lower temperature (-40 ºC) was required to efficiently attain 1,2 glycosylic linkages with complete α-selectivity. The deallylations of compounds **25**-**27** were performed by allylic substitutions mediated by a palladium complex to yield the corresponding lactols **28-30.** Finally, conversion to the trichloroacetimidates **2** - **4** were carried out using sodium hydride as base.

Scheme 6. Assembly of Oligomannosylating Reagents **2**−**4** for the Synthesis of **PIM$_4$**−**PIM$_6$**^{a}

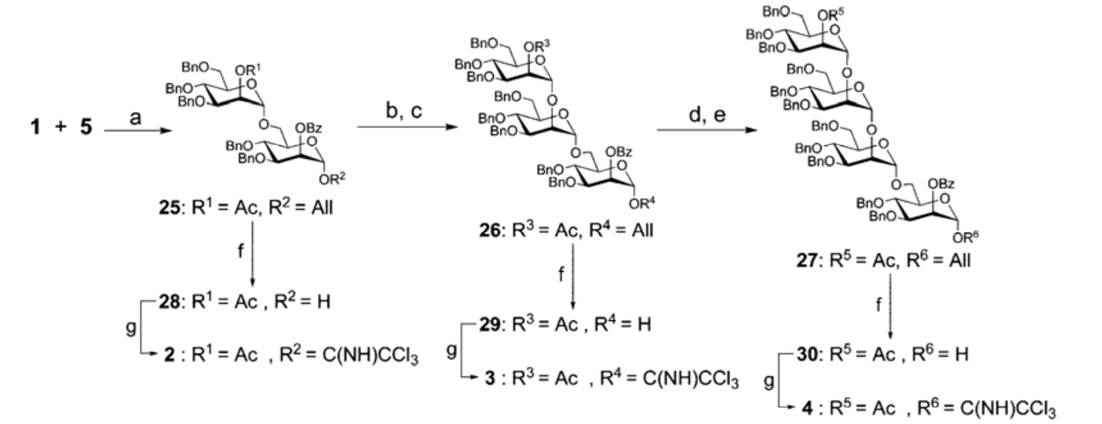

^{a} Reagents and conditions: (a) TMSOTf, CH_2Cl_2, −10 °C, quant.; (b) AcCl, MeOH, CH_2Cl_2, 0 °C, 91%; (c) **1**, TMSOTf, −40 °C, Toluene, 95%; (d) AcCl, MeOH, CH_2Cl_2, 0 °C, 84%; (e) **1**, TMSOTf, Toluene, −40 °C, 96%; (f) $Pd(OAc)_2$, MeOH, PPh_3, Et_2NH, 77% for **28**, 95% for **29**, and 83% for **30**; (g) Cl_3CCN, NaH, rt, 85% for **2**, 86% for **3**, and 89% for **4**.

Assembly of protected PIM backbones. Prior to phosphorylation, all protected PIM oligosaccharide backbones were obtained by late-state glycosylations (Table 2). Following these glycosylations all ester protecting groups were removed with NaOMe in MeOH at elevated temperature before masking the free hydroxyl groups with benzyl groups. These protecting group manipulations were performed to avoid the persistence of *O*-benzoate protecting groups under Birch conditions in the final step.[39]

Coupling between mannosyl phosphate **1** and inositol **23** gave pseudodisaccharide **31**, the backbone of **PIM$_1$**. To access the **PIM$_2$** backbone, pseudotrisaccharide fragment **8** was directly used as the starting material to be transformed into backbone **32**. The glycosylation products from couplings (Table 2, entry 3-5) between the oligomannosyl trichloroacetimidates (**1-3**) and the common pseudotrisaccharide **8** were cleanly achieved at -10 ºC. After quenching with triethylamine, the concentrated crude products were directly used to obtain the benzylated products in good yields in the next two steps. When the larger structure **4** was applied for the glycosylation, the coupling became more sluggish resulting in the hydrolysis of **4**. A higher temperature (0 ºC) was needed to obtain the 4 + 3 glycosylation product **46** (see experimental section). Pseudoheptasaccharide **46** was the largest oligosaccharide assembled in this series and consisted of fragments of all other smaller oligosaccharides. Thus, **46** was analyzed extensively by C-H coupled HSQC to confirm its structural identity. 2D-NMR data elucidated six anomeric proton signals with typical[38] α-manno $J_{C1,H1}$ couplings.

Table 2. Assembly of Fully Protected **PIM$_1$–PIM$_6$** Backbones: Union of (oligo)Mannosyl Fragment (**X**) and Inositiol-Containing Pseudosaccharide Fragment (**Y**)

a) Glycosylation (except entry 2)
b) NaOMe / MeOH, 50 °C, 24 h
c) BnBr, NaH, 0 °C to rt, 12 h

X + Y → **Differentially Protected PIM$_2$ - PIM$_6$**

Entry	X	Y	Glycosylation Conditions	Products	Yields a) ; b) ; c)
1	**1**	**23**	TMSOTf, -40 °C, Et_2O	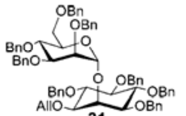 **31**	a) 69%; b) and c) quant. (2 steps)
2	not applied	**8**	No Glycosylation	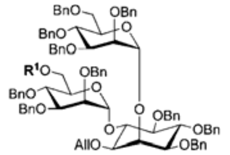 **32**: **R^1 = Bn**	b) and c) 90% (2 steps)
3	**1**	**8**	TMSOTf, -10 °C, CH_2Cl_2	**33**: **R^1** = 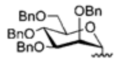	a), b), and c) 89% (3 steps)
4	**2**	**8**	TMSOTf, -10 °C, CH_2Cl_2	**34**: **R^1** = 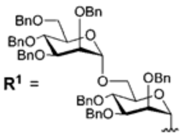	a), b), and c) 89% (3 steps)
5	**3**	**8**	TMSOTf, -10 °C, CH_2Cl_2	**35**: **R^1** = 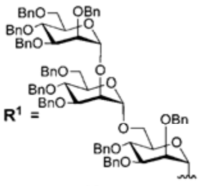	a), b), and c) 73% (3 steps)
6	**4**	**8**	TMSOTf, 0 °C, CH_2Cl_2	**36**: **R^1** = 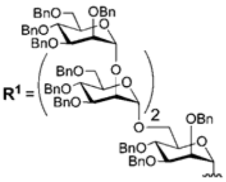	a) 64%; b) and c) 97% (2 steps)

Removal of *O*-allyl protecting group on the inositol moiety of oligosaccharide backbone 24, 31 - 36. Protocols to cleave the C-1 *O*-allyl group on inositol attached to oligosaccharides, performed by using $PdCl_2$, have been reported to give moderate yields.[32, 40-43] This was observed in our study as well. Several precedents to remove the *O*-allyl group were investigated on substrate **31** (Scheme 7 and Table 3). The hydrogen activated iridium complex Ir{(COD)[$PH_3(C_6H_5)_2$]$_2$ }PF_6 was found to be the most efficient reagent to isomerize the allyl group to its corresponding enol ether. In the same pot, a catalytic amount of *p*-toluenesulfonic acid (*p*-TsOH) was added to cleave the enol ether and liberate the C1 hydroxyl of pseudodisaccharide **38** in quantitative yield. This two step procedure was applied to the larger oligosaccharides **32** to **36** as well. However, while the isomerizations mediated by the iridium complex worked smoothly, an excess of *p*-TsOH (10 equiv.) was required to cleave the enol ether and furnish **39** - **43** (Scheme 7, entry 3).

Scheme 7. Removal of Allyl Protecting Groups on C1 *myo*-Inositol of Fully Protected **PI** and **PIM$_2$−PIM$_6$**

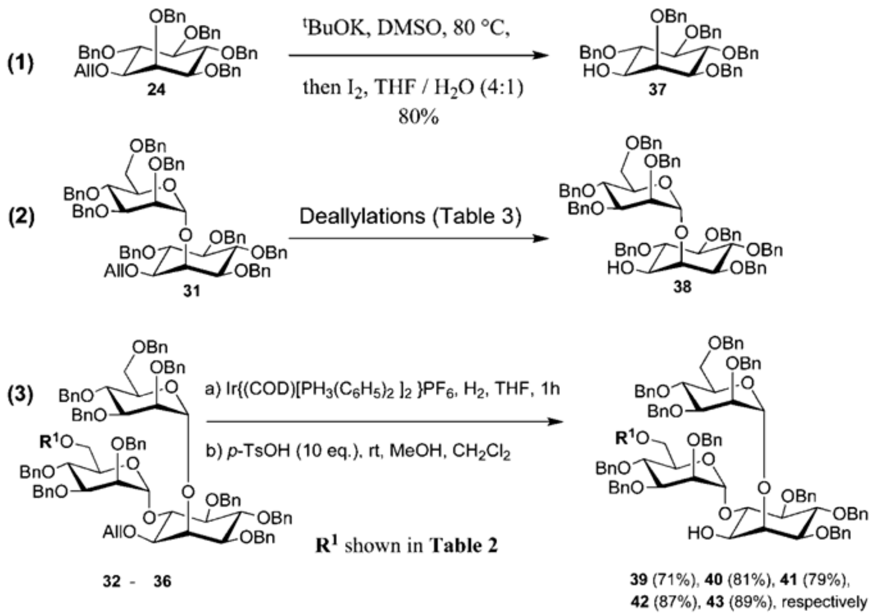

Table 3. Removal of Allyl Protecting Group on Pseudo-Disaccharide **31**

entry	conditions	yield
1	^{t}BuOK, DMSO, 80 EC, then I$_2$, THF/H$_2$O TMSOTf	10%, (decompostion)
2	Pd(OAc)$_2$, PPh$_3$, HNEt$_2$, CH$_2$Cl$_2$/MeOH (2:1)	no reaction
3	[Ir(COD)(PCH3Ph$_2$)$_2$]PF$_6$ (cat.), H$_2$, THF then I$_2$ in THF/H$_2$O (2:1)	30%
4	[Ir(COD)(PCH3Ph$_2$)$_2$]PF$_6$ (cat.), H$_2$, THF then *p*-TsOH (cat.) in DCM/MeOH (1:3)	**quantitative**

Phosphorylations and global deprotections by Birch reduction. The phosphate moiety accompanied with a terminal thiol linker was installed on the inositol C1 hydroxyl group of the oligosaccharide backbone **37** - **43** using a H-phosphonate (Scheme 8). Substrates **37** - **43** were treated with pivaloyl chloride in the presence of the linker **44** and pyridine. Subsequently, in the same pot, the H-phosphonate diesters were oxidized with iodine and water to provide the fully benzylated phosphodiester analogs **45** as triethylamine salts in excellent yields. Global removal of benzyl protecting groups of analogs **45**(**a-g**) was achieved by Birch reduction. The fully protected compounds were treated with sodium dissolved in ammonia to furnish the final products **PI** and **PIM$_1$** - **PIM$_6$** (Figure 2). Small amounts of incompletely reduced products were observed containing some remaining benzyl groups. These side products were separated by extraction with chloroform and converted to the final products by re-submission to Birch reduction. The final products were formed as a mixture of monomers and disulfide dimers. Treatment with one equivalent of tris(carboxyethyl) phosphine hydrochloride (TCEP) immediately prior to conjugation of the final compounds ensured that **PI** and **PIM$_1$** - **PIM$_6$** were present in monomeric form.

Scheme 8. Phosphorylation of Oligosaccharides **37**−**43** and Global Deprotection under Birch Reduction Conditions[a]

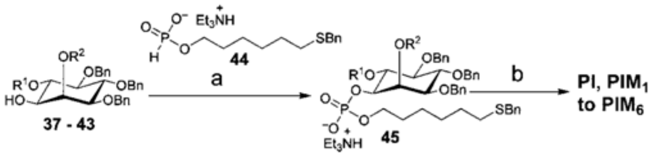

[a] Reagents and conditions: (a) i. **44**, PivCl, pyridine, ii. I_2, H_2O, pyridine, 90% to quant., 2 steps; (b) i. Na/NH_3 (l) /*t*-BuOH, −78 °C, ii. MeOH, 65% for **PI**, 43% for **PIM$_1$**, 56% for **PIM$_2$**, 91% for **PIM$_3$**, 65% for **PIM$_4$**, 88% for **PIM$_5$**, and 84% for **PIM$_6$**.

Preliminary experiments to determine biological activities of synthetic PI and PIMs. To demonstrate the utility of the synthetic PIM compounds equipped with a thiol linker for biochemical studies, synthetic **PI** and **PIMs** were used to study their interactions with the protein DC-SIGN on a microarray (Figure 3). **PI** and **PIMs** were immobilized on a maleimide activated glass slide following established protocols.[44] The binding of these compounds to DC-SIGN was monitored. DC-SIGN is an important receptor on dendritic cells and contributes to the initiation of a pro-inflammatory response by host cells.[45-47] One of the functions of DC-SIGN is the recognition of evolutionary conserved pathogenic structures that are secreted or exposed on the surface of viruses or bacteria.[46, 48-50] Upon binding to DC-SIGN, the antigens are internalized, processed and later presented on the surface of dendritic cells together with costimulatory molecules.[51, 52] Mycobacteria also use DC-SIGN as a receptor to enter dendritic cells.[51]

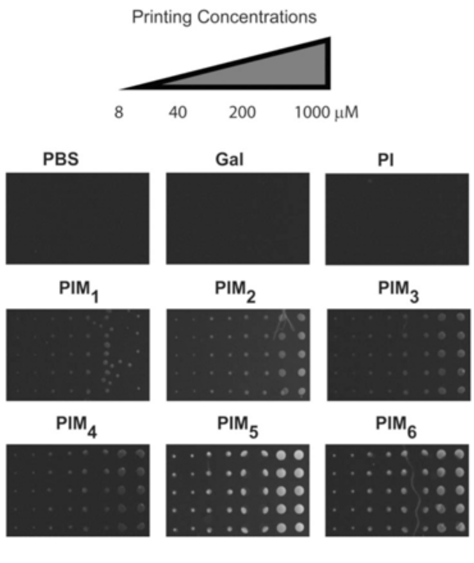

Figure 3. Fluorescent scanning of PIM microarray incubated with DC-SIGN and susequently with fluorescein conjugated antihuman DC-SIGN antibody (1 h). A PI and PIM immobilized glass slide was incubated with a solution of DC-SIGN (1 μg/100 μL) in HEPES buffer containing 1% BSA, 20 mM $CaCl_2$, and 0.5% Tween-20 at room temperature for 1 h. The slide was washed thoroughly and incubated with a solution of fluorescein conjugated antihuman DC-SIGN antibody (0.5 μg/100 μL) in HEPES buffer containing 1% BSA and 0.5% Tween-20 at room temperature for 1 h. The slide was washed thoroughly and scanned by a fluorescent microarray scanner. (PBS = Phosphate-buffered saline, Gal = Galactose)

A glass slide with the immobilized **PI** and **PIM$_1$** - **PIM$_6$** was incubated with a DC-SIGN solution in buffer at room temperature to allow DC-SIGN to bind to the immobilized PIMs. Excess DC-SIGN was washed off and bound DC-SIGN was detected by incubation with a fluorescein-conjugated anti-DC-SIGN antibody. The difference in DC-SIGN binding affinity to the synthetic PIM compounds was assessed semi-quantitatively by monitoring the fluorescence intensity via a fluorescence scanner. Synthetic PIMs bind to DC-SIGN in a specific manner (Figure 3). Although both synthetic analogs of the most abundant PIM_2 and PIM_6 are recognized by DC-SIGN, the larger synthetic oligosaccharides **PIM_5** and **PIM_6** bound to DC-SIGN to a greater extent. This observation underlines the significance of the α−1,2- mannose motif present in both PIMs and ManLAM structures.[53]

An important feature of natural PIMs is their ability to induce an immune response by host cells. To investigate immunostimulatory effects of these synthetic PIMs on three Balb/c mice per group were prime-boost immunized with the model antigen keyhole-limpet hemocyanin (KLH) covalently linked to **PIM_2** or **PIM_6**. While pre-immunized mice did not display an anti-KLH antibody response, immunization with KLH resulted in detectable anti-KLH antibody levels. Antibody levels were slightly increased by coupling of **PIM_2** to KLH and markedly higher when mice were immunized with KLH coupled to **PIM_6** (Figure 4). Recognition of the PIMs by pattern recognition receptors on antigen-presenting cells might provide a danger signal, thereby facilitating enhanced uptake of the model antigen and increased expression of costimulatory molecules. Though antibody levels were lower than in mice immunized with Freund's adjuvant, this finding highlights the potential of PIMs to stimulate immune responses.

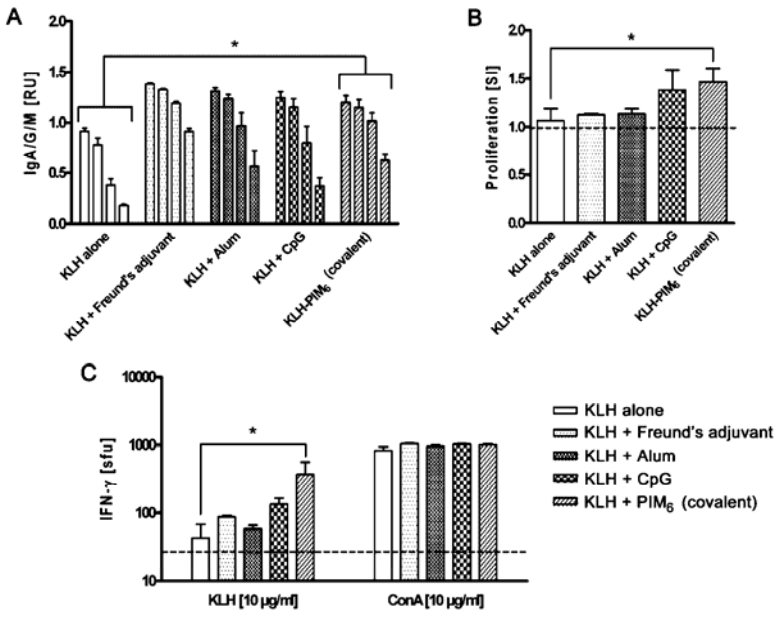

Figure 4. Immunization studies in mice with the model antigen KLH coupled to PIM_6. On day 0, four C57BL/6 mice per group (6−8 weeks) were s.c. immunized with KLH alone, KLH in complete Freund's adjuvant, KLH with alum, KLH with CpG or KLH covalently linked to **PIM_6**. On day 10, mice received a boost immunization with KLH alone, KLH in incomplete Freund's adjuvant, KLH with alum, KLH with CpG, or KLH−**PIM_6**. (A) On day 17 post immunization blood was taken from the saphenous vein of the immunized mice and levels of anti-KLH antibodies (sum of IgA, IgG and IgM) were measured by ELISA in serial dilutions of the sera (1:1000, 1:2000, 1:10000, 1:50000, duplicates for each mouse). Data are presented as mean ± SEM for each group of mice. Statistical analysis was performed with Student's *t* test (*, $p < 0.05$). (B) On day 20 post immunization, 2×10^5 splenocytes were restimulated with KLH (10 μg/ml) for 24 h and cell proliferation was measured. The results are expressed as a stimulation index (SI) which is the net proliferation of spleen cell cultures stimulated with 10 μg/ml KLH divided by the net proliferation of spleen cell cultures in medium. Data are presented as mean ± SEM for each group of mice. Statistical analysis was performed with Student's *t* test (*, $p < 0.05$). The dashed line represents proliferation of spleen cells from unimmunized mice. (C) On day 20, 2×10^5 splenocytes were stimulated with KLH (10 μg/ml) or Concanavalin A (ConA, 10 μg/ml) in a 96-Well plate coated with antimouse-IFN-γ and the frequency of IFN-γ producing cells was determined by ELISpot analysis. The results are expressed as *spot forming units* (sfu) which is the number of cells producing IFN-γ in each well. Data are presented as mean ± SEM for each group of mice. Statistical analysis was performed with Student's *t* test (*, $p < 0.05$). The dashed line represents IFN-γ production of cells cultivated in medium (unspecific background).

The synthetic **PI** and **PIM_5 - PIM_6** described here will be suitable for conjugation with other appropriate surfaces such as fluorescent nanocrystals, beads or fluorophores to generate probes for cellular assays. Such tools may shed light on the mechanism by which PIM structures on *Mtb* can influence bacterial trafficking in host cells. The synthetic compounds can also be attached to affinity columns in search for proteins or enzymes in cell lysates that interact with PIMs. Moreover, the synthetic PIMs can be used as substrates to explore biosynthetic pathways of the PIMs.

We are investigating the possibility of applying synthetic PIMs as antigens to elicit an immune response against *Mtb* as well as their adjuvant properties *in vivo*. For these purposes, the synthetic compounds can be conjugated to different model antigens.

Conclusion

In this study, the efficient synthesis of all PIMs including phosphatidylinositol (**PI**) and **PIM$_1$** to **PIM$_6$** was reported. Robust and practical synthetic protocols were developed by utilizing mannosyl bicyclic and tricyclic orthoesters and mannosyl phosphates. The key intermediate orthoesters allowed for rapid and scalable syntheses of mannoside building blocks and the glycosylations of the mannosyl phosphates resulted in excellent yields and stereoselectivity. All synthetic PIMs are equipped with a thiol linker to be readily immobilized on microarray surfaces. Thus, the synthetic PIMs represent tools for various biological studies. An application of the synthetic **PI** and **PIMs** for interaction with the protein DC-SIGN was demonstrated. The difference in DC-SIGN binding affinity among synthetic PI and PIM compounds was observed in a specific manner. Immunization experiments in mice revealed the potential of synthetic PIMs to serve as immune stimulators.

References

[1] Koul, A.; Herget, T.; Klebl, B. and Ullrich, A., *Nat. Rev. Microbiol.* **2004**, *2*, 189-202.

[2] Boshoff, H. I. and Barry, C. E., *Nat. Rev. Microbiol.* **2005**, *3*, 70-80.

[3] McMurray, D. N.; Carlomagno, M. A.; Mintzer, C. L. and Tetzlaff, C. L., *Infect. Immun.* **1985**, *50*, 555-559.

[4] Russell, D. G., *Nat. Rev. Microbiol.* **2007**, *5*, 39-47.

[5] Sacchettini, J. C.; Rubin, E. J. and Freundlich, J. S., *Nat. Rev. Microbiol.* **2008**, *6*, 41-52.

[6] Martin, C., *Eur. Respir. J* **2005**, *26*, 162-167.

[7] Nunn, P.; Williams, B.; Floyd, K.; Dye, C.; Elzinga, G. and Raviglione, M., *Nat. Rev. Immunol.* **2005**, *5*, 819-826.

[8] Russell, D. G., *Nat. Rev. Mol. Cell. Biol.* **2001**, *2*, 569-577.

[9] Sharma, S. K. and Mohan, A., *Chest* **2006**, *130*, 261-272.

[10] Malin, A. S. and Young, D. B., *BMJ.* **1996**, *312*, 1495.

[11] Sharma, S. K. and Mohan, A., *Indian J. Med. Res.* **2004**, *120*, 354-376.

[12] Hoppe, H. C.; de Wet, B. J.; Cywes, C.; Daffe M. and Ehlers, M. R., *Infect. Immun.* **1997**, *65*, 3896-3905.

[13] Brennan, P. J., *Tuberculosis* **2003**, *83*, 91-97.

[14] Crick, D. C.; Mahapatra, S. and Brennan, P. J., *Glycobiology* **2001**, *11*, 107R-118R.

[15] Berg, S.; Kaur, D.; Jackson, M. and Brennan, P. J., *Glycobiology* **2007**, *17*, 35-56R.

[16] Chatterjee, D. and Khoo, K. H., *Glycobiology* **1998**, *8*, 113-120.

[17] Villeneuve, C.; Gilleron, M.; Maridonneau-Parini, I.; Daffe, M.; Astarie-Dequeker, C. and Etienne, G., *J. Lipid. Res.* **2005**, *46*, 475-483.

[18] Sundaramurthy, V. and Pieters, J., *Microbes Infect.* **2007**, *9*, 1671-1679.

[19] Apostolou, I.; Takahama, Y.; Belmant, C.; Kawano, T.; Huerre, M.; Marchal, G.; Cui, J.; Taniguchi, M.; Nakauchi, H.; Fournie, J. J.; Kourilsky, P. and Gachelin, G., *Proc. Natl. Acad. Sci. U. S. A.* **1999**, *96*, 5141-5146.

[20] Nigou, J.; Gilleron, M.; Rojas, M.; Garcia, L. F.; Thurnher, M. and Puzo, G.; *Microbes Infect.* **2002**, *4*, 945-953.

[21] de la Salle, H.; Mariotti, S.; Angenieux, C.; Gilleron, M.; Garcia-Alles, L. F.; Malm, D.; Berg, T.; Paoletti, S.; Maitre, B.; Mourey, L.; Salamero, J.; Cazenave, J. P.; Hanau, D.; Mori, L.; Puzo, G. and De Libero, G., *Science* **2005**, *310*, 1321-1324.

[22] Rojas, R. E.; Thomas, J. J.; Gehring, A. J. Hill, P. J.; Belisle, J. T.; Harding, C. V. and Boom, W. H., *J. Immunol.* **2006**, *177*, 2959-2968.

[23] Vliegenthart, J. F., *FEBS Lett.* **2006**, *580*, 2945-2950.

[24] Thorson, L. M.; Doxsee, D.; Scott, M. G.; Wheeler, P. and Stokes, R. W., *Infect. Immun.* **2001**, *69*, 2172-2179.

[25] Torrelles, J. B.; Azad, A. K. and Schlesinger, L. S., *J. Immunol.* **2006**, *177*, 1805-1816.

[26] Elie, C. J. J.; Dreef, C. E.; Verduyn, R.; Vandermarel, G. A.; Van Boom, J. H., *Tetrahedron* **1989,** *45*, 3477-3486.

[27] Elie, C. J. J.; Verduyn, R.; Dreef, C. E.; Brounts, D. M.; Vandermarel, G. A.; Van Boom, J. H., *Tetrahedron* **1990,** *46*, 8243-8254.

[28] Elie, C. J. J.; Verduyn, R.; Dreef, C. E.; Vandermarel, G. A.; Van Boom, J. H., *J. Carbohydr. Chem.* **1992,** *11*, 715-739.

[29] Watanabe, Y.; Yamamoto, T.; Ozaki, S., *J. Org. Chem.* **1996,** *61*, 14-15.

[30] Watanabe, Y.; Yamamoto, T.; Okazaki, T., *Tetrahedron* **1997,** *53*, 903-918.

[31] Stadelmaier, A.; Schmidt, R. R., *Carbohydr. Res.* **2003,** *338*, 2557-2569.

[32] Jayaprakash, K. N.; Lu, J.; Fraser-Reid, B., *Bioorg. Med. Chem. Lett.* **2004,** *14*, 3815-3819.

[33] Stadelmaier, A.; Biskup, M. B.; Schmidt, R. R., *Eur. J. Org. Chem.* **2004**, 3292-3303.

[34] Ravida, A.; Liu, X.; Kovacs, L. and Seeberger, P. H., *Org. Lett.* **2006**, *8*, 1815-1818.

[35] Liu, X.; Wada, R.; Boonyarattanakalin, S.; Castagner B. and Seeberger, P. H., *Chem. Commun.* **2008**, DOI: 10.1039/b804069a.

[36] Jia, Z. J., Olsson, L. and Fraser-Reid, B. *J. Chem. Soc., Perkin Trans. 1* **1998**, 631.

[37] Liu, X.; Stocker, B. L. andSeeberger, P. H. *J. Am. Chem. Soc.* **2006**, *128*, 3638-3648.

[38] Podlasek, C. A.; Wu, J.; Stripe, W. A.; Bondo, P. B. and Serianni, A. S., *J. Am. Chem. Soc* **1995**, *117*, 8635-8644.

[39] Kwon, Y. U.; Soucy, R. L.; Snyder, D. A. and Seeberger, P. H., *Chem. Eur. J.* **2005**, *11*, 2493-2504.

[40] Cid, M. B.; Alfonso, F. and Martin-Lomas, M., *Synlett* **2003**, 1370-1372.

[41] Liu, X. and Seeberger, P. H., *Chem. Commun.* **2004**, 1708-1709.

[42] Vishwakarma, R. A. and Menon, A. K., *Chem. Commun.* **2005**, 453-455.

[43] Liu, X.; Kwon, Y. U. and Seeberger, P. H., *J. Am. Chem. Soc.* **2005**, *127*, 5004-5005.

[44] de Paz, J. L.; Horlacher, T. and Seeberger, P. H., *Methods Enzymol.* **2006**, *415*, 269-292.

[45] van Kooyk, Y. and Geijtenbeek, T. B., *Nat. Rev. Immunol.* **2003**, *3*, 697-709.

[46] Cambi, A. and Figdor, C. G., *Curr Opin Cell Biol* **2003**, *15*, 539-546.

[47] Banchereau, J. and Steinman, R. M., *Nature* **1998**, *392*, 245-252.

[48] Cambi, A.; Koopman, M. and Figdor, C. G., *Cell. Microbiol.* **2005**, *7*, 481-488.

[49] Su, S. V.; Hong, P.; Baik, S.; Negrete, O. A.; Gurney, K. B. and Lee, B., *J. Biol. Chem.* **2004**, *279*, 19122-19132.

[50] Geijtenbeek, T. B.; Engering, A. and Van Kooyk, Y., *J. Leukoc. Biol.* **2002**, *71*, 921-931.

[51] De Libero, G. and Mori, L., *Nat. Rev. Immunol.* **2005**, *5*, 485-496.

[52] De Libero, G. and Mori, L., *FEBS Lett.* **2006**, *580*, 5580-5587.

[53] Koppel, E. A.; Ludwig, I. S.; Hernandez, M. S.; Lowary, T. L.; Gadikota, R. R.; Tuzikov, A. B.; Vandenbroucke-Grauls, C. M.; van Kooyk, Y.; Appelmelk, B. J. and Geijtenbeek, T. B., *Immunobiology* **2004**, *209*, 117-127.

[54] Takahashi, H.; Kittaka, H. and Ikegami, S., *J. Org. Chem.* **2001**, 66, 2705-2716.

<u>เอกสารแนบหมายเลข 3</u>

Output จากโครงการวิจัยที่ได้รับทุนจาก สกว.

1. ผลงานตีพิมพ์ในวารสารวิชาการนานาชาติ (ระบุชื่อผู้แต่ง ชื่อเรื่อง ชื่อวารสาร ปี เล่มที่ เลขที่ และหน้า) หรือผลงานตามที่คาดไว้ในสัญญาโครงการ

(1) **Boonyarattanakalin, S.**; Liu, X.; Michieletti, M.; Lepenies, B.; and Seeberger, P. H. “Chemical Synthesis of All Phosphatidylinositol Mannoside (PIM) Glycans from Mycobacterium tuberculosis” *J. Am. Chem. Soc.* **2008**, 130, 16791-16799 (*Impact Factor = 8.091*).

(2) Kikkeri, R.; Kamena, F.; Gupta, T.; Hossain, L. H.; **Boonyarattanakalin, S.**; Gorodyska, G.; Beurer, E.; Coullerez, G.; Textor, M.; and Seeberger, P. H. “Ru(II) Glycodendrimers as Probes to Study Lectin-Carbohydrate Interactions and Electrochemically Measure Monosaccharide and Oligosaccharide Concentrations” *Langmuir*, **2010**, *26*, 1520. (*Impact Factor = 4.097*)

2. อื่นๆ (เช่น ผลงานตีพิมพ์ในวารสารวิชาการในประเทศ การเสนอผลงานในที่ประชุมวิชาการ หนังสือ การจดสิทธิบัตร)

Proceedings:

(1) Sungsilp, M., Yongyat, C., Ruchirawat, S. and **Boonyarattanakalin, S.** “Synthesis of tricyclic orthoesters of mannose for ring-opening oligomerization toward D-mannopyranan”. Proceedings of Pure and Applied Chemistry International Conference (PACCON 2010), 21-23 January 2010, Ubon Ratchathani, Thailand, 760-763.

(2) **Boonyarattanakalin, S.** and Seeberger, P. H. “Convergent Synthesis of Phosphatidylinositol Hexamannoside Glycan of Mycobacterium tuberculosis”. Proceedings of the Pure and Applied Chemistry International Conference (PACCON 2009), 14-16 January 2009, Phitsanulok, Thailand, 446-449.

J|A|C|S
ARTICLES

Published on Web 11/17/2008

Chemical Synthesis of All Phosphatidylinositol Mannoside (PIM) Glycans from *Mycobacterium tuberculosis*

Siwarutt Boonyarattanakalin,[†,‡] Xinyu Liu,[†,§] Mario Michieletti,[†,||] Bernd Lepenies,[†] and Peter H. Seeberger*,[†]

Laboratory for Organic Chemistry, Swiss Federal Institute of Technology (ETH) Zürich, Wolfgang-Pauli-Str. 10, HCI F312, 8093 Zürich, Switzerland, and Sirindhorn International Institute of Technology, Thammasat University, P.O. Box 22 Thammasat-Rangsit Post Office, Pathumthani 12121, Thailand

Received August 8, 2008; E-mail: seeberger@org.chem.ethz.ch

Abstract: The emergence of multidrug-resistant tuberculosis (TB) and problems with the BCG tuberculosis vaccine to protect humans against TB have prompted investigations into alternative approaches to combat this disease by exploring novel bacterial drug targets and vaccines. Phosphatidylinositol mannosides (PIMs) are biologically important glycoconjugates and represent common essential precursors of more complex mycobacterial cell wall glycolipids including lipomannan (LM), lipoarabinomannan (LAM), and mannan capped lipoarabinomannan (ManLAM). Synthetic PIMs constitute important biochemical tools to elucidate the biosynthesis of this class of molecules, to reveal PIM interactions with host cells, and to investigate the function of PIMs as potential antigens and/or adjuvants for vaccine development. Here, we report the efficient synthesis of all PIMs including phosphatidylinositol (PI) and phosphatidylinositol mono- to hexa-mannoside (PIM_1 to PIM_6). Robust synthetic protocols were developed for utilizing bicyclic and tricyclic orthoesters as well as mannosyl phosphates as glycosylating agents. Each synthetic PIM was equipped with a thiol-linker for immobilization on surfaces and carrier proteins for biological and immunological studies. The synthetic PIMs were immobilized on microarray slides to elucidate differences in binding to the dendritic cell specific intercellular adhesion molecule-grabbing nonintegrin (DC-SIGN) receptor. Synthetic PIMs served as immune stimulators during immunization experiments in C57BL/6 mice when coupled to the model antigen keyhole-limpet hemocyanin (KLH).

Introduction

Tuberculosis (TB) is a complex disease and a major cause of mortality worldwide.[1−3] Despite the development of new treatments, TB remains a global health concern.[4,5] Annually, there are more than seven million new cases and two million deaths caused by TB.[6] Coinfection with HIV leads to an exacerbation of the disease[4] and contributes to higher mortality in HIV patients.[6,7] Programs to combat TB in many countries have failed to eradicate TB,[8] partly due to the spread of multidrug-resistant TB[9] and the low efficacy of the BCG vaccine. Therefore, the exploration of novel drug targets and vaccines against *Mycobacterium tuberculosis* (*Mtb*), the main causative pathogen of TB, is essential.

Among pathogenic bacteria, *Mtb* causes more deaths in humans than any other pathogen.[6,10,11] Approximately one-third of the world population has already been infected by *Mtb*.[4] *Mtb* is an intracellular pathogen that has evolved to persist efficiently in infected macrophages.[4,8,12] The composition of the *Mtb* cell wall is important for the interaction with host cells during the initial steps of the infection. Later, cell wall components play a crucial role in modulating the pro-inflammatory response by macrophages and also serve as a protective barrier to prevent antituberculosis agents from permeating inside. Consequently, the antibiotics used for the treatment of tuberculosis require long-term administration.[5] Mortality in people living in developing countries is high since their access to these antibiotics is often limited and compliance with treatment courses is low.

The major components of the mycobacterial cell wall are the mycoyl arabinogalactan-peptidoglycan (mAGP) complex and interspersed glycolipids including ManLAM, LAM, LM, and

[†] Swiss Federal Institute of Technology (ETH) Zürich.
[‡] Sirindhorn International Institute of Technology.
[§] Current address: Department of Biological Chemistry and Molecular Pharmacology, Harvard Medical School, 240 Longwood Avenue, Boston, MA 02115.
[||] Visiting Ph.D. student from Università degli Studi del Piemonte Orientale "Amedeo Avogadro", Novara, Italy.

(1) Koul, A.; Herget, T.; Klebl, B.; Ullrich, A. *Nat. Rev. Microbiol.* **2004**, *2*, 189–202.
(2) Boshoff, H. I.; Barry, C. E. *Nat. Rev. Microbiol.* **2005**, *3*, 70–80.
(3) McMurray, D. N.; Carlomagno, M. A.; Mintzer, C. L.; Tetzlaff, C. L. *Infect. Immun.* **1985**, *50*, 555–559.
(4) Russell, D. G. *Nat. Rev. Microbiol.* **2007**, *5*, 39–47.
(5) Sacchettini, J. C.; Rubin, E. J.; Freundlich, J. S. *Nat. Rev. Microbiol.* **2008**, *6*, 41–52.
(6) Martin, C. *Eur. Respir. J.* **2005**, *26*, 162–167.
(7) Nunn, P.; Williams, B.; Floyd, K.; Dye, C.; Elzinga, G.; Raviglione, M. *Nat. Rev. Immunol.* **2005**, *5*, 819–826.
(8) Russell, D. G. *Nat. Rev. Mol. Cell. Biol.* **2001**, *2*, 569–577.
(9) Sharma, S. K.; Mohan, A. *Chest* **2006**, *130*, 261–272.
(10) Malin, A. S.; Young, D. B. *BMJ* **1996**, *312*, 1495.
(11) Sharma, S. K.; Mohan, A.; Indian, J. *Med. Res.* **2004**, *120*, 354–376.
(12) Hoppe, H. C.; de Wet, B. J.; Cywes, C.; Daffe, M.; Ehlers, M. R. *Infect. Immun.* **1997**, *65*, 3896–3905.

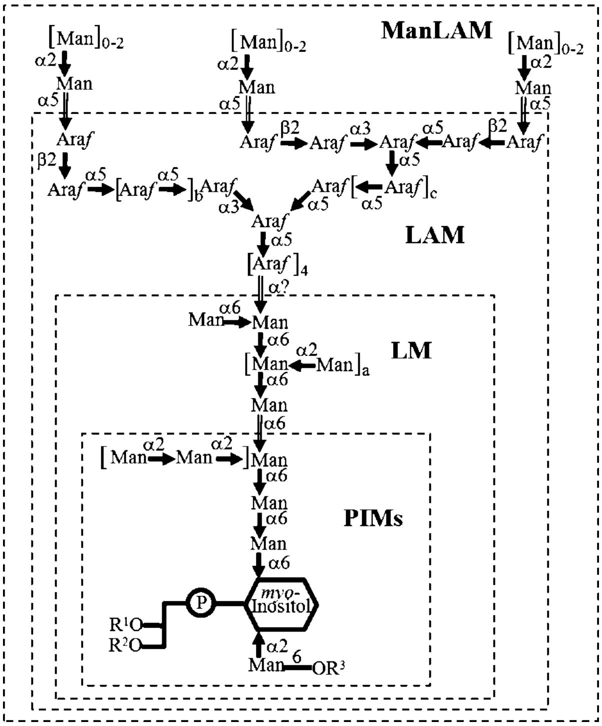

Figure 1. Structural features of PIMs, LM, LAM, and ManLAM of *Mycobacterium tuberculosis*. PIMs are the common precursors of more complex components of the mycobacterial cell wall including lipomannan (LM), lipoarabinomannan (LAM), and mannan capped lipoarabinomannan (ManLAM). (a, b, and c are varied; typically, R^2 is tuberculostearic acid, R^1 and R^3 are various fatty acids.)

PIMs. While the mAGP complex is covalently attached to the bacterial plasma membrane, the glycolipids are noncovalently attached through their phosphatidyl-*myo*-inositol (PI) anchor.[13−15] PIMs constitute the only conserved substructure of LM, LAM, and ManLAM (Figure 1). The inositol residue of PI is mannosylated at the C-2 position to form PIM_1 and further at the C-6 position to form PIM_2, one of the two most abundant naturally occurring PIMs, along with PIM_6. Further α-1,6 mannosylations give rise to PIM_3 and PIM_4—the common biosynthetic precursors for PIM_5, PIM_6, and the much larger LM structures. LAM is constituted by attachment of arabinans—the repeating units of α-1,5 arabinose terminated with a single *β*-1,2 arabinose to mannose units of LM. The nonreducing end arabinose in the arabinan moiety of LAM can be capped at the C-5 position with one or two α-mannose units to furnish ManLAM.

Among the surface components involved in the *Mtb* interaction with host cells, PIMs play a crucial role in the modulation of the host immune response.[16−23] The functional importance of PIMs was emphasized by the finding that PIMs bind to receptors on both phagocytic[17,24,25] and nonphagocytic[12] mammalian cells. Recently, it has been shown that PIMs, but neither LAM nor ManLAM interact with the VLA-5 on $CD4^+$ T lymphocytes and induce the activation of this integrin.[22] These findings suggest that PIMs are not only secreted to the extracellular environment, but also exposed on the surface of *Mtb* to interact with host cells.

Although different functions have been ascribed to the PIMs, it remains to be determined whether and to which extent the different PIM substructures display biological activity. A better understanding of the mycobacterial cell wall biosynthesis is required to be able to counteract with the problems of drug resistance and bacterial persistence. Synthetic PIMs represent important biochemical tools to elucidate biosynthetic pathways and to reveal interactions with receptors on host cells. PIMs are potential vaccine antigens and/or adjuvants.

Several synthetic PIMs containing fewer mannoside units have been synthesized employing various chemical methodologies.[26−33] In contrast to PIM_3 and PIM_4 that contain only α-1,6 mannosidic linkages, PIM_5 and PIM_6 also incorporate α-1,2 mannosides that might contribute to different biological activities of these PIMs. None of the studies to date utilized synthetic PIMs that contain linkers for immobilization. Coupling of synthetic PIMs to carrier proteins, beads, quantum dots, microarray or surface plasmon resonance (SPR) surfaces opens a host of options for biochemical studies. Here, we report the efficient synthesis of the carbohydrate portion of all PIMs including phosphatidylinositol (**PI**) and $\mathbf{PIM_1}$ to $\mathbf{PIM_6}$ (Figure 2). The native diacylglycerol phosphate at the C-1 position of *myo*-inositol is replaced by a 6-thiohexyl phosphate residue for immobilization of the synthetic PIMs on surfaces.

Results and Discussion

Retrosynthetic Analysis. The overall structure of the synthetic PIM targets (Figure 2) can be attained by the convergent union of oligomannosides with D-*myo*-inositol containing pseudosaccharides and a thiol-terminated phosphate linker (Scheme 1). Late-stage couplings between protected oligosaccharide fragments (**1**−**4**) and **8** allow for parallel syntheses of the intermediates for all target molecules. The key glycosylations in these syntheses are the couplings between mannosyl phosphate **1**, oligomannosyl trichloroacetimidates (**2**−**4**) and the common

(13) Brennan, P. J. *Tuberculosis* **2003**, *83*, 91–97.
(14) Crick, D. C.; Mahapatra, S.; Brennan, P. J. *Glycobiology* **2001**, *11*, 107R–118R.
(15) Berg, S.; Kaur, D.; Jackson, M.; Brennan, P. J. *Glycobiology* **2007**, *17*, 35–56R.
(16) Chatterjee, D.; Khoo, K. H. *Glycobiology* **1998**, *8*, 113–120.
(17) Villeneuve, C.; Gilleron, M.; Maridonneau-Parini, I.; Daffe, M.; Astarie-Dequeker, C.; Etienne, G. *J. Lipid. Res.* **2005**, *46*, 475–483.
(18) Sundaramurthy, V.; Pieters, J. *Microbes Infect.* **2007**, *9*, 1671–1679.
(19) Apostolou, I.; Takahama, Y.; Belmant, C.; Kawano, T.; Huerre, M.; Marchal, G.; Cui, J.; Taniguchi, M.; Nakauchi, H.; Fournie, J. J.; Kourilsky, P.; Gachelin, G. *Proc. Natl. Acad. Sci. U.S.A.* **1999**, *96*, 5141–5146.
(20) Nigou, J.; Gilleron, M.; Rojas, M.; Garcia, L. F.; Thurnher, M.; Puzo, G. *Microbes Infect.* **2002**, *4*, 945–953.
(21) de la Salle, H.; et al. *Science* **2005**, *310*, 1321–1324.
(22) Rojas, R. E.; Thomas, J. J.; Gehring, A. J.; Hill, P. J.; Belisle, J. T.; Harding, C. V.; Boom, W. H. *J. Immunol.* **2006**, *177*, 2959–2968.
(23) Vliegenthart, J. F. *FEBS Lett.* **2006**, *580*, 2945–2950.
(24) Thorson, L. M.; Doxsee, D.; Scott, M. G.; Wheeler, P.; Stokes, R. W. *Infect. Immun.* **2001**, *69*, 2172–2179.
(25) Torrelles, J. B.; Azad, A. K.; Schlesinger, L. S. *J. Immunol.* **2006**, *177*, 1805–1816.
(26) Elie, C. J. J.; Dreef, C. E.; Verduyn, R.; Vandermarel, G. A.; Van Boom, J. H. *Tetrahedron* **1989**, *45*, 3477–3486.
(27) Elie, C. J. J.; Verduyn, R.; Dreef, C. E.; Brounts, D. M.; Vandermarel, G. A.; Van Boom, J. H. *Tetrahedron* **1990**, *46*, 8243–8254.
(28) Elie, C. J. J.; Verduyn, R.; Dreef, C. E.; Vandermarel, G. A.; Van Boom, J. H. *J. Carbohydr. Chem.* **1992**, *11*, 715–739.
(29) Watanabe, Y.; Yamamoto, T.; Ozaki, S. *J. Org. Chem.* **1996**, *61*, 14–15.
(30) Watanabe, Y.; Yamamoto, T.; Okazaki, T. *Tetrahedron* **1997**, *53*, 903–918.
(31) Stadelmaier, A.; Schmidt, R. R. *Carbohydr. Res.* **2003**, *338*, 2557–2569.
(32) Jayaprakash, K. N.; Lu, J.; Fraser-Reid, B. *Bioorg. Med. Chem. Lett.* **2004**, *14*, 3815–3819.
(33) Stadelmaier, A.; Biskup, M. B.; Schmidt, R. R. *Eur. J. Org. Chem.* **2004**, 3292–3303.

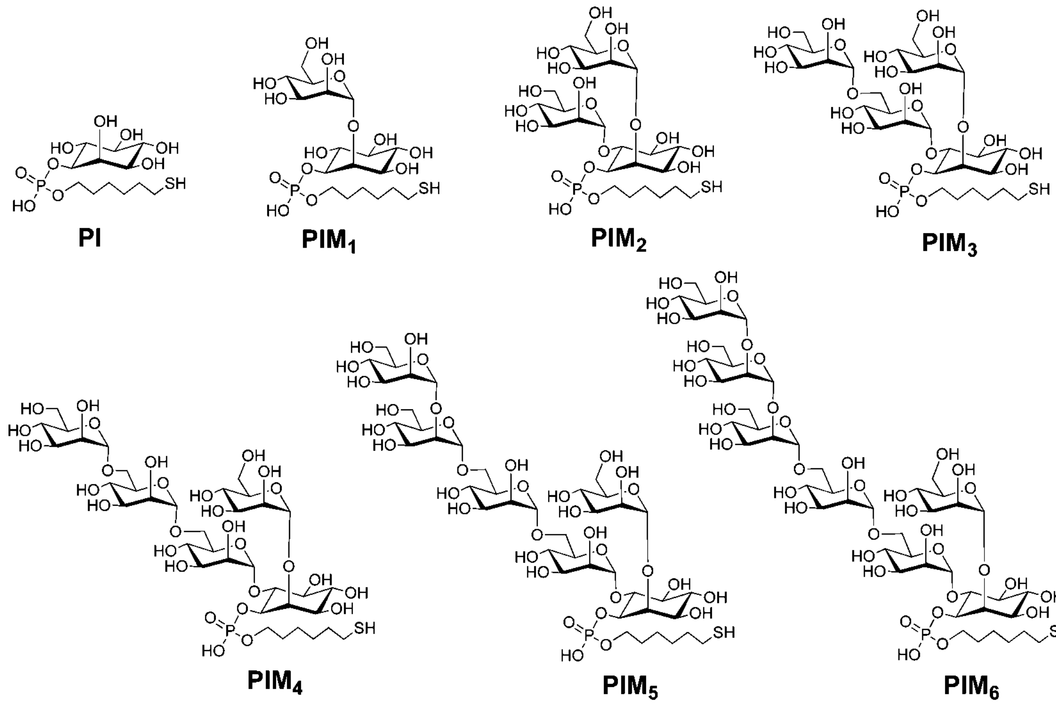

Figure 2. Structures of synthetic **PI** and **PIM$_1$** to **PIM$_6$**.

Scheme 1. Retrosynthetic Analysis for the Assembly of Synthetic PIMs

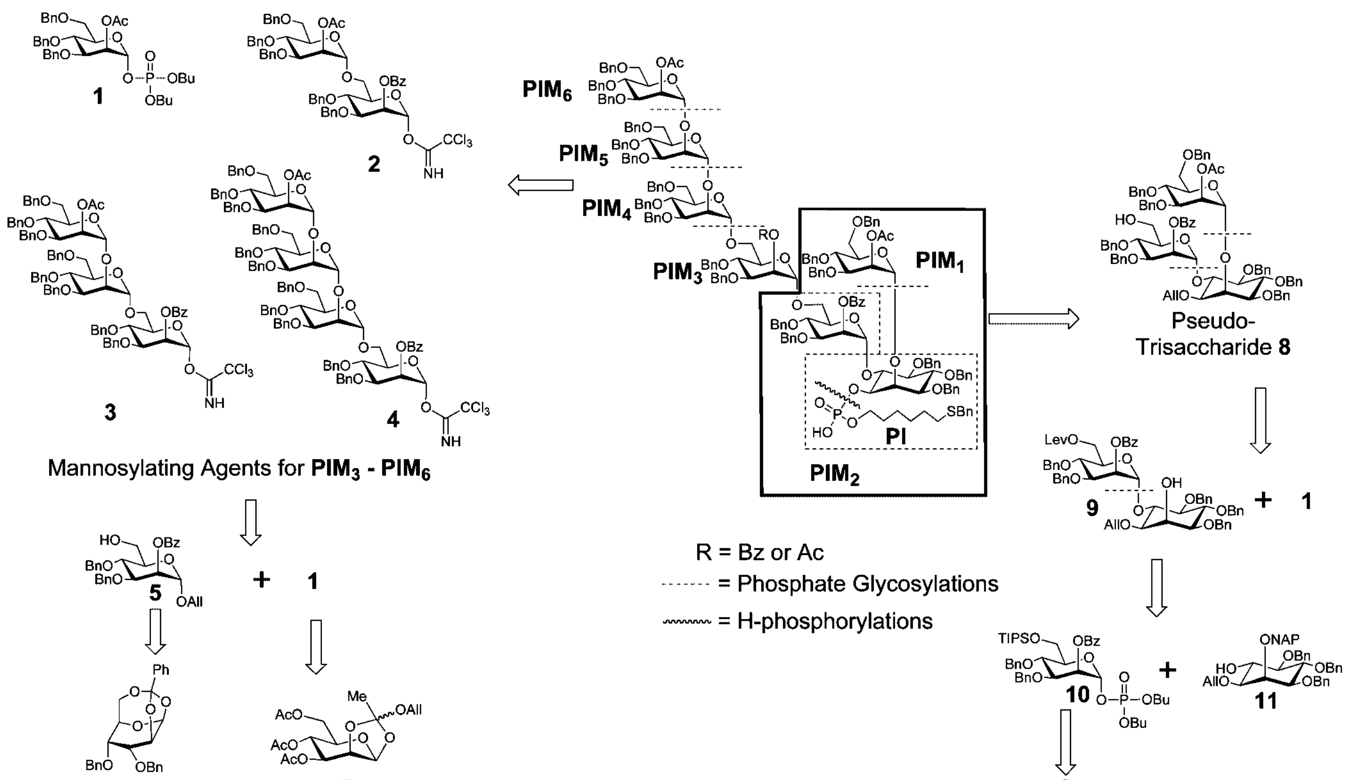

pseudotrisaccharide **8**. The two main carbohydrate moieties are coupled, followed by protecting group manipulations. Subsequently, a phosphate diester linker is installed using an H-phosphonate followed by oxidation of phosphorus. Since the target molecules contain sulfur that is known to deactivate the Pd/C catalyst, the permanent benzyl protecting groups are globally removed via Birch reduction.

The stereoselectivity of each glycosydic bond formation is ensured by neighboring C-2 acyl participating groups. In this study, we employed an anomeric dibutyl phosphate ester as a leaving group for the mannose building blocks that can be readily prepared. This method proved advantageous when compared to previous PIM syntheses. Three mannose building blocks (**1**, **5**, and **10**) are needed in addition to the inositol building block.

Scheme 2. Efficient Multi-Gram Preparations of Mannose Building Blocks via Bicyclic and Tricyclic Orthoester Intermediates[a]

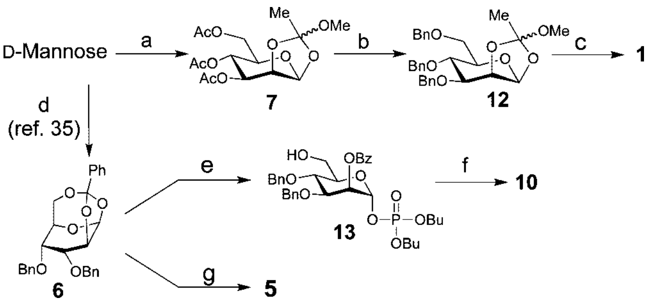

[a] Reagents and conditions: (a) i. Ac_2O, $HClO_4$ (cat.), ii. HBr/HOAc, iii. MeOH, Lutidine, 90%, three steps; (b) i. NaOMe/MeOH/THF, ii. NaH, BnBr, DMF, quant. two steps; (c) $HOP(O)(OBu)_2$, 4 Å MS 93%; (d) ref 35 - i. BzCl, Py, ii. HBr/HOAc, iii. AllOH, Lutidine, iv. NaOMe/MeOH/THF, reflux, v. CSA, MeCN, vi. NaH, BnBr, DMF, 70%, six steps; (e) $HOP(O)(OBu)_2$, 4 Å MS, 97%; (f) TIPSCl, NEt_3, DMAP, CH_2Cl_2, 91%; (g) AllOH, BF_3-Et_2O, CH_2Cl_2, 99%.

Scheme 3. Modified Synthesis of 1-*O*-Acetyl-3,4,5-tri-*O*-benzyl-*myo*-inositol (**16**)[a]

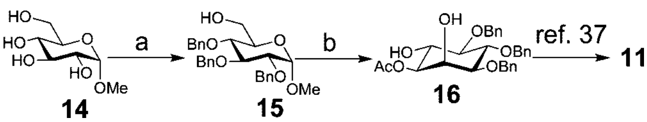

[a] Reagents and conditions: (a) i. Imidazole, TIPSCl, DMF 0 °C to rt, ii. NaH, BnBr, DMF, 0 °C to rt, iii. TBAF, THF, 99%, three steps; (b) i. SO_3−Py, DIPEA, DMSO, CH_2Cl_2, 0 °C to rt, ii. K_2CO_3, Ac_2O, MeCN, reflux, iii. $Hg(CF_3COO)_2$, Acetone/H_2O (4:1), rt, 1 h, then NaOAc (aq), NaCl (aq), 0 °C to rt, iv. $NaBH(CH_3COO)_3$, AcOH, MeCN, 0 °C to rt, 40%, four steps.

Syntheses of Monosaccharide Building Blocks. Mannosyl building blocks **1**, **5**, and **10** were synthesized from mannose bicyclic and tricyclic orthoesters (**6**, **12**, Scheme 2).[34,35] Starting from D-mannose, mannosyl phosphate **1** was accessed in six steps by dibutyl phosphoric acid opening of the bicyclic orthoester **7**. Mannosyl tricyclic orthoester **6** is readily available from D-mannose over six high yielding steps.[35] This process required only one purification at the last step and gave **6** in 70% overall yield. The versatile intermediate **6** was opened by allyl alcohol upon activation with $BF_3 \cdot Et_2O$ to afford **5** in excellent yield. Treatment of orthoester **6** with dibutyl phosphate selectively opened the tricyclic orthoester to furnish glycosyl phosphate **13**, leaving the C-6 hydroxyl group unprotected. The installation of a triisopropylsilyl (TIPS) group was straightforward and furnished building block **10**.

The previously reported synthetic route to the differentially protected *myo*-inositol by Fraser-Reid et al.[36] was modified (Scheme 3). Methyl glucopyranose was quantitatively converted to **15** in three consecutive steps. A Parikh-Doering reaction oxidized the primary hydroxyl group in **15** to an aldehyde in quantitative yield. Using this oxidation, we avoided complications arising from the urea byproduct created when dicyclohexylcarbodiimide (DCC) was used as activator. The sulfate byproduct was readily removed by water extraction. The partially protected *myo*-inositol **16** was prepared from **15** in 40% yield over four consecutive steps. The allyl and NAP protecting groups were introduced at C1 and C2 of the D-*myo*-inositol respectively as previously described[37] to furnish **11**, ready for further decoration at the C6 hydroxyl group.

Scheme 4. Assembly of *myo*-Inositol Containing Pseudotrisaccharide **8**[a]

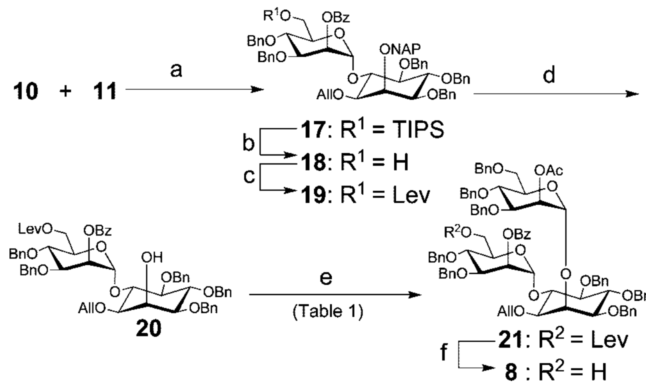

[a] Reagents and conditions: (a) TMSOTf, Toluene, −40 °C, 90%; (b) AcCl, MeOH, CH_2Cl_2, 0 °C, quant.; (c) LevOH, DIPC, DMAP, quant.; (d) DDQ, CH_2Cl_2, MeOH, 0 °C, 95%; (e) **1**, TBDMSOTf, Toluene, −40 °C, 95%, (see Table 1); (f) H_2NNH_3OAc, MeOH, rt, 89%.

Table 1. Effects of Promoter and Temperature on the Glycosylation of Glycosyl Phosphate **1** and *myo*-inositol Intermediate **20**

entry	promoter	temperature (°C)	yield (%)
1	TMSOTf	−40	15
2	TBDMSOTf	−40	27
3	TBDMSOTf	−10	57
4	TBDMSOTf	rt	55
5	**TBDMSOTf**	**0**	**95**

Assembly of *myo*-Inositol Containing Pseudosaccharides. The *myo*-inositol containing pseudotrisaccharide **8** was assembled in a stepwise manner. Glycosylation of inositol **11** with mannosyl phosphate **10** that contained a C6-TIPS ether as a temporary protecting group was found to be optimal at −40 °C, in toluene, and promoted by a stoichiometric amount of TMSOTf (Scheme 4). Under these conditions the reaction gave a good yield with complete α-selectivity. To sustain further glycosylations, the temporary TIPS protecting group was replaced by the levulinoyl (Lev) group. The presence of TIPS rather than Lev on the C6 hydroxyl group of **10** was found necessary to balance its reactivity with inositol **10** to obtain high yield and selectivity, as observed in a previous study.[37] Treatment of **19** with DDQ unmasked the C2 hydroxyl group on inositol to give **20** that served in turn as nucleophile during the next mannosylation.

The second mannosylation on the C2 hydroxyl group of pseudodisaccharide **20** was found to be nontrivial (Table 1). Activation by TMSOTf afforded the desired pseudodisaccharide **21** in just 15% yield (Table 1, Entry 1). Decomposition of **1** to form the anomeric alcohol was observed instead. Switching the promoter from TMSOTf to the milder activator TBDMSOTf dramatically improved the yield of the desired product (Table 1, Entry 2). This observation suggested a possible reactivity mismatch between highly activated **1** and less activated **20**. The glycosylation was thus improved by reducing the reactivity of **1** with TBDMSOTf. The activity of the less reactive **20** was increased by higher reaction temperatures. Product **21** was

(34) Ravida, A.; Liu, X.; Kovacs, L.; Seeberger, P. H. *Org. Lett.* **2006**, *8*, 1815–1818.
(35) Liu, X.; Wada, R.; Boonyarattanakalin, S.; Castagner, B.; Seeberger, P. H. *Chem. Commun.* **2008**, 3510–3512.
(36) Jia, Z. J.; Olsson, L.; Fraser-Reid, B. *J. Chem. Soc., Perkin Trans. 1* **1998**, 631.
(37) Liu, X.; Stocker, B. L.; Seeberger, P. H. *J. Am. Chem. Soc.* **2006**, *128*, 3638–3648.

Scheme 5. Protecting Group Manipulations on *myo*-Inositol **16** for PI Intermediate **23** and PIM_1 Intermediate **24**[a]

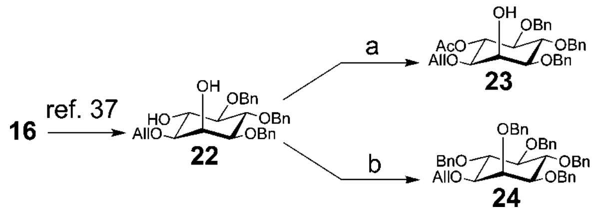

[a] Reagents and conditions: (a) Ac_2O, DMAP, Py, 70%; (b) NaH, BnBr, DMF, 0 °C to rt, quant.

obtained in excellent yield (95%) and selectivity by performing the glycosylation at 0 °C (Table 1, Entry 5). The α linkages in **21** were confirmed by 2D NMR. $^1H-^{13}C$ coupled HSQC NMR indicated $^1H1-^{13}C1$ coupling constants ($J_{C1,H1}$) of 178 Hz at the anomeric position of the mannose connected to the C2 of inositol and 182 Hz at the anomeric position of the mannose on C6 of inositol. $J_{C1,H1}$ of β mannosidic linkages are typically lower at around 159 Hz.[38]

Removal of the Lev group in **21** was achieved by treatment with hydrazine acetate in methanol and required careful monitoring. Longer reaction times resulted predominantly in the reduction of the allyl moiety to a propyl group. Partially protected inositol **16** was subjected to protecting group manipulations to furnish the inositol intermediates for **PI** and $\mathbf{PIM_1}$ (Scheme 5). Based on reactivity differences, the equatorial C6 hydroxyl group of the diol **22** was selectively acetylated to afford **23** as the intermediate en route to $\mathbf{PIM_1}$. The **PI** intermediate **24** was obtained in parallel by benzylation of the common intermediate **22**.

Assembly of Oligomannoside Fragments. The oligomannoside trichloroacetimidates **2**, **3**, and **4** were assembled in linear fashion (Scheme 6). All glycosylations employed mannosyl phosphate **1** and TMSOTf as activator. The α-1,6 glycosydic bond was readily formed at 0 °C in quantitative yield. A lower temperature (−40 °C) was required to efficiently install 1,2 glycosylic linkages with complete α-selectivity. Deallylation of **25**−**27** was performed by allylic substitutions mediated by a palladium complex to yield the corresponding anomeric alcohols **28**−**30**. Finally, conversion to the glycosyl trichloroacetimidates **2**−**4** was carried out using sodium hydride as base.

Assembly of Protected PIM Backbones. Prior to phosphorylation, all protected PIM oligosaccharide backbones were obtained by late-state glycosylations (Table 2). Following these glycosylations all ester protecting groups were removed with sodium methoxide in methanol at elevated temperature before masking the free hydroxyl groups as benzyl ethers. These protecting group manipulations were performed to avoid the persistence of *O*-benzoate protecting groups under Birch conditions in the final deprotection.[39]

Coupling between mannosyl phosphate **1** and inositol **23** gave pseudodisaccharide **31**, the backbone of $\mathbf{PIM_1}$. To access the $\mathbf{PIM_2}$ backbone, pseudotrisaccharide fragment **8** was directly used as the starting material to be transformed into backbone **32**. The glycosylation products from couplings (Table 2, entry 3−5) between the oligomannosyl trichloroacetimidates (**1**−**3**) and the common pseudotrisaccharide **8** were cleanly achieved at −10 °C. After quenching with triethylamine, the concentrated crude products were directly converted to obtain the benzylated products. When the larger structure **4** was used for glycosylation, the coupling became more sluggish and resulted in the hydrolysis of **4**. A higher temperature (0 °C) was needed to obtain the 4 + 3 glycosylation product **46** (see Experimental Section). Pseudoheptasaccharide **46** was the largest oligosaccharide assembled in this series and consisted of fragments of all smaller oligosaccharides. Thus, **46** was analyzed extensively by C−H coupled HSQC to confirm its structural identity. 2D-NMR data elucidated six anomeric proton signals with typical[38] α-manno $J_{C1,H1}$ couplings.

Removal of *O*-Allyl Protecting Group on Inositol. Protocols to cleave the C-1 *O*-allyl group on inositol attached to oligosaccharides, performed by using $PdCl_2$, have been reported to give moderate yields.[32,40−43] This literature precedence was reflected in our study as well. Different methods to remove the *O*-allyl group were explored on substrate **31** (Scheme 7 and Table 3). The hydrogen activated iridium complex $Ir\{(COD)[PH_3(C_6H_5)_2]_2\}PF_6$ was found to be the most efficient reagent to isomerize the allyl group to the corresponding enol ether. In the same pot, a catalytic amount of *p*-toluenesulfonic acid (*p*-TsOH) was added to cleave the enol ether and liberate the C1 hydroxyl of pseudodisaccharide **38** in quantitative yield. This two step procedure was applied to the larger oligosaccharides **32** to **36** as well. However, while the isomerizations mediated by the iridium complex worked smoothly, an excess of *p*-TsOH (10 equiv) was required to cleave the enol ether and furnish **39** - **43** (Scheme 7, entry 3).

Phosphorylation and Global Deprotection. The phosphate moiety accompanied by a terminal thiol linker was installed on the inositol C1 hydroxyl group of the oligosaccharide backbone **37**−**43** using a H-phosphonate (Scheme 8). Substrates **37**−**43** were treated with pivaloyl chloride in the presence of linker **44** and pyridine. Subsequently, in the same pot, the H-phosphonate diesters were oxidized with iodine and water to provide the fully benzylated phosphodiesters **45** as triethylamine salts in excellent yield. Global removal of benzyl protecting groups of analogs **45a**−**g** was achieved under Birch reduction conditions. The fully protected compounds were treated with sodium dissolved in ammonia to furnish the final products **PI** and $\mathbf{PIM_1}$−$\mathbf{PIM_6}$ (Figure 2). Small amounts of incompletely reduced products were observed containing some remaining benzyl groups. These side products were separated by extraction with chloroform and converted to the final products by resubmission to Birch reduction. The final products were formed as a mixture of monomers and disulfide dimers. Treatment with one equivalent of tris(carboxyethyl) phosphine hydrochloride (TCEP) immediately prior to conjugation of the final compounds ensured that **PI** and $\mathbf{PIM_1}$−$\mathbf{PIM_6}$ were present as monomers.

PIM Microarrays to Determine Binding to DC-SIGN. To study the interactions of synthetic **PI** and **PIMs** with the protein DC-SIGN on a microarray, **PI** and **PIMs** were immobilized on a maleimide activated glass slide via their thiol handle following established protocols (Figure 3).[44] DC-SIGN is an important receptor on dendritic cells and contributes to the initiation of a pro-inflammatory response by host cells.[45−47] One of the functions of DC-SIGN is the recognition of evolutionary

(38) Podlasek, C. A.; Wu, J.; Stripe, W. A.; Bondo, P. B.; Serianni, A. S. *J. Am. Chem. Soc.* **1995**, *117*, 8635–8644.
(39) Kwon, Y. U.; Soucy, R. L.; Snyder, D. A.; Seeberger, P. H. *Chem.−Eur. J.* **2005**, *11*, 2493–2504.
(40) Cid, M. B.; Alfonso, F.; Martin-Lomas, M. *Synlett* **2003**, 1370–1372.
(41) Liu, X.; Seeberger, P. H. *Chem. Commun.* **2004**, 1708–1709.
(42) Vishwakarma, R. A.; Menon, A. K. *Chem. Commun.* **2005**, 453–455.
(43) Liu, X.; Kwon, Y. U.; Seeberger, P. H. *J. Am. Chem. Soc.* **2005**, *127*, 5004–5005.

Scheme 6. Assembly of Oligomannosylating Reagents **2**−**4** for the Synthesis of **PIM$_4$**−**PIM$_6$**[a]

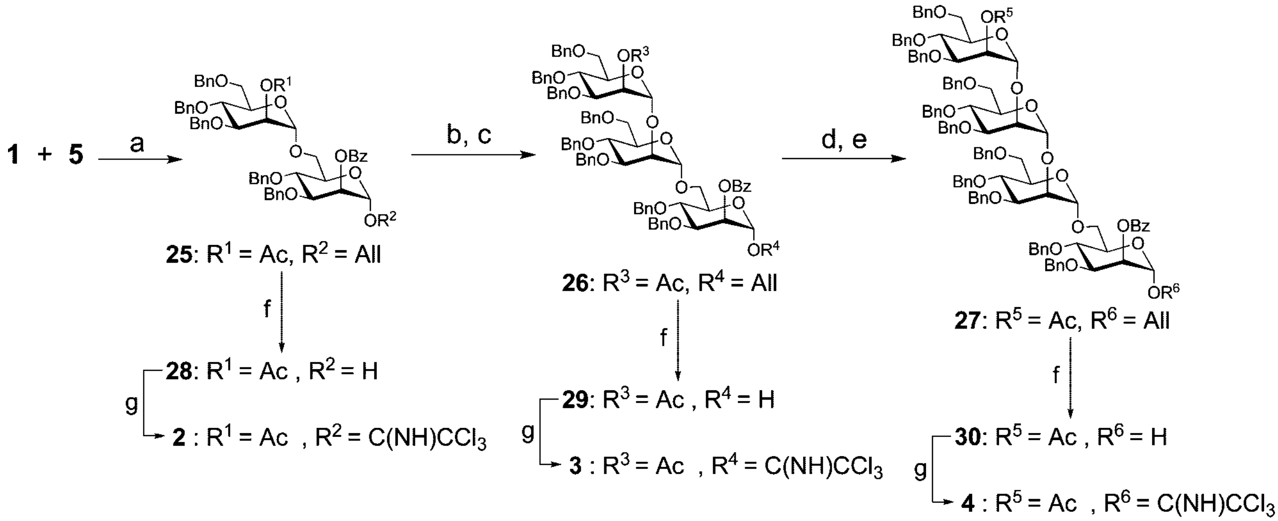

[a] Reagents and conditions: (a) TMSOTf, CH_2Cl_2, −10 °C, quant.; (b) AcCl, MeOH, CH_2Cl_2, 0 °C, 91%; (c) **1**, TMSOTf, −40 °C, Toluene, 95%: (d) AcCl, MeOH, CH_2Cl_2, 0 °C, 84%; (e) **1**, TMSOTf, Toluene, −40 °C, 96%; (f) $Pd(OAc)_2$, MeOH, PPh_3, Et_2NH, 77% for **28**, 95% for **29**, and 83% for **30**; (g) Cl_3CCN, NaH, rt, 85% for **2**, 86% for **3**, and 89% for **4.**

conserved pathogenic structures that are secreted or exposed on the surface of viruses or bacteria.[46,48−50] Upon binding to DC-SIGN, the antigens are internalized, processed and later presented on the surface of dendritic cells together with costimulatory molecules.[51,52] Mycobacteria also use DC-SIGN as a receptor to enter dendritic cells.[51]

Glass slides printed with the immobilized **PI** and **PIM$_1$**−**PIM$_6$** were incubated with a DC-SIGN solution in buffer at room temperature to allow DC-SIGN to bind to the immobilized PIMs. Excess DC-SIGN was washed off and bound DC-SIGN was detected by incubation with a fluorescein-conjugated anti-DC-SIGN antibody. The difference in DC-SIGN binding affinity to the synthetic PIM compounds was assessed semiquantitatively by monitoring the fluorescence intensity via a fluorescence scanner (for fluorescent intensity data, see Supporting Information). Synthetic PIMs bind to DC-SIGN in a specific manner (Figure 3). Although both synthetic analogs of the most abundant **PIM$_2$** and **PIM$_6$** are recognized by DC-SIGN, the larger synthetic oligosaccharides **PIM$_5$** and **PIM$_6$** bound to DC-SIGN to a greater extent. This observation underlines the significance of the α-1,2- mannose motif present in both PIMs and ManLAM structures.[53]

Adjuvant Activity of PIMs. An important feature of natural PIMs is their ability to induce a host cell immune response. To investigate immunostimulatory effects of these synthetic PIMs four C57BL/6 mice per group were prime-boost immunized with the model antigen keyhole-limpet hemocyanin (KLH) covalently linked to **PIM$_6$**. As expected, immunization with the pure antigen KLH resulted in detectable anti-KLH antibody levels. Antibody production in the presence of the well-established adjuvants Freund's adjuvant, alum and CpG, increased substantially. In comparison, conjugation of **PIM$_6$** glycan to KLH also resulted in a marked increase of anti-KLH antibodies that was statistically significant for each serum dilution compared to KLH alone (Figure 4A). To address the mechanism causing the increased antibody production after covalent attachment of **PIM$_6$** to KLH, we restimulated spleen cells of immunized mice with KLH *ex vivo* and measured proliferation. Spleen cell proliferation of mice that had been immunized with KLH−**PIM$_6$** was significantly increased indicating that T cell priming was stimulated by **PIM$_6$** glycan (Figure 4B). It is also known that adjuvant properties not only depend on antibody production and T cell proliferation, but also on other T effector functions such as cytokine production. To this end, we measured IFN-γ production of T cells by ELISpot analysis. The frequency of IFN-γ producing T cells in spleen was determined upon restimulation of T cells with KLH. The ability of T cells to produce IFN-γ was increased in spleen cells of mice that had been immunized with KLH−**PIM$_6$** conjugate (Figure 4C). The effect was even stronger than with the well-established adjuvants Freund's adjuvant, alum or CpG, which highlights the immunostimulatory capacity of synthetic **PIM$_6$** glycan. Concanavalin A was used as a positive control since it serves as a T cell mitogen and stimulates all T cells to the same extent.

Recognition of **PIM$_6$** by pattern recognition receptors on antigen-presenting cells might provide a danger signal, thereby facilitating enhanced uptake of the model antigen and increased expression of costimulatory molecules. The effect of **PIM$_6$** on T cell proliferation and T cell effector functions such as IFN-γ production clearly indicates that antigen presentation by APCs and T cell activation are increased by **PIM$_6$** glycan.

The synthetic **PI** and **PIM$_5$**−**PIM$_6$** described here will be suitable for conjugation with other appropriate surfaces such as fluorescent nanocrystals, beads or fluorophores to generate probes for cellular assays. Such tools may shed light on the mechanism

(44) de Paz, J. L.; Horlacher, T.; Seeberger, P. H. *Methods Enzymol.* **2006**, *415*, 269–292.
(45) van Kooyk, Y.; Geijtenbeek, T. B. *Nat. Rev. Immunol.* **2003**, *3*, 697–709.
(46) Cambi, A.; Figdor, C. G. *Curr. Opin. Cell Biol.* **2003**, *15*, 539–546.
(47) Banchereau, J.; Steinman, R. M. *Nature* **1998**, *392*, 245–252.
(48) Cambi, A.; Koopman, M.; Figdor, C. G. *Cell. Microbiol.* **2005**, *7*, 481–488.
(49) Su, S. V.; Hong, P.; Baik, S.; Negrete, O. A.; Gurney, K. B.; Lee, B. *J. Biol. Chem.* **2004**, *279*, 19122–19132.
(50) Geijtenbeek, T. B.; Engering, A.; Van Kooyk, Y. *J. Leukoc. Biol.* **2002**, *71*, 921–931.
(51) De Libero, G.; Mori, L. *Nat. Rev. Immunol.* **2005**, *5*, 485–496.
(52) De Libero, G.; Mori, L. *FEBS Lett.* **2006**, *580*, 5580–5587.
(53) Koppel, E. A.; Ludwig, I. S.; Hernandez, M. S.; Lowary, T. L.; Gadikota, R. R.; Tuzikov, A. B.; Vandenbroucke-Grauls, C. M.; van Kooyk, Y.; Appelmelk, B. J.; Geijtenbeek, T. B. *Immunobiology* **2004**, *209*, 117–127.

Table 2. Assembly of Fully Protected $\mathbf{PIM_1}$−$\mathbf{PIM_6}$ Backbones: Union of (oligo)Mannosyl Fragment (**X**) and Inositiol-Containing Pseudosaccharide Fragment (**Y**)

X + Y → a) Glycosylation (except entry 2); b) NaOMe / MeOH, 50 °C, 24 h; c) BnBr, NaH, 0 °C to rt, 12 h → **Differentially Protected PIM_2 - PIM_6**

Entry	X	Y	Glycosylation Conditions	Products	Yields a) ; b) ; c)
1	**1**	**23**	TMSOTf, -40 °C, Et_2O	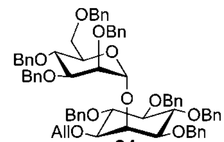 **31**	a) 69%; b) and c) quant. (2 steps)
2	not applied	**8**	No Glycosylation	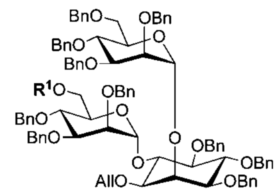 **32**: $\mathbf{R^1}$ = Bn	b) and c) 90% (2 steps)
3	**1**	**8**	TMSOTf, -10 °C, CH_2Cl_2	**33**: $\mathbf{R^1}$ = 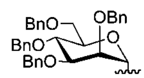	a), b), and c) 89% (3 steps)
4	**2**	**8**	TMSOTf, -10 °C, CH_2Cl_2	**34**: $\mathbf{R^1}$ = 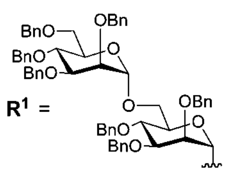	a), b), and c) 89% (3 steps)
5	**3**	**8**	TMSOTf, -10 °C, CH_2Cl_2	**35**: $\mathbf{R^1}$ = 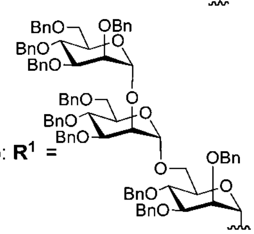	a), b), and c) 73% (3 steps)
6	**4**	**8**	TMSOTf, 0 °C, CH_2Cl_2	**36**: $\mathbf{R^1}$ = 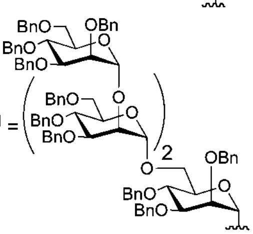	a) 64%; b) and c) 97% (2 steps)

by which PIM structures on *Mtb* can influence bacterial trafficking in host cells. The synthetic compounds can also be attached to affinity columns in search for proteins or enzymes in cell lysates that interact with PIMs. Moreover, the synthetic PIMs can be used as substrates to explore biosynthetic pathways of the PIMs.

We are investigating the possibility of applying synthetic PIMs as antigens to elicit an immune response against *Mtb* as well as their adjuvant properties *in vivo*. For these purposes, the synthetic compounds can be conjugated to different model antigens.

Conclusion

In this study, the efficient synthesis of all PIMs including phosphatidylinositol (**PI**) and $\mathbf{PIM_1}$ to $\mathbf{PIM_6}$ was reported. A robust and practical synthesis to the PIM molecules was developed utilizing mannosyl bicyclic and tricyclic orthoesters and mannosyl phosphates. The key intermediate orthoesters allowed for rapid and scalable syntheses of mannoside building blocks and the glycosylations of the mannosyl phosphates resulted in excellent yields and stereoselectivity. All synthetic PIMs are equipped with a thiol linker to be readily immobilized on microarray surfaces. Thus, the synthetic PIMs represent tools for various biological studies. An application of the synthetic **PI** and **PIMs** for interaction with the protein DC-SIGN was

(54) Takahashi, H.; Kittaka, H.; Ikegami, S. *J. Org. Chem.* **2001**, *66*, 2705–2716.

Scheme 7. Removal of Allyl Protecting Groups on C1 *myo*-Inositol of Fully Protected **PI** and **PIM₂**−**PIM₆**

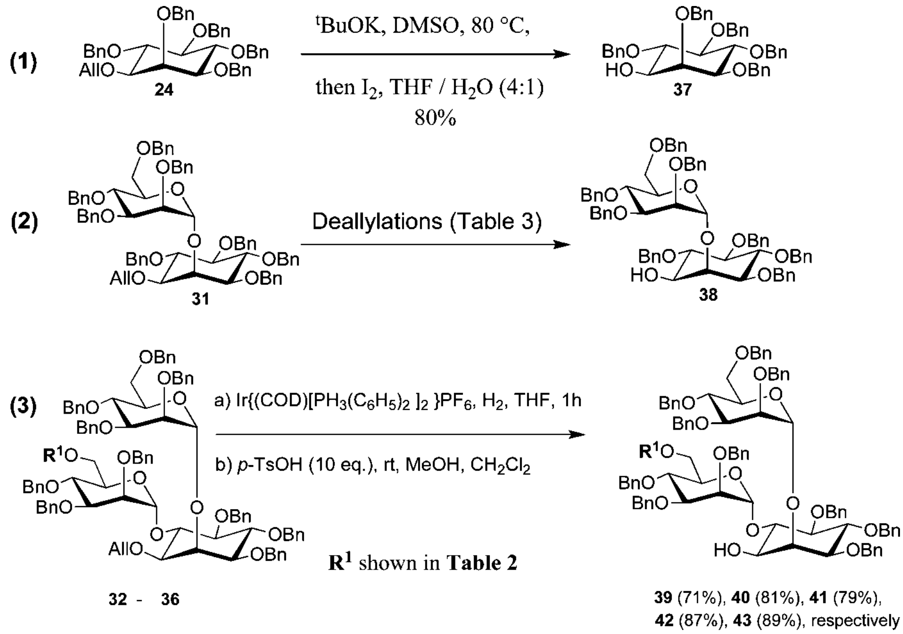

Table 3. Removal of Allyl Protecting Group on Pseudo-Disaccharide **31**

entry	conditions	yield
1	ᵗBuOK, DMSO, 80 EC, then I_2, THF/H_2O TMSOTf	10%, (decompostion)
2	$Pd(OAc)_2$, PPh_3, $HNEt_2$, CH_2Cl_2/MeOH (2:1)	no reaction
3	$[Ir(COD)(PCH3Ph_2)_2]PF_6$ (cat.), H_2, THF then I_2 in THF/H_2O (2:1)	30%
4	$[Ir(COD)(PCH3Ph_2)_2]PF_6$ (cat.), H_2, THF then *p*-TsOH (cat.) in DCM/MeOH (1:3)	**quantitative**

Scheme 8. Phosphorylation of Oligosaccharides **37**−**43** and Global Deprotection under Birch Reduction Conditions[a]

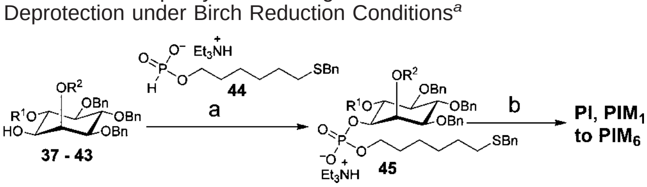

[a] Reagents and conditions: (a) i. **44**, PivCl, pyridine, ii. I_2, H_2O, pyridine, 90% to quant., 2 steps; (b) i. Na/NH_3 (l) /*t*-BuOH, −78 °C, ii. MeOH, 65% for **PI**, 43% for **PIM₁**, 56% for **PIM₂**, 91% for **PIM₃**, 65% for **PIM₄**, 88% for **PIM₅**, and 84% for **PIM₆**.

demonstrated. The difference in DC-SIGN binding affinity among synthetic PI and PIM compounds was observed in a specific manner. Immunization experiments in mice revealed the potential of synthetic PIMs to serve as immune stimulators.

Experimental Section

Immunization of Mice and Detection of anti-KLH Antibody Levels in Sera. Preparation of keyhole limpet hemocyanin (KLH) in complete/incomplete Freund's adjuvant was performed by mixing KLH with Freund's adjuvant in a 1:1 volume ratio. For coupling of **PIM₆** to KLH, **PIM₆** was incubated with Tris(2-carboxyethyl)phosphine HCl (TCEP) in equal molar ratio for one hour at rt. A molar excess of **PIM₆** was then coupled to KLH using the Imject Maleimide Activated mcKLH Kit (Pierce, Rockford, IL) according to manufacturer's instructions. **PIM₆**−KLH conjugate was purified by gel filtration chromatography and the protein concentration in the eluate was determined by measuring the absorption at a wavelength of 280 nm.

Female C57BL/6 mice (6−8 weeks old) were housed in the HCI rodent center, ETH Zürich, and were provided food and water *ad libitum*. On day 0 four mice per group were *s.c.* immunized with KLH alone (group 1), KLH in complete Freund's adjuvant (group 2), KLH with alum (group 3), KLH with CpG (group 4) or KLH coupled to **PIM₆** (group 5). On day 10, mice received a boost immunization with KLH alone (group 1), KLH in incomplete Freund's adjuvant (group 2), KLH with alum (group 3), KLH with CpG (group 4) or KLH coupled to **PIM₆** (group 5). The amount of KLH was adjusted to 50 μg per mouse and immunization. On day

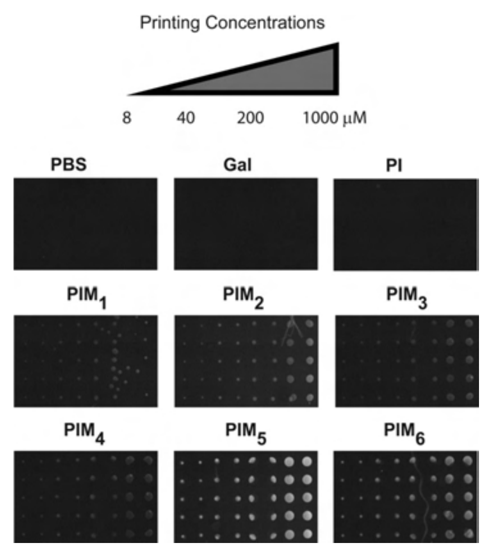

Figure 3. Fluorescent scanning of PIM microarray incubated with DC-SIGN and susequently with fluorescein conjugated antihuman DC-SIGN antibody (1 h). A PI and PIM immobilized glass slide was incubated with a solution of DC-SIGN (1 μg/100 μL) in HEPES buffer containing 1% BSA, 20 mM $CaCl_2$, and 0.5% Tween-20 at room temperature for 1 h. The slide was washed thoroughly and incubated with a solution of fluorescein conjugated antihuman DC-SIGN antibody (0.5 μg/100 μL) in HEPES buffer containing 1% BSA and 0.5% Tween-20 at room temperature for 1 h. The slide was washed thoroughly and scanned by a fluorescent microarray scanner. (PBS = Phosphate-buffered saline, Gal = Galactose)

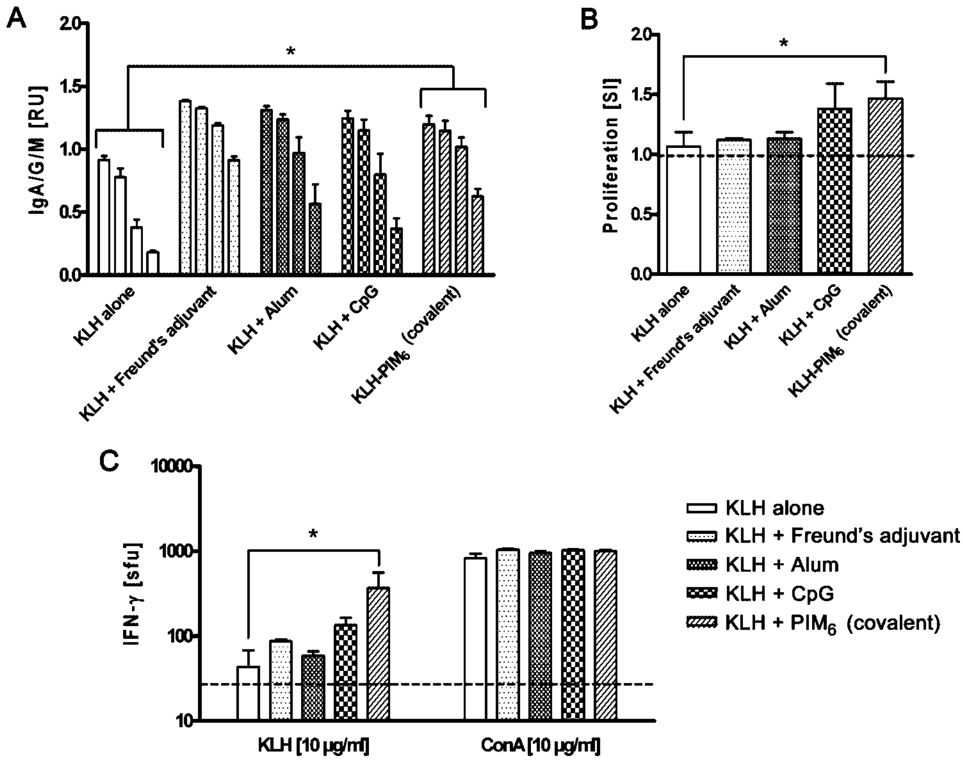

Figure 4. Immunization studies in mice with the model antigen KLH coupled to PIM_6. On day 0, four C57BL/6 mice per group (6−8 weeks) were s.c. immunized with KLH alone, KLH in complete Freund's adjuvant, KLH with alum, KLH with CpG or KLH covalently linked to **PIM_6**. On day 10, mice received a boost immunization with KLH alone, KLH in incomplete Freund's adjuvant, KLH with alum, KLH with CpG, or KLH−**PIM_6**. (A) On day 17 post immunization blood was taken from the saphenous vein of the immunized mice and levels of anti-KLH antibodies (sum of IgA, IgG and IgM) were measured by ELISA in serial dilutions of the sera (1:1000, 1:2000, 1:10000, 1:50000, duplicates for each mouse). Data are presented as mean ± SEM for each group of mice. Statistical analysis was performed with Student's *t* test (*, $p < 0.05$). (B) On day 20 post immunization, 2×10^5 splenocytes were restimulated with KLH (10 μg/ml) for 24 h and cell proliferation was measured. The results are expressed as a stimulation index (SI) which is the net proliferation of spleen cell cultures stimulated with 10 μg/ml KLH divided by the net proliferation of spleen cell cultures in medium. Data are presented as mean ± SEM for each group of mice. Statistical analysis was performed with Student's *t* test (*, $p < 0.05$). The dashed line represents proliferation of spleen cells from unimmunized mice. (C) On day 20, 2×10^5 splenocytes were stimulated with KLH (10 μg/ml) or Concanavalin A (ConA, 10 μg/ml) in a 96-Well plate coated with antimouse-IFN-γ and the frequency of IFN-γ producing cells was determined by ELISpot analysis. The results are expressed as *spot forming units* (sfu) which is the number of cells producing IFN-γ in each well. Data are presented as mean ± SEM for each group of mice. Statistical analysis was performed with Student's *t* test (*, $p < 0.05$). The dashed line represents IFN-γ production of cells cultivated in medium (unspecific background).

17, blood was taken from the saphenous vein and serum was separated from the clotted blood by centrifugation. All animal experiments were in accordance with local Animal Ethics Committee regulations.

Levels of anti-KLH antibodies in sera of immunized mice were measured by ELISA. Briefly, Microlon microplates (Greiner, Frickenhausen, Germany) were coated with 10 μg/mL KLH in 0.05 M Na_2CO_3 buffer (pH 9.6) at 4 °C overnight. After blocking with 1% BSA/PBS for two hours at rt and washing with 0.05% Tween-20/PBS plates were incubated with serial dilutions of sera (diluted in 0.1% BSA/PBS) for two hours. Plates were then washed three times with 0.05% Tween-20/PBS and incubated with HRP-conjugated goat-antimouse IgG+A+M antibody in a dilution of 1:1000 (Invitrogen, Basel, Switzerland). Detection was performed by using the 3,3′,5,5′-Tetramethylbenzidine Liquid Substrate System (Sigma-Aldrich, Buchs, Switzerland) according to manufacturer's instructions.

T Cell Proliferation and ELISpot Analysis. On day 20 after the first immunization, mice were sacrificed and spleens were removed. RBCs were lysed by adding hypotonic ammonium chloride solution. Single cell suspensions were cultivated at 2×10^5 cells per well in 96-well plates for 24 h in the presence of medium or KLH (10 μg/mL) for restimulation of T cells *ex vivo*. Proliferation of spleen cells was measured using the CellTiter 96 AQueous One Solution Cell Proliferation Assay (Promega, Madison, WI) according to the manufacturer's instructions.

ELISpot analysis was performed on day 20 after the first immunization using a mouse IFN-γ ELISpot Kit (R&D Systems, Minneapolis, MN). Briefly, 2×10^5 spleen cells per well were stimulated for 24 h in the presence of medium, KLH (10 μg/mL) or the T cell mitogen concanavalin A (ConA, 10 μg/mL). Spot development was performed according to the manufacturer's instructions and the number of spots was determined using an ELISpot reader (AID, Straussberg, Germany).

Statistical Analysis. Statistical analyses were performed applying unpaired Student's *t* test. All statistical analyses were performed with the Prism software (Graph Pad Software, San Diego, CA).

Acknowledgment. This research was supported by ETH Zürich, the Swiss National Science Foundation (SNF Grant 200121-101593), and the Roche Research Foundation (postdoctoral fellowship for S.B.). S.B. thanks Thailand Research Fund for financial support.

Supporting Information Available: Complete synthetic procedures, NMR spectral copies of all new compounds and complete ref 21. This material is available free of charge via the Internet at http://pubs.acs.org.

JA806283E

SUPPORTING INFORMATION

Chemical Synthesis of All Phosphatidylinositol Mannoside (PIM) Glycans from *Mycobacterium tuberculosis*

Siwarutt Boonyarattanakalin,[†‡] *Xinyu Liu*[†§] *Mario Michieletti,*[†¶] *Bernd Lepenies*[†]

and Peter H. Seeberger[†]*

Laboratory for Organic Chemistry, Swiss Federal Institute of Technology (ETH) Zürich Wolfgang-Pauli-Str. 10, HCI F312, 8093 Zürich, Switzerland and Sirindhorn International Institute of Technology, Thammasat University, P.O.Box 22 Thammasat-Rangsit Post Office, Pathumthani 12121, Thailand

seeberger@org.chem.ethz.ch

† Swiss Federal Institute of Technology (ETH) Zürich

‡ Sirindhorn International Institute of Technology

§ Current address: Department of Biological Chemistry and Molecular Pharmacology, Harvard Medical School, 240 Longwood Avenue, Boston, MA, 02115, USA

¶ Visiting Ph.D. student from Università degli Studi del Piemonte Orientale “Amedeo Avogadro”, Novara, Italy

Complete ref. 21

[21] de la Salle, H.; Mariotti, S.; Angenieux, C.; Gilleron, M.; Garcia-Alles, L. F.; Malm, D.; Berg, T.; Paoletti, S.; Maitre, B.; Mourey, L.; Salamero, J.; Cazenave, J. P.; Hanau, D.; Mori, L.; Puzo, G. and De Libero, G., *Science* **2005**, *310*, 1321-1324.

Semi-quantitative analysis of the microarray data.

Spot intensities were quantified by densitometric analysis using the program Quantity One (Bio-Rad Laboratories, Hercules, CA). Data are expressed as mean for the second highest concentration of spotted PIMs (200 μM).

Fluorescence Intensities (by densitometric analysis):

PBS	no binding
PI	no binding
PIM_1	6939
PIM_2	14710
PIM_3	7334
PIM_4	10040
PIM_5	33500
PIM_6	19660

General information for Chemical Synthesis: All chemicals used were reagent grade and used as supplied except where noted. All reactions were performed in oven-dried glassware under an inert atmosphere unless noted otherwise. Reagent grade *N*,*N*-dimethylformamide (DMF) was dried over activated molecular sieves prior to use. Pyridine, triethylamine (NEt_3) and acetonitrile (MeCN) were distilled over CaH_2 prior to use. Dichloromethane (CH_2Cl_2), toluene and tetrahydrofuran (THF) were purified by a Cycle-Tainer Solvent Delivery System unless noted otherwise. Analytical thin layer chromatography (TLC) was performed on Merck silica gel 60 F254 plates (0.25mm). Compounds were visualized by UV irradiation or dipping the plate in a cerium sulfate-ammonium molybdate (CAM) solution. Flash column chromatography was carried out using forced flow of the indicated solvent on Fluka Kieselgel 60 (230-400 mesh). Gel filtration chromatography was carried out using Sephadex LH-20 from Amersham Biosciences. ^{1}H, ^{13}C and ^{31}P NMR spectra were recorded on a Varian Mercury 300 (300 MHz), Bruker DRX500 (500 MHz), or, Bruker DRX600 (600 MHz) spectrometer in $CDCl_3$ with chemical shifts referenced to internal standards $CDCl_3$ (7.26 ppm ^{1}H, 77.0 ppm ^{13}C) unless otherwise stated. ^{31}P spectra are reported in δ value relative to H_3PO_4 (0.0 ppm) as an external reference. Splitting patterns are indicated as s, singlet; d, doublet; t, triplet; q, quartet; brs, broad singlet for ^{1}H NMR data. NMR chemical shifts (δ) are reported in ppm and coupling constants (*J*) are reported in Hz. High resolution mass spectral (HRMS) analyses were performed by the MS-service at the Laboratory for Organic Chemistry (LOC) at ETH Zürich. High-resolution MALDI and ESI mass spectra were run on an IonSpec Ultra instrument. IR spectra were recorded on a Perkin-Elmer 1600 FTI R spectrometer. Optical rotations were measured using a Perkin-Elmer 241 polarimeter.

General procedures for glycosylations: Glycosylating agent and nucleophile were co-evaporated with anhydrous toluene (3x) *in vacuo* and placed under high vacuum for at least 4 h. Glycosylations were performed without molecular sieves. Under argon atmosphere, the glycosylating agent and nucleophile mixtures were dissolved in a solvent at room temperature (rt) before being cooled to a desired temperature (0 °C by ice-water bath, - 10 °C by ice-acetone bath, and - 40 °C by dry ice-acetonitrile bath). A promoter (TMSOTf or TBDMSOTf) was added to this reaction solution in one portion via syringe. After the reaction had finished, excess triethylamine (NEt_3) was added to quench the reaction at the reaction temperature. The reaction mixture was concentrated *in vacuo* and purified by flash silica column chromatography or directly used as a starting material in the next reaction.

1-*O*-Allyl-2-*O*-benzoyl-3,4-di-*O*-benzyl-α-D-mannopyranose (**5**): To a solution of tricyclic orthoester **6** (309 mg, 0.692 mmol) and allyl alcohol (0.94 mL, 13.840 mmol) in CH_2Cl_2 (1.50 mL) at 0 °C, $BF_3{\cdot}Et_2O$ was added (8.5 μL, 0.067 mmol) in one portion. The mixture was stirred for 2 h at 0 °C and quenched by excess NEt_3 (50 μL). The resulting mixture was purified by flash silica column chromatography (cyclohexane / EtOAc gradient 9:1 to 4:1) to obtain the title compound **5** (332 mg, 99%) as a colorless syrup. R_f 0.64 (cyclohexane / EtOAc = 6 : 4); $[\alpha]_D^{r.t.}$= + 0.6 (*c* = 1.0, $CHCl_3$); ^1H NMR (500 MHz, $CDCl_3$) δ: 8.09 – 7.94 (m, 2H), 7.61 – 7.10 (m, 13H), 5.84 (ddd, *J* = 5.7, 10.9, 15.7, 1H), 5.57 (dd, *J* = 1.9, 3.0, 1H), 5.30 – 5.08 (m, 2H), 4.93 (d, *J* = 1.57, 1H), 4.77 – 4.50 (m, 4H), 4.20 – 3.64 (m, 7H), 1.86 (brs, 1 H); ^{13}C NMR (75 MHz, $CDCl_3$) δ: ^{13}C NMR (75 MHz, $CDCl_3$) δ = 165.49, 138.05, 137.81, 133.15, 129.76, 129.69, 128.37, 128.30, 128.19, 128.04, 127.83, 127.70, 127.50, 117.81, 96.93, 78.14, 75.28, 74.02, 71.89, 71.55, 69.14, 68.31, 62.11. HRMS-MALDI (*m/z*): $[M+Na]^+$ calculated for $C_{30}H_{32}O_7Na$, 527.2040; Found: 527.2039.

Dibutyl-(2-*O*-benzoyl-3,4-di-*O*-benzyl-6-*O*-triisopropylsilyl–α-D-mannopyranosyl) phosphate (**10**): To a solution of dibutyl phosphate **13** (3.0 g, 4.568 mmol), DMAP (664 mg, 5.435 mmol) and pyridine (10 mL) in CH_2Cl_2 (12 mL) at rt, triisopropylsilyl chloride (TIPSCl, 1.30 mL, 6.082 mmol) was added in one portion. The mixture was stirred for 36 h at rt and filtered to remove suspension solid. The filtrate was concentrated *in vacuo*. The resulting crude product was purified by flash silica column chromatography (cyclohexane / EtOAc) to obtain the title compound **10** (3.3 g, 91%) as a colorless syrup. R_f 0.29 (cyclohexane / EtOAc = 4 : 1); $[\alpha]_D^{r.t.}$= – 5.0 (c = 1.0, $CHCl_3$); ^{1}H NMR (300 MHz, $CDCl_3$) δ 8.23 – 8.03 (m, 2H), 7.69 – 7.14 (m, 13H), 5.77 (dd, J = 1.9, 6.4, 1H), 5.73 – 5.65 (m, 1H), 5.06 – 4.47 (m, 4H), 4.40 – 3.82 (m, 9H), 1.84 – 1.59 (m, 4H), 1.56 – 1.30 (m, 4H), 1.28 – 1.03 (m, 21H), 0.99 – 0.93 (m, 6H); ^{13}C NMR (75 MHz, $CDCl_3$) δ 165.19, 138.40, 137.71, 133.17, 129.93, 129.48, 128.24, 128.20, 127.95, 127.78, 127.56, 96.03, 95.96, 77.36, 75.40, 74.38, 73.20, 71.89, 68.83, 68.69, 67.93, 67.85, 67.77, 61.85, 32.40, 32.36, 32.31, 32.27, 18.77, 18.15, 18.11, 13.71, 12.16; ^{31}P NMR (121 MHz, $CDCl_3$) δ – 2.67. HRMS-MALDI (*m/z*): $[M+Na]^+$ calculated for $C_{44}H_{65}O_{10}PSiNa$, 835.3997; Found: 835.3992.

1-*O*-Methyl-2,3,4-tri-*O*-benzyl-α-D-gluopyranose (**15**): To a cooled solution (0 °C) of 1-*O*-methyl-α-D-gluopyranose (3.66 g, 18.85 mmol) and imidazole (3.86 g, 56.55 mmol) in DMF (30 mL), TIPSCl (4.43 mL, 20.70 mmol) was added dropwise over a period of 15 minutes. After 24 h at rt, the reaction was diluted with water (100 mL) and extracted with CH_2Cl_2 (3 x 60 mL). The combined organic layer was washed with brine, dried over Na_2SO_4, concentrated *in vacuo*, and placed under high vacuum. A solution of this crude product and BnBr (11.2 mL, 94.28 mmol) in DMF (100 mL) was cooled to 0 °C and NaH (60% in mineral oil, 3.77 g, 94.28 mmol) was added. The reaction mixture was allowed to warm to rt. After 12 h at rt, the reaction mixture was transferred to a separatory funnel and carefully quenched by minimum amount of MeOH and water (100 mL). The reaction mixture was extracted with Et_2O (3 x 100 mL). The combined organic layer was washed with brine, dried over Na_2SO_4, and concentrated *in vacuo*. The crude product was combined with TBAF·H_2O (solid, 12 g, 36.03 mmol) and THF (20 mL) was added. The reaction solution was stirred at rt for 12 h, diluted with H_2O, and extracted with EtOAc (3x). The combined organic layer was washed with brine, dried over Na_2SO_4, concentrated *in vacuo*, and purified by flash silica column chromatography (cyclohexane / EtOAc gradient) to obtain the title compound **15** as a colorless syrup (9.0 g, 99%, 3 steps). R_f 0.44 (cyclohexane / EtOAc = 1 : 1); $[\alpha]_D^{r.t.}$= +27.5 (c = 1.0, $CHCl_3$); ^{1}H NMR (400 MHz, $CDCl_3$) δ 7.40 – 7.07 (m, 15H), 5.14 – 4.33 (m, 7H), 3.93 (t, J = 9.3, 1H), 3.74 – 3.65 (m, 1H), 3.64 – 3.51 (m, 2H), 3.50 – 3.35 (m, 2H), 3.28 (s, 3H), 1.60 (s, 1H); ^{13}C NMR (75 MHz, $CDCl_3$) δ 138.58, 137.97, 128.37, 128.30, 128.02, 127.93, 127.86, 127.77, 127.52, 98.11, 81.93, 79.92, 77.46, 77.34, 77.03, 76.61, 75.76, 75.03, 73.43, 70.65, 61.85, 55.22; HRMS-MALDI (m/z): $[M+Na]^+$ calculated for $C_{28}H_{32}O_6Na$, 487.2091; Found: 487.2091.

1-*O*-Acetyl-3,4,5-tri-*O*-benzyl-D-*myo*-inositol (**16**): To a cooled solution of compound **15** (10.5 g, 22.60 mmol) in CH_2Cl_2 (250 mL) at 0 °C, SO_3·Py (14.4 g, 90.41 mmol) was added, immediately followed by addition of *N*,*N*-diisopropylethylamine (DIPEA, 20.7 mL, 158.22 mmol). The reaction mixture was stirred at 0 °C for 10 min and DMSO (24.5 mL, 316.44 mmol) was added to this reaction in one portion via syringe. After 2 h at 0 °C, the reaction was diluted with saturated aqueous $NaHCO_3$ (200 mL) and extracted with Et_2O (3 x 200 mL). The combined organic layer was washed with brine, dried over Na_2SO_4, concentrated *in vacuo*, and placed under high vacuum for 4 h. The aldehyde crude product was dissolved in MeCN (300 mL). Then, Ac_2O (12.7 mL, 135.62 mmol) and K_2CO_3 (12.5 mg, 90.41 mmol) were added to the same flask. The reaction mixture was refluxed for 12 h and allowed to cool to rt. In a separatory funnel, the reaction mixture was diluted with saturated aqueous $NaHCO_3$ (300 mL) and extracted with Et_2O (3 x 200 mL). The combined organic layer was washed with brine, dried over Na_2SO_4, concentrated *in vacuo*, and placed under high vacuum for 4 h. The acetyl enolate crude product was dissolved in a mixture of acetone (280 mL) and water (65 mL). To this solution, $(CF_3COO)_2Hg$ (11.57 g, 27.12 mmol) was added at rt. After 1h, the reaction solution was cooled to 0 °C. To this reaction, aqueous NaOAc (9 mL of 3 M, 27.13 mmol) was added, immediately followed by addition of brine (31 mL). The reaction was allowed to slowly warm to rt and stirred at rt for 12h. In a separatory funnel, the reaction mixture was diluted with saturated aqueous $NaHCO_3$ (300 mL) and extracted with Et_2O (3 x 200 mL). The combined organic layer was washed with brine, dried over Na_2SO_4, concentrated *in vacuo*, and placed under high vacuum for 4 h. The crude product from Ferrier rearrangement was dissolved in MeCN (100 mL) and this solution was transferred to a cooled (0 °C) solution of $NaBH(CH_3COO)_3$ (24.0 g, 113.00 mmol) in a mixture of AcOH (110 mL) and MeCN (110 mL). The reaction was allowed to warm to rt and stirred at rt for 12h. In a separatory funnel, the reaction mixture was diluted with saturated aqueous $NaHCO_3$ (300 mL) and extracted with Et_2O (3 x 200 mL). The combined organic layer was washed with brine, dried over Na_2SO_4, concentrated *in vacuo*, and purified by flash silica column chromatography (cyclohexane / EtOAc gradient started from 100% cyclohexane to 7: 3 to 6:4 to 1:1, the major product is the desired product) to obtain the title compound **16** (4.45 g, 40%, 4 steps) as a colorless syrup. NMR spectra are the same as reported in literature.[1]

(2-*O*-Benzoyl-3,4-di-*O*-benzyl-6-*O*-triisopropylsilyl-α-D-mannopyranosyl)-(1→6)- 1-*O*-allyl-2-*O*-napthylmethyl-3,4,5-tri-*O*-benzyl-D-*myo*-inositol (**17**): Following the general procedures for glycosylations, a glycosylation of mannosyl phosphate **10** (122 mg, 0.150 mmol) and inositol **11** (86 mg, 0.136 mmol) promoted by TMSOTf (29 μL, 0.150 mmol) was carried out in toluene (4 mL) at - 40 °C for 2 h. After being quenched by NEt_3 (60 μL), the reaction mixture was concentrated *in vacuo* and purified by flash silica column chromatography (cyclohexane / EtOAc) to obtain the title compound **17** in quantitative yield as a white solid. R_f 0.51 (cyclohexane / EtOAc = 4 : 1); $[\alpha]_D^{r.t.}$= – 6.8 (*c* = 1.0, $CHCl_3$); b.p. = 130.5 – 132 °C; ^{1}H NMR (300 MHz, $CDCl_3$) δ 8.24 – 8.15 (m, 2H), 7.92 – 7.78 (m, 4H), 7.68 – 7.58 (m, 2H), 7.55 – 7.44 (m, 4H), 7.44 – 7.13 (m, 25H), 6.12 – 5.91 (m, 1H), 5.79 (dd, *J* = 1.9, 3.0, 1H), 5.58 (d, *J* = 1.5, 1H), 5.37 – 5.15 (m, 2H), 5.10 – 4.60 (m, 12H), 4.40 – 3.89 (m, 8H), 3.61 (brs, 2H), 3.52 – 3.24 (m, 3H), 1.20 – 1.03 (m, 21H); ^{13}C NMR (75 MHz, $CDCl_3$) δ 165.54, 139.26, 138.58, 138.31, 138.26, 138.23, 136.20, 134.37, 133.11, 132.89, 132.85, 130.19, 129.96, 128.33, 128.26, 128.14, 128.03, 127.97, 127.92, 127.86, 127.64, 127.59, 127.51, 127.35, 127.12, 126.43, 126.18, 125.84, 125.64, 117.65, 98.60, 82.02, 81.80, 81.44, 80.89, 78.48, 76.20, 75.90, 75.50, 74.97, 74.08, 73.97, 73.20, 72.85, 72.32, 71.59, 71.46, 69.42, 62.04, 18.26, 18.20, 12.15; HRMS-MALDI (*m/z*): $[M+Na]^+$ calculated for $C_{77}H_{88}O_{12}SiNa$, 1255.5937; Found: 1255.5911.

(2-*O*-Benzoyl-3,4-di-*O*-benzyl-6-*O*-levuniloyl-α-D-mannopyranosyl)-(1→6)-1-*O*-allyl-2-*O*-(2-*O*-acetyl-3,4,6-tri-*O*-benzyl-α-D-mannopyranosyl)-3,4,5-tri-*O*-benzyl- D-*myo*-inositol (**21**): Following the general procedures for glycosylations, a glycosylation of mannosyl phosphate **1** (225 mg, 0.217 mmol) and pseudodisaccharide **20** (238 mg, 0.347 mmol) promoted by TBDMSOTf (85 μL, 0.370 mmol) was carried out in toluene (5 mL) at 0 °C for 1 h. After being quenched by NEt_3 (100 μL), the reaction mixture was concentrated *in vacuo* and purified by flash silica column chromatography (cyclohexane / EtOAc gradient) to obtain the title compound **21** (311.1 mg, 95 %) as a colorless syrup. R_f 0.33 (cyclohexane / EtOAc = 7 : 3); $[\alpha]_D^{r.t.}$= + 9.3 (*c* = 1.0, $CHCl_3$); ^1H NMR (600 MHz, $CDCl_3$) δ 8.11 – 8.05 (m, 2H), 7.60 – 7.54 (m, 1H), 7.49 – 7.42 (m, 2H), 7.38 – 7.09 (m, 40H), 5.96 – 5.85 (m, 1H), 5.65 (dd, *J* = 2.1, 2.9, 1H), 5.53 (d, *J* = 1.8, 1H), 5.42 (dd, *J* = 2.0, 2.9, 1H), 5.23 – 5.17 (m, 1H), 5.12 (d, *J* = 1.8, 1H), 5.11 – 5.09 (m, 1H), 5.00 – 4.68 (m, 8H), 4.65 – 4.25 (m, 9H), 4.20 – 3.78 (m, 12H), 3.51 (dd, *J* = 3.5, 10.8, 1H), 3.36 – 3.23 (m, 4H), 2.74 – 2.42 (m, 4H), 2.08 (s, 3H), 2.07 (s, 3H); ^{13}C NMR (151 MHz, $CDCl_3$) δ = 172.27, 169.89, 165.44, 138.74, 138.54, 138.38, 138.22, 138.10, 138.04, 137.97, 137.86, 133.89, 133.12, 130.12, 129.93, 128.46, 128.38, 128.37, 128.35, 128.27, 128.21, 128.20, 128.17, 128.00, 127.98, 127.92, 127.86, 127.65, 127.57, 127.55, 127.51, 127.50, 127.47, 127.38, 117.95, 99.09, 98.25, 81.32, 81.30, 80.87, 78.78, 78.21, 77.58, 76.24, 75.97, 75.69, 75.03, 74.99, 74.10, 73.62, 73.39, 72.53, 72.12, 71.69, 71.48, 71.34, 69.72, 68.74, 68.66, 68.55, 62.83, 37.98, 29.76, 27.80, 21.09; HRMS-MALDI (*m/z*): $[M+Na]^+$ calculated for $C_{91}H_{96}O_{20}Na$, 1531.6387; Found: 1531.6372.

(2-*O*-Benzoyl-3,4-di-*O*-benzyl-α-D-mannopyranosyl)-(1→6)-1-*O*-allyl-2-*O*-(2-*O*-acetyl-3,4,6-tri-*O*-benzyl-α-D-mannopyranosyl)-3,4,5-tri-*O*-benzyl-D-*myo*-inositol (8): A solution of trisaccharide 21 (840 mg, 0.556 mmol) and hydrazine acetate (256 mg, 2.782 mmol) in a mixture of CH_2Cl_2 (30 mL) and

MeOH (15 mL) was stirred at rt. After 4 h, although there was a small amount of the starting material 21 left, the reaction was quenched by adding pyridine (15 mL) and acetone (15 mL) in order to avoid the reduction of the allyl group on the desired product by hydrazine acetate. The reaction mixture was concentrated *in vacuo* and purified by flash silica column chromatography (cyclohexane / EtOAc) to obtain the title compound 8 (698.9 mg, 89 %) as a colorless syrup. R_f 0.40 (cyclohexane / EtOAc = 7 : 3); $[\alpha]_D^{r.t.}$= + 14.1 (*c* = 1.0, $CHCl_3$); ^{1}H NMR (600 MHz, $CDCl_3$) δ 8.08 – 8.03 (m, 2H), 7.59 – 7.53 (m, 1H), 7.48 – 7.41 (m, 2H), 7.38 – 7.08 (m, 40H), 5.95 – 5.83 (m, 1H), 5.65 (dd, *J* = 1.9, 3.1, 1H), 5.54 (d, *J* = 1.8, 1H), 5.46 (dd, *J* = 1.9, 3.0, 1H), 5.22 – 5.18 (m, 1H), 5.17 (d, *J* = 1.7, 1H), 5.09 (dd, *J* = 1.4, 10.4, 1H), 4.97 – 4.51 (m, 14H), 4.43 – 4.26 (m, 3H), 4.18 – 3.76 (m, 10H), 3.55 – 3.23 (m, 7H), 2.08 (s, 3H), 1.86 (brs, 1H); ^{13}C NMR (151 MHz, $CDCl_3$) δ 170.07, 165.57, 138.80, 138.70, 138.44, 138.20, 138.17, 137.96, 137.92, 133.86, 133.07, 130.03, 129.94, 128.43, 128.40, 128.36, 128.34, 128.24, 128.23, 128.21, 128.19, 127.99, 127.94, 127.92, 127.88, 127.69, 127.53, 127.49, 127.43, 127.37, 117.91, 98.76, 98.20, 81.45, 81.41, 81.10, 78.78, 77.98, 77.42, 77.33, 76.14, 75.75, 75.69, 75.17, 74.98, 74.12, 73.42, 72.51, 71.85, 71.60, 71.56, 71.46, 71.41, 71.24, 69.07, 68.62, 68.59, 61.49, 21.11; HRMS-MALDI (*m/z*): $[M+Na]^+$ calculated for $C_{86}H_{90}O_{18}Na$, 1433.6019; Found: 1433.5996.

1-*O*-Allyl-6-*O*-acetyl-3,4,5-tri-*O*-benzyl-D-*myo*-inositol (**23**): A solution of inositol **22** (255 mg, 0.520 mmol) and DMAP (63.52 mg, 0.520 mmol) in pyridine (13 mL) was cooled to 0 °C. Acetyl chloride (199 μL, 2.782 mmol) was added dropwise to the reaction solution over a period of 10 min. The reaction solution was stirred at 0 °C and quenched by adding water (1 mL) dropwise. The reaction mixture was concentrated *in vacuo* and purified by flash silica column chromatography (cyclohexane / EtOAc) to obtain the title compound **23** (194 mg, 70 %) as a colorless syrup. R_f 0.30 (cyclohexane / EtOAc = 7 : 3); $[\alpha]_D^{r.t.}$ = – 9.3 (*c* = 1.0, $CHCl_3$); ^{1}H NMR (300 MHz, $CDCl_3$) δ 7.39 – 7.23 (m, 15H), 5.82 (ddd, *J* = 5.7, 10.8, 16.0, 1H), 5.46 (dd, *J* = 9.9, 9.9 1H), 5.26 (dd, *J* = 1.48, 1.49, 1H), 5.21 – 5.15 (m, 1H), 4.93 – 4.60 (m, 6H), 4.24 – 4.19 (m, 1H), 4.15 – 4.05 (m, 1H), 4.00 – 3.94 (m, 1H), 3.46 – 3.40

(m, 2H), 3.24 (dd, *J* = 2.7, 9.9, 1H), 2.49 (s, 1H), 1.95 (s, 3H); HRMS-MALDI (*m/z*): $[M+Na]^+$ calculated for $C_{32}H_{36}O_7Na$, 555.2369; Found: 555.2371.

1-*O*-Allyl-2,3,4,5,6-penta-*O*-benzyl-D-*myo*-inositol (**24**): A solution of inositol **22** (100 mg, 0.204 mmol) and benzyl bromide (136 μL, 1.142 mmol) in DMF (4 mL) was cooled to 0 °C. NaH (60% in mineral oil, 46 mg, 1.142 mmol) was added to the reaction solution. The reaction was allowed to warm to rt. After 12 h at rt, the reaction was quenched by carefully adding MeOH (1 mL). The reaction mixture was diluted with EtOAc (20 mL), washed with water (2x) and brine, dried over $MgSO_4$ and concentrated *in vacuo*. The crude product was purified by flash silica column chromatography (cyclohexane / EtOAc) to obtain the title compound **24** in quantitative yield as a colorless syrup. NMR spectra are the same as reported in literature.[2]

Allyl (2-*O*-acetyl-3,4,6-tri-*O*-benzyl-α-D-mannopyranosyl)-(1→6)-2-*O*-benzoyl-3,4-di-*O*-benzyl-α-D-mannopyranoside (25): Following the general procedures for glycosylations, a glycosylation of mannosyl phosphate **1** (224.0 mg, 0.327 mmol) and mannose **5** (150.0 mg, 0.297 mmol) promoted by TMSOTf (63 μL, 0.327 mmol) was carried out in CH_2Cl_2 (5 mL) at - 10 °C for 1 h. After being quenched by NEt_3 (100 μL), the reaction mixture was concentrated *in vacuo* and purified by flash silica column chromatography (cyclohexane / EtOAc) to obtain the title compound **25** as a colorless syrup in quantitative yield. NMR spectra are the same as reported in literature.[3]

Allyl (2-*O*-acetyl-3,4,6-tri-*O*-benzyl-α-D-mannopyranosyl)-(1→2)-(3,4,6-tri-*O*-benzyl-α-D-mannopyranosyl)-(1→6)-2-*O*-benzoyl-3,4-di-*O*-benzyl-α-D-mannopyrano- side (26): Following the general procedures for glycosylations, a glycosylation of mannosyl phosphate **1** (384.3 mg, 0.561 mmol) and dimannose **25a** (R^1 = H, R^2 = All, 477.7 mg, 0.510 mmol) promoted by TMSOTf (108 μL, 0.561 mmol) was carried out in toluene (8 mL) at - 40 °C for 2 h. After being quenched by NEt_3 (160 μL), the reaction mixture was concentrated *in vacuo* and purified by flash silica column chromatography (cyclohexane / EtOAc) to obtain the title compound **26** (682.6 mg, 95 %) as a colorless syrup. NMR spectra are the same as reported in literature.[4]

Allyl (2-*O*-acetyl-3,4,6-tri-*O*-benzyl-α-D-mannopyranosyl)-(1→2)-(3,4,6-tri-*O*-benzyl-α-D-mannopyranosyl)-(1→2)-(3,4,6-tri-*O*-benzyl-α-D-mannopyranosyl)-(1→6)-2-*O*-benzoyl-3,4-di-*O*-benzyl-α-D-mannopyranoside (27): Following the general procedures for glycosylations, a glycosylation of mannosyl phosphate **1** (172.5 mg, 0.252 mmol) and trimannose **26a** (R^3 = H, R^4 = All, 230.0 mg, 0.168 mmol) promoted by TMSOTf (48 μL, 0.252 mmol) was carried out in toluene (2 mL) at - 40 °C for 2 h. After being quenched by NEt_3 (100 μL), the reaction mixture was concentrated *in vacuo* and purified by flash silica column chromatography (cyclohexane / EtOAc) to obtain the title compound **27** (296.1 mg, 96 %) as a colorless syrup. NMR spectra are the same as reported in literature.[4]

General Procedures to Prepare Oligomannosyl Trichloroacetimidates (**2, 3, and 4**): To a solution of $Pd(OAc)_2$ (0.2 equiv.) in MeOH (400 μL), PPh_3 (0.6 equiv.) was added at rt. The reaction mixture was stirred at rt for 6 h and Et_2NH was added (0.2 equiv.). The reaction mixture was further stirred at rt for 15 min and oligomannose **25**, **26** or **27** (1 equiv., ~ 200 mg) in CH_2Cl_2 (~ 2 mL) was added via syringe in one portion. The reaction solution was stirred at rt for 12 h, concentrated *in vacuo*, and purified by flash silica column chromatography (cyclohexane / EtOAc) to obtain the hemiacetals **28** (77 %), **29** (95 %), or **30** (83 %) as colorless syrup. A solution of an hemiacetal (**28**, **29** or **30, ~** 0.2 mmol) and trichloroacetonitrile (~ 2.0 mmol) in CH_2Cl_2 (~ 2 mL) was cooled to 0 °C and added NaH (~ 0.02 mmol). The reaction mixture was stirred at 0 °C for 10 min and at rt for 1 h before concentrated *in vacuo* at 33°C. The reaction crude was coevaporated with toluene and purified by flash silica column chromatography (cyclohexane / EtOAc) to obtain the title compounds **2** (85 %), **3** (86 %), or **4** (89 %) as colorless syrup.

(2-*O*-Acetyl-3,4,6-tri-*O*-benzyl-α-D-mannopyranosyl)-(1→2)-(3,4,6-tri-*O*-benzyl-α-D-mannopyranosyl)-(1→6)-2-*O*-benzoyl-3,4-di-*O*-benzyl-α-D-mannopyranosyl trichloroacetimidate (**3**): R_f 0.53 (cyclohexane / EtOAc = 7 : 3); $[\alpha]_D^{r.t.}$= + 19.8 (*c* = 1.0, $CHCl_3$); ^{1}H NMR (300 MHz, $CDCl_3$) δ 8.73 (s, 1H), 8.18 – 8.07 (m, 2H), 7.58 – 7.09 (m, 43H), 6.39 (d, *J* = 1.8, 1H), 5.81 – 5.72 (m, 1H), 5.60 – 5.52 (m, 1H), 5.11 (d, *J* = 1.4, 1H), 5.01 (d, *J* = 1.4, 1H), 4.96 – 4.31 (m, 16H), 4.23 – 3.53 (m, 16H), 2.15 (s, 3H); ^{13}C NMR (75 MHz, $CDCl_3$) δ 170.08, 165.37, 159.56, 138.49, 138.44, 138.39, 138.15, 138.09, 137.94, 137.89, 137.31, 133.44, 129.80, 129.44, 128.52, 128.30, 128.24, 128.16, 128.08, 127.93, 127.78, 127.71, 127.65, 127.56, 127.43, 127.40, 127.31, 127.25, 99.51, 98.72, 95.03, 90.67, 79.51, 78.05, 77.69, 75.22, 74.98, 74.57, 74.37, 74.14, 73.57, 73.42, 73.30, 73.05, 71.81, 68.93, 68.70, 67.72, 65.84, 21.11; HRMS-MALDI (*m/z*): $[M+Na]^+$ calculated for $C_{85}H_{86}ClNO_{18}Na$, 1433.6019; Found: 1433.5996.

1-*O*-Allyl-2-*O*-(2,3,4,6-tetra-*O*-benzyl-α-D-mannopyranosyl)-3,4,5,6-tetra-*O*-benzyl-D-*myo*-inositol (**31**): Following the general procedures for glycosylations, a glycosylation of mannosyl phosphate **1** (273.8 mg, 0.400 mmol) and inositol **23** (194.0 mg, 0.364 mmol) promoted by TMSOTf (76 μL, 0.400 mmol) was carried out in Et_2O (8 mL) at - 40 °C for 1.5 h. After being quenched by NEt_3 (150 μL), the reaction mixture was concentrated *in vacuo* and purified by flash silica column chromatography (cyclohexane / EtOAc) to obtain 1-*O*-allyl-2-*O*-(2-*O*-acetyl-3,4,6-tri-*O*-benzyl-α-D-mannopyranosyl)-3,4,5-tri-*O*-benzyl-6-*O*-acetyl-D-*myo*-inositol **31*p*** (266.0 mg, 70 %) as a colorless syrup. $[\alpha]_D^{r.t.}$= + 14.5 (*c* = 1.0, $CHCl_3$); ^{1}H NMR (300 MHz, $CDCl_3$) δ 7.49 – 7.07 (m, 30H), 5.93 – 5.70 (m, 1H), 5.57 (dd, *J* = 2.1, 2.7, 1H), 5.46 (t, *J* = 10.0, 1H), 5.28 – 5.21 (m, 2H), 5.21 – 5.11 (m, 2H), 4.93 – 4.70 (m, 6H), 4.68 – 4.53 (m, 4H), 4.47 – 4.23 (m, 3H), 4.21 – 4.04 (m, 2H), 4.03 – 3.84 (m, 4H), 3.59 – 3.18 (m, 5H), 2.17 – 2.10 (m, 3H), 1.97 (s, 3H); ^{13}C NMR (75 MHz, $CDCl_3$) δ 169.68, 169.61, 138.57, 138.29, 138.21, 138.06, 137.89, 137.84, 134.02, 128.48, 128.30, 128.25, 128.10, 128.03, 127.84, 127.77, 127.55, 127.41, 127.35, 127.18, 117.00, 99.09, 81.18, 81.12, 78.62, 76.62, 75.80, 75.55, 74.99, 74.01, 73.35, 72.93, 72.69, 72.42, 71.45, 71.37, 68.48, 21.23, 21.13; HRMS-MALDI (*m/z*): $[M+Na]^+$ calculated for $C_{61}H_{66}O_{13}Na$, 1029.4396; Found: 1029.4400

To a solution of pseudodisaccharide **31*p*** (266 mg, 0.288 mmol) in a mixture of CH_2Cl_2 (1 mL) and MeOH (3 mL), a solution of NaOMe in MeOH (1.150 μL of 0.288 M, 0.180 mmol, freshly prepared from Na(s) and MeOH) was added at rt. The reaction was stirred at rt for 2 d, concentrated *in vacuo*, and filtered through a short plug of silica gel to obtain a yellow syrup. A solution of this crude product and BnBr (121 μL, 1.018 mmol) in DMF (8 mL) was cooled to 0 °C and NaH (60% in mineral oil, 40.7 mg, 1.018 mmol) was added. The reaction mixture was allowed to warm to rt. After 5 h at rt, the reaction was quenched by carefully adding MeOH (1 mL) dropwise. The reaction mixture was diluted with EtOAc (20 mL), washed with water (2x) and brine, dried over $MgSO_4$, and concentrated *in vacuo*. The crude product was purified by flash silica column chromatography (cyclohexane / EtOAc) to obtain the title compound **31** in quantitative yield (2 steps) as a colorless syrup. NMR spectra are the same as reported in literature. [26]

(2,3,4,6-Tetra-*O*-benzyl-α-D-mannopyranosyl)-(1→6)-1-*O*-allyl-2-*O*-(2,3,4,6-tetra-*O*-benzyl-α-D-mannopyranosyl)-3,4,5-tri-*O*-benzyl-D-*myo*-inositol (**32**): To a solution of pseudotrisaccharide **8** (59.7 mg, 0.042 mmol) in a mixture of THF (1 mL) and MeOH (1 mL) a solution of NaOMe in MeOH (168 μL of 0.250 M, 0.042 mmol, freshly prepared from Na(s) and MeOH) was added at rt. The reaction was stirred at rt for 3 d and neutralized with acid resin (methanol washed Amberlite IR-120). The resin was filtered off and the reaction solution was concentrated *in vacuo* and placed under high vacuum for 4 h. A solution of this crude product and BnBr (20 μL, 0.168 mmol) in DMF (4 mL) was cooled to 0 °C and NaH (60% in mineral oil, 7 mg, 0.168 mmol) was added. The reaction mixture was allowed to warm to rt. After 12 h at rt, the reaction mixture was transferred to a separatory funnel and carefully quenched by minimum amount of MeOH and water (10 mL). The reaction mixture was extracted with EtOAc (3 x 10 mL). The combined organic layer was washed with brine, dried over Na_2SO_4, and concentrated *in* *vacuo*. The crude product was purified by flash silica column chromatography (cyclohexane / EtOAc) to obtain the title compound **32** (58 mg, 90 %, 2 steps) as a colorless syrup. R_f 0.27 (hexanes / EtOAc = 3 : 1); $[\alpha]_D^{r.t.}$= + 26.4 (*c* = 1.8, $CHCl_3$); ^{1}H NMR (500 MHz, $CDCl_3$) δ 7.41 – 6.96 (m, 55H), 5.70 (ddd, *J* = 5.5, 10.6, 22.7, 1H), 5.48 (d, *J* = 1.7, 1H), 5.22 (d, *J* = 1.4, 1H), 5.21 – 5.16 (m, 1H), 5.08 – 5.04 (m, 1H), 4.93 – 4.25 (m, 22H), 4.20 – 3.72 (m, 13H), 3.49 (dd, *J* = 3.7, 10.7, 1H), 3.42 – 3.07 (m, 6H); ^{13}C NMR (126 MHz, $CDCl_3$) δ 139.36, 139.14, 139.05, 138.98, 138.83, 138.71, 138.61, 138.61, 138.58, 138.30, 138.30, 134.17, 128.66, 128.55, 128.52, 128.51, 128.42, 128.41, 128.39, 128.37, 128.33, 128.31, 128.27, 128.25, 128.18, 128.09, 128.04, 128.03, 128.02, 127.82, 127.79, 127.71, 127.68, 127.65, 127.63, 127.59, 127.53, 127.46, 127.44, 117.99, 98.95, 98.91, 82.01, 81.72, 81.57, 80.41, 79.19, 78.97, 76.19, 75.86, 75.21, 75.14, 75.04, 74.85, 74.77, 73.58, 73.46, 72.65, 72.60, 72.46, 72.26, 72.16, 72.07, 71.79, 71.28, 71.00, 69.19, 68.84; HRMS-MALDI (*m/z*): $[M+Na]^+$ calculated for $C_{98}H_{102}O_{16}Na$, 1557.7030; Found: 1557.7030.

(2,3,4,6-Tetra-*O*-benzyl-α-D-mannopyranosyl)-(1→6)-(2,3,4,-tri-*O*-benzyl-α-D-mannopyranosyl)-(1→6)-1-*O*-allyl-2-*O*-(2,3,4,6-tetra-*O*-benzyl-α-D-mannopyrano- syl)-3,4,5-tri-*O*-benzyl-D-*myo*-inositol (**33**): Following the general procedures for glycosylations, a glycosylation of mannosyl phosphate **1** (54.0, 0.079 mmol) and pseudotrisaccharide **8** (70.0 mg, 0.049 mmol) promoted by TMSOTf (12 μL, 0.064 mmol) was carried out in CH_2Cl_2 (3 mL) at - 10 °C for 1 h. After being quenched by NEt_3 (40 μL), the reaction mixture was concentrated *in vacuo*. To a solution of this crude product in THF (2 mL), a solution of NaOMe in MeOH (2.00 mL of 0.250 M, 0.500 mmol, freshly prepared from Na(s) and MeOH) was added at rt. The reaction was stirred at 50 °C for 12 h and neutralized with acid resin (methanol washed Amberlite IR-120). The reaction mixture was filtered through a short plug of silica gel, concentrated *in vacuo* and placed under high vacuum for 4 h. A solution of this crude product and BnBr (59 μL, 0.496 mmol) in DMF (4 mL) was cooled to 0 °C and NaH (60% in mineral oil, 20 mg, 0.496 mmol) was added. The reaction mixture was allowed to warm to rt. After 12 h at rt, the reaction mixture was transferred to a separatory funnel and carefully quenched by minimum amount of MeOH and water (10 mL). The reaction mixture was extracted with EtOAc (3 x 10 mL). The combined organic layer was washed with brine, dried over Na_2SO_4, and concentrated *in vacuo*. The crude product was purified by general procedures for glycosylations flash silica column chromatography (cyclohexane / EtOAc) to obtain the title compound **33** (86.5 mg, 89 %, 3 steps) as a colorless syrup. R_f 0.27 (cyclohexane / EtOAc = 4 : 1); $[\alpha]_D^{r.t.}$= + 35.6 (c = 1.0, $CHCl_3$); ^{1}H NMR (300 MHz, $CDCl_3$) δ 7.50 – 7.09 (m, 70H), 5.77 (ddd, *J* = 5.4, 10.6, 22.5, 1H), 5.50 (d, *J* = 1.1, 1H), 5.29 (brs, 1.5H), 5.23 (d, *J* = 1.3, 0.5H), 5.15 (d, *J* = 0.9, 0.5H), 5.11 (brs, 1.5H), 5.08 – 4.76 (m, 7H), 4.76 – 4.26 (m, 22H), 4.26 – 3.80 (m, 15H), 3.62 – 3.13 (m, 10H); ^{13}C NMR (126 MHz, $CDCl_3$) δ 139.32, 139.17, 139.14, 138.96, 138.93, 138.88, 138.85, 138.65, 138.63, 138.62, 138.28, 138.23, 134.19, 128.74, 128.67, 128.64, 128.58, 128.57, 128.53, 128.48, 128.44, 128.42, 128.34, 128.33, 128.29, 128.22, 128.13, 128.05, 128.01, 127.97, 127.92, 127.89, 127.76, 127.74, 127.70, 127.67, 127.65, 127.62, 127.59, 127.54, 127.52, 127.48, 127.43, 127.31, 117.94, 99.12, 98.88, 98.18, 81.90, 81.64, 81.46, 80.75, 79.57, 79.22, 78.98, 76.95, 76.10, 76.01, 75.90, 75.28, 75.24, 75.12, 75.00, 74.93, 74.86, 74.81, 74.58, 73.58, 73.52, 72.88, 72.78, 72.43, 72.41, 72.14, 71.89, 71.57, 71.20, 70.53, 69.24, 69.08, 65.47; ESI-MS (*m/z*): $[M+NH_4]^{1+}$ calculated for $C_{125}H_{134}NO_{21}$, 1984.9; Found: 1984.4 as a dominant peak.

(2,3,4,6-Tetra-*O*-benzyl-α-D-mannopyranosyl)-(1→6)-(2,3,4,-tri-*O*-benzyl-α-D-mannopyranosyl)-(1→6)-(2,3,4,-tri-*O*-benzyl-α-D-mannopyranosyl)-(1→6)-1-*O*-allyl-2-*O*-(2,3,4,6-tetra-*O*-benzyl-α-D-mannopyranosyl)-3,4,5-tri-*O*-benzyl-D-*myo*-inositol (**34**): Following the general procedures for glycosylations, a glycosylation of mannosyl imidate **2** (102.0, 0.094 mmol) and pseudotrisaccharide **8** (110.0 mg, 0.078 mmol) promoted by TMSOTf (1.8 µL, 0.008 mmol) was carried out in CH_2Cl_2 (3 mL) at - 10 °C for 1 h. After being quenched by NEt_3 (10 µL), the reaction mixture was concentrated *in vacuo*. To a solution of this crude product in THF (2 mL), a solution of NaOMe in

MeOH (3.1 mL of 0.250 M, 0.780 mmol, freshly prepared from Na(s) and MeOH) was added at rt. The reaction was stirred at 60 °C for 18 h and neutralized with acid resin (methanol washed Amberlite IR-120). The reaction mixture was filtered through a short plug of silica gel, concentrated *in vacuo* and placed under high vacuum for 4 h. A solution of this crude product and BnBr (52 μL, 0.441 mmol) in DMF (4 mL) was cooled to 0 °C and NaH (60% in mineral oil, 23.5 mg, 0.588 mmol) was added. The reaction mixture was allowed to warm to rt. After 12 h at rt, the reaction mixture was transferred to a separatory funnel and carefully quenched by minimum amount of MeOH and water (10 mL). The reaction mixture was extracted with EtOAc (3 x 10 mL). The combined organic layer was washed with brine, dried over Na_2SO_4, and concentrated *in vacuo*. The crude product was purified by flash silica column chromatography (cyclohexane / EtOAc) to obtain the title compound **34** (166.4 mg, 89 %, 3 steps) as a colorless syrup. R_f 0.30 (cyclohexane / EtOAc = 7 : 3); $[\alpha]_D^{r.t.}$= + 38.7 (*c* = 1.0, $CHCl_3$); ^1H NMR (500 MHz, $CDCl_3$) δ 7.47 – 7.05 (m, 85H), 5.82 – 5.68 (m, 1H), 5.45 (brs, 1H), 5.24 (brs, 1.5H), 5.21 (brs, 0.5H), 5.12 (brs, 0.5H), 5.09 (brs, 1.5H), 5.07 – 4.76 (m, 9H), 4.75 – 4.30 (m, 27H), 4.22 – 3.79 (m, 18H), 3.69 – 3.48 (m, 5H), 3.46 – 3.09 (m, 8H); ^{13}C NMR (126 MHz, $CDCl_3$) δ 139.27, 139.22, 139.19, 139.17, 139.16, 138.94, 138.93, 138.90, 138.89, 138.80, 138.72, 138.69, 138.64, 138.62, 138.55, 138.35, 138.32, 134.25, 128.84, 128.64, 128.60, 128.57, 128.53, 128.51, 128.49, 128.49, 128.46, 128.43, 128.41, 128.38, 128.34, 128.33, 128.30, 128.23, 128.11, 128.07, 128.02, 127.98, 127.95, 127.87, 127.77, 127.76, 127.73, 127.72, 127.70, 127.67, 127.60, 127.56, 127.51, 127.43, 127.37, 127.29, 117.97, 99.34, 99.02, 98.72, 98.55, 81.88, 81.65, 81.50, 80.93, 79.84, 79.45, 79.34, 79.03, 77.63, 77.38, 77.28, 77.12, 76.09, 76.03, 75.97, 75.61, 75.29, 75.24, 75.19, 75.16, 74.99, 74.95, 74.94, 74.58, 74.15, 73.63, 73.57, 72.95, 72.89, 72.84, 72.58, 72.50, 72.46, 72.31, 72.23, 72.19, 71.86, 71.66, 71.63, 71.46, 71.26, 70.64, 69.42, 69.29, 65.88, 65.82; HRMS-MALDI (*m/z*): $[M+Na]^+$ calculated for $C_{152}H_{158}O_{26}Na$, 2422.0934; Found: 2422.0995.

(2,3,4,6-Tetra-*O*-benzyl-α-D-mannopyranosyl)-(1→2)-(3,4,6-tri-*O*-benzyl-α-D-mannopyranosyl)-(1→6)-(2,3,4,-tri-*O*-benzyl-α-D-mannopyranosyl)-(1→6)-(2,3,4,-tri-*O*-benzyl-α-D-mannopyranosyl)-(1→6)-1-*O*-allyl-2-*O*-(2,3,4,6-tetra-*O*-benzyl-α-D-mannopyranosyl)-3,4,5-tri-*O*-benzyl-D-*myo*-inositol) (**35**): Following the general procedures for glycosylations, a glycosylation of mannosyl imidate **3** (128.0 mg, 0.085 mmol) and pseudotrisaccharide **8** (100.0 mg, 0.071 mmol) promoted by TMSOTf (1.6 μL, 0.007 mmol) was carried out in CH_2Cl_2 (4 mL) at - 10 °C for 1 h. After being quenched by NEt_3 (10 μL), the reaction mixture was concentrated *in vacuo*. To a solution of this crude product in THF (2 mL), a solution of NaOMe in MeOH (2.8 mL of 0.250 M, 0.710 mmol, freshly prepared from Na(s) and MeOH) was added at rt. The reaction was stirred at 60 °C for 12 h and neutralized with acid resin (methanol washed Amberlite IR-120). The reaction mixture was filtered through a short plug of silica gel, concentrated *in vacuo* and placed under high vacuum for 4 h. A solution of this crude product and BnBr (84 μL, 0.709 mmol) in DMF (4 mL) was cooled to 0 °C and NaH (60% in mineral oil, 28.3 mg, 0.709 mmol) was added. The reaction mixture was allowed to warm to rt. After 16 h at rt, the reaction mixture was transferred to a separatory funnel and carefully quenched by minimum amount of MeOH and water (10 mL). The reaction mixture was extracted with EtOAc (3 x 10 mL). The combined organic layer was washed with brine, dried over Na_2SO_4, and concentrated *in vacuo*. The crude product was purified by flash silica column chromatography (cyclohexane / EtOAc) to obtain the title compound **35** (145.0 mg, 73 %, 3 steps) as a colorless syrup. R_f 0.56 (cyclohexane / EtOAc = 7 : 3); $[\alpha]_D^{r.t.}$= + 38.5 (*c* = 1.0, $CHCl_3$); ^1H NMR (500 MHz, $CDCl_3$) δ 7.50 – 7.06 (m, 100H), 5.77 (ddd, *J* = 5.5, 10.6, 22.6, 1H), 5.49 (d, *J* = 1.4, 1H), 5.29 – 5.25 (m, 1.5H), 5.25 – 5.21 (m, 1.5H), 5.15 – 5.10 (m, 1H), 5.08 – 4.87 (m, 8H), 4.86 – 4.77 (m, 3H), 4.76 – 4.33 (m, 32H), 4.25 – 4.03 (m, 6H), 4.03 – 3.82 (m, 16H), 3.82 – 3.53 (m, 4H), 3.53 – 3.11 (m, 11H); ^{13}C NMR (126 MHz, $CDCl_3$) δ 139.33, 139.31, 139.18, 139.16, 139.13, 139.08, 139.02, 138.97, 138.93, 138.89, 138.86, 138.84, 138.81, 138.73, 138.70, 138.65, 138.42, 138.35, 138.34, 134.27, 128.84, 128.71, 128.68, 128.67, 128.65, 128.60, 128.55, 128.52, 128.50, 128.45, 128.43, 128.43, 128.38, 128.35, 128.25, 128.16, 128.12, 128.11, 128.09, 128.04, 128.01, 127.99, 127.97, 127.88, 127.79, 127.78, 127.73, 127.72, 127.69, 127.67, 127.62, 127.55, 127.42, 127.30, 127.19, 127.14, 117.98, 99.62, 99.56, 99.33, 99.06, 98.56, 81.87, 81.69, 81.57, 80.98, 80.22, 79.99, 79.78, 79.41, 79.03, 77.27, 76.15, 76.00, 75.62, 75.31, 75.25, 75.15, 74.94, 74.88, 74.81, 74.69, 74.55, 74.34, 74.07, 73.64, 73.61, 73.53, 72.95, 72.92, 72.62, 72.60, 72.52, 72.42, 72.41, 72.33, 72.29, 72.23, 72.17, 72.08, 71.56, 71.43, 71.28, 71.21, 70.67, 69.39, 69.31, 69.19, 66.30, 66.21; HRMS-MALDI (*m/z*): $[M+Na]^+$ calculated for $C_{179}H_{186}O_{31}Na$, 2854.2870; Found: 2854.2804.

(2,3,4,6-Tetra-*O*-benzyl-α-D-mannopyranosyl)-(1→2)-(3,4,6-tri-*O*-benzyl-α-D-mannopyranosyl)-(1→2)-(3,4,6-tri-*O*-benzyl-α-D-mannopyranosyl)-(1→6)-(2,3,4,-tri-*O*-benzyl-α-D-mannopyranosyl)-(1→6)-(2,3,4,-tri-*O*-benzyl-α-D-mannopyranosyl)-(1→6)-1-*O*-allyl-2-*O*-(2,3,4,6-tetra-*O*-benzyl-α-D-mannopyranosyl)-3,4,5-tri-*O*-benzyl-D-*myo*-inositol) (**36**): Following the general procedures for glycosylations, a glycosylation of mannosyl imidate **4** (164.0 mg, 0.084 mmol) and pseudotrisaccharide **8** (99.0 mg, 0.070 mmol) promoted by TMSOTf (1.6 μL, 0.007 mmol) was carried out in CH_2Cl_2 (6 mL) at 0 °C for 1 h. After being quenched by NEt_3 (10 μL), the reaction mixture was concentrated *in vacuo* and purified by recycling size exclusion HPLC (eluent = 100% $CHCl_3$) to obtain (2-*O*-acetyl-3,4,6-tri-*O*-benzyl-α-D-mannopyranosyl)-(1→2)-(3,4,6-tri-*O*-benzyl-α-D-mannopyranosyl)-(1→2)-(3,4,6-tri-*O*-benzyl-α-D-mannopyranosyl)-(1→6)-(2-*O*-benzoyl-3,4,-di-*O*-benzyl-α-D-mannopyranosyl)-(1→6)-(2-*O*-benzoyl-3,4,-di-*O*-benzyl-α-D-mannopyranosyl)-(1→6)-1-*O*-allyl-2-*O*-(2-*O*-acetyl-3,4,6-tri-*O*-benzyl-α-D-mannopyranosyl)-3,4,5-tri-*O*-benzyl-D-*myo*-inositol) **36*p*** (143.0 mg, 64 %) as a colorless syrup. The remaining pseudotrisaccharide starting material **8** was also recovered (27.5 mg, 28%) as a colorless syrup. R_f 0.44 (cyclohexane / EtOAc = 7 : 3); $[\alpha]_D^{r.t}$ = + 25.9 (*c* = 1.0, $CHCl_3$); ^1H NMR (600 MHz, $CDCl_3$) δ 8.17 – 8.01 (m, 4H), 7.50 – 6.87 (m, 101H), 5.90 (ddd, *J* = 5.7, 10.5, 22.8, 1H), 5.76 (dd, *J* = 2.0, 2.9, 1H), 5.74 (dd, *J* = 2.1, 2.9, 1H), 5.56 (dd, *J* = 1.9, 3.2, 1H), 5.54 (d, *J* = 1.7, 1H), 5.42 (dd, *J* = 2.0, 3.0, 1H), 5.26 (d, *J* = 1.6, 1H), 5.24 – 5.19 (m, 1H), 5.16 (d, *J* = 1.6, 1H), 5.10 (s, 1.5H), 5.09 – 5.08 (m, 0.5H), 5.05 – 4.68 (m, 15H), 4.68 – 4.61 (m, 3H), 4.60 – 4.49 (m, 10H), 4.48 – 4.21 (m, 12H), 4.21 – 4.07 (m, 6H), 4.07 – 3.85 (m, 14H), 3.85 – 3.75 (m, 4H), 3.63 (m, 3H), 3.46 (m, 4H), 3.40 – 3.26 (m, 7H), 3.23 – 3.12 (m, 2H), 2.11 (s, 3H), 2.05 (s, 3H); ^{13}C NMR (151 MHz, $CDCl_3$) δ 170.09, 169.80, 165.60, 165.29, 138.88, 138.74, 138.73, 138.66, 138.64, 138.61, 138.55, 138.49, 138.42, 138.34, 138.21, 138.17, 138.11, 138.08, 138.03, 137.97, 137.92, 137.77, 137.58, 133.83, 133.17, 130.16, 130.11, 129.86, 129.81, 128.55, 128.49, 128.44, 128.43, 128.40, 128.38, 128.37, 128.36, 128.33, 128.30, 128.27, 128.25, 128.24, 128.21, 128.18, 128.13, 128.09, 128.05, 127.96, 127.90, 127.86, 127.85, 127.77, 127.75, 127.74, 127.67, 127.61, 127.59, 127.57, 127.52, 127.51, 127.48, 127.45, 127.39, 127.36, 127.34, 127.09, 127.01, 126.91, 126.78, 117.94, 100.39, 99.39, 99.20, 98.89, 98.85, 98.37, 81.44, 81.28, 80.78, 79.17, 78.84, 78.76, 78.35, 77.47, 75.82, 75.72, 75.14, 75.04, 75.00, 74.96, 74.76, 74.75, 74.60, 74.53, 74.50, 74.12, 74.00, 73.97, 73.40, 73.39, 73.28, 73.24, 72.63, 72.44, 72.21, 72.13, 72.03, 71.89, 71.65, 71.51, 71.46, 71.44, 71.31, 71.11, 70.71, 70.46, 68.96, 68.79, 68.70, 68.64, 68.62, 68.60, 68.51, 68.31, 66.03, 65.51, 21.16, 21.04; ESI-MS (*m/z*): $[M+2(NH_4)]^{2+}$ calculated for $C_{196}H_{210}N_2O_{40}{}^{2+}$, 1615.7; Found: 1615.5 as a dominant peak.

To a solution of pseudoheptasaccharide **36*p*** (120 mg, 0.037 mmol) in THF (3 mL) a solution of NaOMe in MeOH (1.50 mL of 0.250 M, 0.375 mmol, freshly prepared from Na(s) and MeOH) was added at rt. The reaction was stirred at 50 °C for 18 h and neutralized with acid resin (methanol washed Amberlite IR-120). The reaction mixture was filtered through a short plug of silica gel, concentrated *in vacuo* and placed under high vacuum for 4 h. A solution of this crude product and BnBr (44.5 μL, 0.375 mmol) in DMF (4 mL) was cooled to 0 °C and NaH (60% in mineral oil, 15.0 mg, 0.375 mmol) was added. The reaction mixture was allowed to warm to rt. After 18 h at rt, the reaction mixture was transferred to a separatory funnel and carefully quenched by minimum amount of MeOH and water (10 mL). The reaction mixture was extracted with EtOAc (3 x 10 mL). The combined organic layer was washed with brine, dried over Na_2SO_4, and concentrated *in vacuo*. The crude product was purified by flash silica column chromatography (cyclohexane / EtOAc) to obtain the title compound **36** (118.7 mg, 97 %, 2 steps) as a colorless syrup. R_f 0.34 (cyclohexane / EtOAc = 7 : 3); $[\alpha]_D^{r.t.}$= + 35.0 (*c* = 1.0, $CHCl_3$); ^1H NMR (300 MHz, $CDCl_3$) δ 7.46 – 7.03 (m, 115H), 5.49 (brs, 1H), 5.29 – 5.17 (m, 3H), 5.04 – 4.78 (m, 9H), 4.78 – 3.99 (m, 46H), 3.99 – 3.50 (m, 29H), 3.49 – 3.15 (m, 6H), 1.70 (brs, 1H); ^{13}C NMR (75 MHz, $CDCl_3$) δ 138.69, 138.62, 138.60, 138.51, 138.47, 138.36, 138.29, 138.28, 138.25, 138.22, 138.06, 137.98, 137.91, 137.80, 128.38, 128.31, 128.21, 128.17, 128.12, 128.08, 128.01, 127.99, 127.91, 127.81, 127.79, 127.71, 127.66, 127.63, 127.57, 127.54, 127.45, 127.36, 127.32, 127.28, 127.21, 127.18, 127.12, 127.07, 100.45, 99.21 (br), 98.81, 98.47, 81.25, 80.44, 80.50, 79.88, 79.85, 78.88, 78.64, 75.56, 75.32, 74.97, 74.86, 74.73, 74.69, 74.53, 74.34, 73.86, 73.31, 73.28, 73.19, 72.72, 72.56, 72.51, 72.33, 72.11, 72.03, 71.95, 71.85, 71.69, 71.52, 71.27, 71.08, 69.26, 69.02, 68.95, 68.85, 66.71, 66.14; HRMS-MALDI (*m/z*): $[M+Na]^+$ calculated for $C_{203}H_{210}O_{36}Na$, 3246.4494; Found: 3246.4406.

General procedures to remove allyl protecting group by the Ir complex to prepare compounds 38 – 43: Each oligosaccharide starting material (**31 – 36**) was coevaporated with toluene (3x) and placed under high vacuum for 4 h prior to the reaction. Under an argon atmosphere, a solution of $Ir\{(COD)[PH_3(C_6H_5)_2]_2\}PF_6$ (cat. i.e. 0.2 equiv.) in THF (distilled over sodium) was degassed by vacuum and gassed with H_2 (g) balloon (~ 5 cycles). The reaction was stirred under H_2 atmosphere at rt for 5 min before the solution was degassed by vacuum and gassed with argon (~ 5 cycles). To this reaction flask, a solution of an allyl protected compound (**31 – 36**, 1 equiv., ~ 0.05 mmol) in THF (1 mL) was added via syringe in one portion at rt. The reaction was stirred at rt for 2 h before concentrated *in* vacuo. The completed isomerization of the terminal allyl group was verified by ^1H NMR. The crude product was treated with *p*-TsOH (0.1 equiv. for **31**, 10 equiv. for **32 – 36)** in a mixture of CH_2Cl_2 and

MeOH (3 : 1, total volume = 2.66 mL) for 12 h at rt. The reaction solution was diluted with EtOAc (20 mL), washed with saturated aqueous $NaHCO_3$ (3x) and brine, dried over Na_2SO_4 and concentrated *in vacuo*. The crude product was purified by flash silica column chromatography (cyclohexane / EtOAc) to obtain the title compounds **38** (quant.); **39** (71%); **40** (81%); **41** (79%); **42** (87%); or **43** (89%) as colorless syrup.

(2,3,4,6-Tetra-*O*-benzyl-α-D-mannopyranosyl)-(1→6)-2-*O*-(2,3,4,6-tetra-*O*-benzyl-α-D-mannopyranosyl)-3,4,5-tri-*O*-benzyl-D-*myo*-inositol (**39**): Colorless syrup, R_f 0.30 (hexanes / EtOAc = 2 : 1); $[\alpha]_D^{r.t.}$= + 36.7 (*c* = 1.35, $CHCl_3$); ^1H NMR (300 MHz, $CDCl_3$) δ 7.54 – 7.10 (m, 55H), 5.48 (brs, 1H), 5.24 (d, *J* = 2.1, 1H), 4.99 – 4.45 (m, 19H), 4.45 – 4.00 (m, 7H), 4.00 – 3.71 (m, 7H), 3.68 – 3.20 (m, 7H), 1.67 (s, 1H); ^{13}C NMR (75 MHz, $CDCl_3$) δ 138.71, 138.48, 138.36, 138.34, 138.21, 138.16, 138.07, 137.92, 137.59, 128.36, 128.22, 128.14, 128.01, 127.95, 127.87, 127.81, 127.77, 127.69, 127.61, 127.53, 127.47, 127.37, 127.27, 127.22, 98.97, 95.48, 81.09, 80.08, 79.97, 79.23, 78.86, 78.31, 75.48, 75.35, 75.32, 75.18, 75.13, 74.95, 74.56, 74.47, 74.19, 73.28, 72.42, 72.38, 71.97, 71.90, 71.69, 71.62, 71.43, 71.14, 69.28, 68.81; HRMS-MALDI (*m/z*): $[M+Na]^+$ calculated for $C_{95}H_{98}O_{16}Na$, 1517.6720; Found: 1517.6747.

(2,3,4,6-tetra-*O*-benzyl-α-D-mannopyranosyl)-(1→6)-(2,3,4,-tri-*O*-benzyl-α-D-mannopyranosyl)-(1→6)-2-*O*-(2,3,4,6-tetra-*O*-benzyl-α-D-mannopyranosyl)-3,4,5-tri-*O*-benzyl-D-*myo*-inositol (**40**): Colorless syrup, R_f 0.36 (cyclohexane / EtOAc = 7 : 3); $[\alpha]_D^{r.t.}$= + 39.1 (*c* = 1.0, $CHCl_3$); ^1H NMR (300 MHz, $CDCl_3$) δ 7.54 – 7.07 (m, 70H), 5.49 (d, *J* = 1.5, 1H), 5.27 (d, *J* = 2.1, 1H), 5.08 – 4.81 (m, 6H), 4.80 – 4.37 (m, 22H), 4.36 – 3.74 (m, 14H), 3.73 – 3.16 (m, 11H), 1.77 (s, 1H); ^{13}C NMR (75 MHz, $CDCl_3$) δ 138.69, 138.57, 138.45, 138.39, 138.35, 138.20, 138.00, 137.92, 128.40, 128.37, 128.33, 128.23, 128.18, 128.12, 128.07, 128.02, 127.96, 127.86, 127.83, 127.73, 127.70, 127.58, 127.45, 127.41, 127.33, 127.28, 127.17, 98.82, 98.15, 96.49, 81.14, 80.52, 79.94, 79.70, 78.77, 78.55, 75.49, 75.33, 75.05, 74.92, 74.65, 74.55, 73.25, 72.46, 72.41, 72.24, 71.96, 71.83, 71.69, 71.65, 71.57, 68.91, 66.05; HRMS-MALDI (*m/z*): $[M+Na]^+$ calculated for $C_{122}H_{126}O_{21}Na$, 1949.8684; Found: 1949.8637.

(2,3,4,6-Tetra-*O*-benzyl-α-D-mannopyranosyl)-(1→6)-(2,3,4,-tri-*O*-benzyl-α-D-mannopyranosyl)-(1→6)-(2,3,4,-tri-*O*-benzyl-α-D-mannopyranosyl)-(1→6)-2-*O*-(2,3,4,6-tetra-*O*-benzyl-α-D-mannopyranosyl)-3,4,5-tri-*O*-benzyl-D-*myo*-inositol (**41**): Colorless syrup, R_f 0.39 (cyclohexane / EtOAc = 7 : 3); $[\alpha]_D^{r.t.}$= + 43.7 (*c* = 1.0, $CHCl_3$); ^1H NMR (300 MHz, $CDCl_3$) δ 7.48 – 7.10 (m, 85H), 5.51 (d, *J* = 1.3, 1H), 5.27 (d, *J* = 2.0, 1H), 5.19 (d, *J* = 1.3, 1H), 5.02 – 4.82 (m, 7H), 4.83 – 4.24 (m, 30H), 4.21 – 3.77 (m, 17H), 3.76 – 3.18 (m, 11H), 1.77 (s, 1H); ^{13}C NMR (75 MHz, $CDCl_3$) δ 138.65, 138.57, 138.40, 138.32, 138.27, 138.21, 138.11, 138.02, 137.94, 137.86, 128.40, 128.37, 128.34, 128.26, 128.22, 128.14, 128.11, 128.09, 128.02, 127.97, 127.85, 127.79, 127.71, 127.64, 127.57, 127.49, 127.42, 127.38, 127.30, 127.27, 127.17, 98.90, 98.41, 98.25, 96.56, 81.24, 80.55, 80.20, 79.97, 79.18, 78.88, 78.65, 75.60, 75.40, 75.02, 74.87, 74.77, 74.71, 74.03, 73.34, 73.31, 72.93, 72.53, 72.31, 72.22, 72.11, 72.05, 71.93, 71.81, 71.76, 71.68, 71.63, 71.27, 69.16, 69.05, 66.41, 65.61; HRMS-MALDI (*m/z*): $[M+Na]^+$ calculated for $C_{149}H_{154}O_{26}Na$, 2382.0621; Found: 2382.0566.

(2,3,4,6-Tetra-*O*-benzyl-α-D-mannopyranosyl)-(1→2)-(3,4,6-tri-*O*-benzyl-α-D-mannopyranosyl)-(1→6)-(2,3,4,-tri-*O*-benzyl-α-D-mannopyranosyl)-(1→6)-(2,3,4,-tri-*O*-benzyl-α-D-mannopyranosyl)-(1→6)-2-*O*-(2,3,4,6-tetra-*O*-benzyl-α-D-mannopy-ranosyl)-3,4,5-tri-*O*-benzyl-D-*myo*-inositol) (**42**): Colorless syrup, R_f 0.38 (cyclohexane / EtOAc = 7 : 3); $[\alpha]_D^{r.t.}$= + 39.2 (*c* = 1.0, $CHCl_3$); ^1H NMR (300 MHz, $CDCl_3$) δ 7.52 – 7.09 (m, 100H), 5.53 (brs, 1H), 5.28 (d, *J* = 1.3, 1H), 5.24 (brs, 1H), 5.07 – 4.86 (m, 8H), 4.85 – 4.40 (m, 32H), 4.39 – 4.04 (m, 8H), 4.04 – 3.75 (m, 17H), 3.74 – 3.19 (m, 13H), 1.79 (s, 1H); ^{13}C NMR (75 MHz, $CDCl_3$) δ 138.71, 138.68, 138.65, 138.56, 138.41, 138.38, 138.28, 138.15, 138.07, 138.00, 137.90, 128.47, 128.41, 128.38, 128.31, 128.25, 128.21, 128.18, 128.16, 128.06, 128.00, 127.90, 127.82, 127.76, 127.66, 127.62, 127.54, 127.47, 127.36, 127.32, 127.24, 127.20, 99.38 (br), 98.91, 98.44, 96.19, 81.32, 80.53, 80.47, 79.90, 79.53, 78.96, 78.72, 75.64, 75.41, 75.07, 75.02, 74.98, 74.92, 74.87, 74.82, 74.70, 74.62, 74.30, 74.04, 73.39, 73.36, 73.30, 72.75, 72.59, 72.29, 72.19, 72.13, 72.07, 72.03, 71.93, 71.89, 71.78, 71.64, 71.62, 71.25, 69.24, 69.11, 66.73, 66.32; HRMS-MALDI (*m/z*): $[M+Na]^+$ calculated for $C_{176}H_{182}O_{31}Na$, 2814.2557; Found: 2814.2484.

(2,3,4,6-Tetra-*O*-benzyl-α-D-mannopyranosyl)-(1→2)-(3,4,6-tri-*O*-benzyl-α-D-mannopyranosyl)-(1→2)-(3,4,6-tri-*O*-benzyl-α-D-mannopyranosyl)-(1→6)-(2,3,4,-tri-*O*-benzyl-α-D-mannopyranosyl)-(1→6)-(2,3,4,-tri-*O*-benzyl-α-D-mannopyranosyl)-(1→6)-2-*O*-(2,3,4,6-tetra-*O*-benzyl-α-D-mannopyranosyl)-3,4,5-tri-*O*-benzyl-D-*myo*-inositol) (**43**): To R_f 0.26 (cyclohexane / EtOAc = 4 : 1); $[\alpha]_D^{r.t.}$= + 37.5 (*c* = 1.0, $CHCl_3$); ^{1}H NMR (500 MHz, $CDCl_3$) δ 7.42 – 6.90 (m, 115H), 5.76 – 5.59 (m, 1H), 5.40 (d, *J* = 1.6, 1H), 5.20 – 5.15 (m, 3.5H), 5.15 – 5.12 (m, 0.5H), 5.07 – 5.01 (m, 1H), 4.98 – 4.69 (m, 12H), 4.67 – 4.17 (m, 37H), 4.16 – 3.95 (m, 7H), 3.94 – 3.70 (m, 20H), 3.69 – 3.55 (m, 2H), 3.54 – 3.42 (m, 3H), 3.40 – 3.16 (m, 8H), 3.15 – 2.98 (m, 3H); ^{13}C NMR (126 MHz, $CDCl_3$) δ139.25, 139.19, 139.10, 139.09, 139.08, 139.01, 138.95, 138.90, 138.87, 138.84, 138.82, 138.78, 138.72, 138.68, 138.65, 138.62, 138.56, 138.35, 138.25, 138.24, 138.10, 134.16, 128.74, 128.71, 128.57, 128.56, 128.51, 128.48, 128.47, 128.43, 128.43, 128.40, 128.39, 128.37, 128.31, 128.29, 128.26, 128.11, 128.09, 128.05, 128.01, 127.99, 127.96, 127.93, 127.92, 127.91, 127.89, 127.88, 127.86, 127.79, 127.66, 127.63, 127.61, 127.60, 127.57, 127.53, 127.47, 127.45, 127.31, 127.12, 127.00, 126.98, 117.90, 100.58, 99.53, 99.41, 99.27, 98.99, 98.58, 81.74, 81.60, 81.47, 80.93, 80.21, 80.14, 80.08, 79.27, 79.09, 78.93, 76.06, 75.92, 75.87, 75.52, 75.22, 75.19, 75.10, 75.04, 74.93, 74.85, 74.78, 74.76, 74.67, 74.50, 74.42, 73.84, 73.71, 73.58, 73.55, 73.52, 73.42, 72.82, 72.80, 72.75, 72.65, 72.62, 72.57, 72.41, 72.35, 72.32, 72.18, 72.15, 72.09, 71.49, 71.37, 71.34, 71.21, 71.03, 70.63, 69.36, 69.21, 69.09, 68.99, 66.19, 66.03; HRMS-MALDI (*m/z*): $[M+Na]^+$ calculated for $C_{206}H_{214}O_{36}Na$, 3286.4807; Found: 3286.4880.

General procedures for phosphorylations to prepare the protected phosphodiesters 45(a-g): Each oligosaccharide (**37 – 43**) was combined with the 6-(S-benzyl)thiohexyl H-phosphonate **44**, coevaporated with pyridine (3x) and placed under high vacuum for 4 h prior to the reaction. To a solution of an oligosaccharide backbone (**37 – 43**, ~ 0.03 mmol) and **44** (0.15 mmol) in pyridine (2 mL), PivCl (0.3 mmol) was added at rt. After 3h at rt, iodine (0.21 mmol) in a mixture of pyridine and water (10 : 1, 300 uL total volume) was added to the reaction solution at rt and stirred for 1 h. The reaction mixture was diluted with CH_2Cl_2 (10 mL) and $Na_2S_2O_3$ (20 mL of 1M) and extracted with CH_2Cl_2 (3 x 10 mL). The combined organic layer was dried over Na_2SO_4(s), concentrated *in vacuo*, purified by flash silica column chromatography (CH_2Cl_2 / MeOH gradient, silica gel was neutralized with 1% NEt_3 in CH_2Cl_2 prior to use) and size exclusion column chromatography (Sephadex LH-20, MeOH / CH_2Cl_2 / NEt_3 = 100 : 100 : 0.05) to obtain compounds **45**(**a-g**) as a colorless syrup (90% to quant.)

Triethylammonium 1-*O*-(6-(S-benzyl)thiohexylphosphonato)-2,3,4,5,6-penta-*O*-benzyl-D-*myo*-inositol (**45a**): Colorless syrup (88%), R_f 0.6 (CH_2Cl_2 / MeOH = 9 : 1); $[\alpha]_D^{r.t.}$= + 7.6 (*c* = 1, $CHCl_3$); ^1H NMR (300 MHz, $CDCl_3$) δ 7.43 – 7.08 (m, 30H), 5.05 – 4.72 (m, 8H), 4.64 (m, *AB*, 2H), 4.54 (brs, 1H), 4.12 – 3.94 (m, 3H), 3.85 – 3.57 (m, 4H), 3.46 (t, *J* = 9.0, 2H), 3.07 (q, *J* = 7.3, 33H), 2.32 (t, *J* = 7.5, $N(C\underline{H}_2CH_3)_3$), 1.50 – 1.40 (m, 3H), 1.33 (t, *J* = 6.0, $N(CH_2C\underline{H}_3)_3$), 1.24 – 1.11 (m, 5H); ^{13}C NMR (75 MHz, $CDCl_3$) δ 139.45, 139.10, 138.63, 138.52, 138.44, 138.37, 128.65, 128.31, 128.17, 127.94, 127.73, 127.36, 127.31, 127.22, 127.06, 126.94, 126.88, 126.74, 83.31, 81.54, 80.87, 80.81, 76.29, 75.79, 75.68, 74.97, 74.48, 72.34, 65.38, 65.30, 46.06 ($N(\underline{C}H_2CH_3)_3$), 36.17, 31.21, 28.99, 28.49, 25.19, 8.74 ($N(CH_2\underline{C}H_3)_3$); ^{31}P NMR (121 MHz, $CDCl_3$) δ – 0.65; HRMS-MALDI (*m/z*): $[M]^+$ calculated for $C_{54}H_{61}O_9PS$, 916.3774; Found: 917.3800.

Triethylammonium 1-*O*-(6-(S-benzyl)thiohexylphosphonato)-2-*O*-(2,3,4,6-tetra-*O*-benzyl-α-D-mannopyranosyl)-3,4,5,6-tetra-*O*-benzyl-D-*myo*-inositol (**45b**): Colorless syrup (88%), R_f 0.1 (CH_2Cl_2 / MeOH = 95 : 5); $[\alpha]_D^{r.t.}$= + 16.4 (*c* = 1, $CHCl_3$); ^1H NMR (300 MHz, $CDCl_3$) δ 7.64 – 7.12 (m, 45H), 5.78 (s, 1H), 5.11 – 4.67 (m, 11H), 4.64 – 4.47 (m, 4H), 4.33 (m, AB, 2H), 4.21 – 4.02 (m, 3H), 3.94 – 3.71 (m, 6H), 3.67 (s, 2H), 3.54 – 3.34 (m, 3H), 3.13 (d, *J* = 10.2, 1H), 2.80 (q, *J* = 7.3, $N(C\underline{H}_2CH_3)_3$), 2.33 (t, *J* = 7.5, 2H), 1.53 – 1.18 (m, 9H), 1.14 (t, *J* = 7.3, $N(CH_2C\underline{H}_3)_3$); ^{13}C NMR (75 MHz, $CDCl_3$) δ 139.12, 138.83, 138.62, 138.59, 138.54, 138.49, 138.46, 138.41, 128.72, 128.35, 128.26, 128.13, 128.11, 128.02, 127.97, 127.88, 127.52, 127.49, 127.41, 127.29, 127.22, 127.07, 126.82, 126.76, 97.84, 83.30, 81.05, 80.95, 79.28, 79.25, 76.20, 75.70, 75.44, 75.08, 74.68, 73.83, 73.13, 72.06, 71.95, 71.41, 71.32, 69.04, 65.49, 65.41, 45.79 ($N(\underline{C}H_2CH_3)_3$), 36.35, 31.43, 29.29, 28.82, 25.32, 9.70 ($N(CH_2\underline{C}H_3)_3$); ^{31}P NMR (121 MHz, $CDCl_3$) δ –0.59; HRMS-MALDI (*m/z*): $[M+Na]^+$ calculated for $C_{81}H_{89}O_{14}PSNa$, 1371.5603; Found: 1371.5600.

Triethylammonium (2,3,4,6-tetra-*O*-benzyl-α-D-mannopyranosyl)-(1→6)-1-*O*-(6-(S-benzyl)thiohexylphosphonato)-2-*O*-(2,3,4,6-tetra-*O*-benzyl-α-D-mannopyranosyl)-3,4,5-tri-*O*-benzyl-D-*myo*-inositol (**45c**): Colorless syrup (95%), R_f 0.52 (CH_2Cl_2 / MeOH = 9 : 1); $[\alpha]_D^{r.t.}$= + 17.1 (*c* = 1.4, $CHCl_3$); ^{1}H NMR (300 MHz, $CDCl_3$) δ 7.51 – 6.95 (m, 60H), 5.75 (brs, 1H), 5.66 (brs, 1H), 4.98 – 4.42 (m, 24H), 4.40 – 3.70 (m, 20H), 3.63 (brs, 2H), 3.50 – 3.02 (m, 8H), 2.94 ($N(C\underline{H}_2CH_3)_3$), 2.27 (t, *J* = 7.3, 2H), 1.51 – 1.22 (m, 8H), 1.16 ($N(CH_2C\underline{H}_3)_3$); ^{13}C NMR (75 MHz, $CDCl_3$ / MeOD = 1 :1) δ 139.46, 139.28, 138.97, 138.86, 138.72, 138.67, 138.64, 138.47, 138.36, 138.17, 128.88, 128.53, 128.51, 128.40, 128.37, 128.36, 128.32, 128.29, 128.25, 128.20, 128.18, 128.14, 128.13, 128.10, 127.99, 127.92, 127.80, 127.74, 127.66, 127.63, 127.55, 127.52, 127.42, 127.39, 127.34, 127.29, 127.24, 127.11, 127.06, 126.98, 98.46, 98.33, 81.52, 80.06, 79.28, 78.98, 78.04, 78.00, 76.23, 75.71, 75.16, 75.11, 74.96, 74.95, 74.85, 74.48, 74.24, 73.71, 73.31, 73.26, 72.25, 71.99, 71.90, 71.67, 71.44, 70.60, 69.03, 68.92, 66.07, 66.04, 45.87 ($N(\underline{C}H_2CH_3)_3$), 36.39, 31.42, 29.18, 28.71, 25.46, 22.75, 8.46 ($N(CH_2\underline{C}H_3)_3$); ^{31}P NMR (121 MHz, $CDCl_3$) δ –0.42; HRMS-MALDI (*m/z*): $[M+Na]^+$ calculated for $C_{108}H_{117}O_{19}Na$, 1803.7540; Found: 1803.7500.

Triethylammonium (2,3,4,6-Tetra-*O*-benzyl-α-D-mannopyranosyl)-(1→6)-(2,3,4,-tri-*O*-benzyl-α-D-mannopyranosyl)-(1→6)-1-*O*-(6-(S-benzyl)thiohexylphosphonato)-2-*O*-(2,3,4,6-tetra-*O*-benzyl-α-D-mannopyranosyl)-3,4,5-tri-*O*-benzyl-D-*myo*-inositol (**45d**): Colorless syrup (99%), R_f 0.44 (CH_2Cl_2 / MeOH = 9 : 1); $[\alpha]_D^{r.t.}$= + 29.2 (*c* = 1.0, $CHCl_3$); ^{1}H NMR (500 MHz, $CDCl_3$) δ 7.54 – 6.93 (m, 75H), 5.62 (brs, 1H), 5.60 (brs, 1H), 5.06 (brs, 1H), 4.98 – 4.17 (m, 30H), 4.15 – 3.69 (m, 15H), 3.59 (s, 2H), 3.52 – 3.03 (m, 10H), 2.70 ($N(C\underline{H}_2CH_3)_3$), 2.24 (t, *J* = 7.3, 2H), 1.51 – 1.05 (m, 8H), 0.99 ($N(CH_2C\underline{H}_3)_3$); ^{13}C NMR (126 MHz, $CDCl_3$) δ 139.52, 139.22, 139.21, 139.04, 139.00, 138.88, 138.83, 138.75, 138.72, 138.62, 138.58, 138.31, 129.01, 128.72, 128.67, 128.54, 128.49, 128.43, 128.42, 128.38, 128.31, 128.29, 128.26, 128.24, 128.18, 128.16, 128.12, 128.05, 128.01, 127.94, 127.86, 127.77, 127.72, 127.69, 127.65, 127.61, 127.58, 127.56, 127.53, 127.46, 127.41, 127.37, 127.21, 127.13, 127.10, 98.93, 98.58, 98.04, 81.62, 81.55, 79.56, 79.51, 79.20, 77.93, 76.39, 76.33, 76.22, 75.88, 75.80, 75.14, 75.06, 74.92, 74.76, 74.52, 73.47, 73.37, 73.32, 72.59, 72.33, 72.28, 72.20, 72.06, 71.96, 71.83, 71.63, 71.59, 71.50, 69.30, 69.02, 66.09, 65.50, 45.41 ($N(\underline{C}H_2CH_3)_3$), 36.56, 31.56, 29.33, 28.88, 25.63, 8.53 ($N(CH_2\underline{C}H_3)_3$); ^{31}P NMR (121 MHz, $CDCl_3$) δ –0.46; ESI-MS (*m/z*): 1) $[M+NH_4]^+$ calculated for $C_{135}H_{149}NO_{24}PS^+$, 2231.0; Found: 2230.7 as a dominant peak.

Triethylammonium (2,3,4,6-Tetra-*O*-benzyl-α-D-mannopyranosyl)-(1→6)-(2,3,4,-tri-*O*-benzyl-α-D-mannopyranosyl)-(1→6)-(2,3,4,-tri-*O*-benzyl-α-D-mannopyrano-syl)-(1→6)-1-*O*-(6-(S-benzyl)thiohexylphosphonato)-2-*O*-(2,3,4,6-tetra-*O*-benzyl-α-D-mannopyranosyl)-3,4,5-tri-*O*-benzyl-D-*myo*-inositol (**45e**): Colorless syrup, R_f 0.56 (CH_2Cl_2 / MeOH = 9 : 1); $[\alpha]_D^{r.t.}$= + 33.8 (*c* = 1.0, $CHCl_3$); ^{1}H NMR (500 MHz, $CDCl_3$) δ 7.52 – 6.93 (m, 90H), 5.61 (brs, 1H), 5.59 (brs, 1H), 5.01 (brs, 1H), 5.00 – 4.18 (m, 38H), 4.15 – 3.73 (m, 18H), 3.67 – 3.19 (m, 15H), 3.12 (t, *J* = 12.0, 2H), 2.71 ($N(C\underline{H}_2CH_3)_3$), 2.24 (t, *J* = 7.26, 2H) 1.47 – 1.06 (m, 9H), 1.00 ($N(CH_2C\underline{H}_3)_3$); ^{13}C NMR (126 MHz, $CDCl_3$) δ = 139.80, 139.42, 139.21, 139.20, 139.15, 139.12, 139.02, 138.96, 138.91, 138.84, 138.82, 138.76, 138.66, 138.65, 138.59, 138.44, 138.39, 129.01, 128.76, 128.67, 128.56, 128.52, 128.51, 128.47, 128.45, 128.42, 128.38, 128.35, 128.33, 128.32, 128.25, 128.21, 128.18, 128.17, 128.04, 128.00, 127.95, 127.82, 127.71, 127.67, 127.64, 127.61, 127.58, 127.54, 127.51, 127.47, 127.42, 127.21, 127.12, 127.11, 99.14, 98.68, 98.64, 98.40, 81.56, 79.77, 79.53, 79.38, 79.27, 76.14, 75.92, 75.11, 74.87, 74.74, 74.44, 74.03, 73.50, 73.37, 72.72, 72.59, 72.50, 72.28, 72.09, 72.05, 71.87, 71.71, 71.62, 71.49, 71.37, 71.25, 70.90, 70.85, 69.31, 65.89, 65.79, 45.43 ($N(\underline{C}H_2CH_3)_3$), 36.56, 31.56, 29.33, 28.88, 25.65, 8.53 ($N(CH_2\underline{C}H_3)_3$); ^{31}P NMR (121 MHz, $CDCl_3$) δ –0.42; ESI-MS (*m/z*): $[M+2(NH_4)]^{2+}$ calculated for $C_{162}H_{181}N_2O_{29}PS^{2+}$, 1340.6; Found: 1341.0 as a dominant peak.

Triethylammonium (2,3,4,6-Tetra-*O*-benzyl-α-D-mannopyranosyl)-(1→2)-(3,4,6-tri-*O*-benzyl-α-D-mannopyranosyl)-(1→6)-(2,3,4,-tri-*O*-benzyl-α-D-mannopyranosyl)-(1→6)-(2,3,4,-tri-*O*-benzyl-α-D-mannopyranosyl)-(1→6)-1-*O*-(6-(S-benzyl)thio-hexylphosphonato)-2-*O*-(2,3,4,6-tetra-*O*-benzyl-α-D-mannopyranosyl)-3,4,5-tri-*O*-benzyl-D-*myo*-inositol) (**45f**): Colorless syrup, R_f 0.53 (CH_2Cl_2 / MeOH = 9 : 1); $[\alpha]_D^{r.t.}$= + 33.2 (*c* = 1.0, $CHCl_3$); ^1H NMR (300 MHz, $CDCl_3$) δ 7.53 – 6.91 (m, 105H), 5.70 (brs, 1H), 5.66 (brs, 1H), 5.19 (d, *J* = 1.6, 1H), 5.06 – 4.22 (m, 44H), 4.18 – 3.97 (m, 9H), 3.96 – 3.77 (m, 14H), 3.74 (t, *J* = 9.4, 1H), 3.68 – 3.61 (m, 3H), 3.56 – 3.25 (m, 9H), 3.22 – 3.04 (m, 3H), 2.83 – 2.67 (m, 6H), 2.28 ($N(C\underline{H}_2CH_3)_3$), 1.51 – 1.10 (m, 10H), 1.03 ($N(CH_2C\underline{H}_3)_3$); ^{13}C NMR (151 MHz, $CDCl_3$) δ 139.61, 139.23, 139.07, 138.99, 138.87, 138.85, 138.81, 138.79, 138.76, 138.74, 138.67, 138.60, 138.56, 138.55, 138.53, 138.47, 138.42, 138.39, 138.17, 138.07, 138.05, 128.78, 128.51, 128.44, 128.39, 128.34, 128.32, 128.27, 128.23, 128.21, 128.18, 128.14, 128.12, 128.11, 128.08, 128.01, 127.96, 127.94, 127.88, 127.85, 127.81, 127.79, 127.78, 127.72, 127.71, 127.67, 127.64, 127.51, 127.41, 127.40, 127.34, 127.29, 127.23, 126.99, 126.97, 126.92, 126.87, 126.79, 126.73, 99.28, 99.20, 98.88, 98.41, 98.17, 81.40, 79.93, 79.67, 79.48, 79.28, 79.12, 75.93, 75.70, 74.95, 74.93, 74.91, 74.81, 74.54, 74.49, 74.28, 74.18, 73.98, 73.68, 73.30, 73.22, 73.16, 72.34, 72.28, 72.09, 72.05, 72.00, 71.81, 71.77, 71.35, 71.05, 70.92, 70.80, 69.09, 69.04, 68.84, 65.92, 45.19 ($N(\underline{C}H_2CH_3)_3$), 36.34, 31.34, 29.71, 29.12, 28.66, 25.43, 8.29 ($N(CH_2\underline{C}H_3)_3$); ^{31}P NMR (121 MHz, $CDCl_3$) δ –0.33;

ESI-MS (*m/z*): $[M+2(NH_4)]^{2+}$ calculated for $C_{189}H_{209}N_2O_{34}PS^{2+}$, 1556.7; Found: 1556.9 as a dominant peak.

Triethylammonium (2,3,4,6-Tetra-*O*-benzyl-α-D-mannopyranosyl)-(1→2)-(3,4,6-tri-*O*-benzyl-α-D-mannopyranosyl)-(1→2)-(3,4,6-tri-*O*-benzyl-α-D-mannopyranosyl)-(1→6)-(2,3,4,-tri-*O*-benzyl-α-D-mannopyranosyl)-(1→6)-(2,3,4,-tri-*O*-benzyl-α-D-mannopyranosyl)-(1→6)-1-*O*-(6-(S-benzyl)thiohexylphosphonato)-2-*O*-(2,3,4,6-tetra-*O*-benzyl-α-D-mannopyranosyl)-3,4,5-tri-*O*-benzyl-D-*myo*-inositol) (**45g**): To R_f 0.33 ($CHCl_3$ / MeOH = 3 : 1); $[\alpha]_D^{r.t.}$= + 46.1 (*c* = 1.0, $CHCl_3$); ^1H NMR (600 MHz, $CDCl_3$) δ 7.56 – 6.80 (m, 120H), 5.67 (brs, 1H), 5.64 (brs, 1H), 5.21 (d, *J* = 1.7, 1H), 5.20 (d, *J* = 1.5, 1H), 5.05 – 4.62 (m, 18H), 4.62 – 4.35 (m, 20H), 4.35 – 4.18 (m, 7H), 4.18 – 3.96 (m, 8H), 3.96 – 3.76 (m, 16H), 3.70 – 3.64 (m, 1H), 3.63 (s, 2H), 3.56 – 3.24 (m, 9H), 3.17 (d, *J* = 10.5, 1H), 3.06 (dd, *J* = 10.4, 24.2, 2H), 2.83 – 2.65 ($N(C\underline{H_2}CH_3)_3$), 2.28 (t, *J* = 7.3, 2H), 1.53 – 1.10 (m, 7H), 1.03 ($N(CH_2C\underline{H_3})_3$); ^{13}C NMR (151 MHz, $CDCl_3$) δ 139.61, 139.21, 139.07, 138.98, 138.90, 138.89, 138.80, 138.75, 138.71, 138.68, 138.66, 138.66, 138.60, 138.57, 138.52, 138.48, 138.47, 138.44, 138.40, 138.16, 138.10, 137.89, 128.79, 128.51, 128.48, 128.44, 128.34, 128.33, 128.28, 128.27, 128.25, 128.24, 128.21, 128.20, 128.17, 128.14, 128.09, 128.07, 128.01, 127.95, 127.93, 127.88, 127.83, 127.79, 127.75, 127.71, 127.69, 127.67, 127.65, 127.55, 127.52, 127.45, 127.38, 127.36, 127.34, 127.31, 127.29, 127.25, 127.22, 126.99, 126.96, 126.90, 126.87, 126.85, 126.71, 126.67, 100.32, 99.31, 99.18, 98.89, 98.42, 98.28, 81.40, 80.00, 79.92, 79.82, 79.28, 79.07, 78.88, 75.94, 75.71, 75.04, 74.95, 74.90, 74.86, 74.82, 74.71, 74.58, 74.53, 74.27, 74.21, 74.16, 73.56, 73.45, 73.36, 73.31, 73.20, 73.16, 72.53, 72.43, 72.38, 72.35, 72.32, 72.13, 72.11, 72.05, 71.98, 71.85, 71.79, 71.33, 71.26, 71.05, 70.84, 70.73, 69.12, 69.09, 68.86, 68.74, 66.07, 65.76, 45.20 ($N(\underline{C}H_2CH_3)_3$), 36.34, 31.34, 29.12, 28.66, 25.43, 8.30 ($N(CH_2\underline{C}H_3)_3$); ^{31}P NMR (121 MHz, $CDCl_3$) δ – 0.38; HRMS-MALDI (*m/z*): $[M+Na]^+$ calculated for $C_{216}H_{229}O_{39}PSNa$, 3532.5286; Found: 3532.5289.

General procedures for Birch reductions to prepare PI and PIM$_1$ - PIM$_6$: At -78 °C (dry ice / acetone bath), ammonia was condensed into a solution of a phosphodiester **45** (~ 0.02 mmol) in a mixture of THF (25 mL) and *t*-BuOH (0.5 mL). Small pieces of Na(s) was added to the reaction to generate a stable dark blue solution for at least 30 min and MeOH was added to the reaction solution. Then, small pieces of Na(s) was again added to the reaction to generate a stable dark blue solution for at least 30 min and MeOH was added to the reaction solution. The reaction was allowed to slowly warm to rt by removing the dry ice / acetone bath and most of the remaining ammonia in the reaction solution was blown off by argon stream. The reaction solution was concentrated *in vacuo*, re-dissolved in water, neutralized with a small amount of acid resin (methanol washed Amberlite IR-120). The resin was filtered off and the mother liquor was concentrated *in vacuo*, re-dissolved in water, and extracted with $CHCl_3$ to remove the less polar partially debenzylated side products. The volume of the aqueous layer was decreased by lyophilzation and the aqueous solution was dialysed to afford the final product **PI**, **PIM$_1$**, **PIM$_2$**, **PIM$_3$**, **PIM$_4$**, **PIM$_5$**, or **PIM$_6$**.

PI: White solid (65%); ^{1}H NMR (300 MHz, D_2O) δ 4.25 (t, *J* = 2.7, 1H), 4.01 – 3.83 (m, 3H), 3.81 – 3.47 (m, 4H), 3.33 (t, *J* = 9.3, 1H), 2.81 – 2.74 (m, 0.2H), 2.42 (t, 1.8H), 1.74 – 1.51 (m, 4H), 1.49 – 1.34 (m, 4H); ^{31}P NMR (121 MHz, $CDCl_3$) δ 0.79; ESI-MS (*m/z*): [M–H]$^-$ calculated for $C_{12}H_{24}O_9PS^-$, 375.0; Found: 374.6 as a dominant peak.

PIM$_1$: White solid (43%); ^{1}H NMR (300 MHz, D_2O) δ 5.13 (d, *J* = 1.5, 1H), 4.32 – 4.25 (m, 1H), 4.13 – 4.06 (m, 1H), 4.04 – 3.53 (m, 12H), 3.31 (t, *J* = 8.8, 1H), 2.88 – 2.68 (m, 0.5H), 2.54 (t, *J* = 7.1, 1.5H), 1.76 – 1.51 (m, 4H), 1.50 – 1.29 (m, 4H); ^{13}C NMR (75 MHz, D_2O) δ 13C NMR (75 MHz, D2O) δ 101.69, 79.27, 76.46, 76.41, 74.43, 72.97, 72.69, 72.08, 72.03, 70.60, 70.37, 70.25, 66.87, 66.68, 66.63, 61.12, 38.42, 33.18, 30.02, 29.97, 29.96, 28.53, 27.51, 27.35, 24.77, 24.60, 23.93; ^{31}P NMR (121 MHz, $CDCl_3$) δ 0.86; HRMS-ESI (*m/z*): [M–H]$^–$ calculated for $C_{18}H_{34}O_{14}PS^{1–}$, 537.1412; Found: 537.1403.

PIM$_2$: White solid (56%); ^{1}H NMR (500 MHz, D_2O) δ 5.04 (s, 1H), 5.02 (s, 1H), 4.19 (s, 1H), 4.06 – 3.42 (m, 20H), 3.23 (t, *J* = 9.2, 1H), 2.65 (t, *J* = 7.2, 2H), 1.65 – 1.45 (m, 4H), 1.44 – 1.22 (m, 4H); ^{13}C NMR (125 MHz, D_2O) δ 101.62, 101.60, 78.96, 78.34, 78.29, 76.68, 73.26, 72.99, 72.84, 70.61, 70.41, 70.25, 70.12, 66.89, 66.79, 66.53, 61.14, 60.92, 38.41, 30.17, 30.12, 28.54, 27.48, 24.85; ^{31}P NMR (121 MHz, $CDCl_3$) δ 0.48; HRMS-ESI (*m/z*): [MS-SM-2H]$^{2-}$ calculated for $C_{48}H_{86}O_{38}P_2S_2^{2-}$, 698.1863; Found: 698.1862.

PIM$_3$: White solid (91%); ^{1}H NMR (600 MHz, D_2O) δ 5.15 (s, 1H), 5.10 (s, 1H), 4.90 (s, 1H), 4.30 (d, *J* = 1.9, 1H), 4.21 – 4.04 (m, 4H), 4.03 – 3.90 (m, 5H), 3.90 – 3.72 (m, 10H), 3.64 (m, 7H), 3.36 (t, *J* = 9.1, 1H), 2.77 (t, *J* = 7.2, 1.7H), 2.54 (t, *J* = 7.1, 0.3H), 1.80 – 1.58 (m, 4H), 1.42 (brs, 4H); ^{13}C NMR (150 MHz, D_2O) δ 104.27, 104.12, 102.26, 81.37, 81.10, 81.06, 79.29, 79.26, 75.68, 75.51, 75.48, 75.43, 73.70, 73.36, 73.31, 73.15, 72.93, 72.73, 72.59, 69.53, 69.39, 69.36, 69.33, 69.28, 69.24, 68.33, 63.69, 63.66, 40.95, 32.60, 32.56, 32.45, 31.02, 30.12, 29.93, 27.32, 27.15; ^{31}P NMR (121 MHz, $CDCl_3$) δ 0.33; HRMS-ESI (*m/z*): [M-H+2Na]$^{+}$ calculated for $C_{30}H_{54}O_{24}PSNa_2^{+}$, 907.2253; Found: 907.2244.

PIM$_4$: White solid (65%); ^{1}H NMR (600 MHz, D_2O) δ 5.17 (d, *J* = 1.8, 1H), 5.12 (d, *J* = 1.5, 1H), 4.90 (d, *J* = 1.6, 1H), 4.90 (d, *J* = 1.6, 1H), 4.35 – 4.28 (m, 1H), 4.22 – 4.16 (m, 1H), 4.15 (dd, *J* = 1.7, 3.2, 1H), 4.12 (dd, *J* = 1.9, 3.3, 1H), 4.10 – 4.06 (m, 1H), 4.03 – 3.89 (m, 8H), 3.89 – 3.73 (m, 13H), 3.73 – 3.55 (m, 8H), 3.37 (td, *J* = 3.3, 9.2, 1H), 2.84 – 2.72 (m, 1.5H), 2.56 (t, *J* = 7.2, 0.5H), 1.80 – 1.56 (m, 4H), 1.52 – 1.36 (m, 4H); ^{13}C NMR (150 MHz, D_2O) δ 104.26, 104.08, 102.22, 102.07, 81.40, 81.36, 81.02, 80.97, 79.09, 79.05, 75.65, 75.46, 75.42, 73.56, 73.47, 73.38, 73.26, 73.09, 72.89, 72.71, 72.69, 72.64, 72.56, 69.47, 69.36, 69.35, 69.22, 69.00, 68.96, 68.38, 68.09, 63.66, 63.61, 40.88, 35.63, 32.62, 32.58, 31.01, 29.94, 29.78, 27.31, 27.14, 26.40; ^{31}P NMR (121 MHz, $CDCl_3$) δ –0.49, –0.48; HRMS-ESI (*m/z*): [M-H]$^{-}$calculated for $C_{36}H_{64}O_{29}PS^{-}$, 1023.2997; Found: 1023.2990.

PIM$_5$: White solid (88%); ^{1}H NMR (500 MHz, D_2O) δ 5.05 (s, 1H), 5.02 (s, 1H), 5.01 (s, 1H), 4.92 (s, 1H), 4.79 (s, 1H), 4.20 (s, 1H), 4.11 – 3.44 (m, 39H), 3.26 (t, *J* = 9.1, 1H), 2.67 (t, *J* = 7.2, 1.5H), 2.41 (t, J = 7.3, 0.4H), 1.66 – 1.47 (m, 4H), 1.32 (m, 4H); ^{13}C NMR (125 MHz, D_2O) δ 102.48, 101.78, 101.61, 99.80, 98.33, 78.93, 78.48, 78.43, 76.64, 76.59, 73.44, 73.17, 72.99, 71.33, 71.05, 71.00, 70.91, 70.62, 70.56, 70.45, 70.42, 70.25, 70.20, 70.18, 70.09, 67.19, 67.15, 66.87, 66.84, 66.73, 66.53, 66.49, 66.20, 65.61, 61.37, 61.18, 61.14, 38.40, 33.17, 30.16, 30.11, 28.54, 27.47, 27.31, 24.85, 24.67, 23.94; ^{31}P NMR (121 MHz, $CDCl_3$) δ 0.38, 0.33; HRMS-ESI (*m/z*): $[M\text{-}H+2Na]^+$ calculated for $C_{42}H_{74}O_{34}PSNa_2^+$, 1231.3322; Found: 1231.3310.

PIM_6: White solid (52%); ^{1}H NMR (500 MHz, D_2O) δ 5.16 (d, J = 1.1, 1H), 5.04 (s, 1H), 4.99 (s, 1H), 4.98 (s, 1H), 4.91 (d, J = 1.4, 1H), 4.77 (s, 1H), 4.18 (s, 1H), 4.10 – 3.91 (m, 5H), 3.90 – 3.40 (m, 37H), 3.24 (t, J = 9.1, 1H), 2.65 (t, J = 7.3, 1H), 2.43 (t, J = 7.3, 0.3 H), 2.27 – 2.21 (m, 0.15H), 1.69 – 1.36 (m, 4H), 1.30 (s, 4H); ^{13}C NMR (125 MHz, D_2O) δ 102.43, 101.78, 101.61, 100.85, 99.81, 98.41, 78.99, 78.94, 78.90, 78.69, 78.49, 78.44, 76.65, 76.60, 73.46, 73.18, 72.98, 71.39, 71.01, 70.93, 70.62, 70.56, 70.46, 70.42, 70.24, 70.20, 70.17, 70.09, 67.31, 67.17, 67.06, 66.87, 66.82, 66.71, 66.54, 66.49, 66.23, 65.57, 61.35, 61.29, 61.16, 61.14, 38.40, 33.17, 30.16, 30.11, 28.54, 27.48, 27.31, 24.84, 24.67, 23.93; ^{31}P NMR (121 MHz, $CDCl_3$) δ –0.50, –0.47; HRMS-ESI (*m/z*): $[M\text{-}H]^-$ calculated for $C_{48}H_{84}O_{39}PS^-$, 1347.4054; Found: 1347.4049.

References:

1. Takahashi, H.; Kittaka, H. and Ikegami, S., *J. Org. Chem.* **2001**, 66, 2705-2716.

2. Elie, C. J. J.; Verduyn, R.; Dreef, C. E.; Brounts, D. M.; Vandermarel, G. A.; Van Boom, J. H., *Tetrahedron* **1990,** *46*, 8243-8254.

3. Kwon, Y. U.; Soucy, R. L.; Snyder, D. A. and Seeberger, P. H., *Chem. Eur. J.* **2005**, *11*, 2493-2504.

4. Liu, X.; Stocker, B. L. and Seeberger, P. H. *J. Am. Chem. Soc.* **2006**, *128*, 3638-3648.

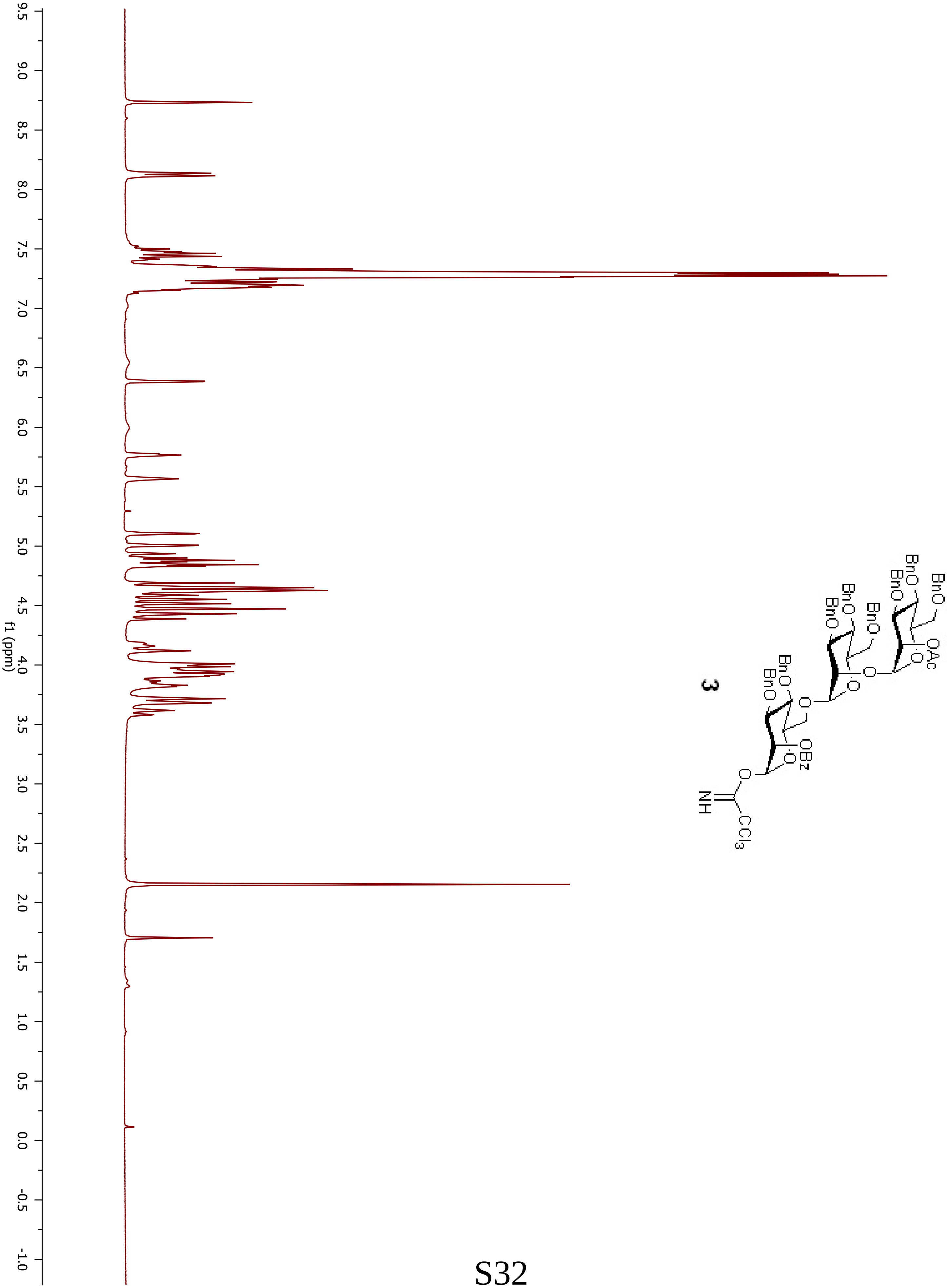
f1 (ppm)
9.5 9.0 8.5 8.0 7.5 7.0 6.5 6.0 5.5 5.0 4.5 4.0 3.5 3.0 2.5 2.0 1.5 1.0 0.5 0.0 -0.5 -1.0
BnO
BnO
BnO
OAc
O
BnO
BnO
BnO
O
BnO
BnO
OBz
O
NH
CCl3
3

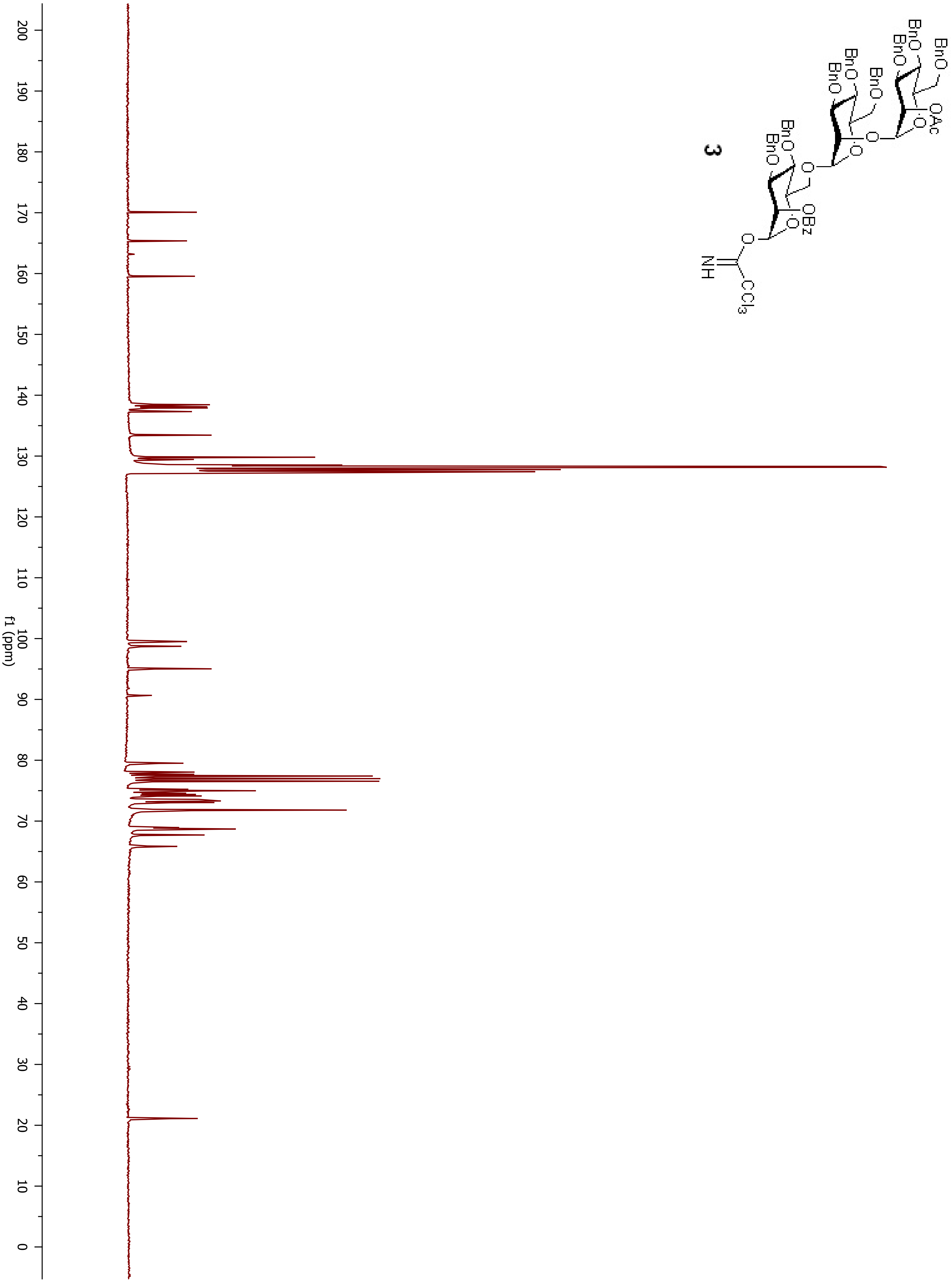

3
f1 (ppm)

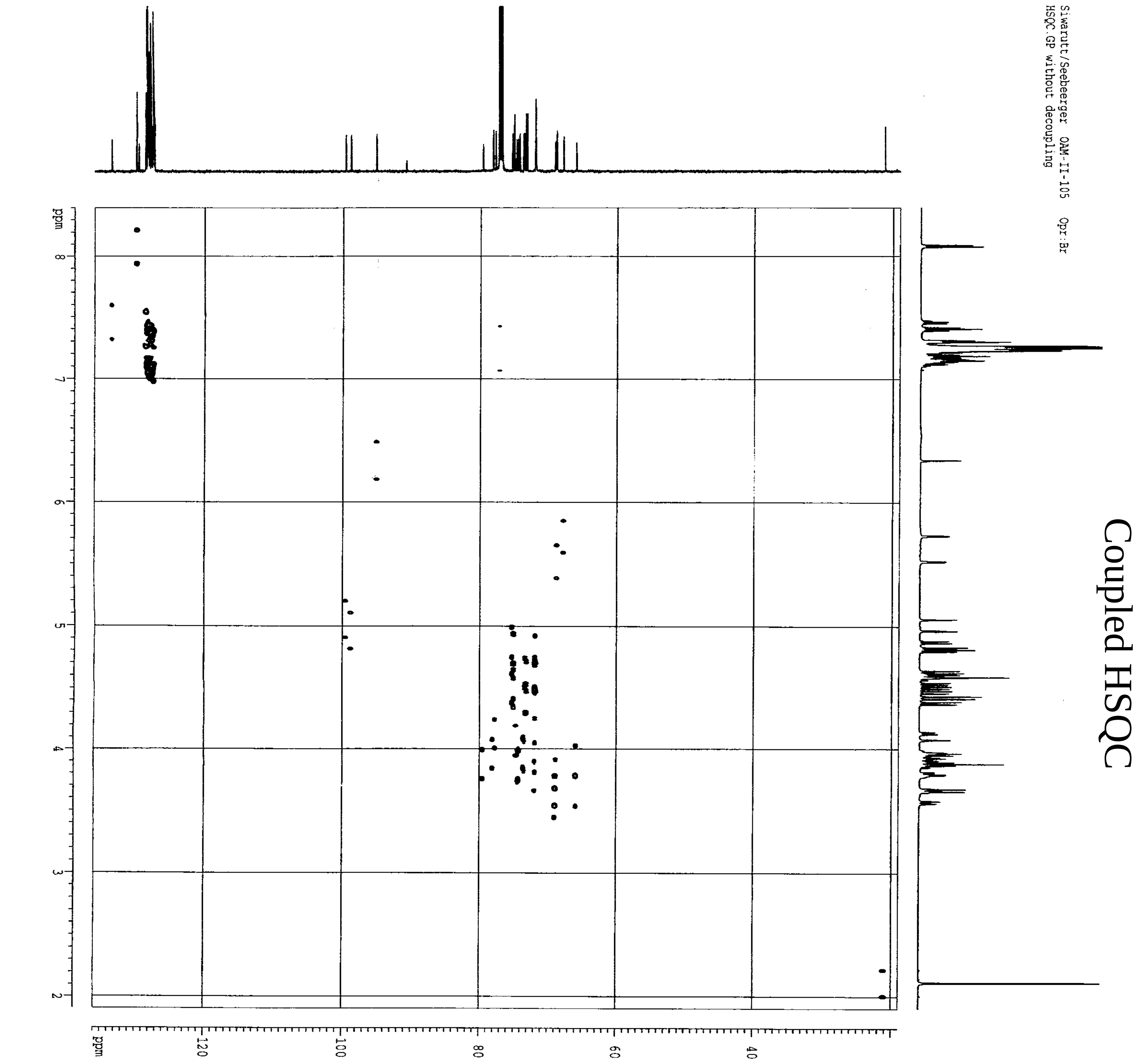
Coupled HSQC
Siwarutt/Seebeerger OAM-II-105 Opr:Br
HSQC.GP without decoupling
ppm

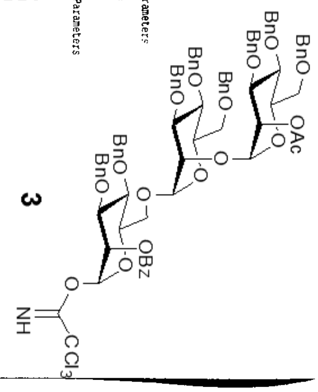
BnO
OAc
OBz
NH
CCl3

3

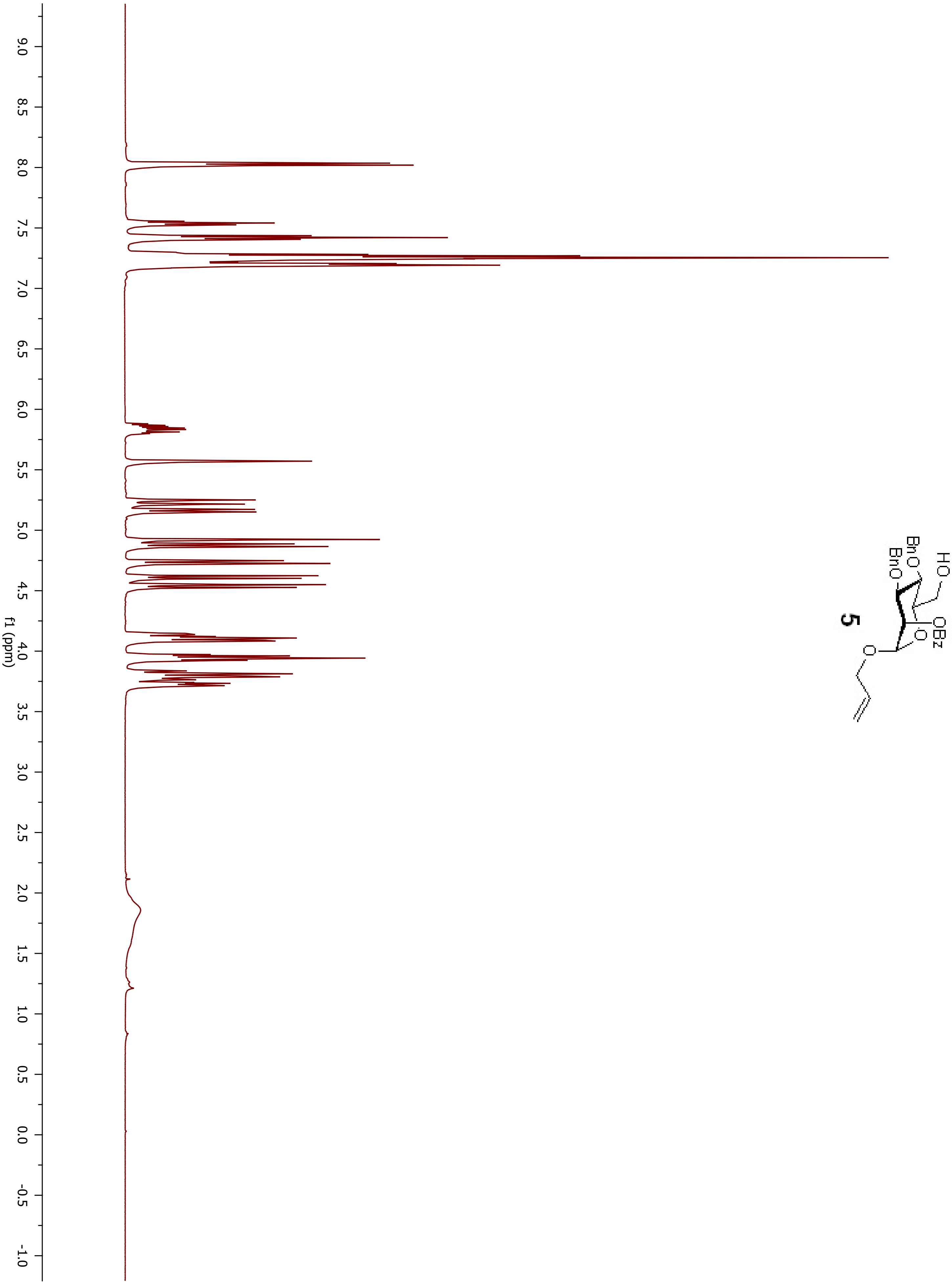
f1 (ppm)
9.0
8.5
8.0
7.5
7.0
6.5
6.0
5.5
5.0
4.5
4.0
3.5
3.0
2.5
2.0
1.5
1.0
0.5
0.0
-0.5
-1.0
HO
BnO
BnO
OBz
O
O
5

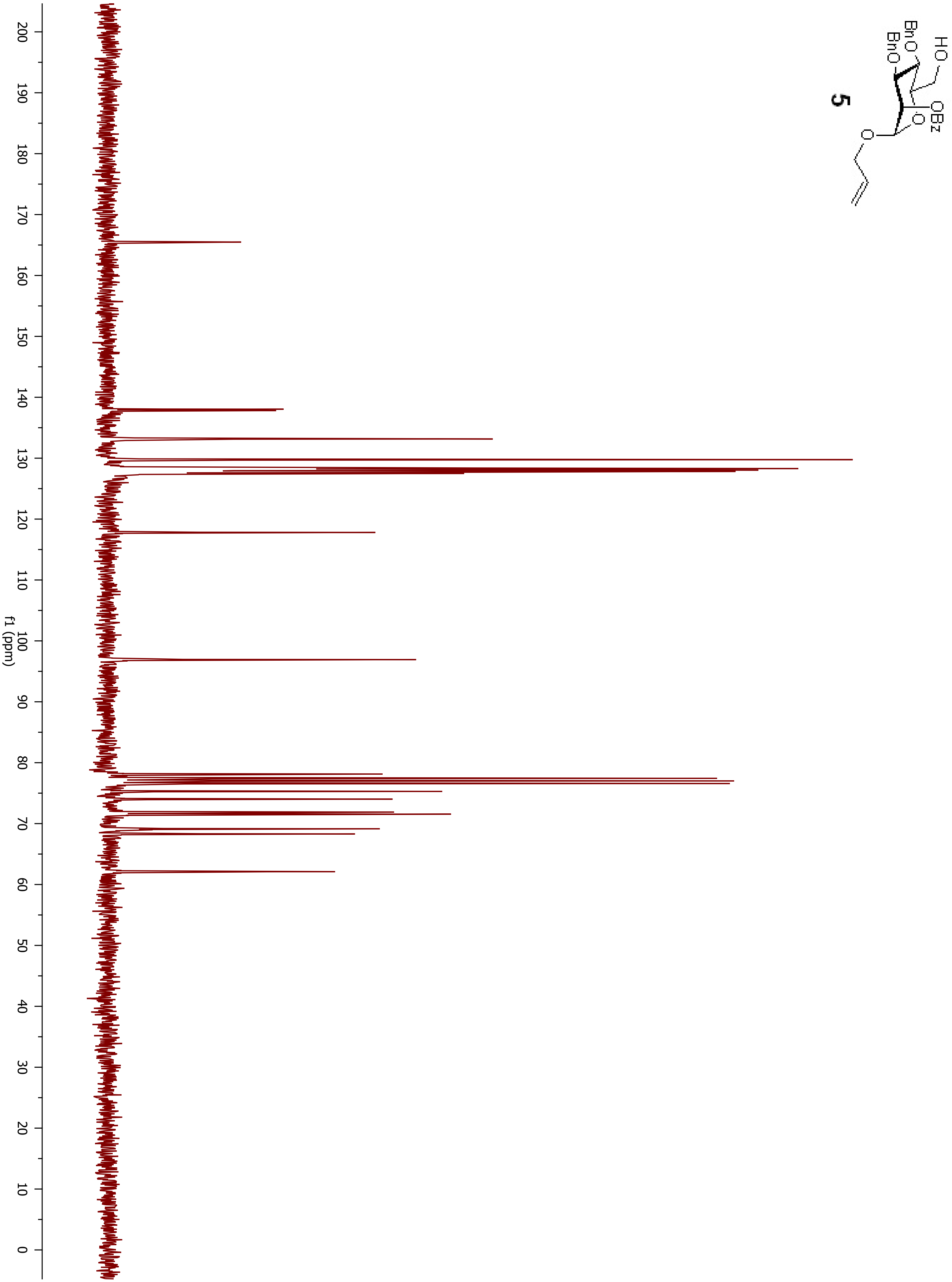
HO
BnO
BnO
OBz
O
O
5
f1 (ppm)

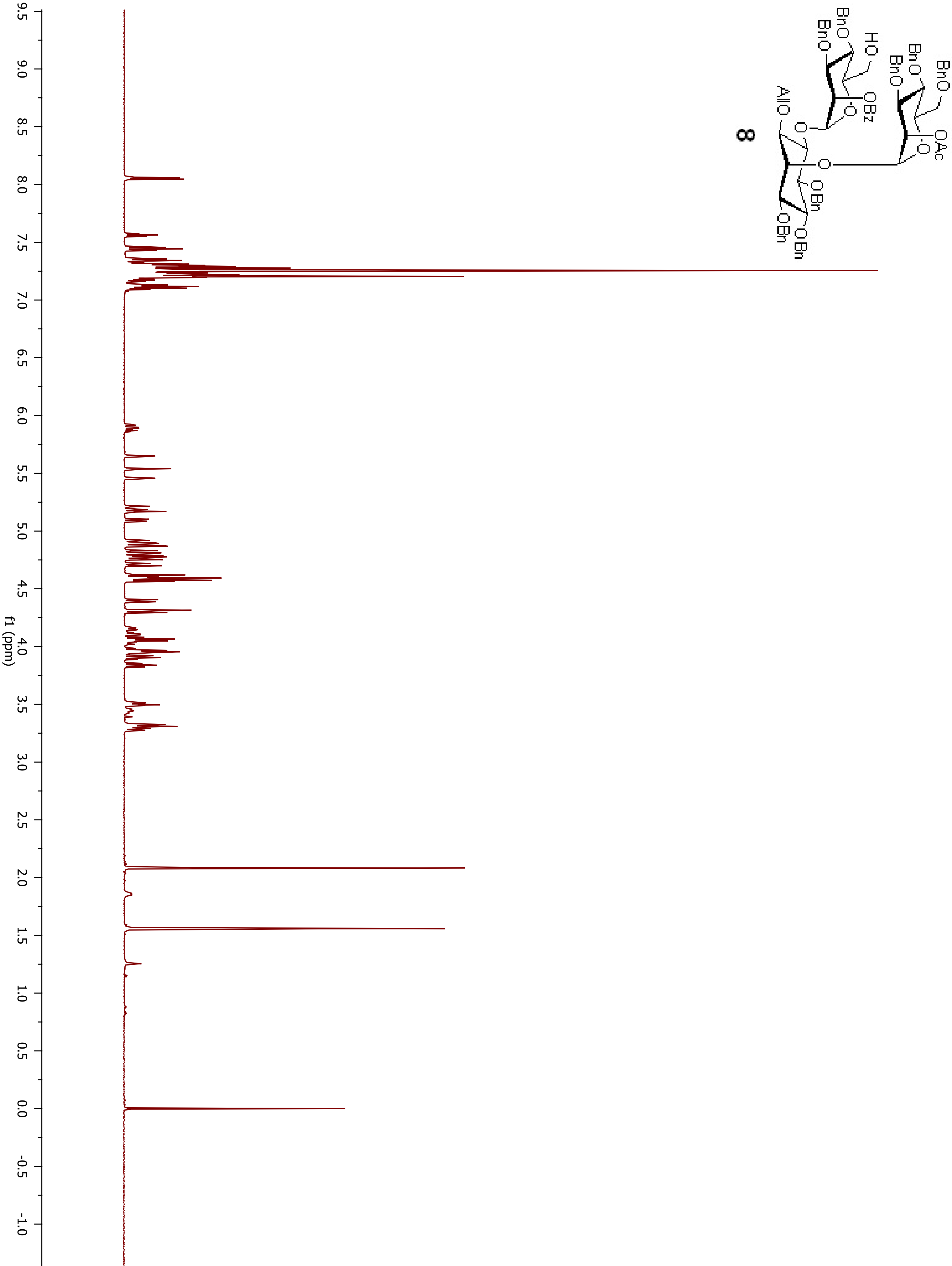
BnO
BnO
BnO
OAc
O
HO
BnO
BnO
OBz
O
O
AllO
OBn
OBn
OBn
8
f1 (ppm)

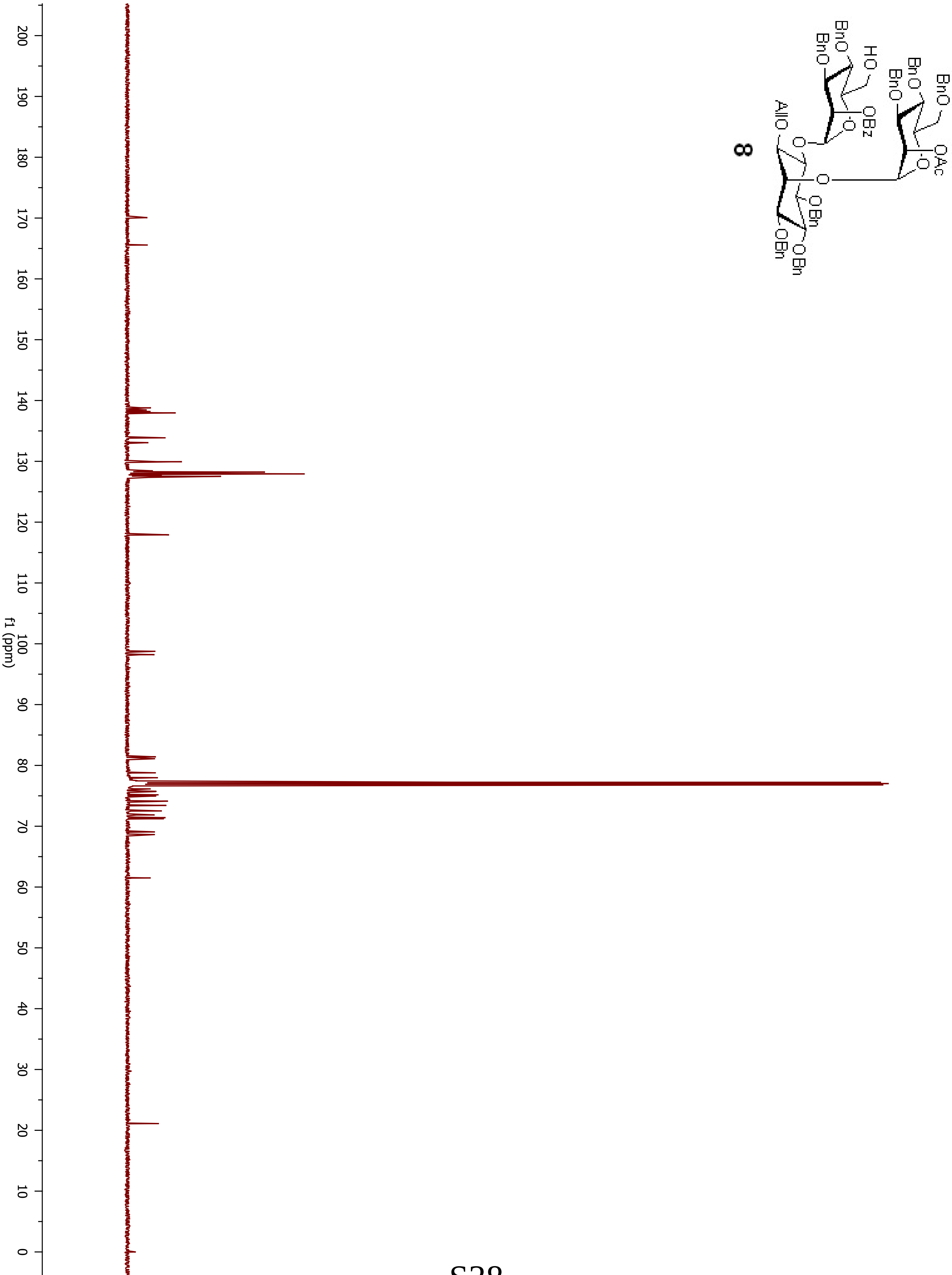
BnO
BnO
BnO
OAc
O
BnO
BnO
HO
OBz
O
AllO
O
O
OBn
OBn
OBn
8
f1 (ppm)
200
190
180
170
160
150
140
130
120
110
100
90
80
70
60
50
40
30
20
10
0

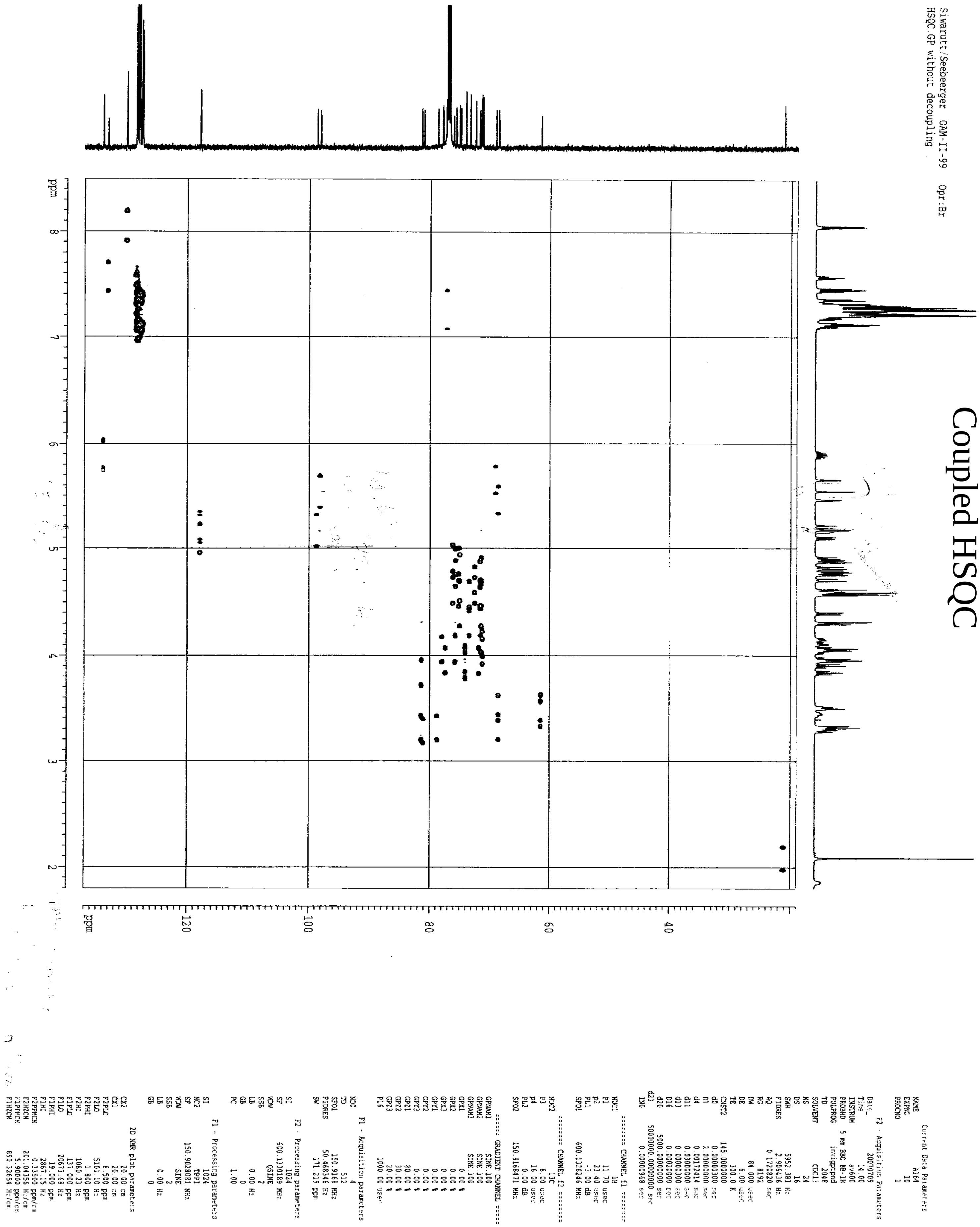
Coupled HSQC
Siwarutt/Seeberger OAM-II-99 Opr:Br
HSQC.GP without decoupling
ppm

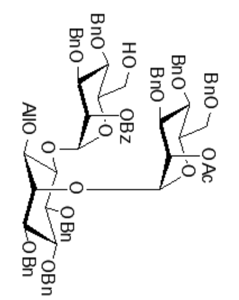
BnO
OAc
BnO
BnO
HO
OBz
BnO
BnO
AllO
OBn
OBn
OBn

8

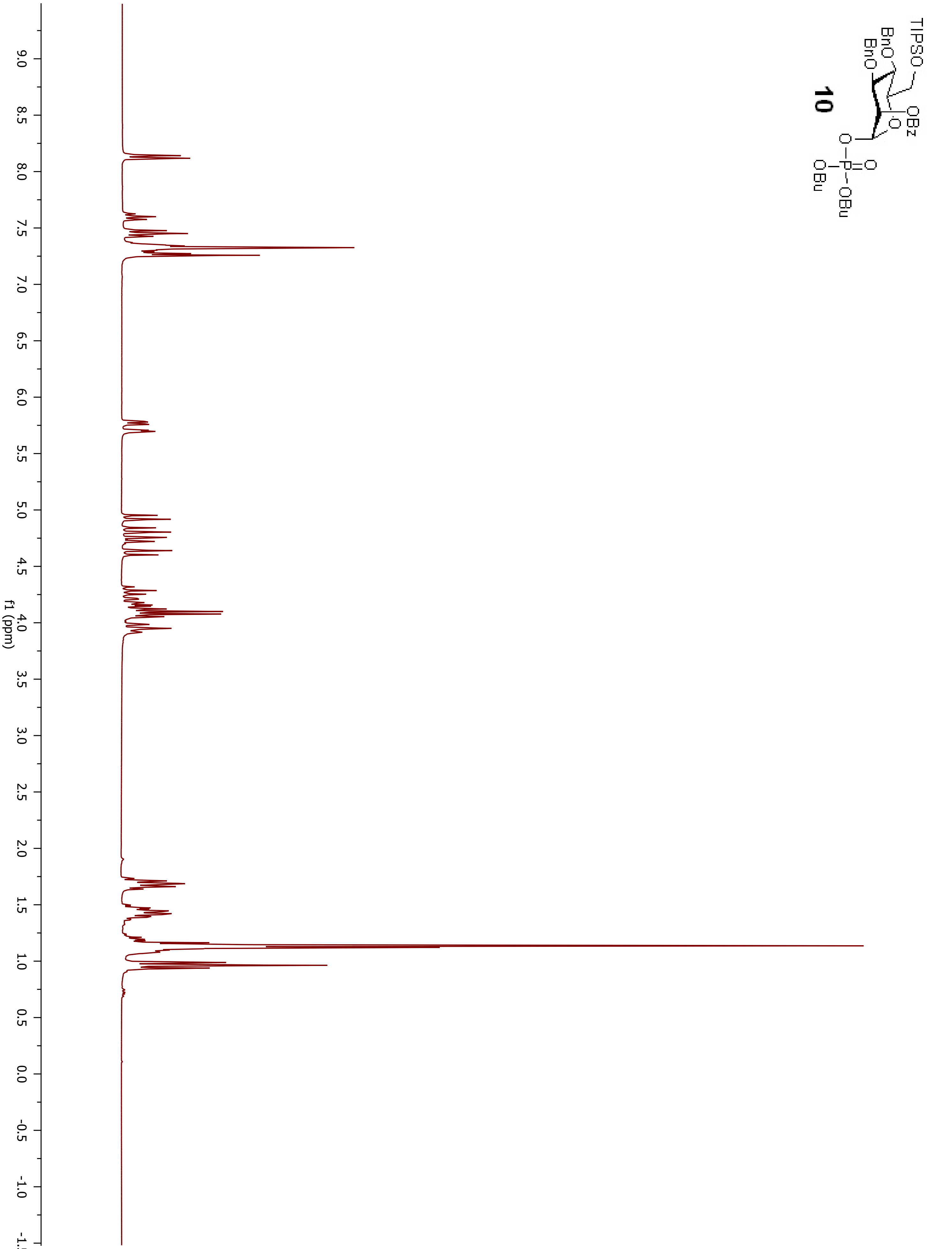
TIPSO
BnO
BnO
OBz
O
O
O
P
OBu
OBu
10
9.0
8.5
8.0
7.5
7.0
6.5
6.0
5.5
5.0
4.5
4.0
3.5
3.0
2.5
2.0
1.5
1.0
0.5
0.0
-0.5
-1.0
-1.5
f1 (ppm)

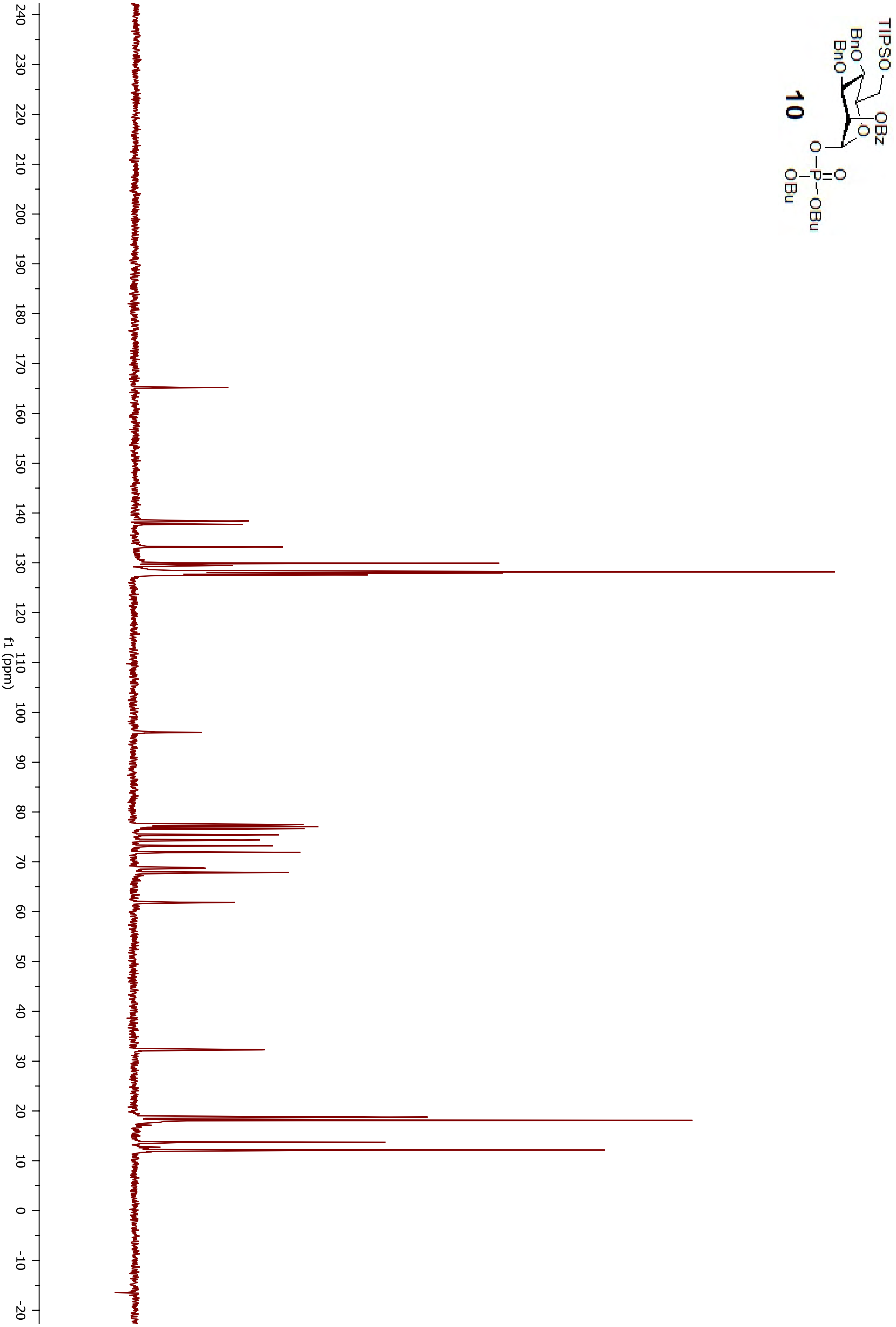

10

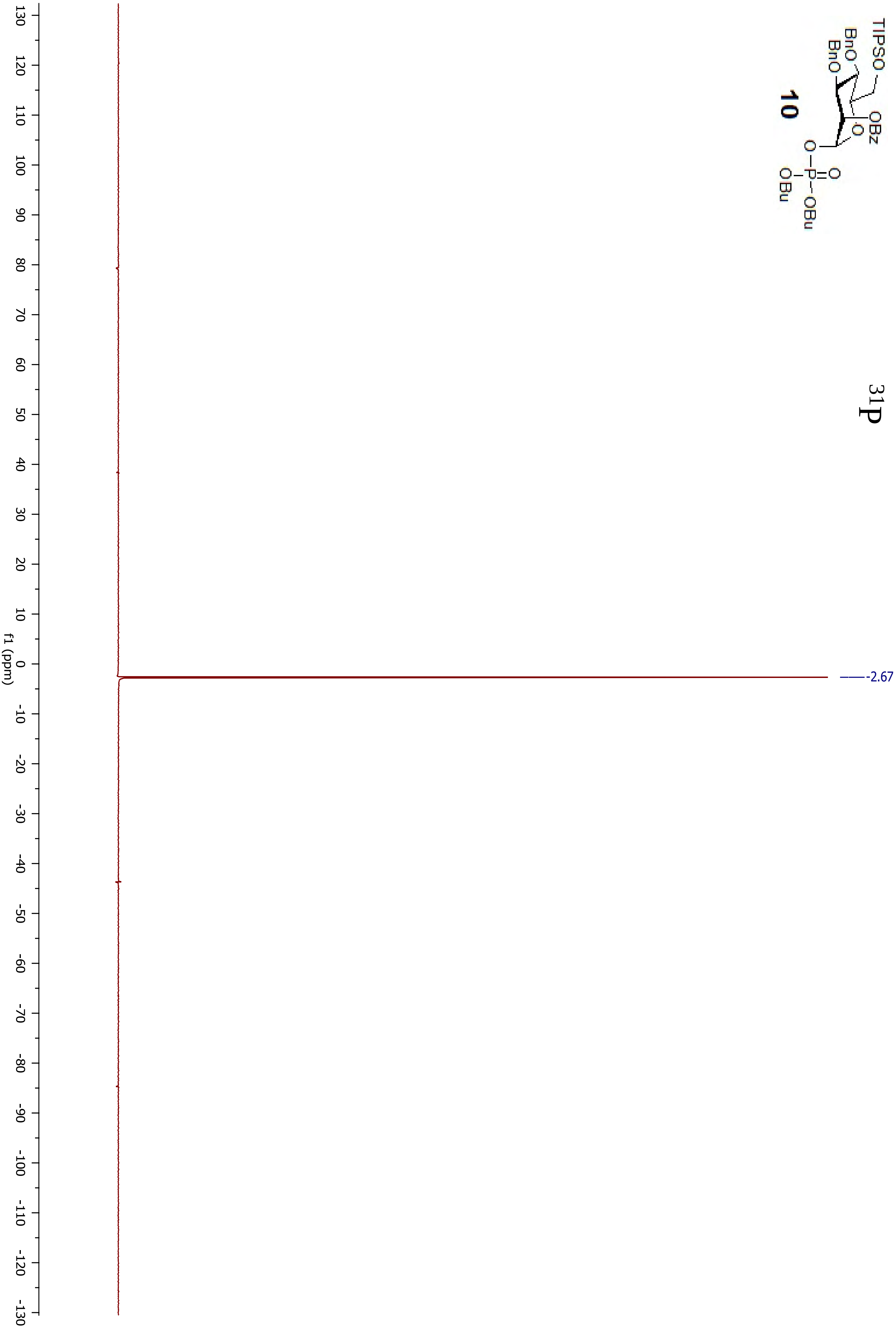

31P
10
TIPSO
BnO
BnO
OBz
O
O
P
OBu
OBu
-2.67
f1 (ppm)

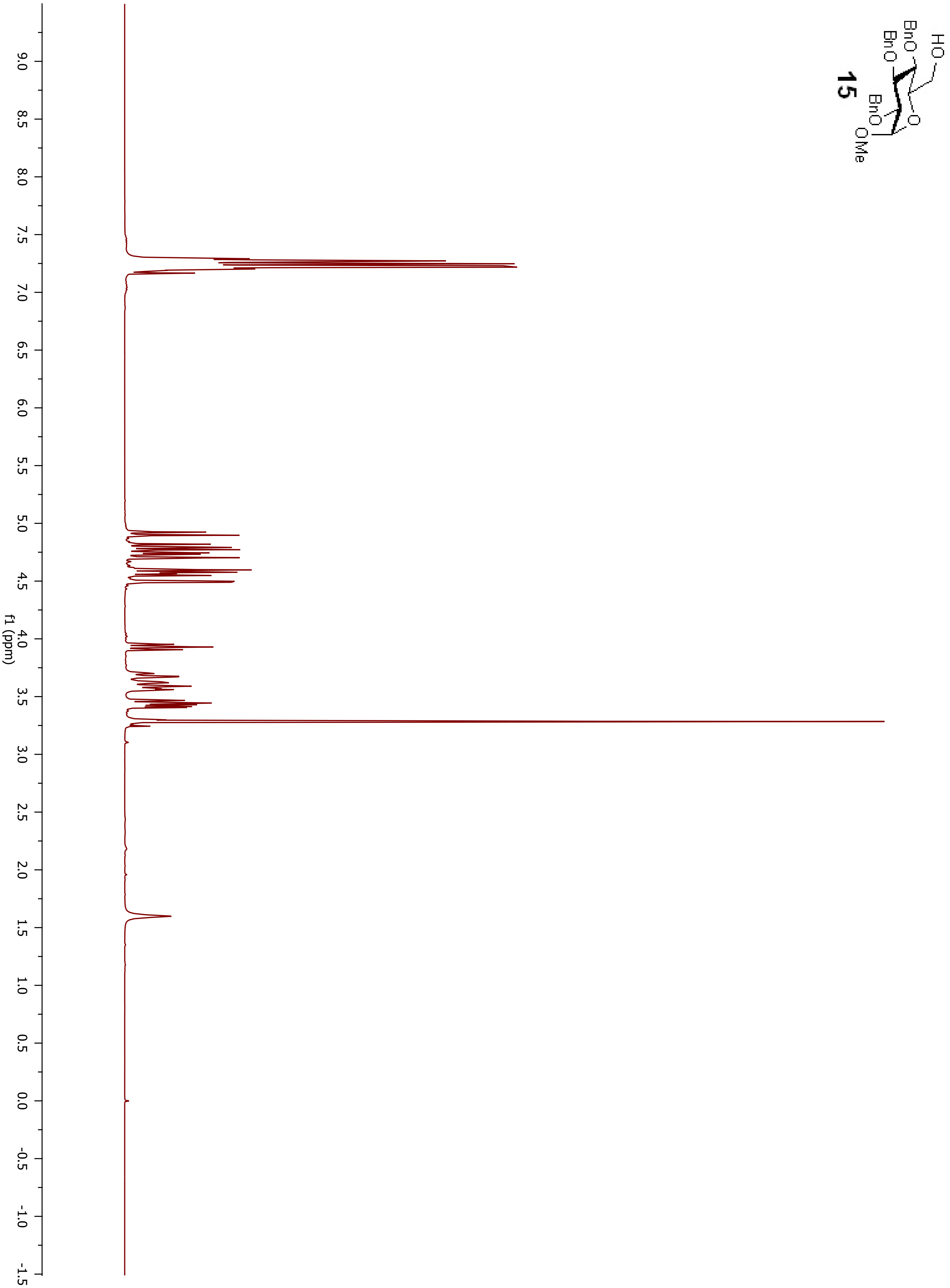
HO
BnO
BnO
O
BnO
OMe
15
f1 (ppm)
9.0
8.5
8.0
7.5
7.0
6.5
6.0
5.5
5.0
4.5
4.0
3.5
3.0
2.5
2.0
1.5
1.0
0.5
0.0
-0.5
-1.0
-1.5

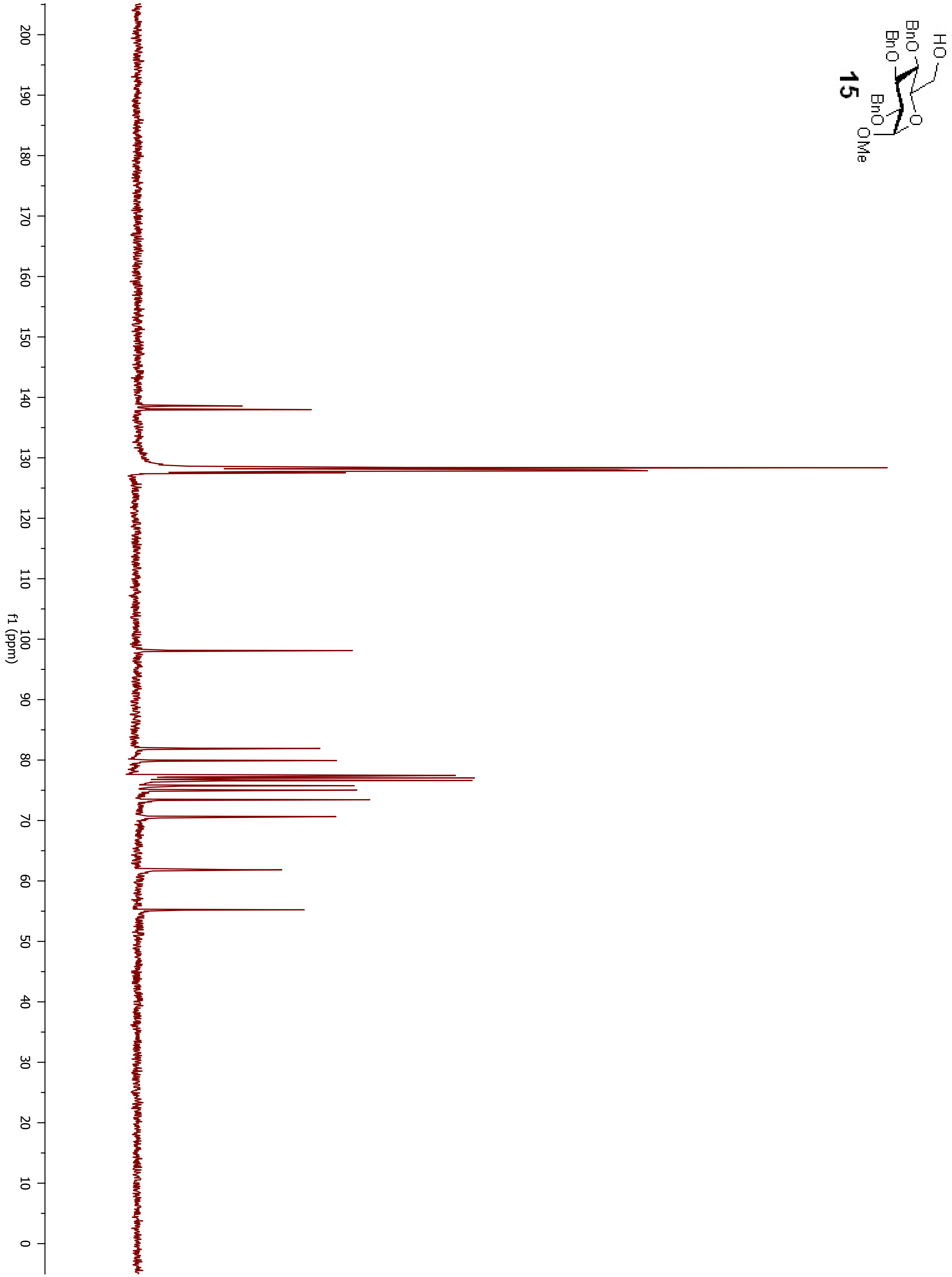
HO
BnO
BnO
BnO
O
OMe
15
f1 (ppm)
200
190
180
170
160
150
140
130
120
110
100
90
80
70
60
50
40
30
20
10
0

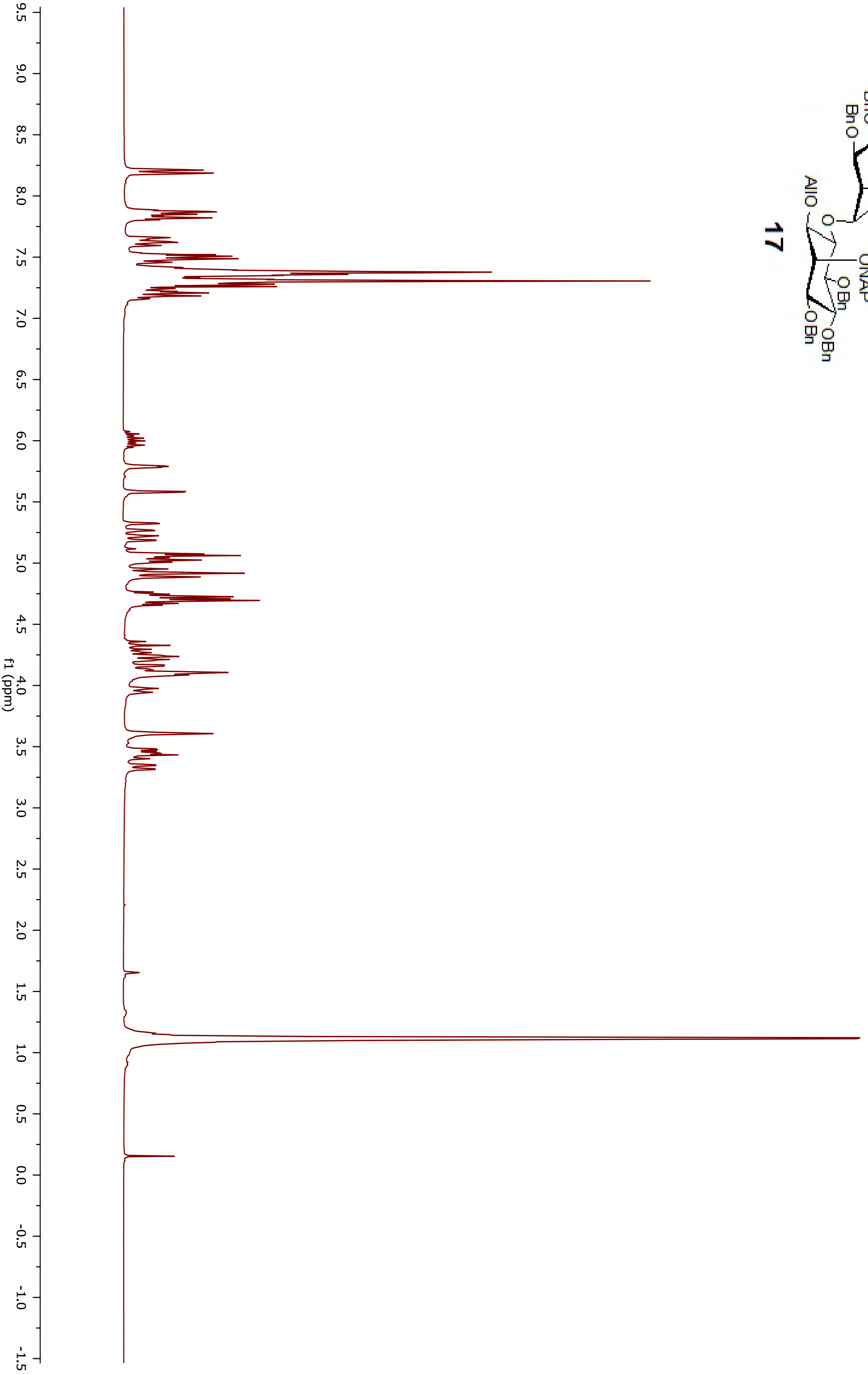
TIPSO
BnO
BnO
OBz
O
AllO
O
ONAP
OBn
OBn
OBn
17
9.5
9.0
8.5
8.0
7.5
7.0
6.5
6.0
5.5
5.0
4.5
4.0
3.5
3.0
2.5
2.0
1.5
1.0
0.5
0.0
-0.5
-1.0
-1.5
f1 (ppm)

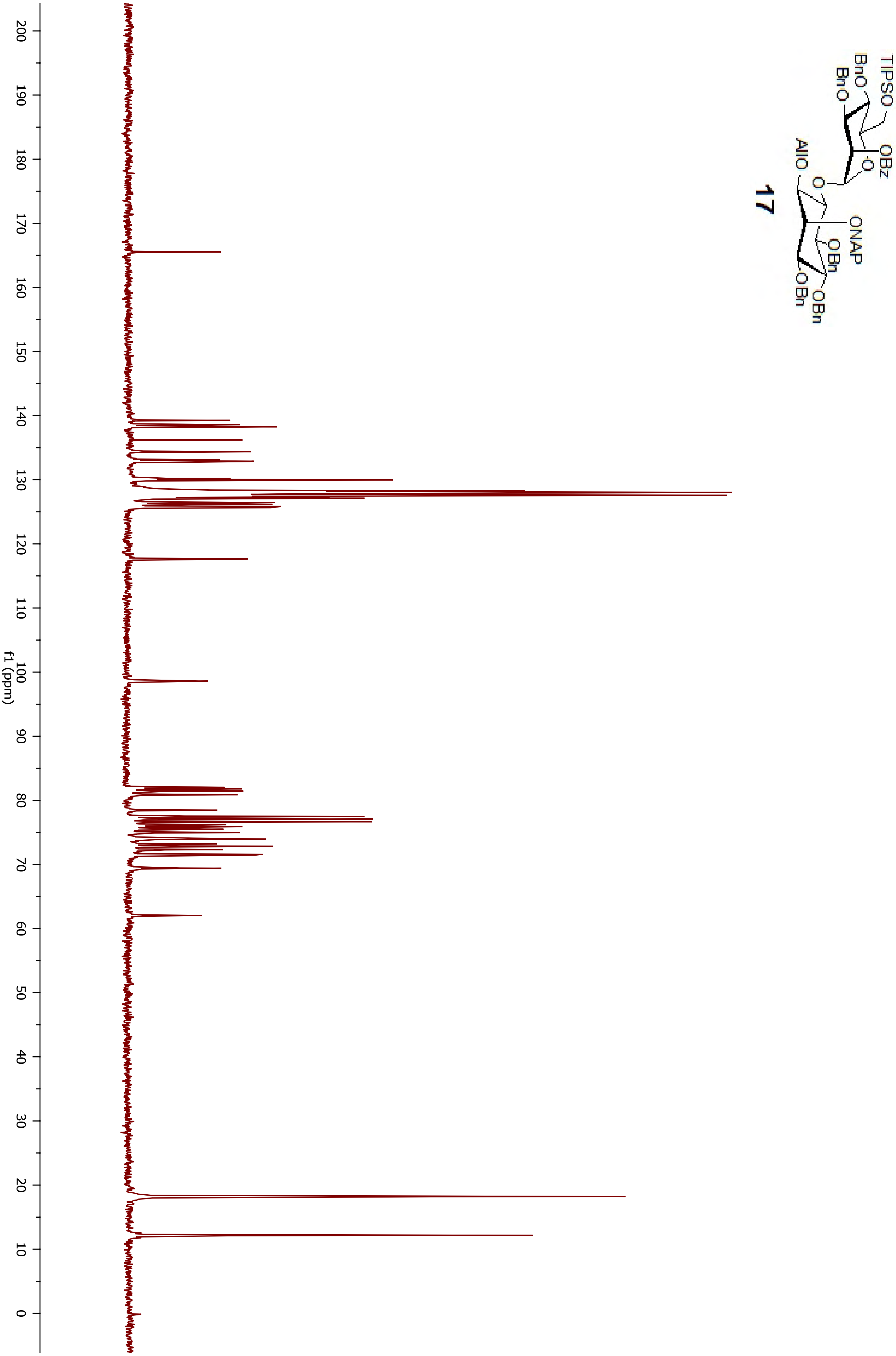
TIPSO
BnO
BnO
OBz
O
O
AllO
ONAP
OBn
OBn
OBn
17
f1 (ppm)

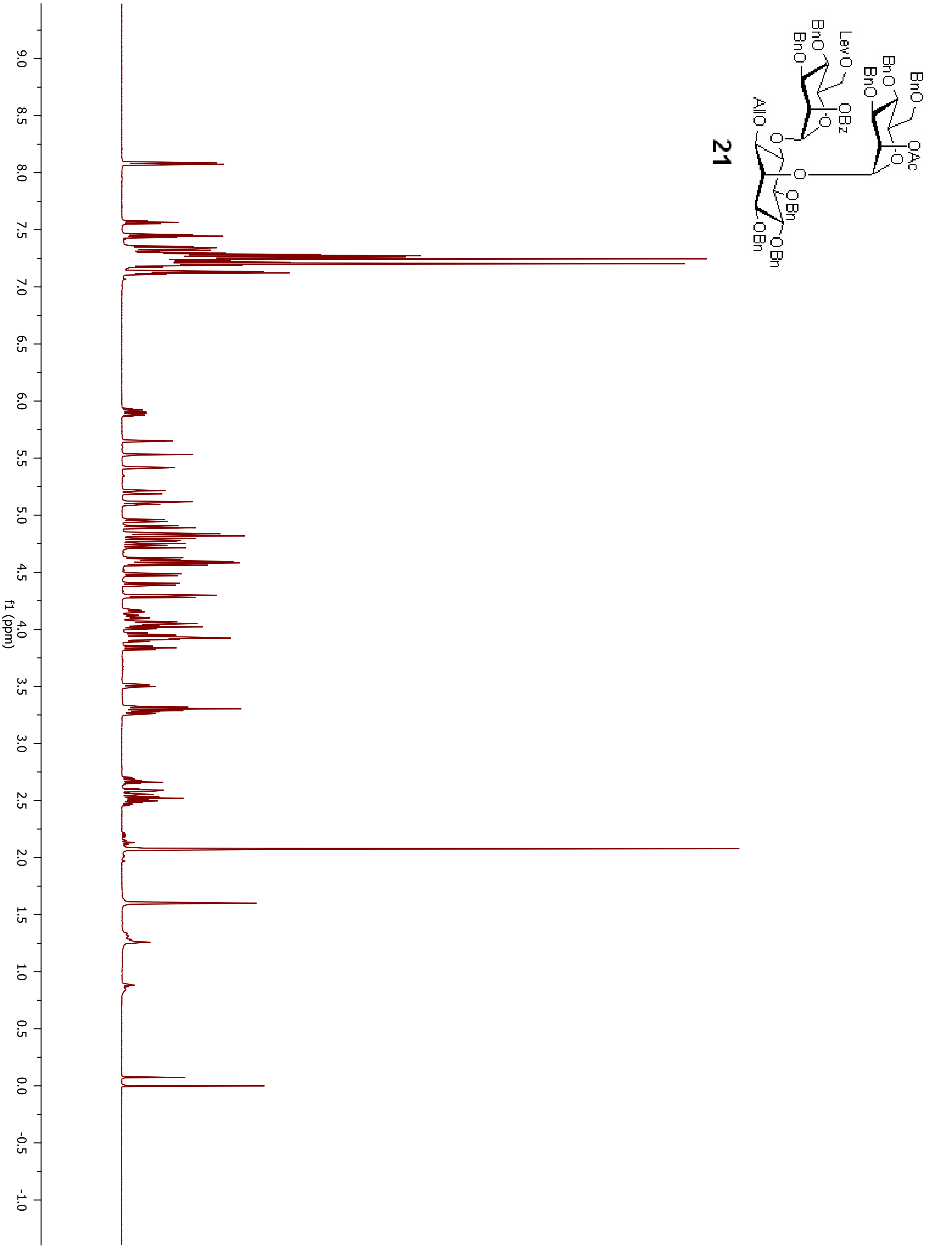

f1 (ppm)
9.0
8.5
8.0
7.5
7.0
6.5
6.0
5.5
5.0
4.5
4.0
3.5
3.0
2.5
2.0
1.5
1.0
0.5
0.0
-0.5
-1.0
BnO
OAc
LevO
OBz
AllO
OBn

21

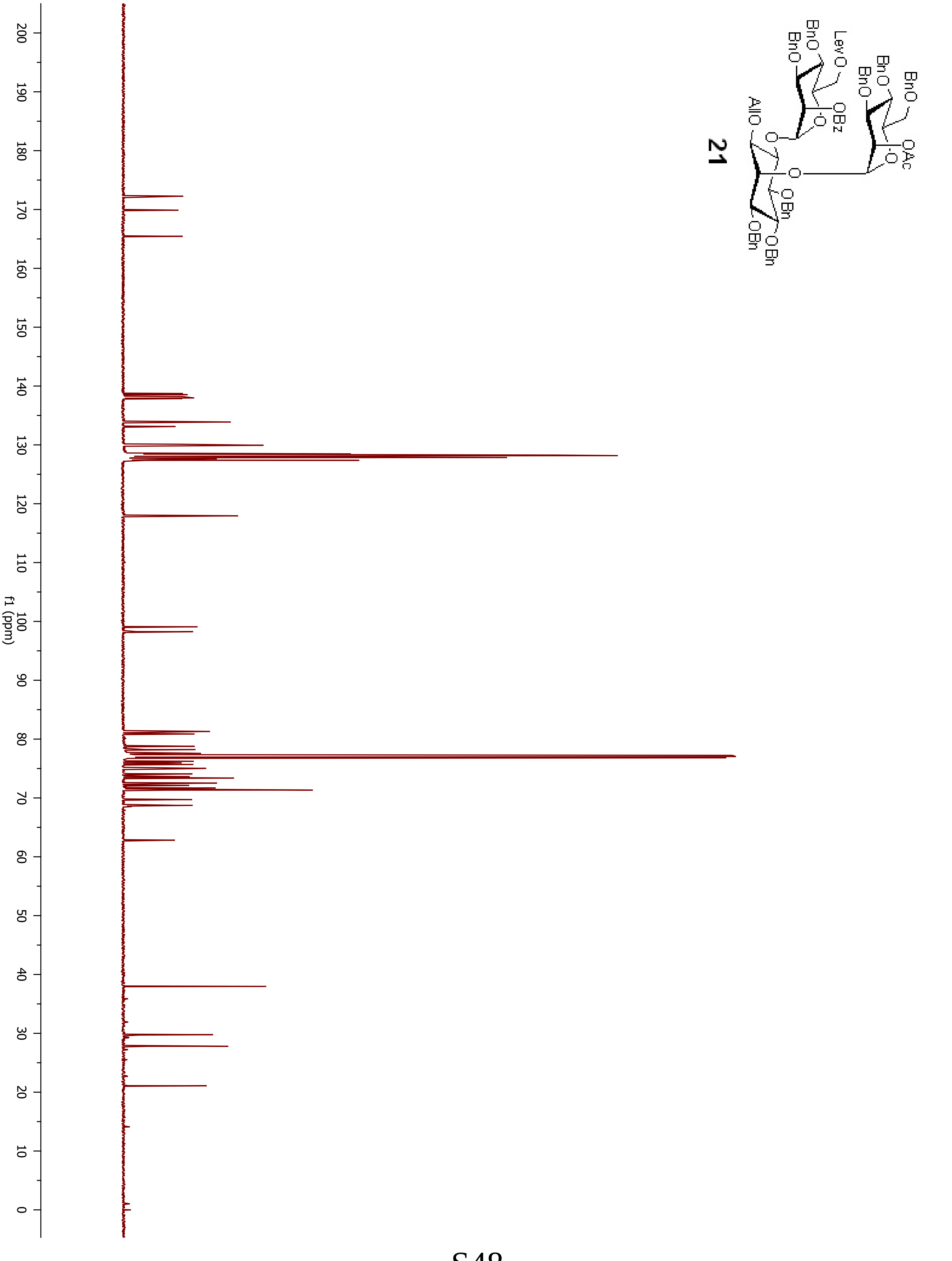
21
BnO
OAc
O
BnO
BnO
OBz
LevO
AllO
OBn
200
190
180
170
160
150
140
130
120
110
100
90
80
70
60
50
40
30
20
10
0
f1 (ppm)

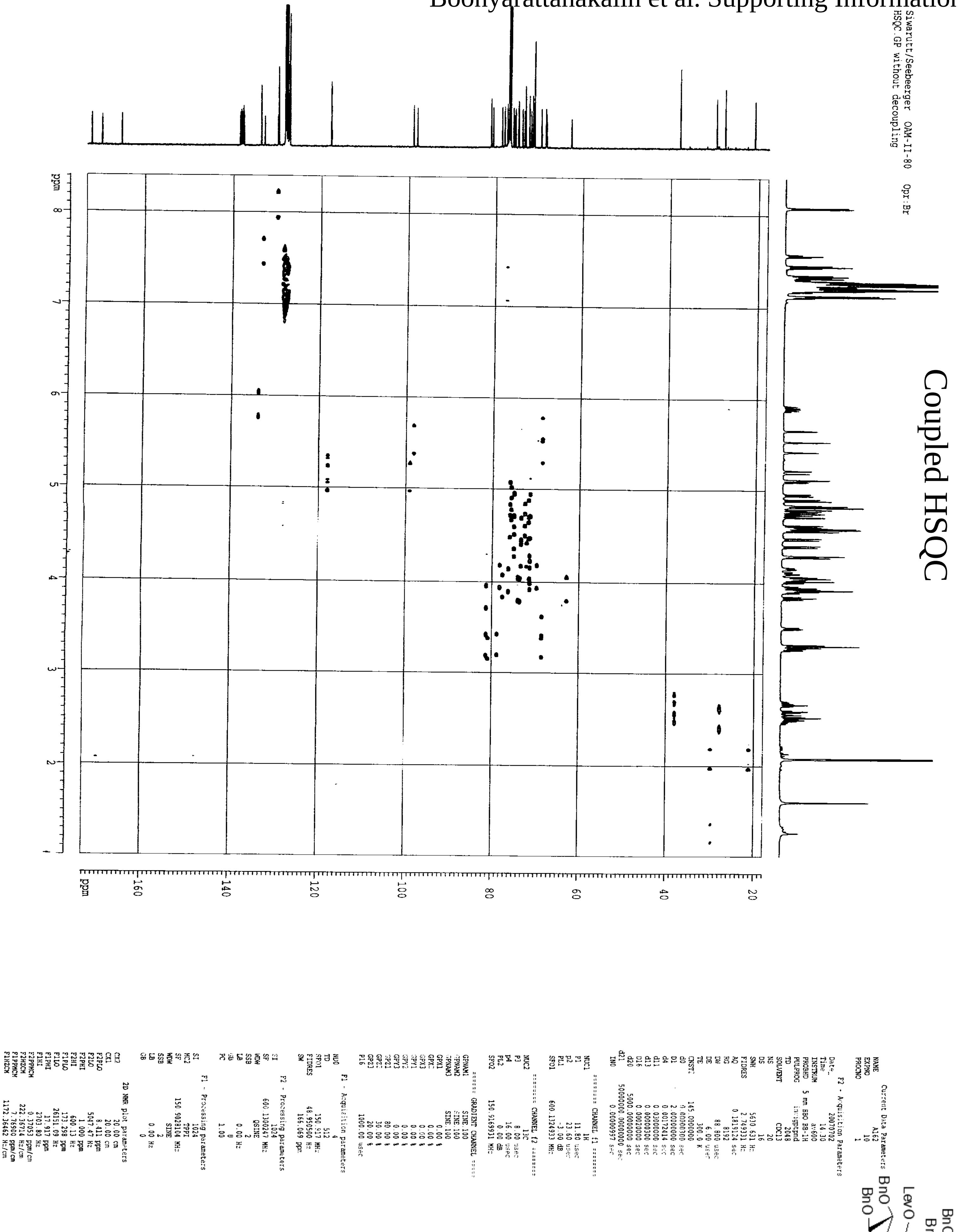
Siwarutt/Seeberger OAM-II-80 Opr:Br
HSQC.GP without decoupling
Coupled HSQC
ppm

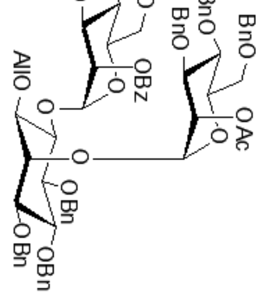
BnO
OAc
BnO
BnO
OBZ
LevO
BnO
BnO
AllO
O
OBn
OBn
OBn

21

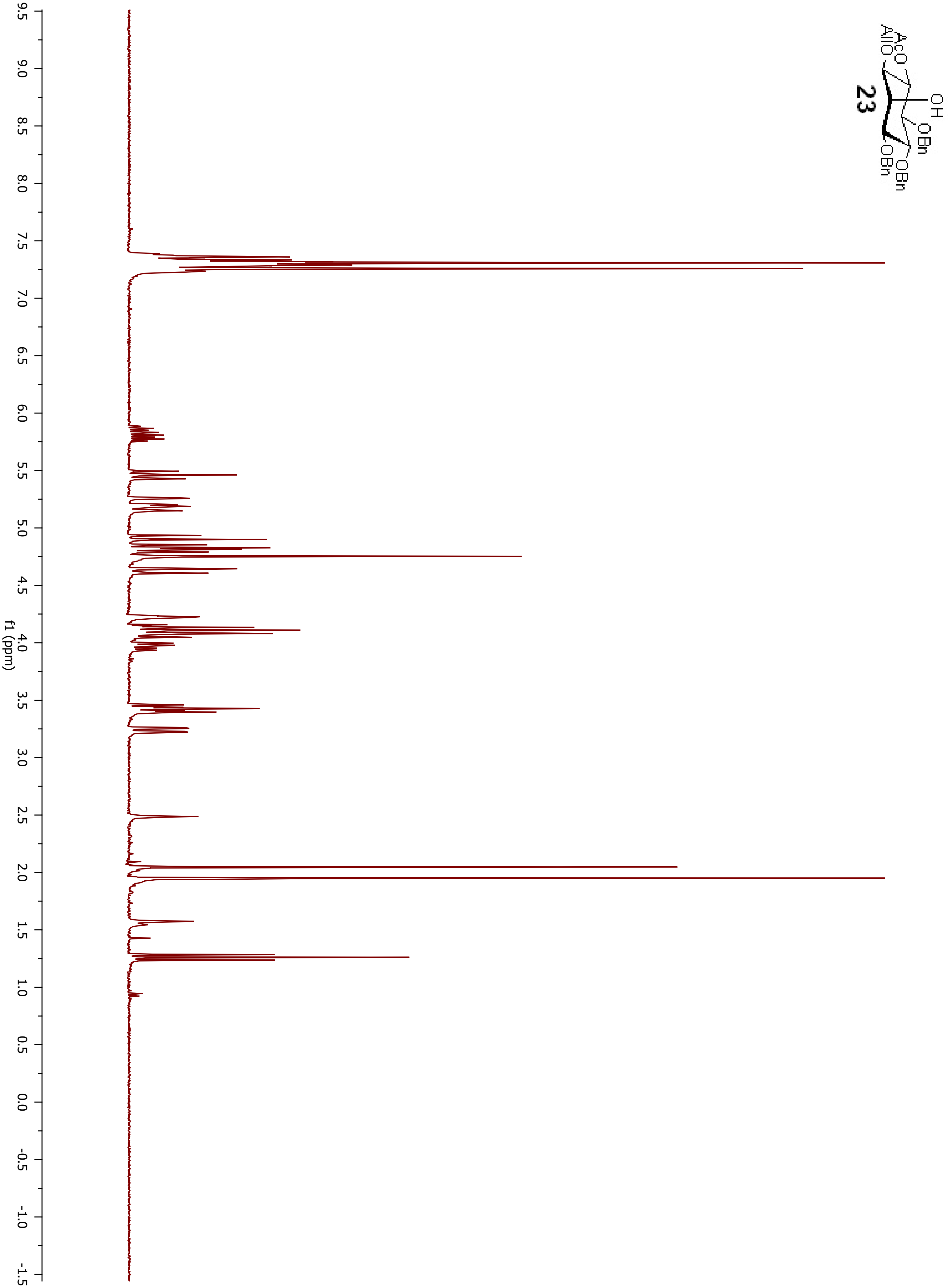
AcO
AllO
OH
OBn
OBn
OBn
23
f1 (ppm)

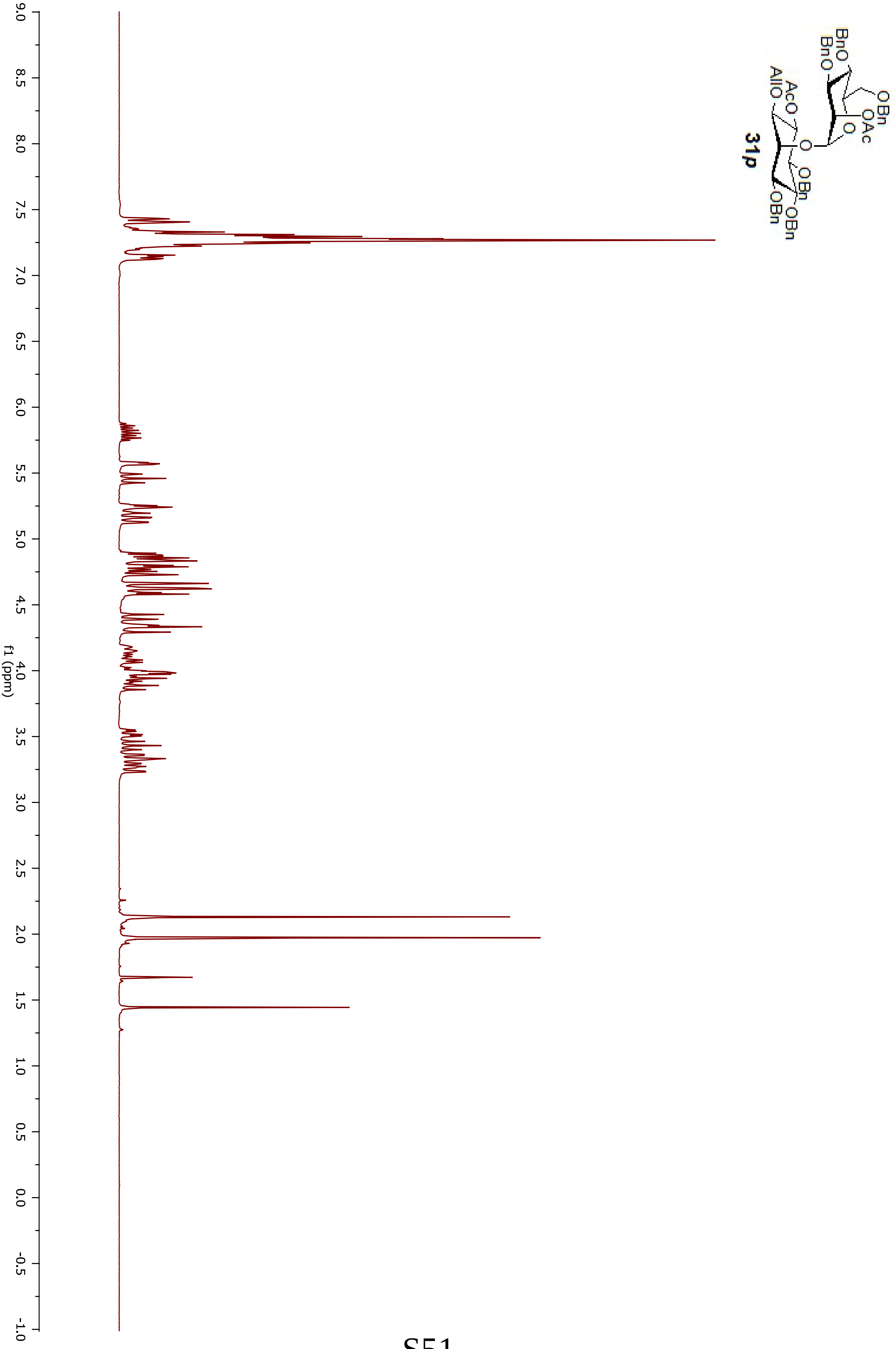
31p
f1 (ppm)

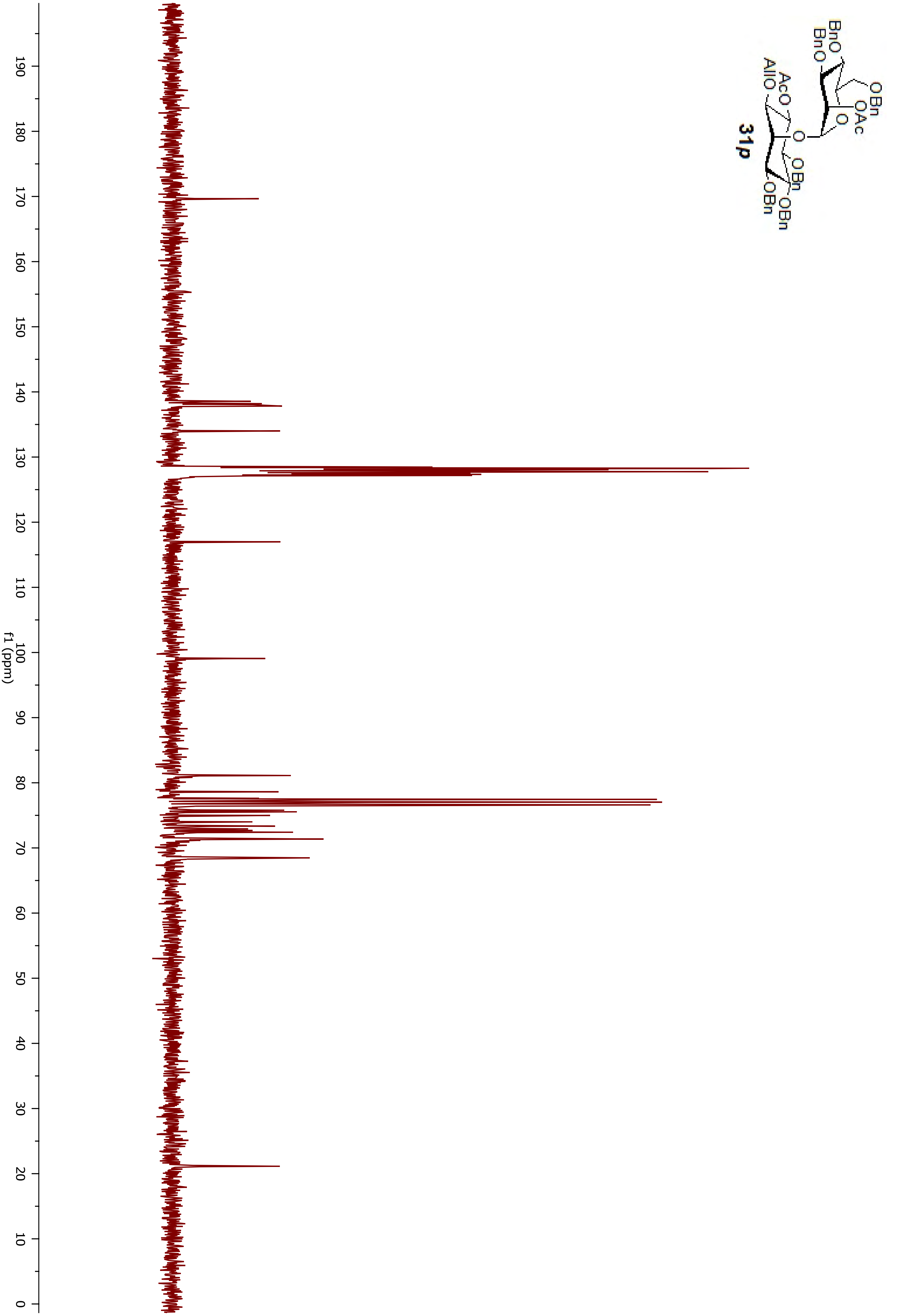
31p
f1 (ppm)

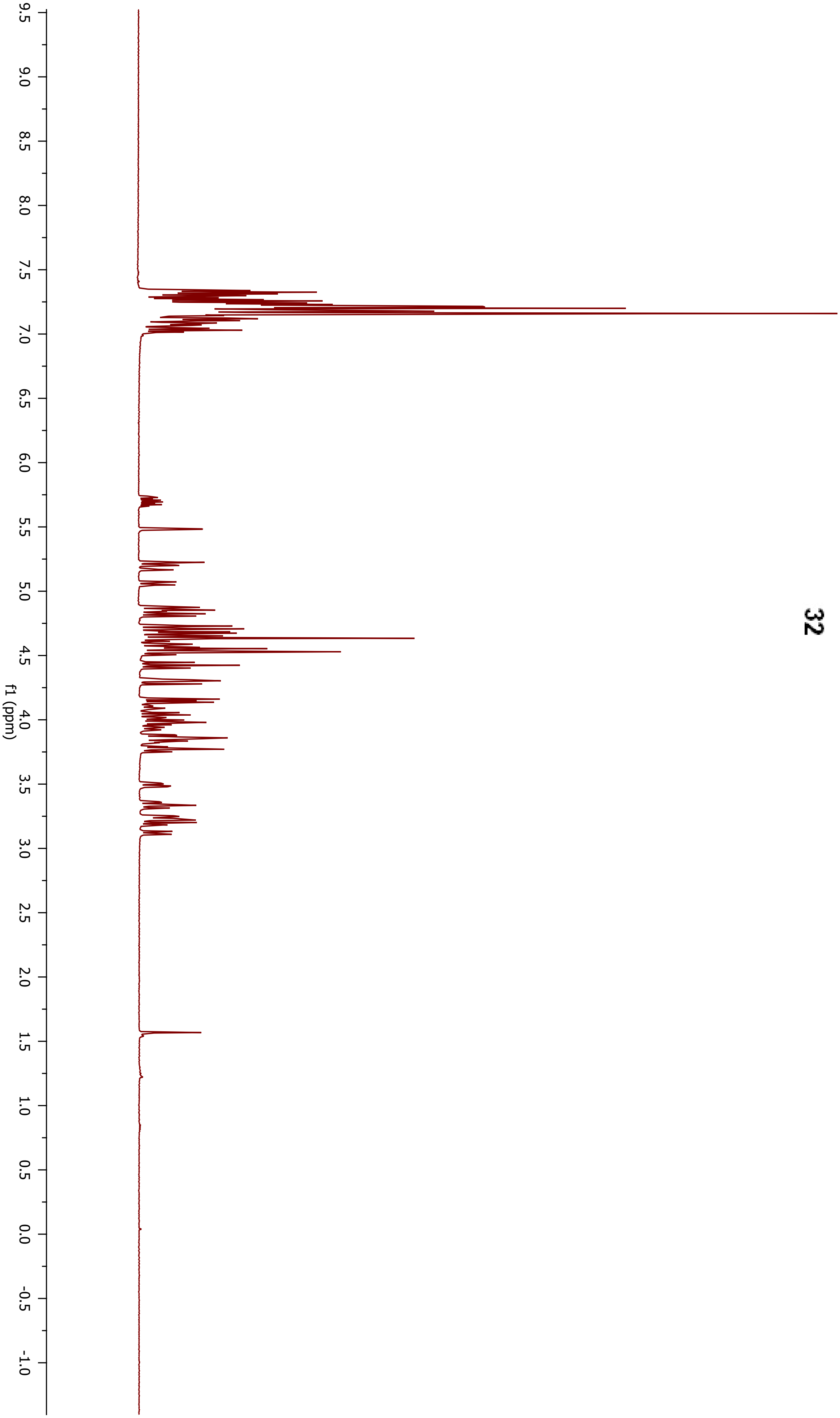

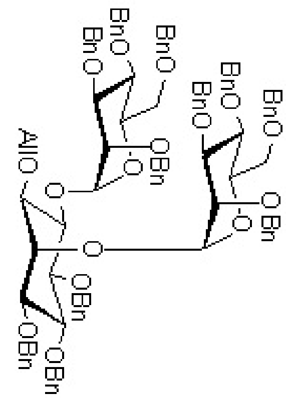

32

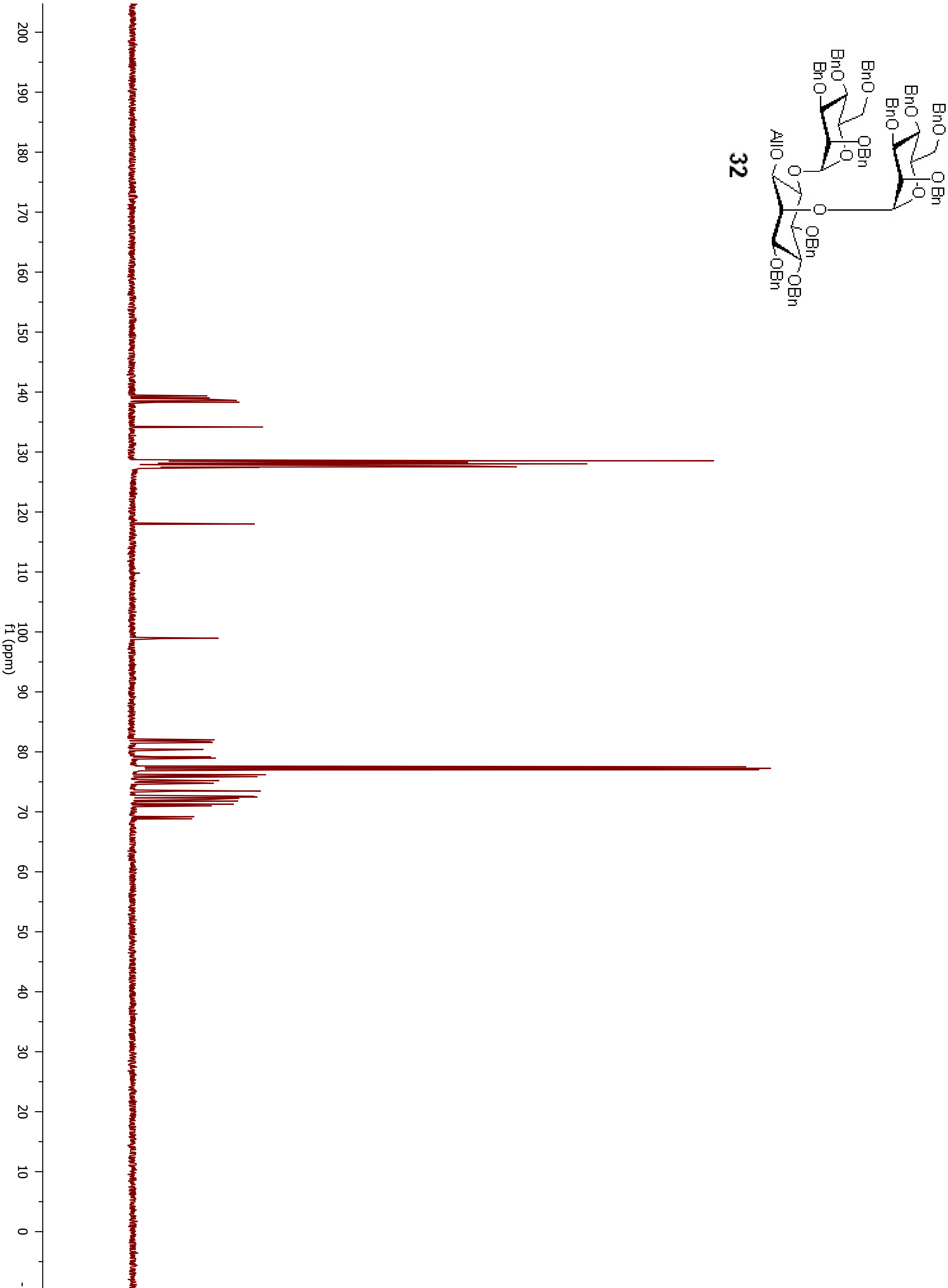

BnO
BnO
BnO
OBn
O
AllO
OBn
OBn
OBn
f1 (ppm)
200
190
180
170
160
150
140
130
120
110
100
90
80
70
60
50
40
30
20
10
0
-10

32

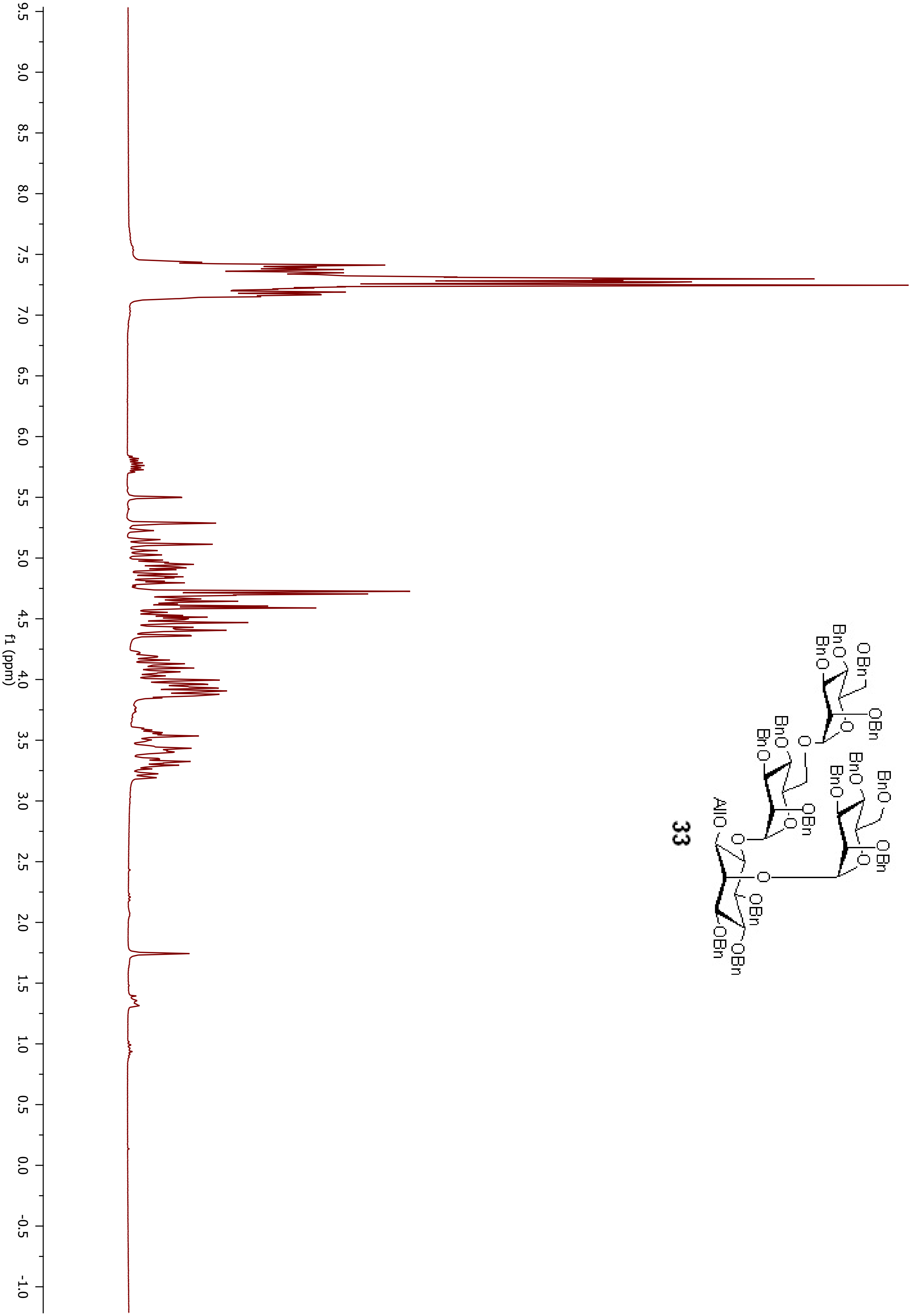

33

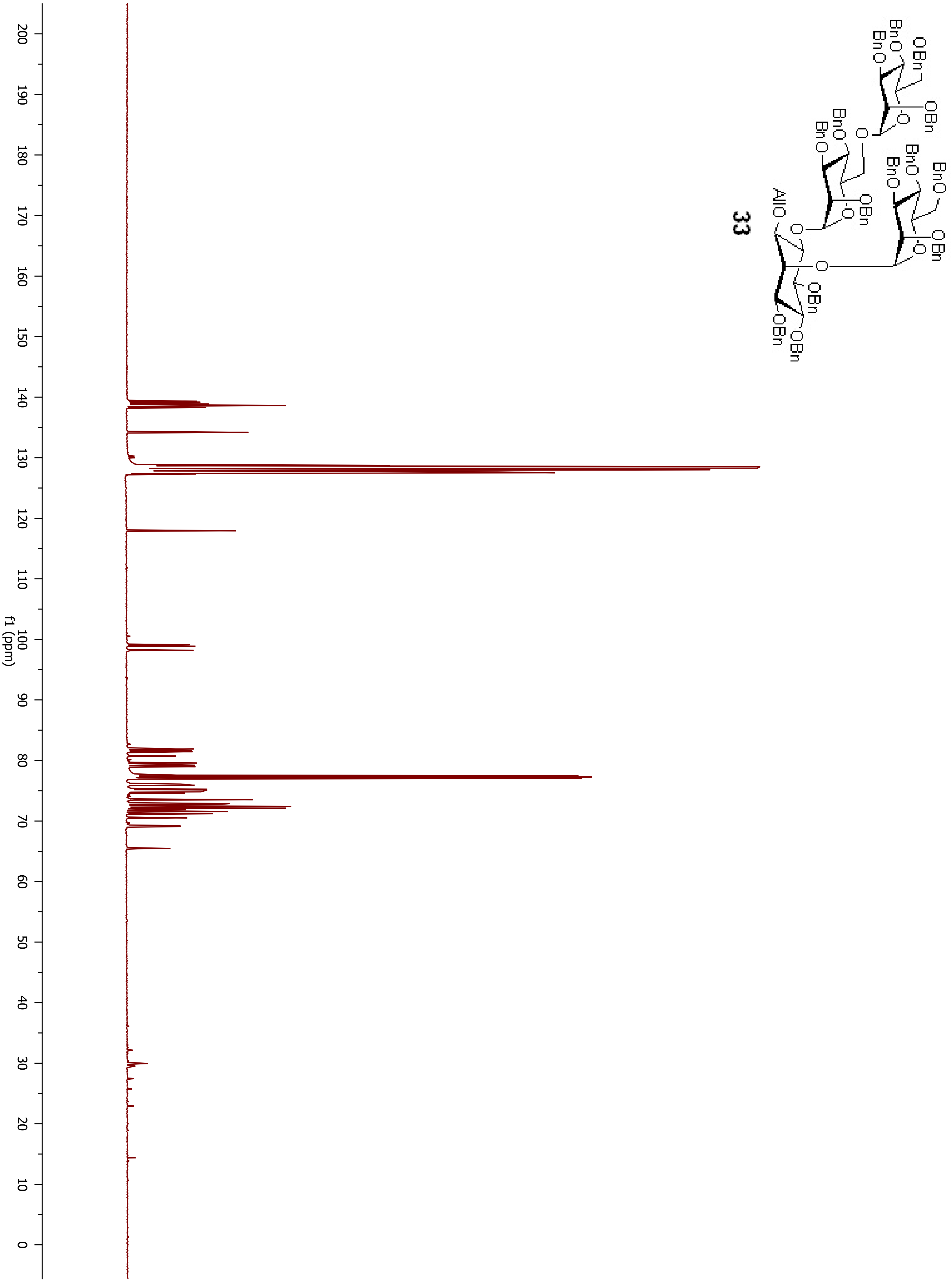
33
f1 (ppm)
200
190
180
170
160
150
140
130
120
110
100
90
80
70
60
50
40
30
20
10
0

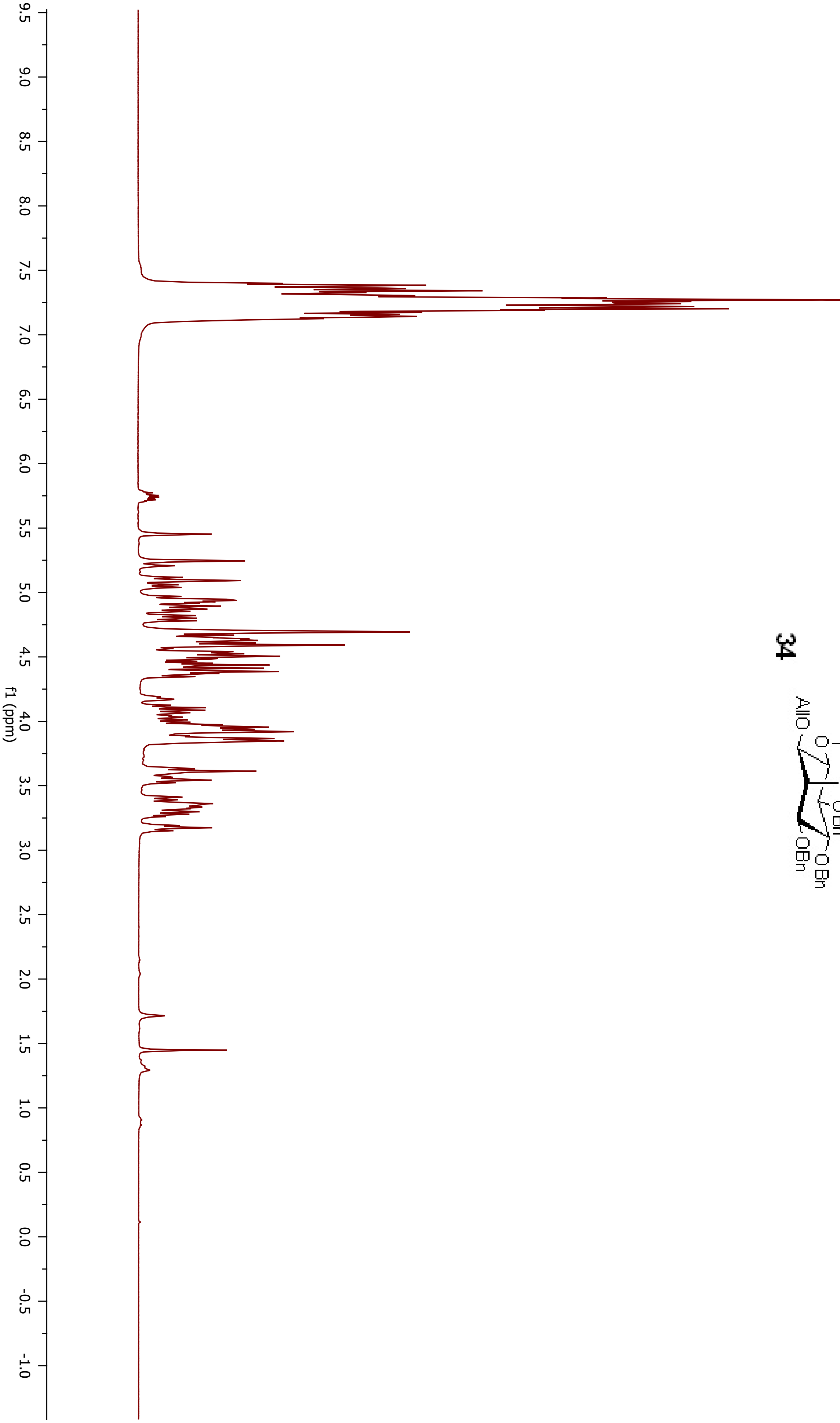
9.5
9.0
8.5
8.0
7.5
7.0
6.5
6.0
5.5
5.0
4.5
4.0
3.5
3.0
2.5
2.0
1.5
1.0
0.5
0.0
-0.5
-1.0
f1 (ppm)

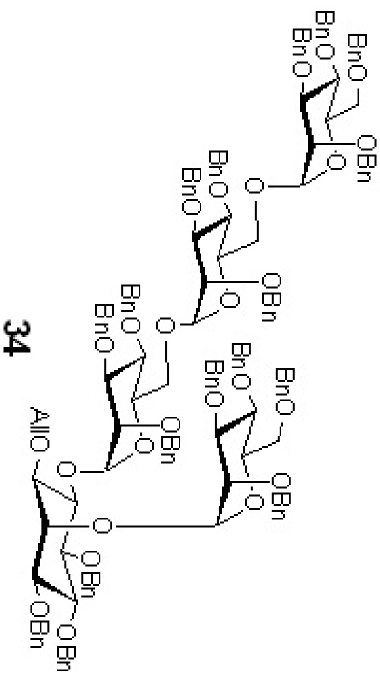
BnO
BnO
BnO
OBn
O
AllO
OBn

34

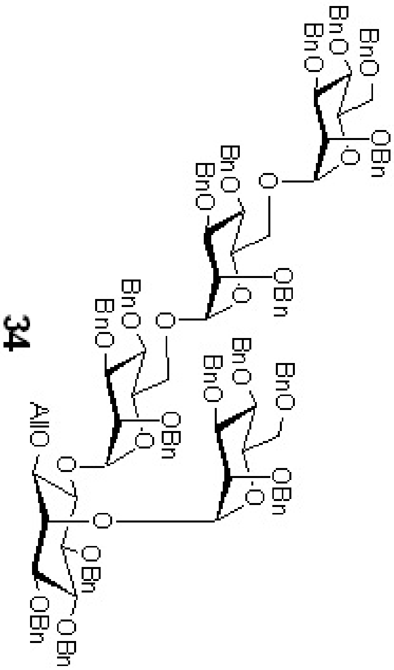
BnO
OBn
AllO

34

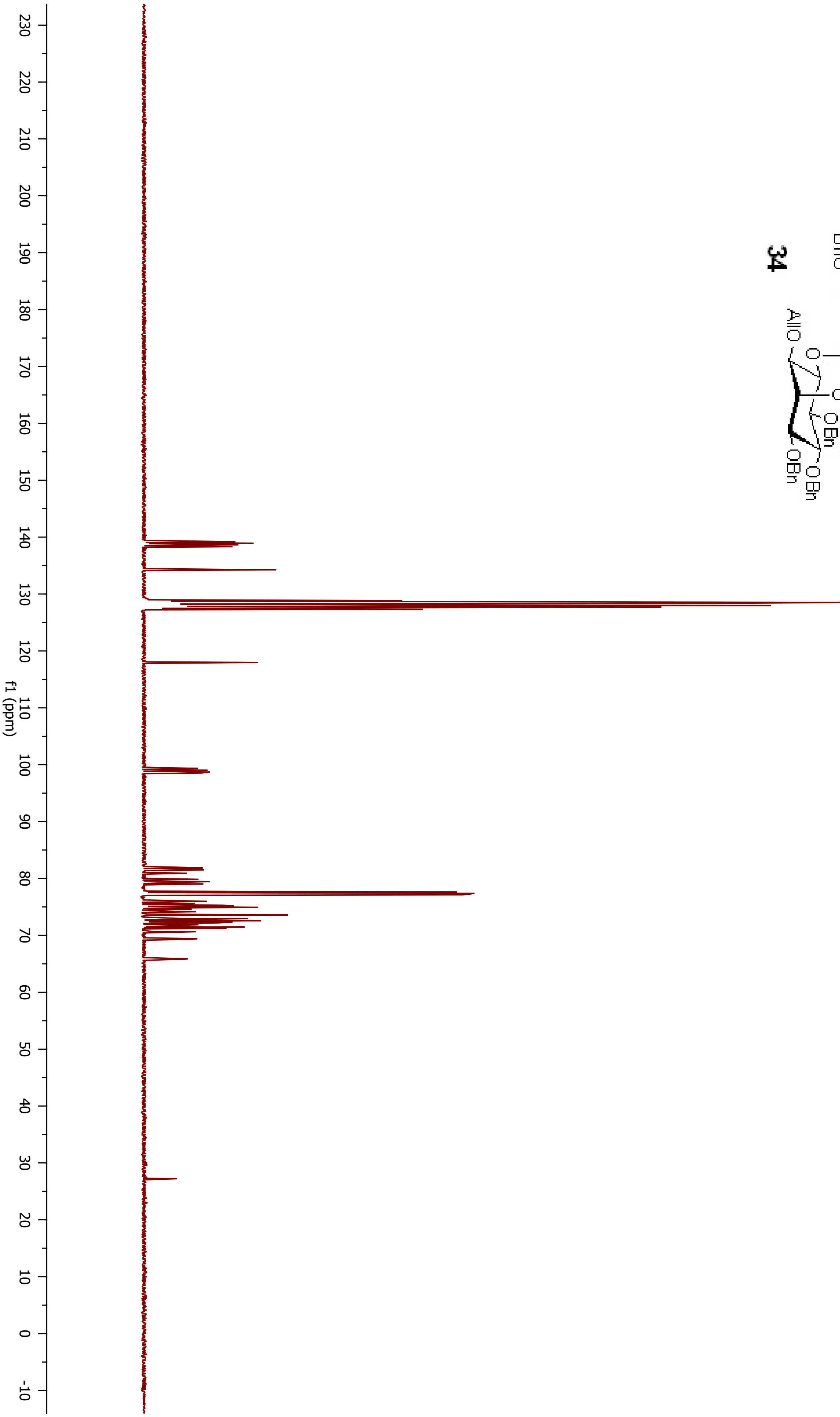
230
220
210
200
190
180
170
160
150
140
130
120
110
100
90
80
70
60
50
40
30
20
10
0
-10
f1 (ppm)

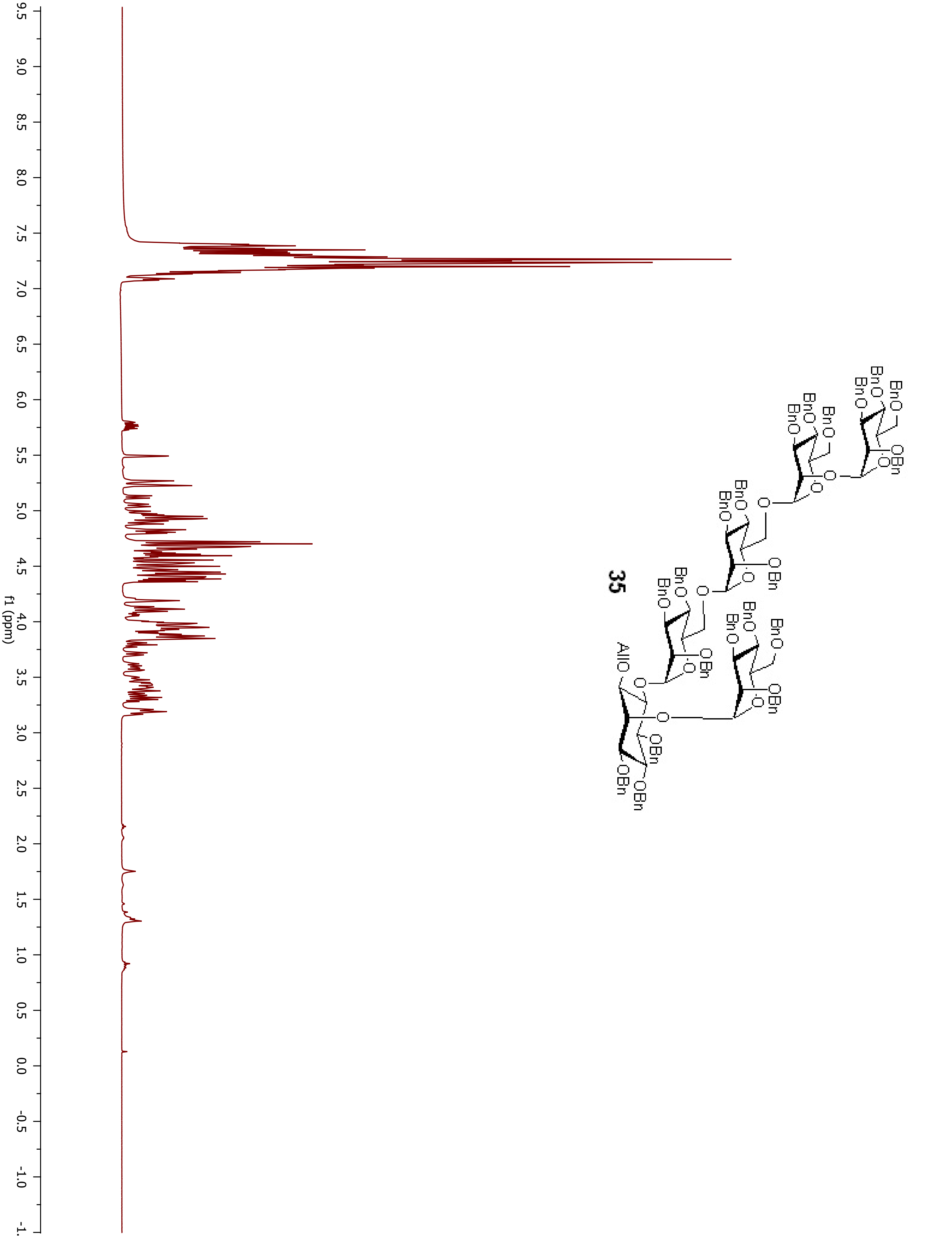
35
f1 (ppm)

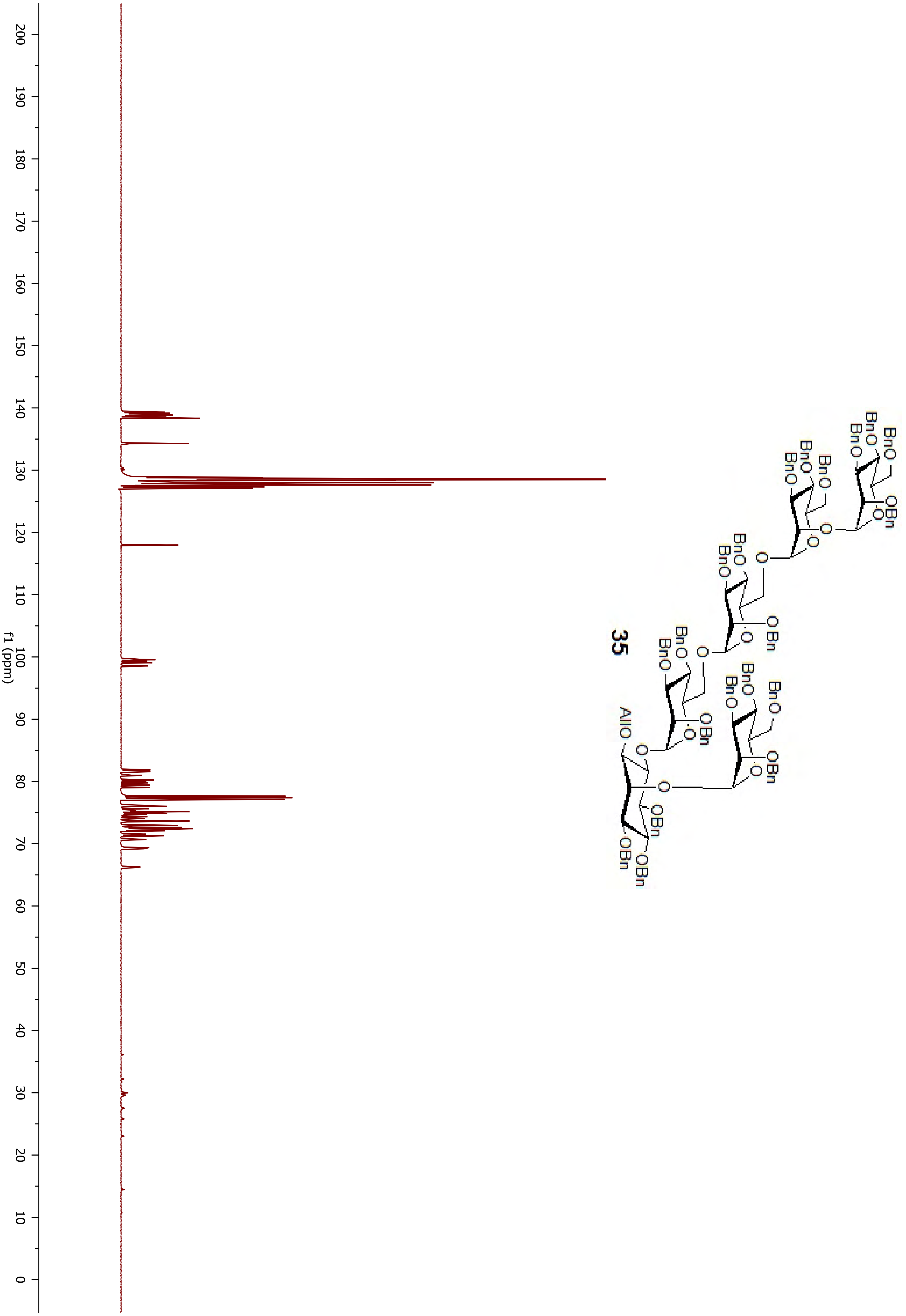
f1 (ppm)
35
AllO
BnO
OBn

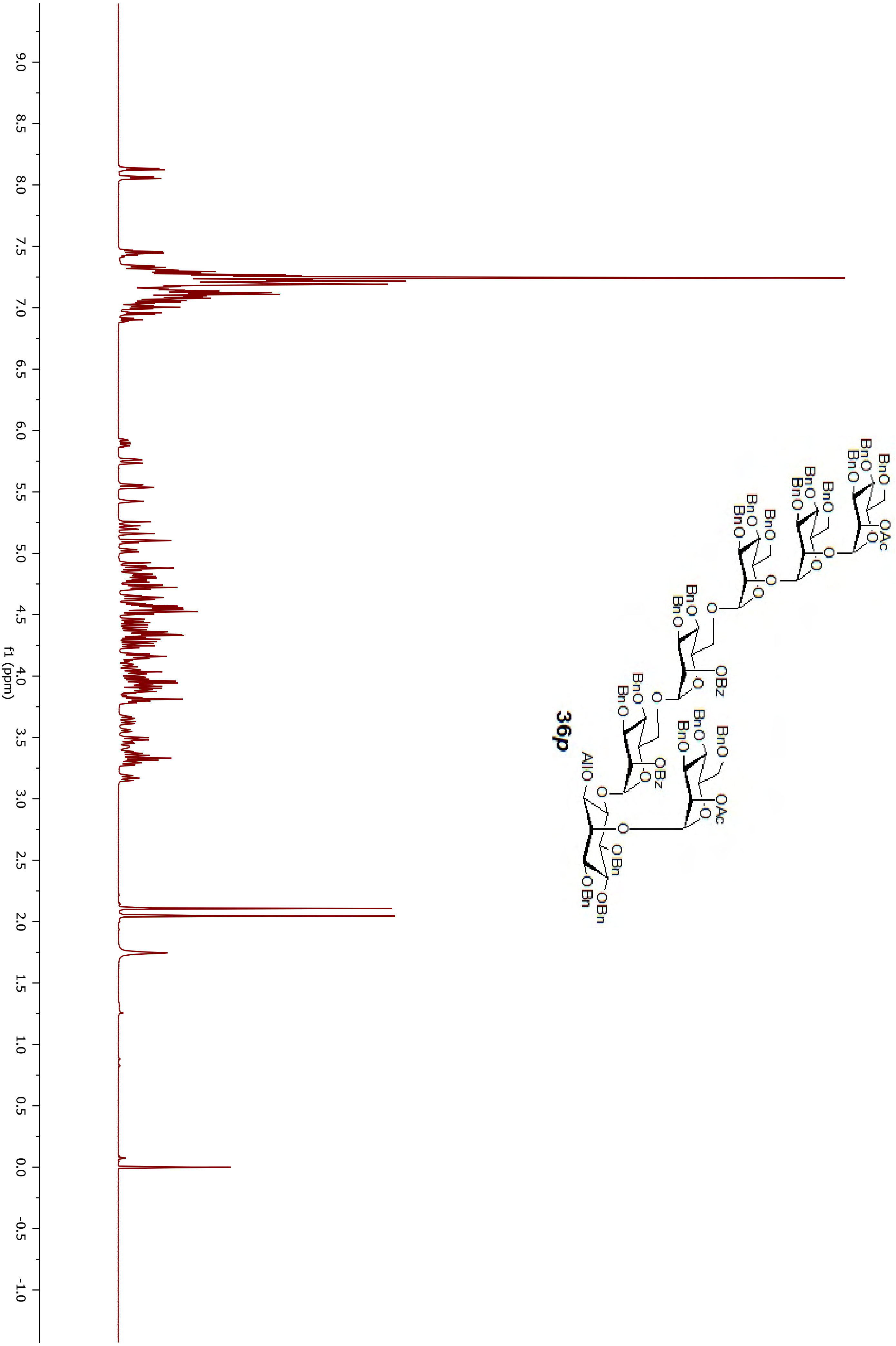

36p

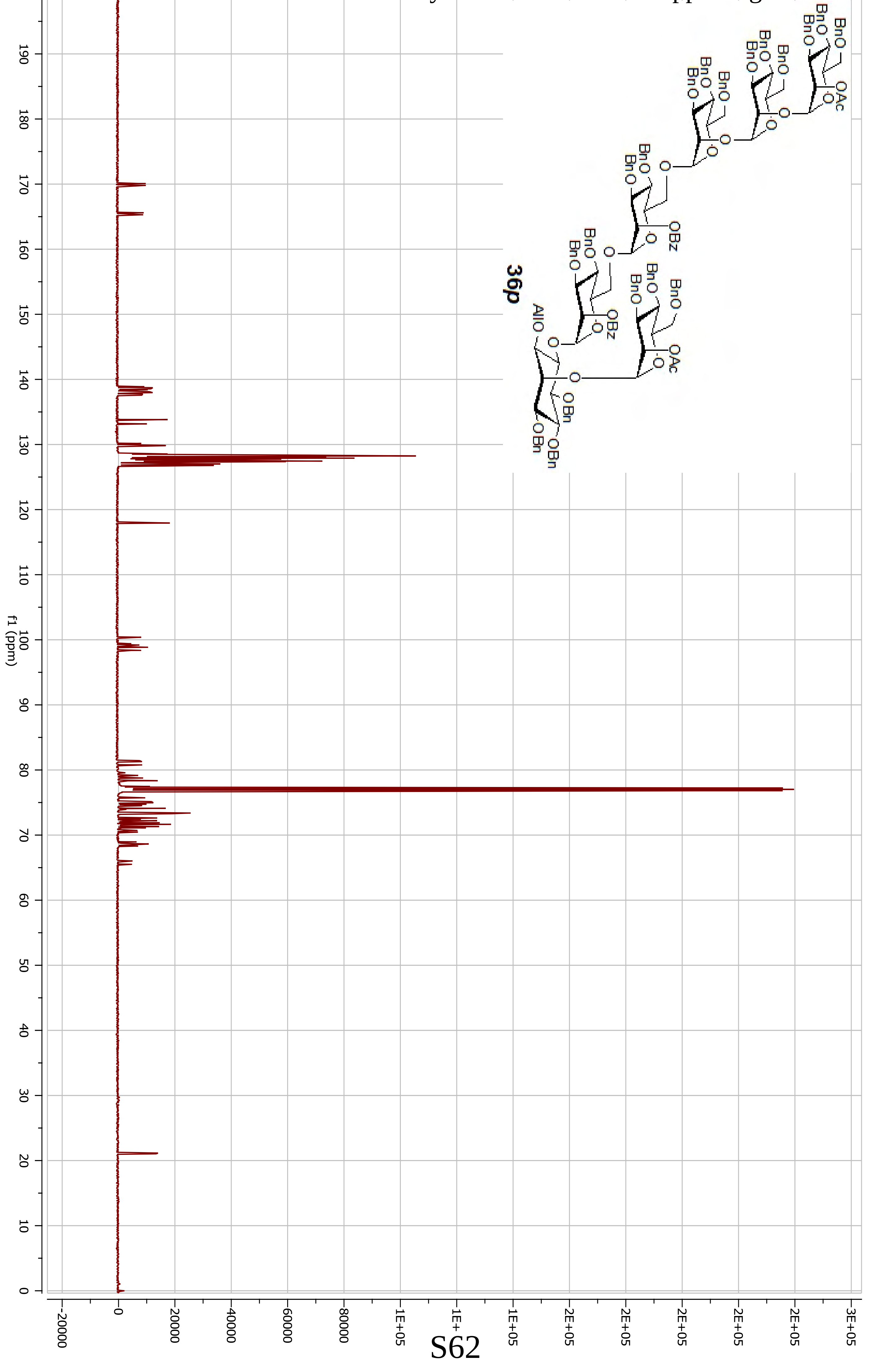
36p
f1 (ppm)

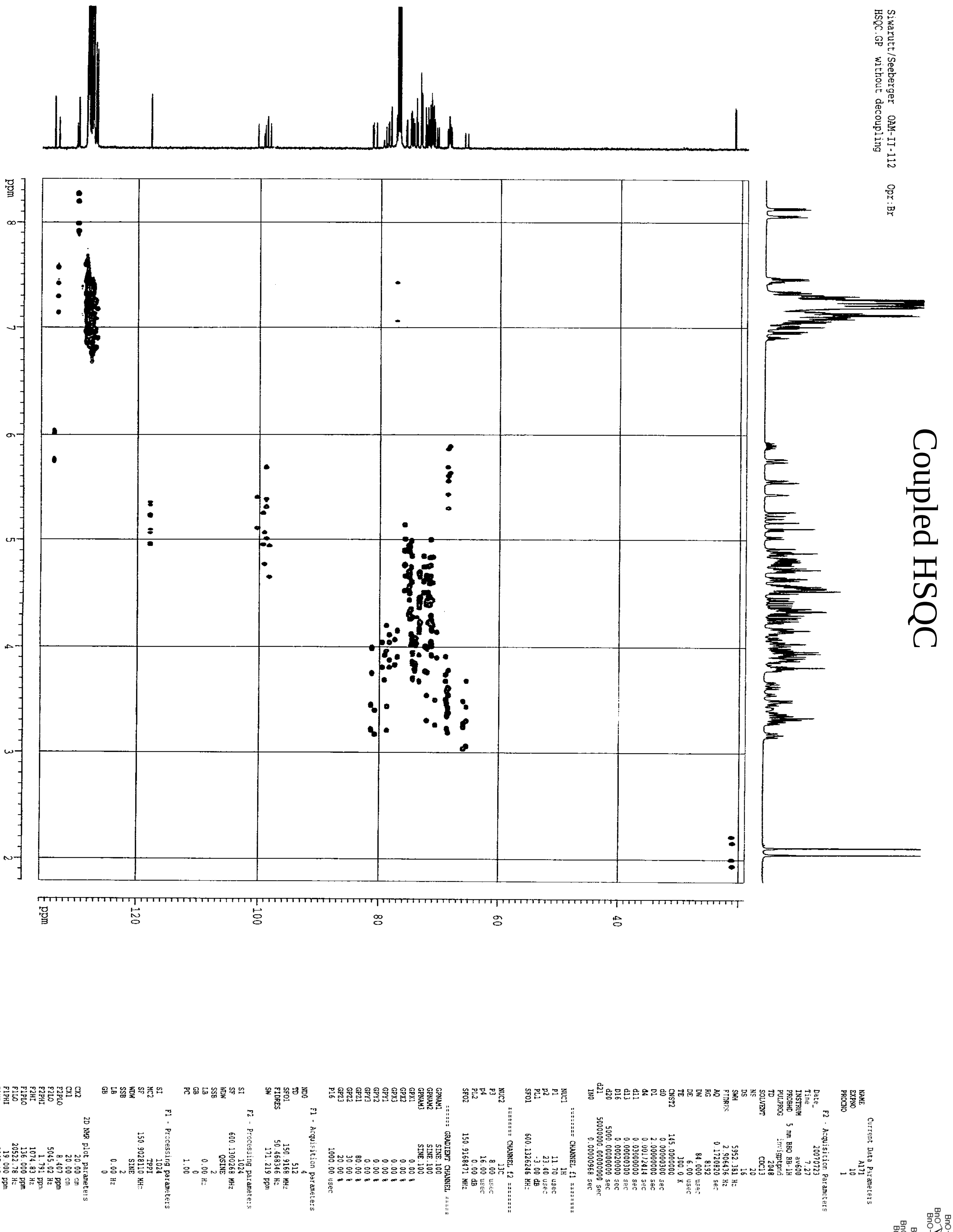
Coupled HSQC
Siwarutt/Seeberger OAM-II-112 Opr:Br
HSQC.GP without decoupling

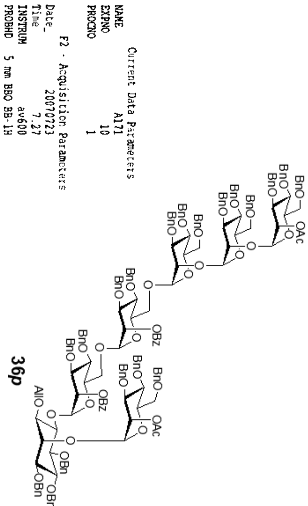

36p

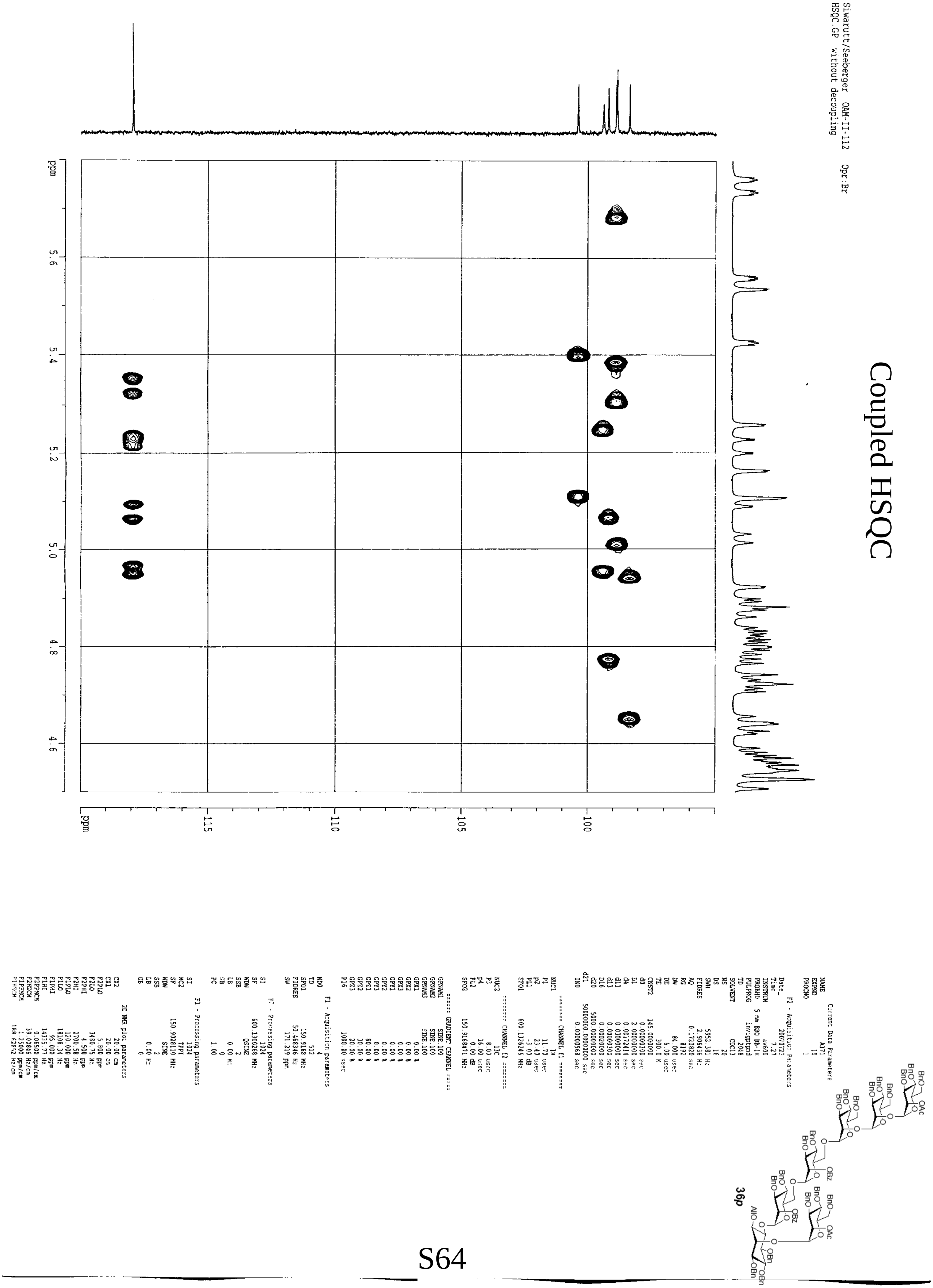
Siwarutt/Seeberger OAM-II-112 Opr:Br
HSQC.GP without decoupling
Coupled HSQC
36p

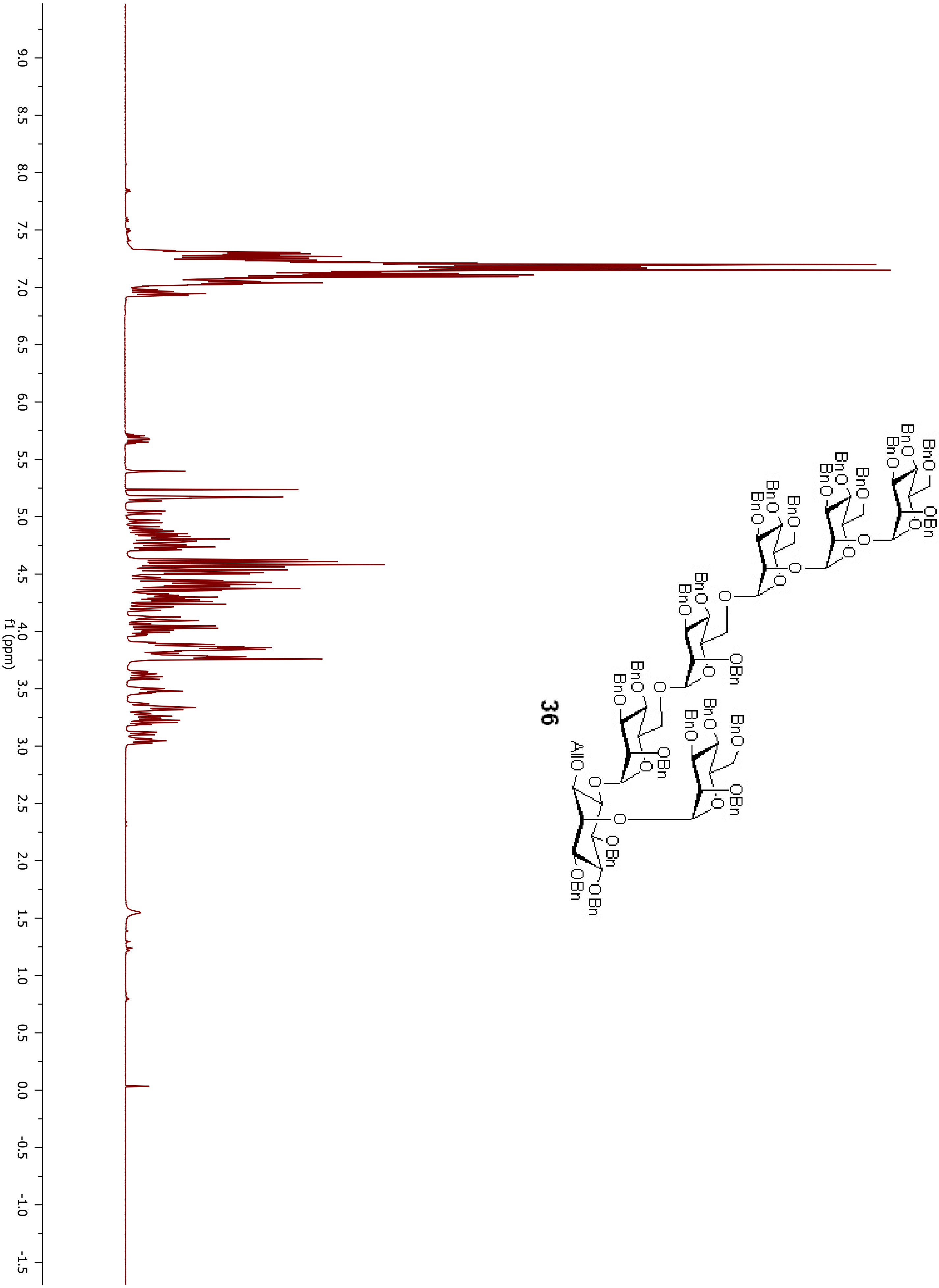
f1 (ppm)
9.0
8.5
8.0
7.5
7.0
6.5
6.0
5.5
5.0
4.5
4.0
3.5
3.0
2.5
2.0
1.5
1.0
0.5
0.0
-0.5
-1.0
-1.5
BnO
OBn
AllO
O

36

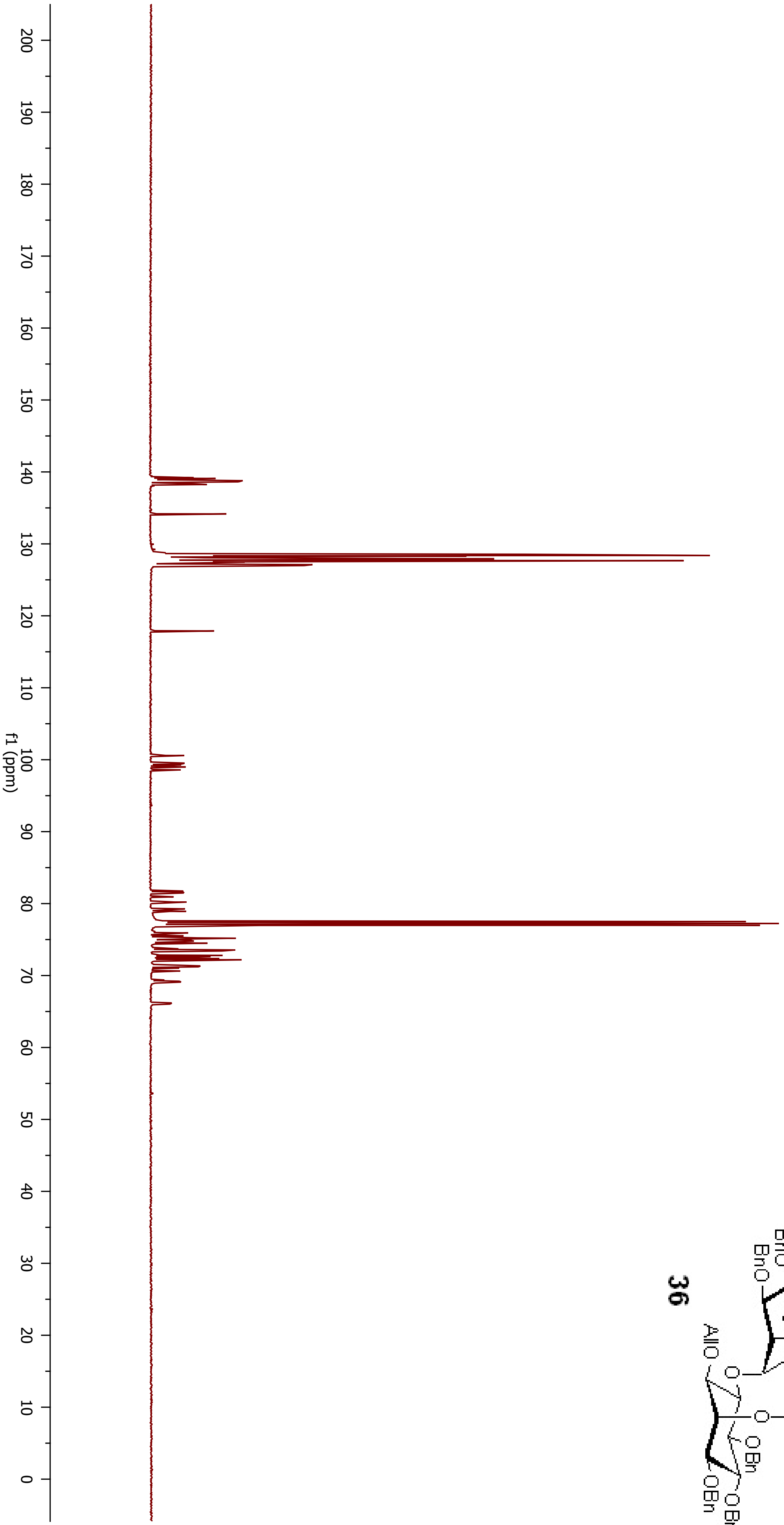

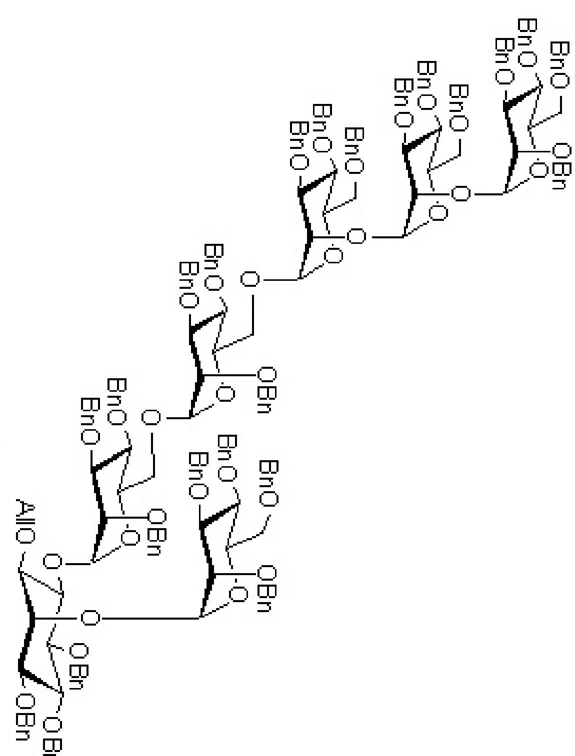

36

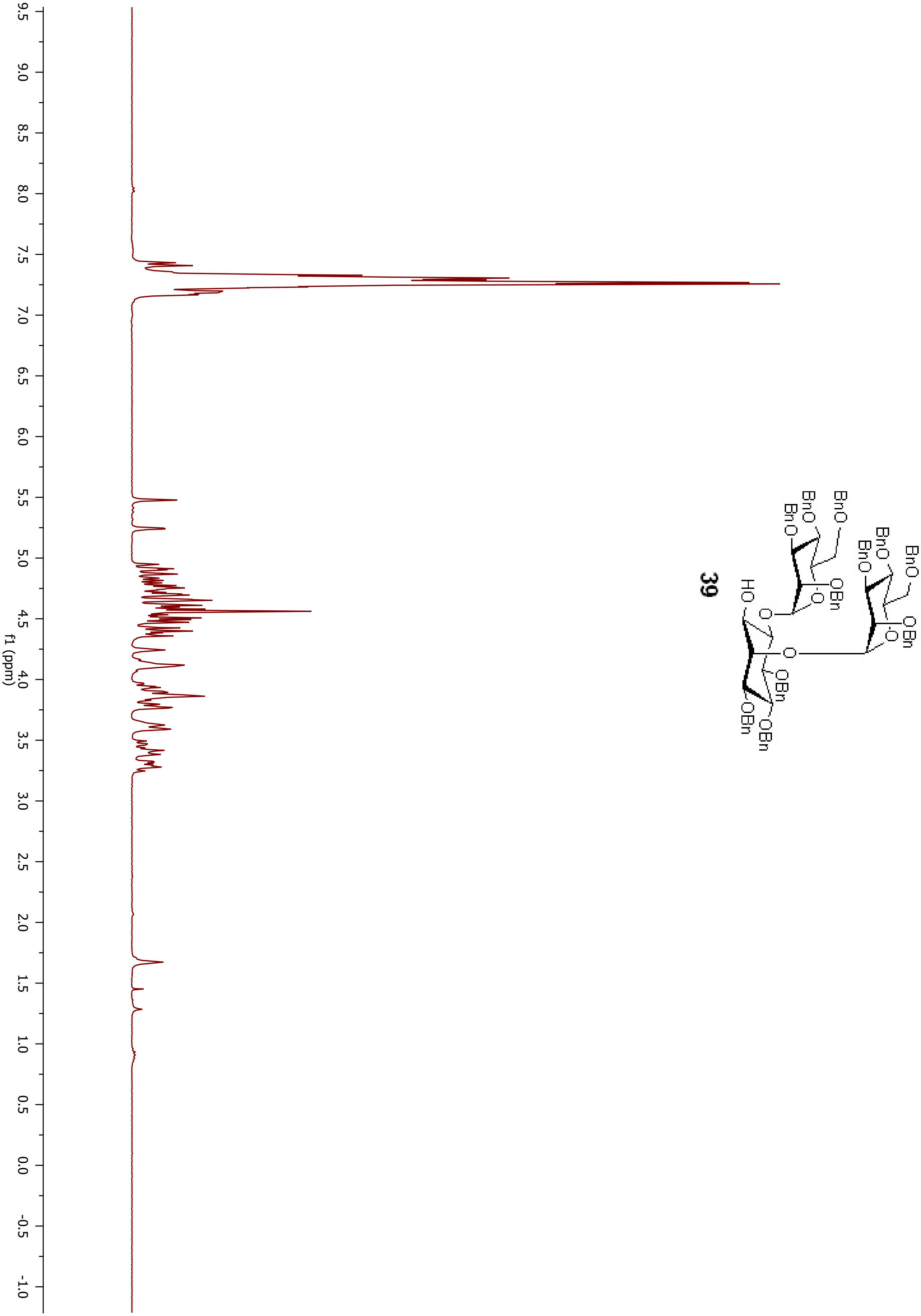
f1 (ppm)
9.5
9.0
8.5
8.0
7.5
7.0
6.5
6.0
5.5
5.0
4.5
4.0
3.5
3.0
2.5
2.0
1.5
1.0
0.5
0.0
-0.5
-1.0
BnO
OBn
HO
O

39

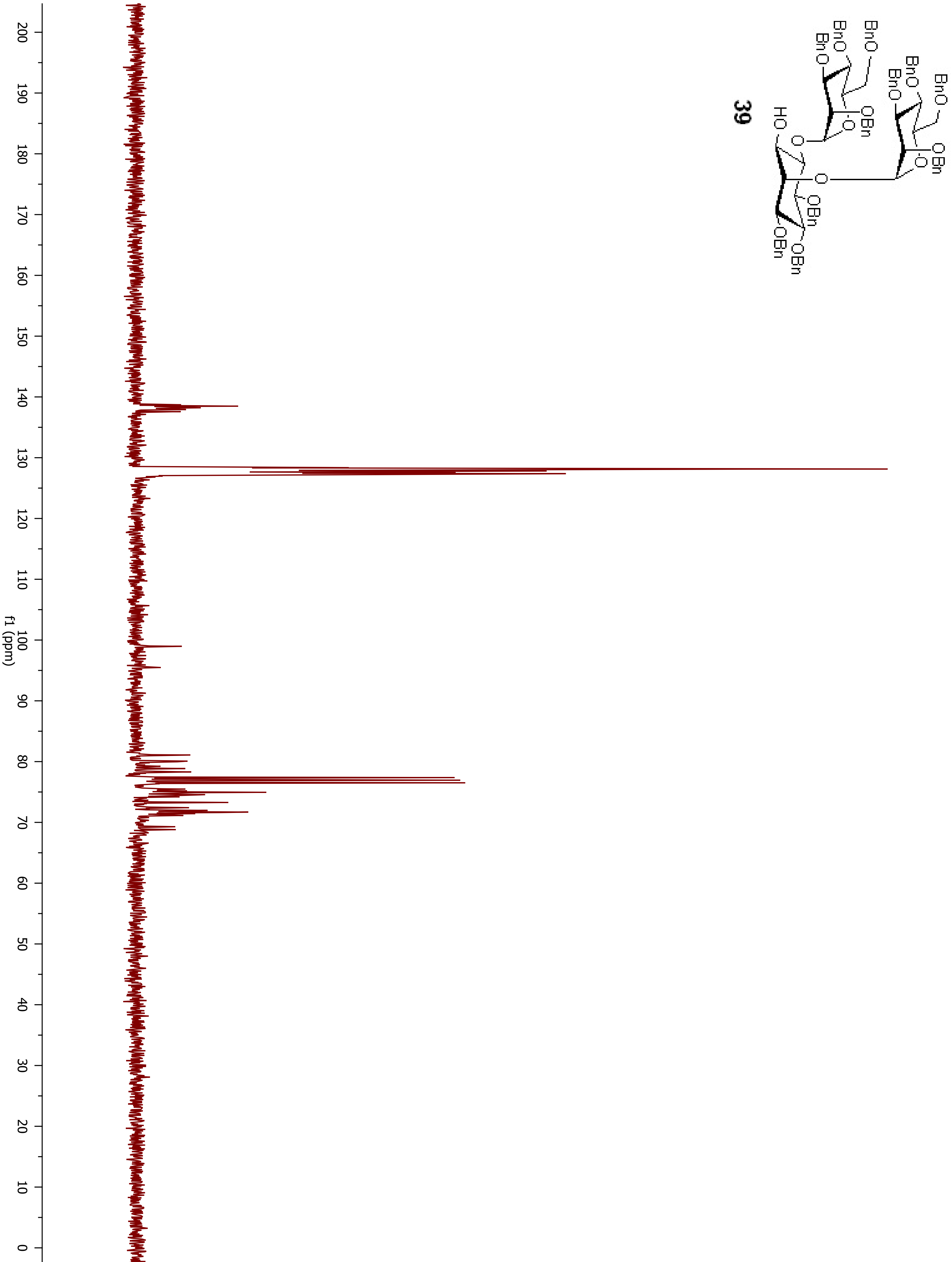
BnO
BnO
BnO
OBn
O
HO
OBn
OBn
OBn
39
f1 (ppm)
200
190
180
170
160
150
140
130
120
110
100
90
80
70
60
50
40
30
20
10
0

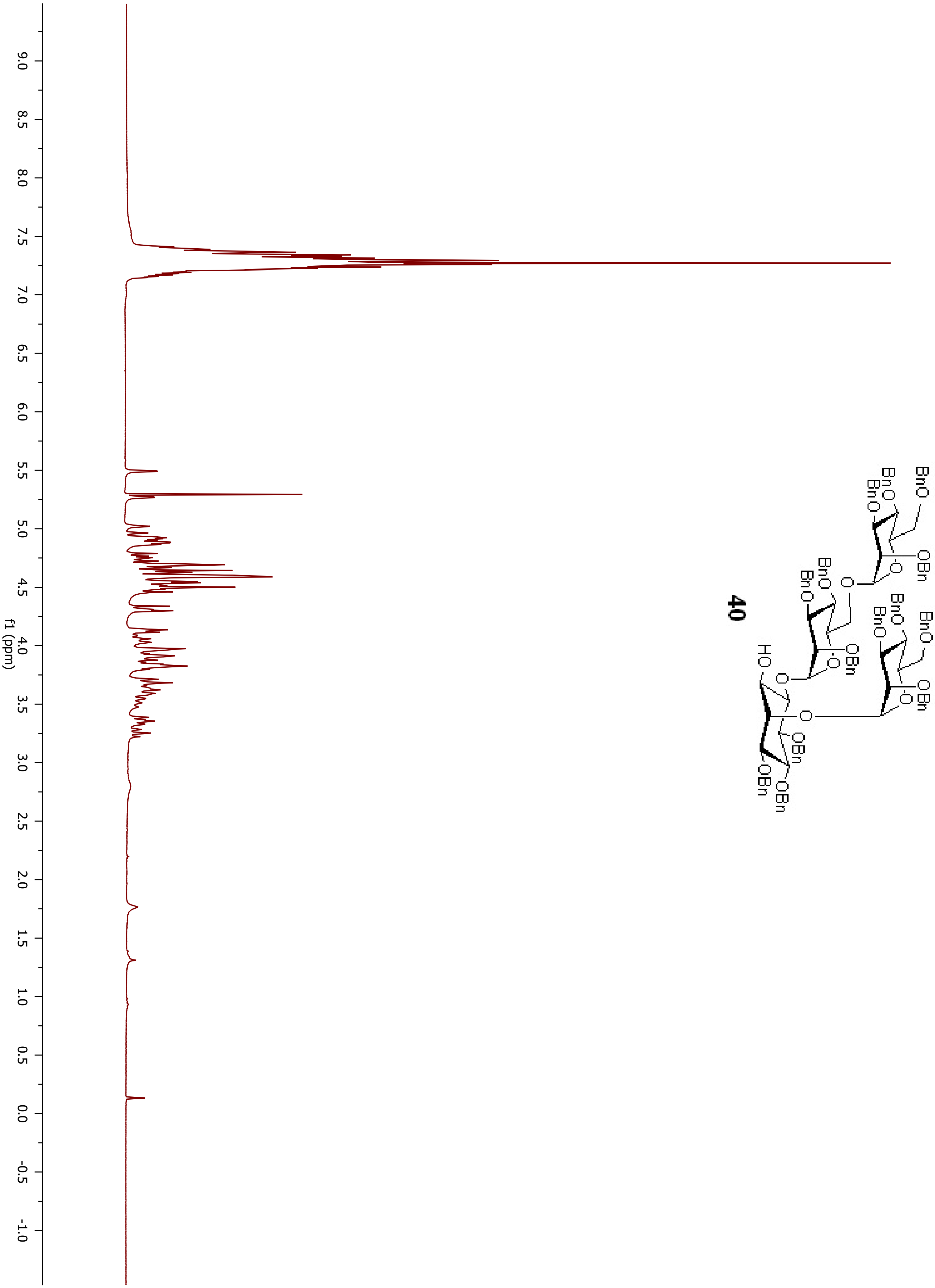
40
BnO
OBn
HO
f1 (ppm)
9.0
8.5
8.0
7.5
7.0
6.5
6.0
5.5
5.0
4.5
4.0
3.5
3.0
2.5
2.0
1.5
1.0
0.5
0.0
-0.5
-1.0

40

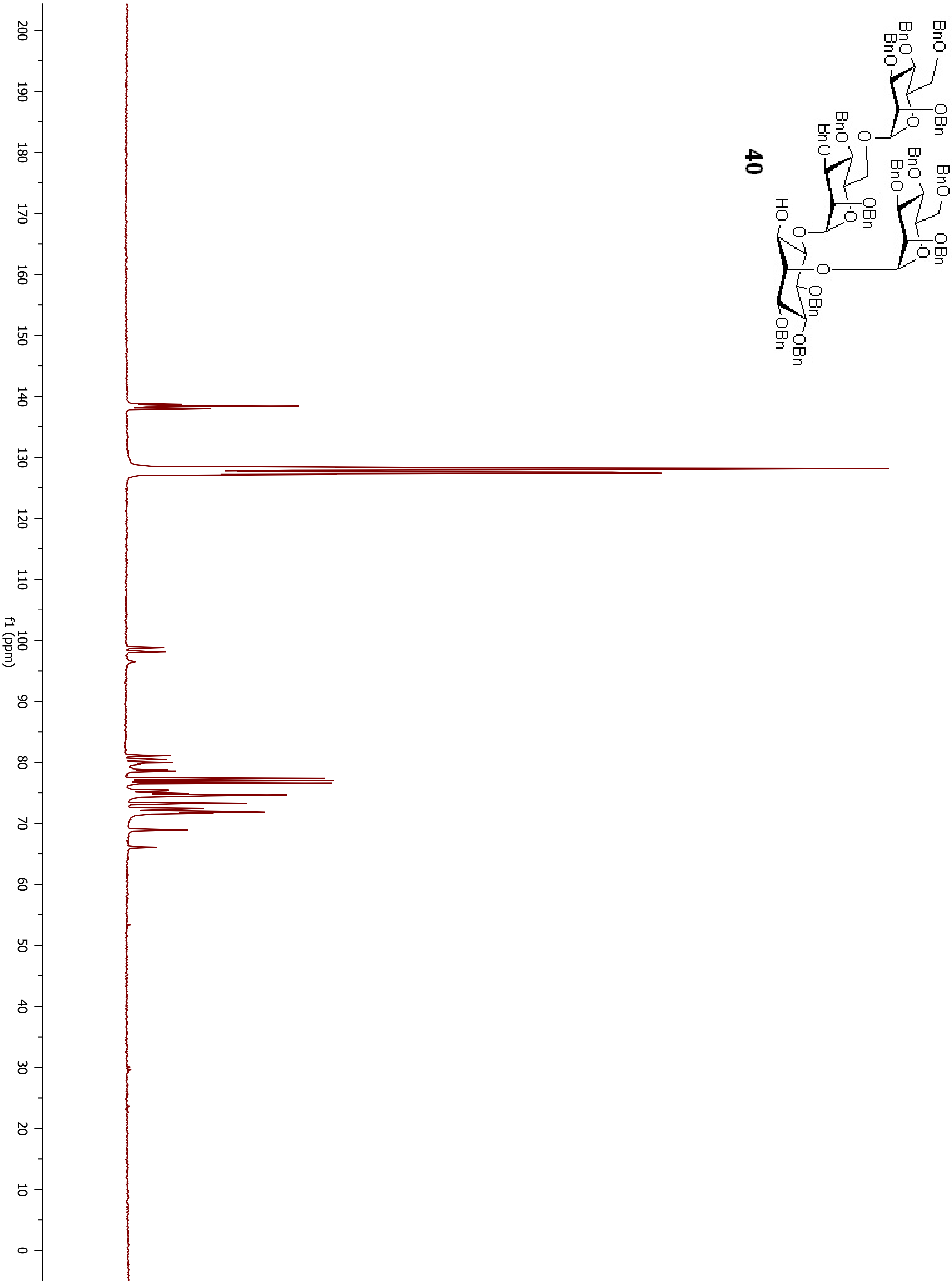
f1 (ppm)
200
190
180
170
160
150
140
130
120
110
100
90
80
70
60
50
40
30
20
10
0

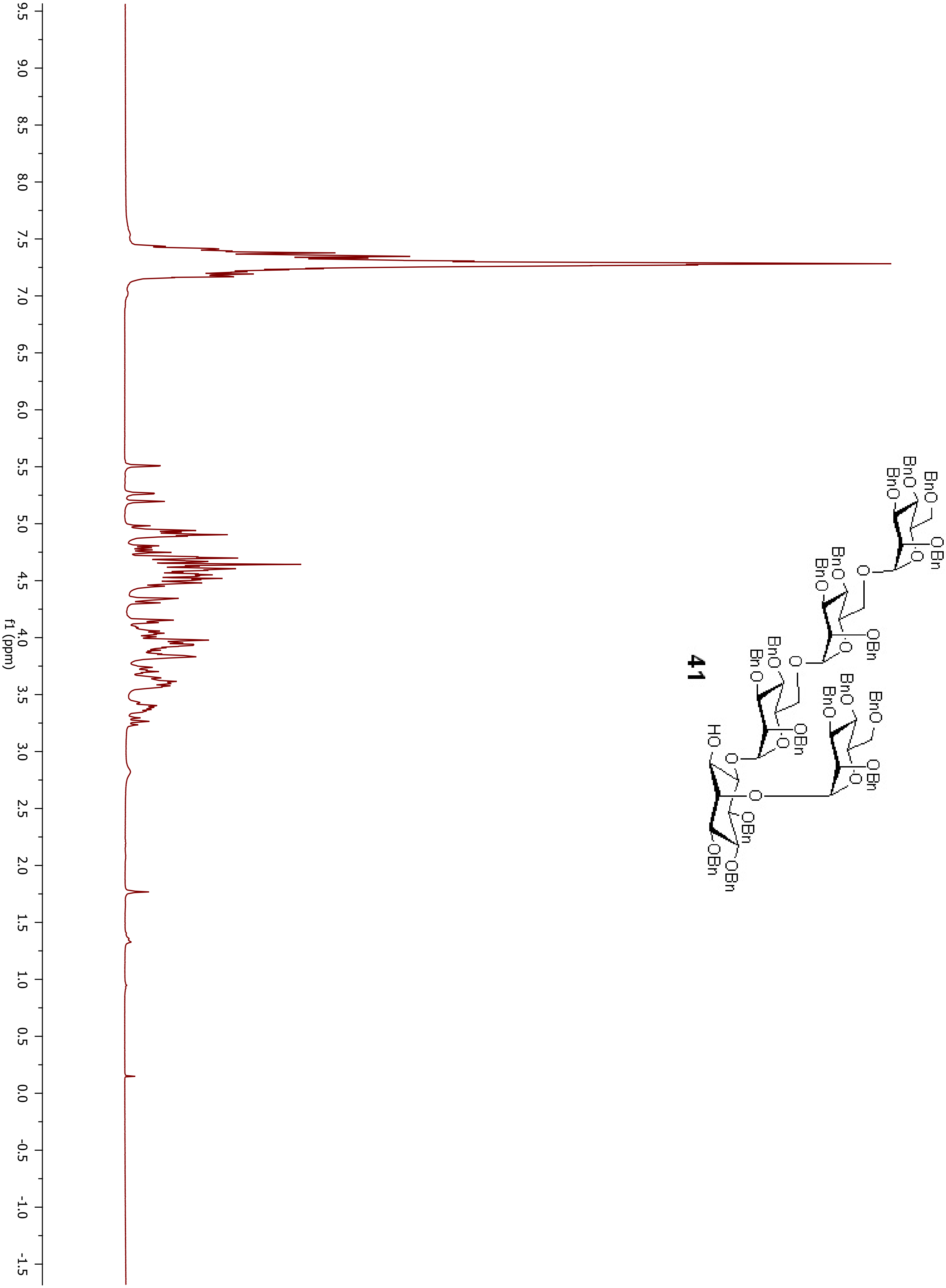
9.5
9.0
8.5
8.0
7.5
7.0
6.5
6.0
5.5
5.0
4.5
4.0
3.5
3.0
2.5
2.0
1.5
1.0
0.5
0.0
-0.5
-1.0
-1.5
f1 (ppm)

41

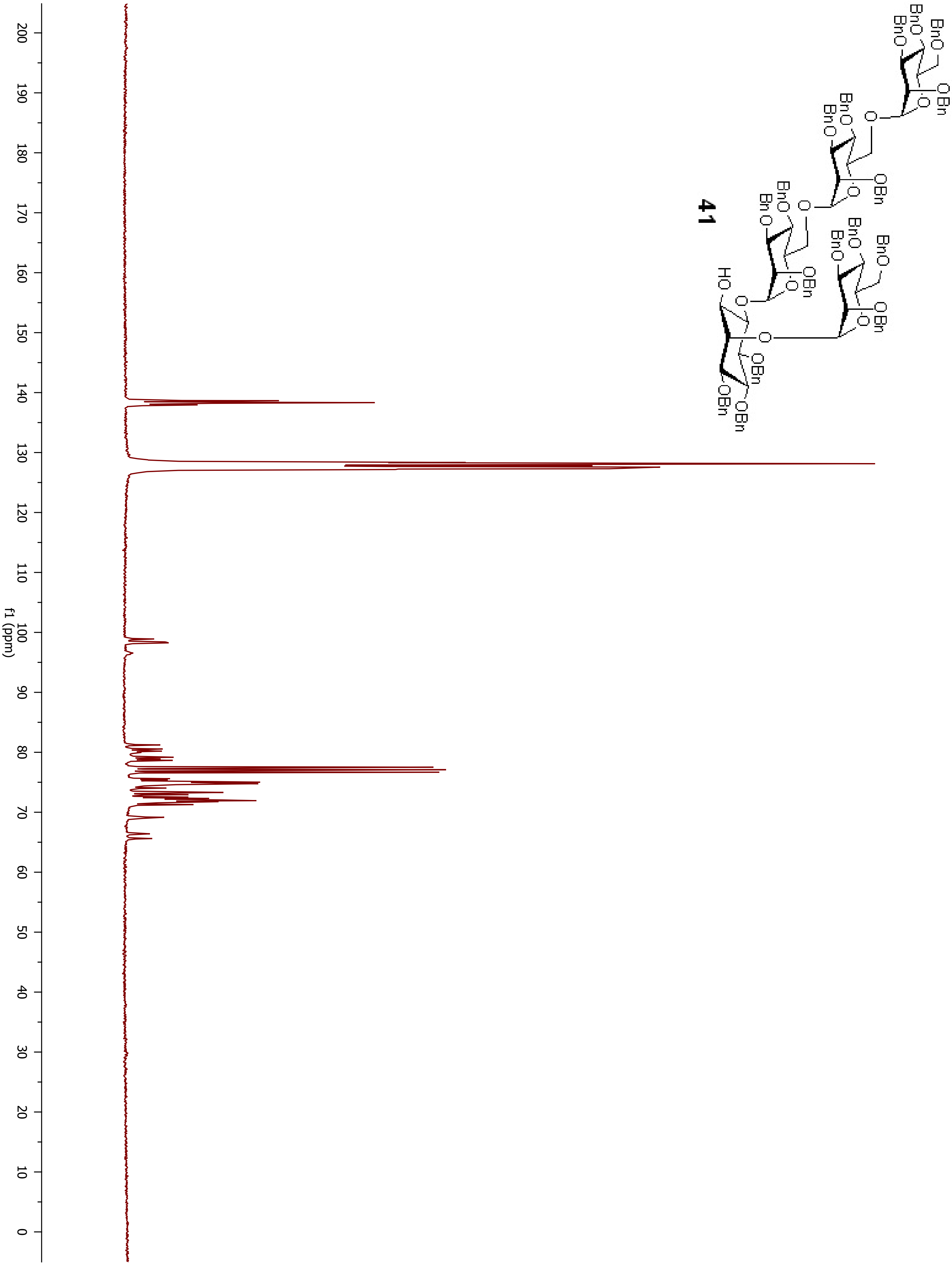

41
BnO
OBn
HO
200
190
180
170
160
150
140
130
120
110
100
90
80
70
60
50
40
30
20
10
0
f1 (ppm)

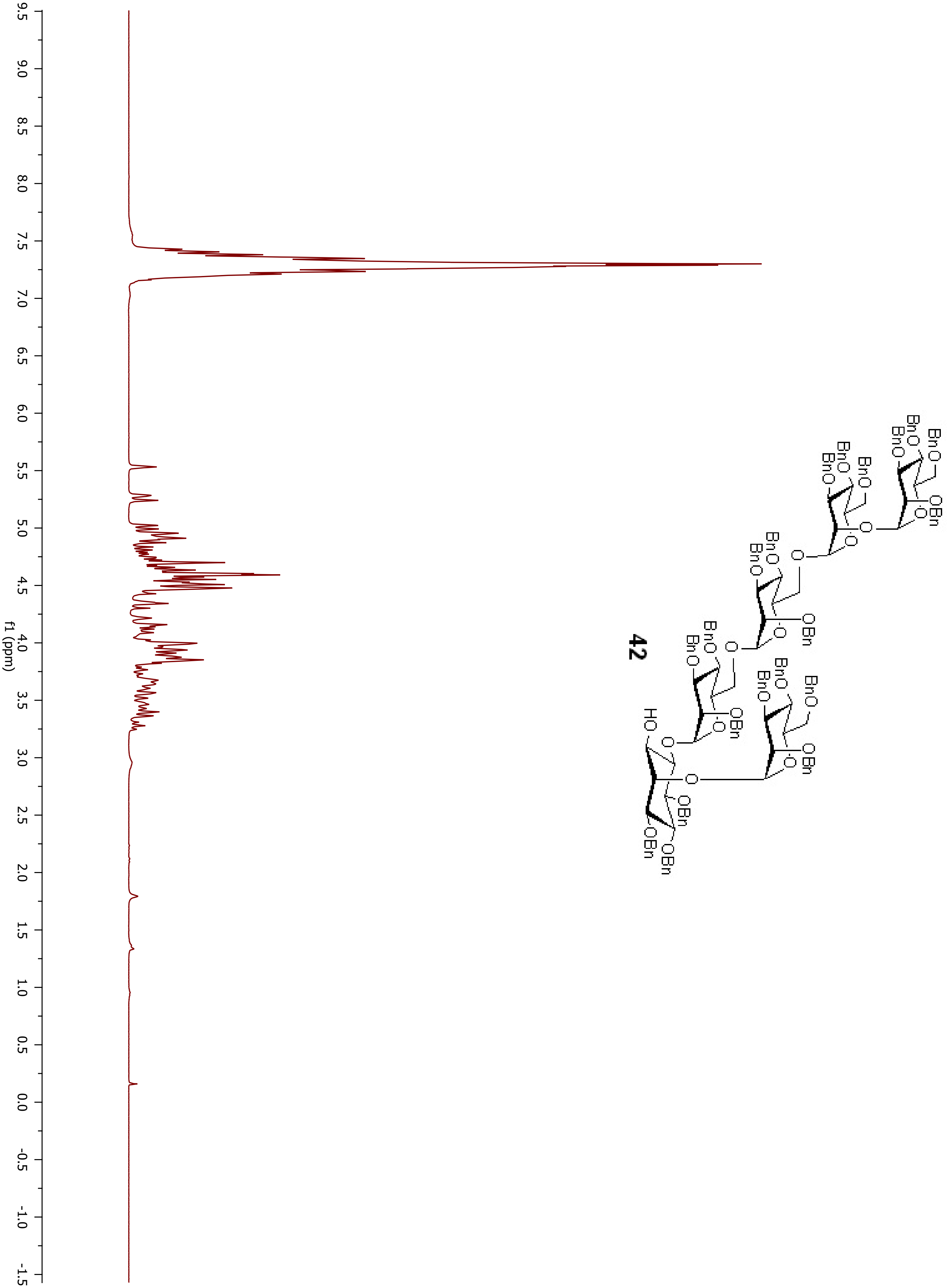
f1 (ppm)
42

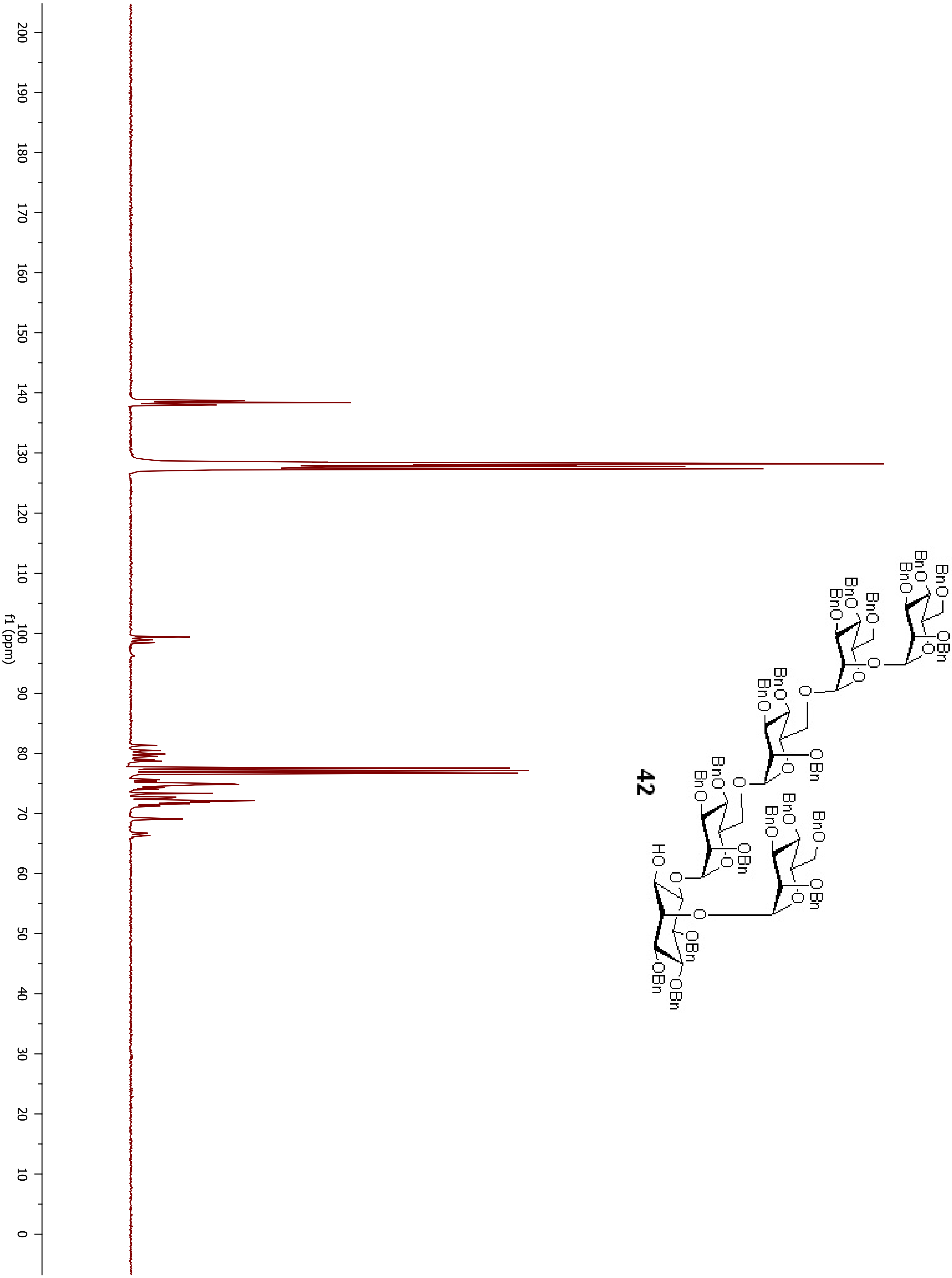
f1 (ppm)
200
190
180
170
160
150
140
130
120
110
100
90
80
70
60
50
40
30
20
10
0
BnO
OBn
HO
O

42

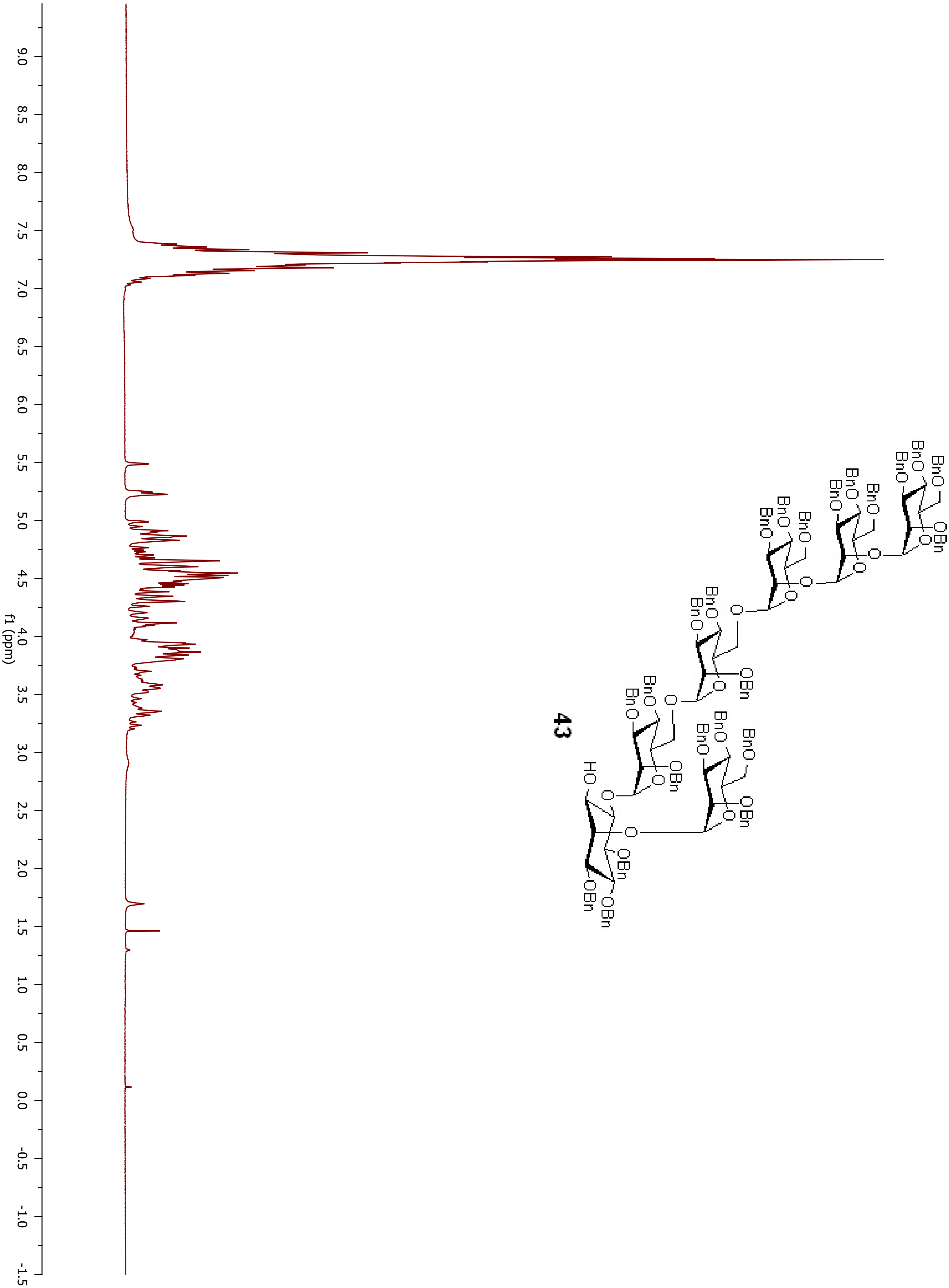
f1 (ppm)
9.0
8.5
8.0
7.5
7.0
6.5
6.0
5.5
5.0
4.5
4.0
3.5
3.0
2.5
2.0
1.5
1.0
0.5
0.0
-0.5
-1.0
-1.5
BnO
OBn
HO
O

43

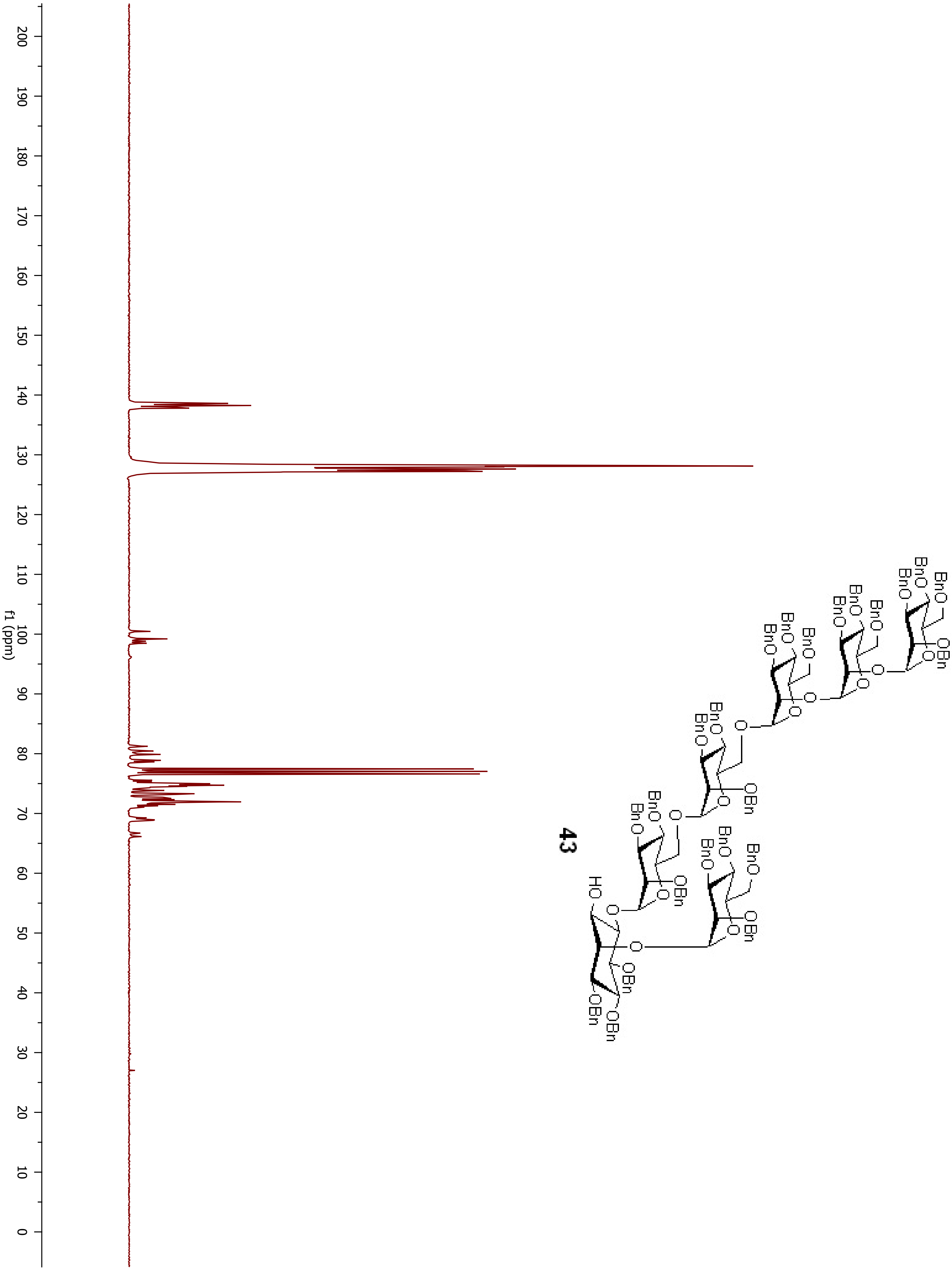
f1 (ppm)
43

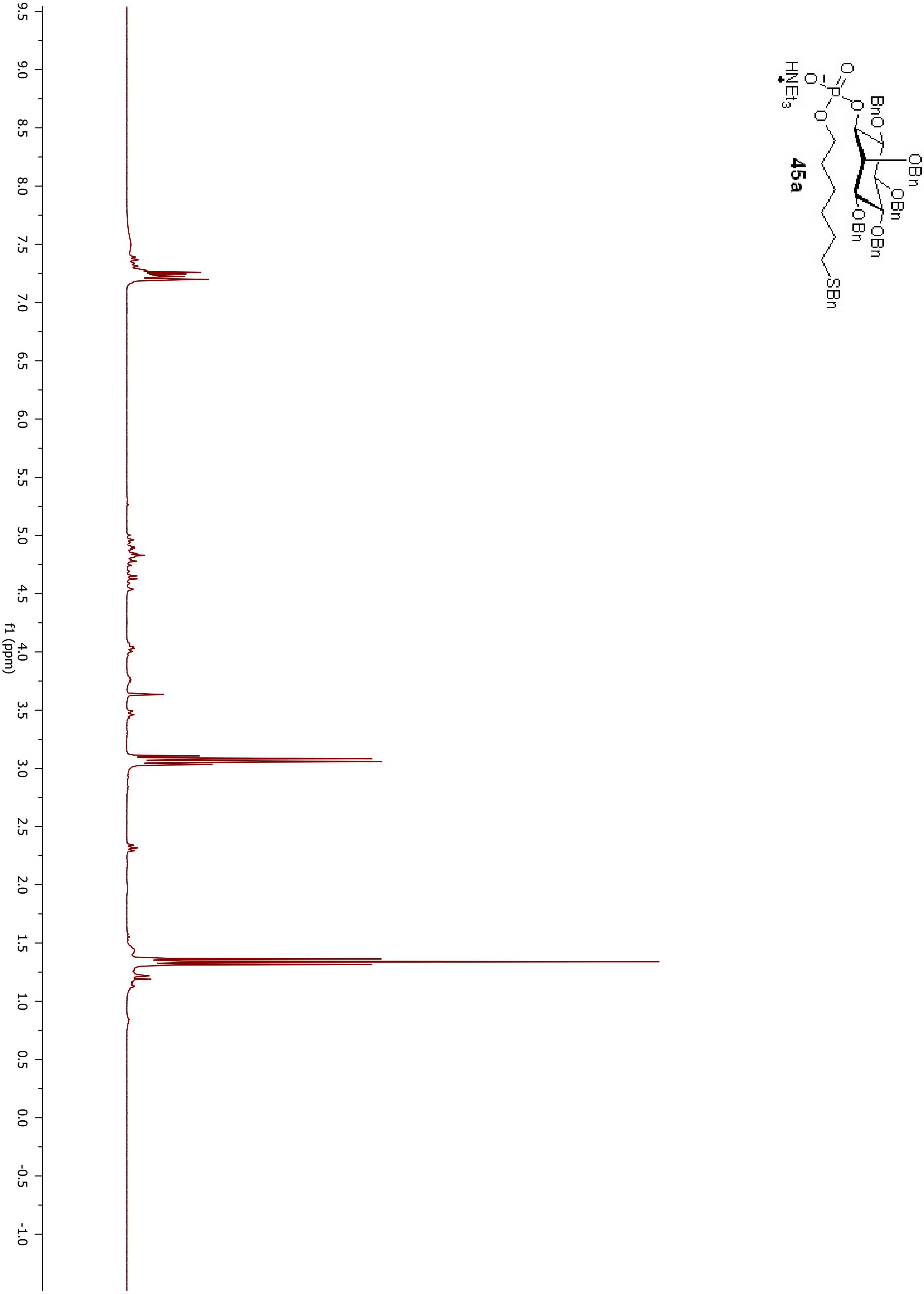
f1 (ppm)
45a

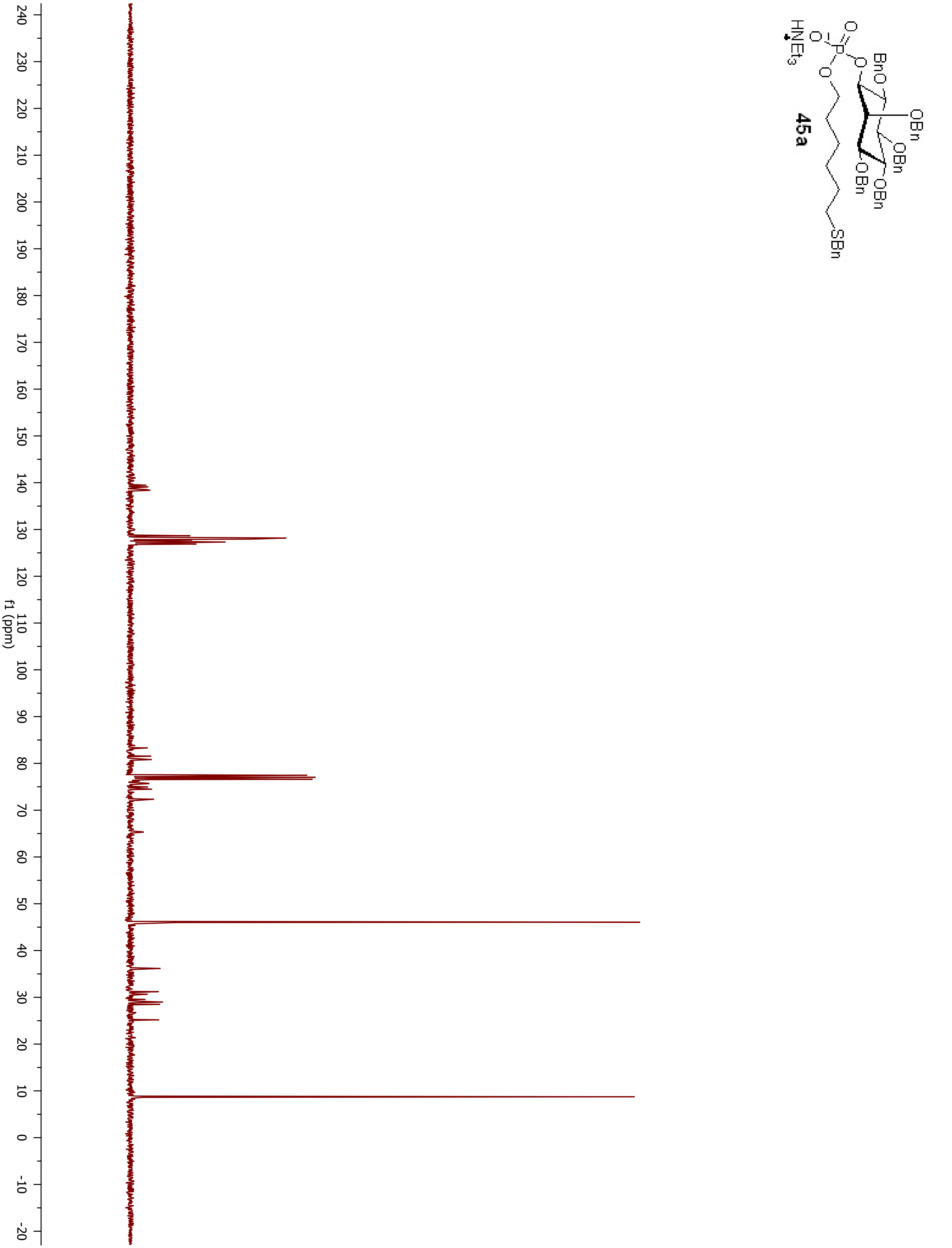
45a
OBn
BnO
SBn
f1 (ppm)
240
230
220
210
200
190
180
170
160
150
140
130
120
110
100
90
80
70
60
50
40
30
20
10
0
-10
-20

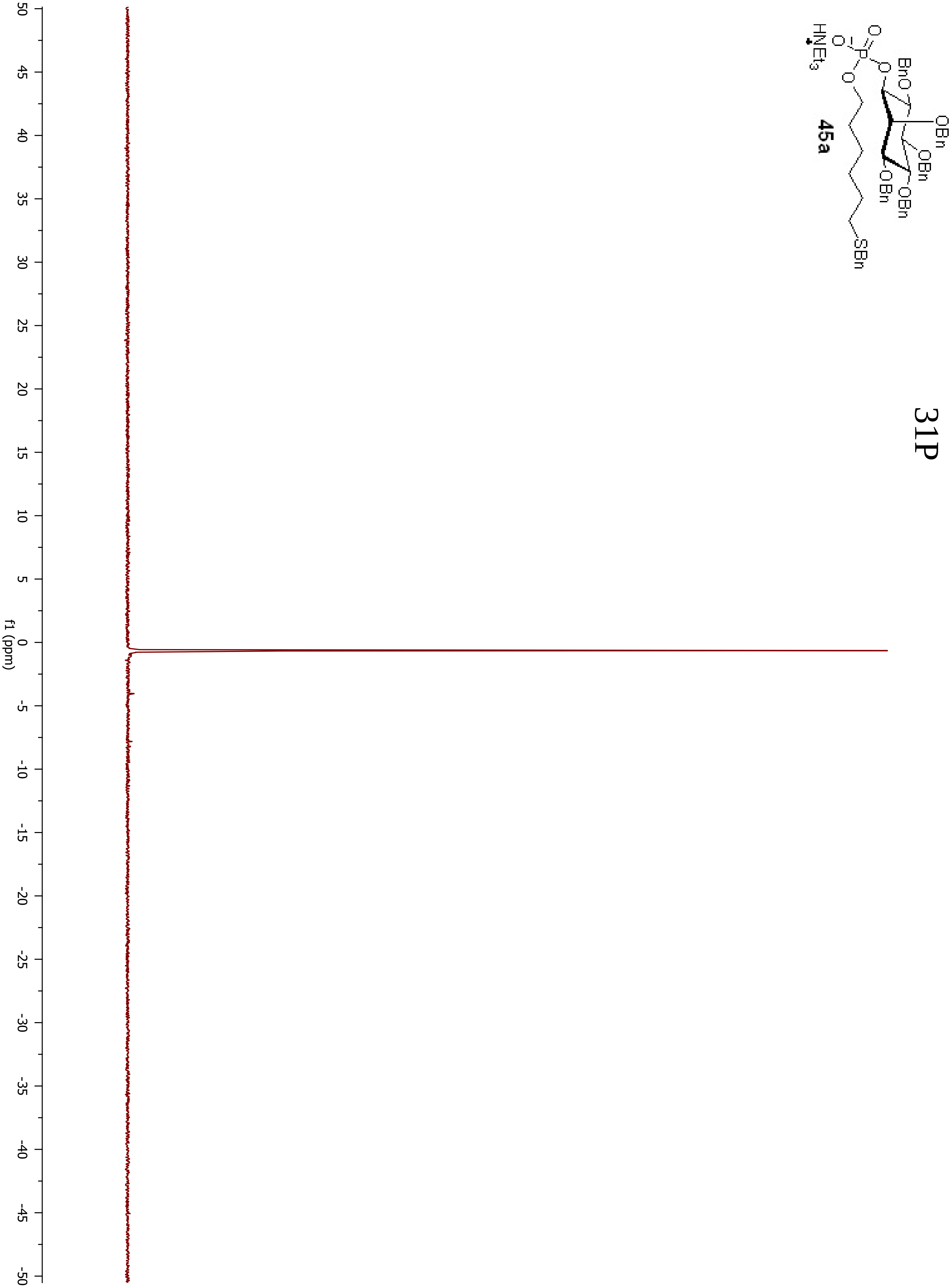
31P
45a
f1 (ppm)

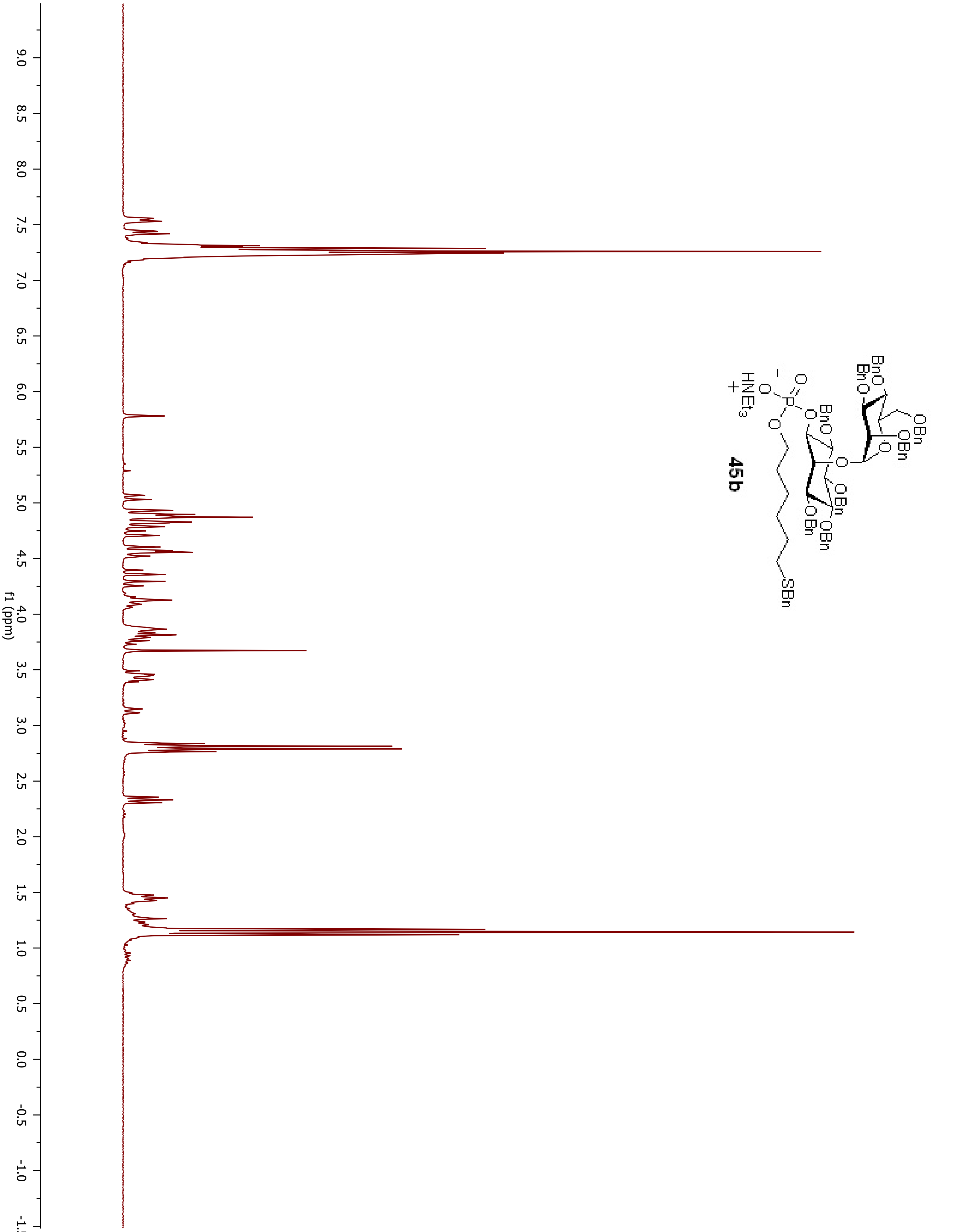
45b
f1 (ppm)
9.0
8.5
8.0
7.5
7.0
6.5
6.0
5.5
5.0
4.5
4.0
3.5
3.0
2.5
2.0
1.5
1.0
0.5
0.0
-0.5
-1.0
-1.5

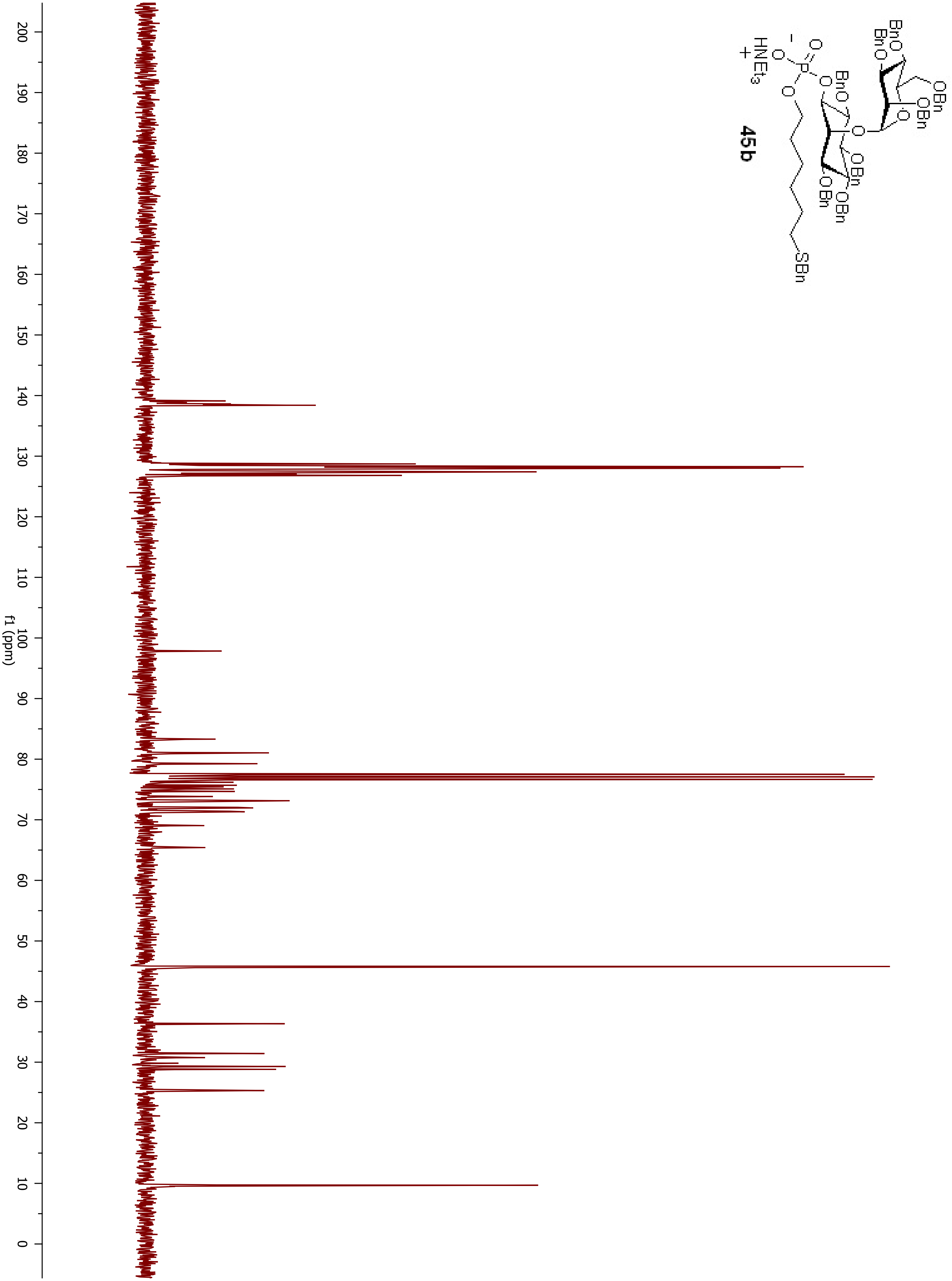
f1 (ppm)
45b

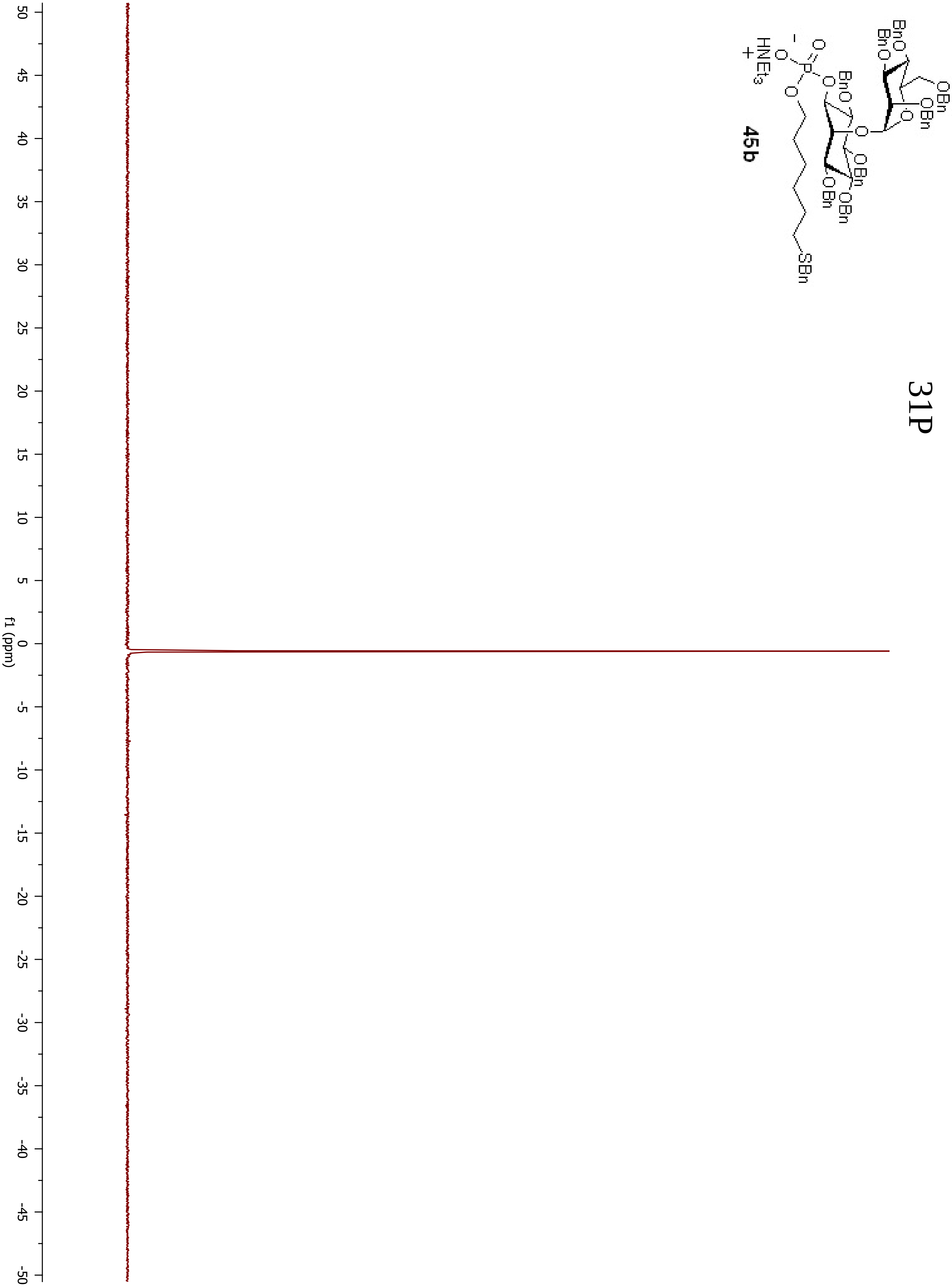
31P
45b
f1 (ppm)

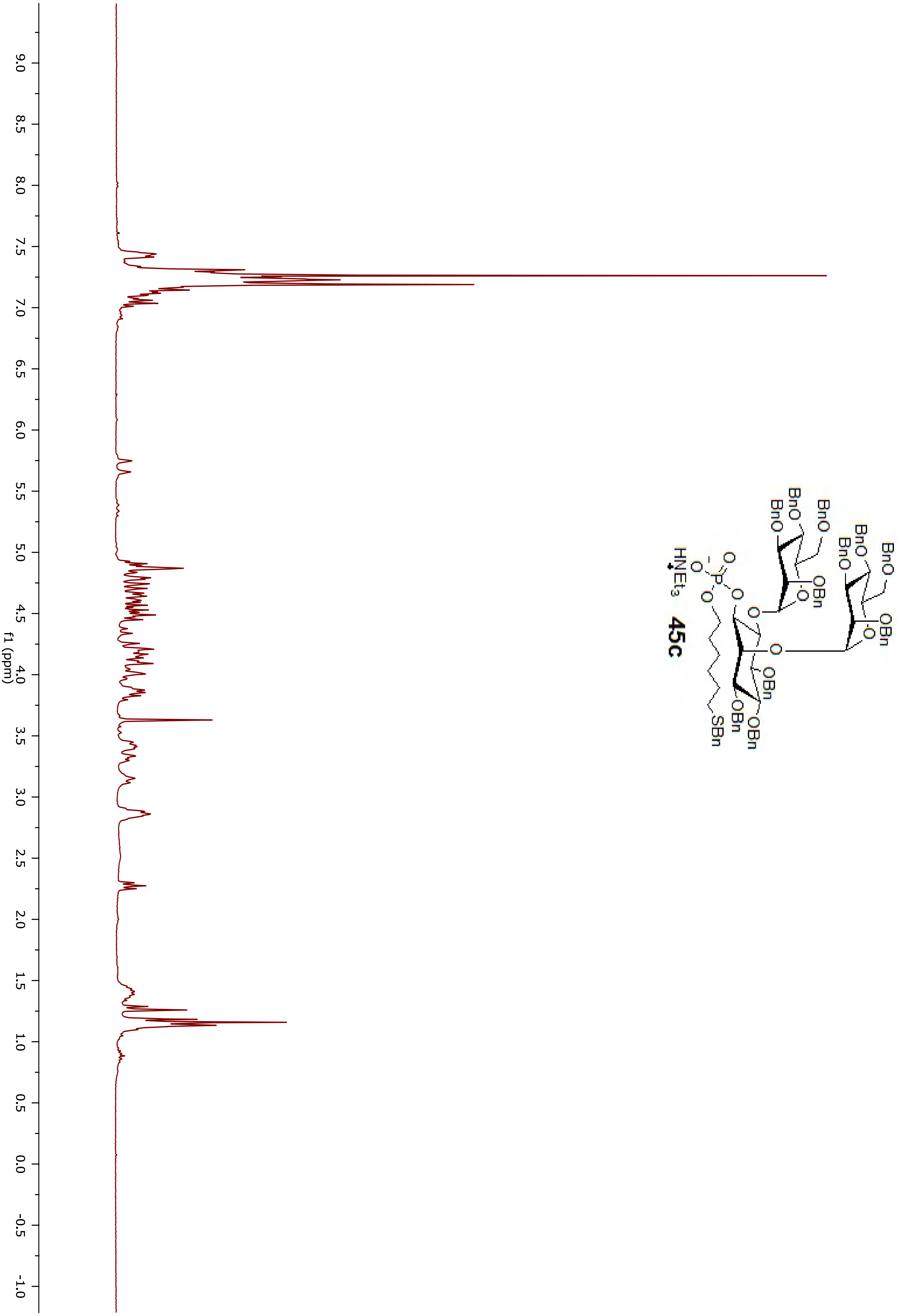
9.0
8.5
8.0
7.5
7.0
6.5
6.0
5.5
5.0
4.5
4.0
3.5
3.0
2.5
2.0
1.5
1.0
0.5
0.0
-0.5
-1.0
f1 (ppm)
BnO
BnO
BnO
OBn
O
BnO
BnO
BnO
OBn
O
O
O
O
OBn
OBn
OBn
O
P
O
O
O
HNEt3
SBn

45c

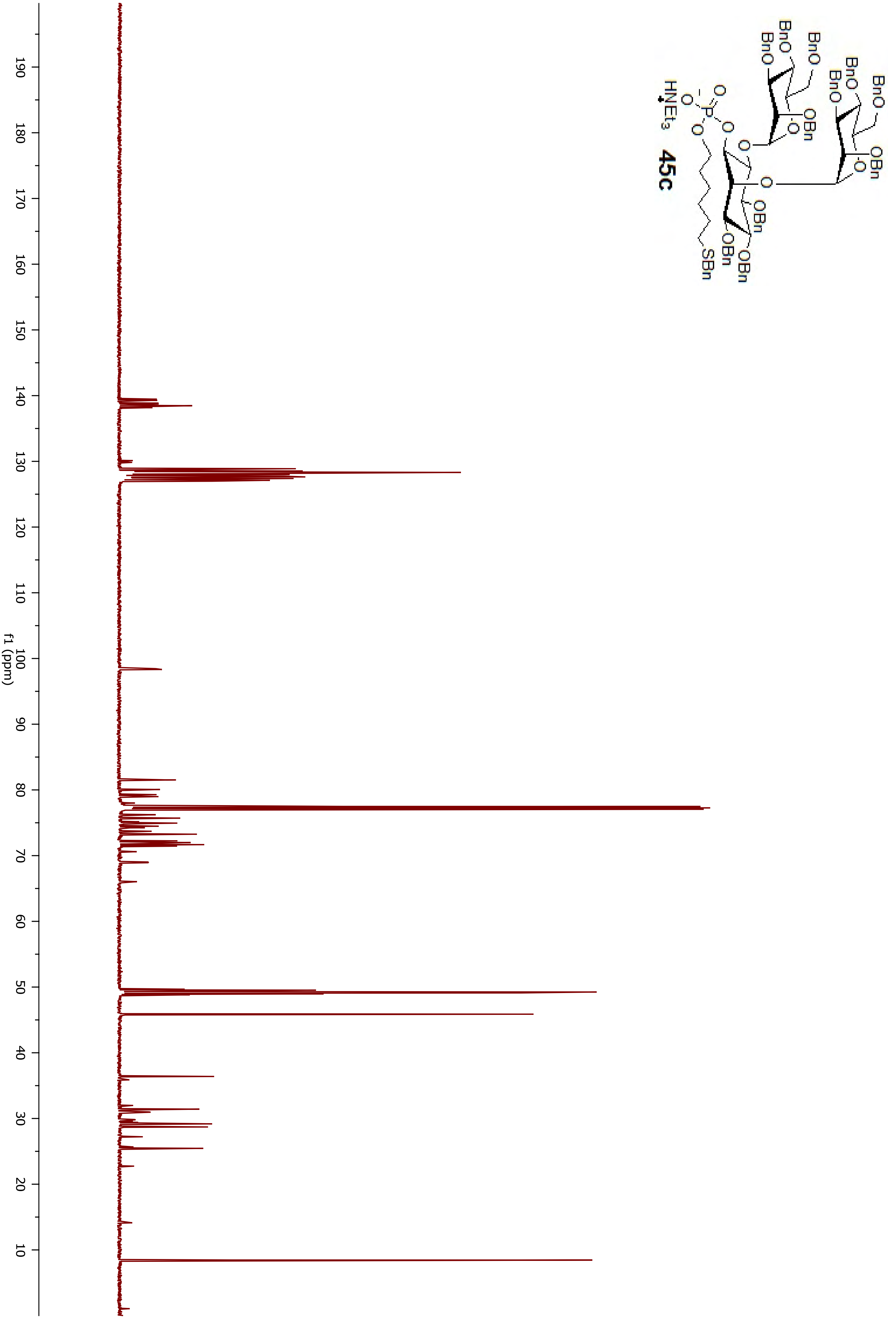
f1 (ppm)
45c

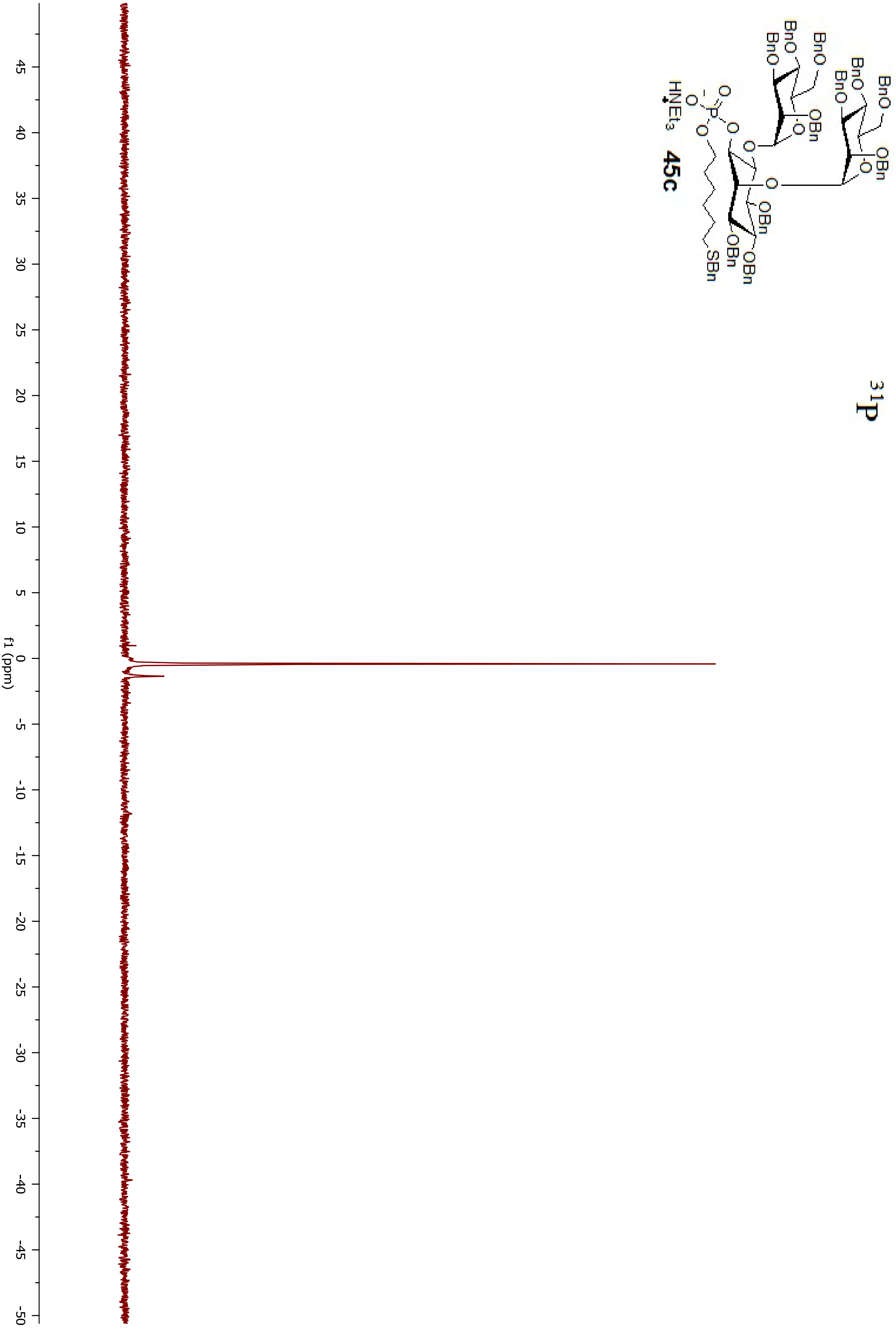
31P
45c
f1 (ppm)

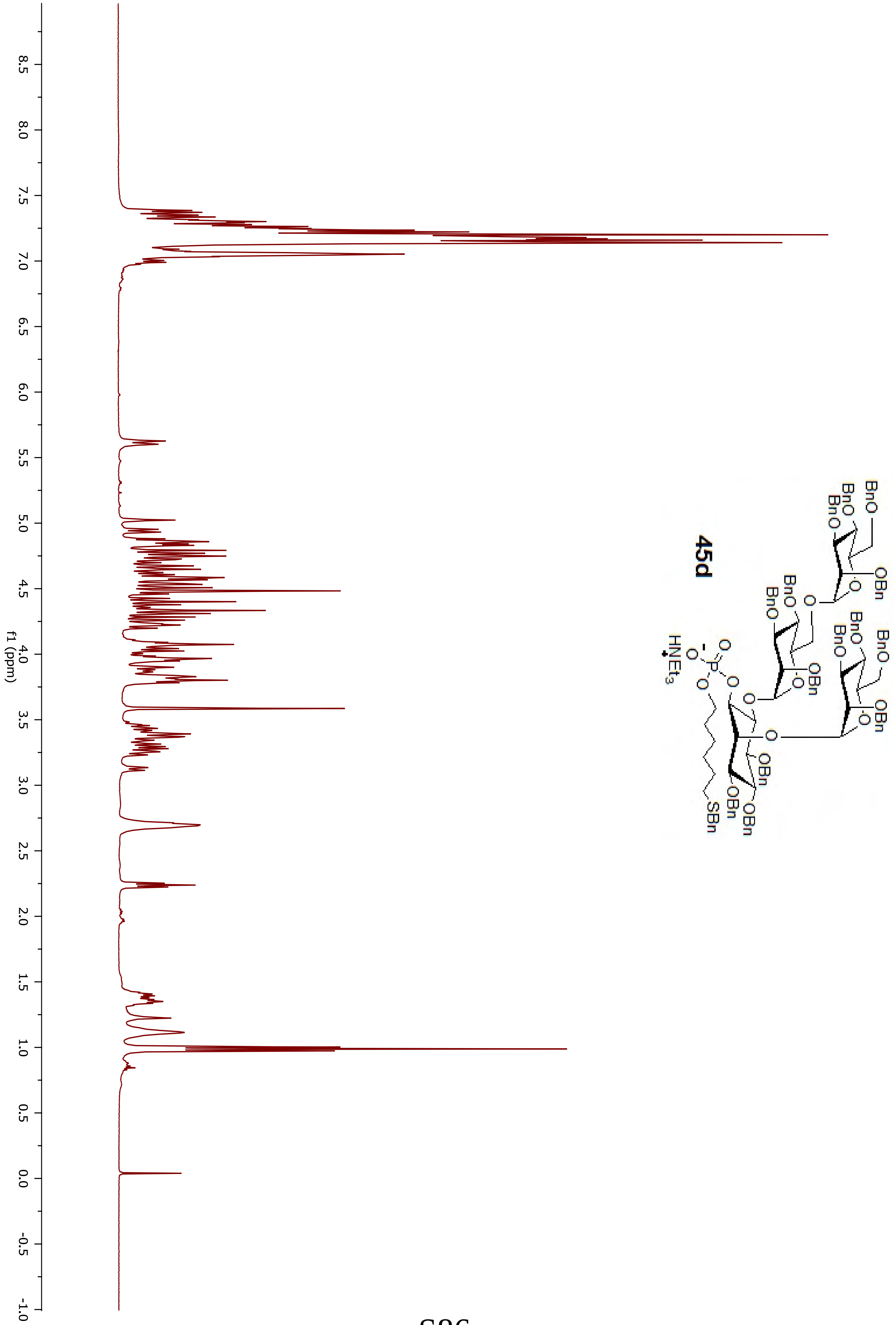
f1 (ppm)
45d

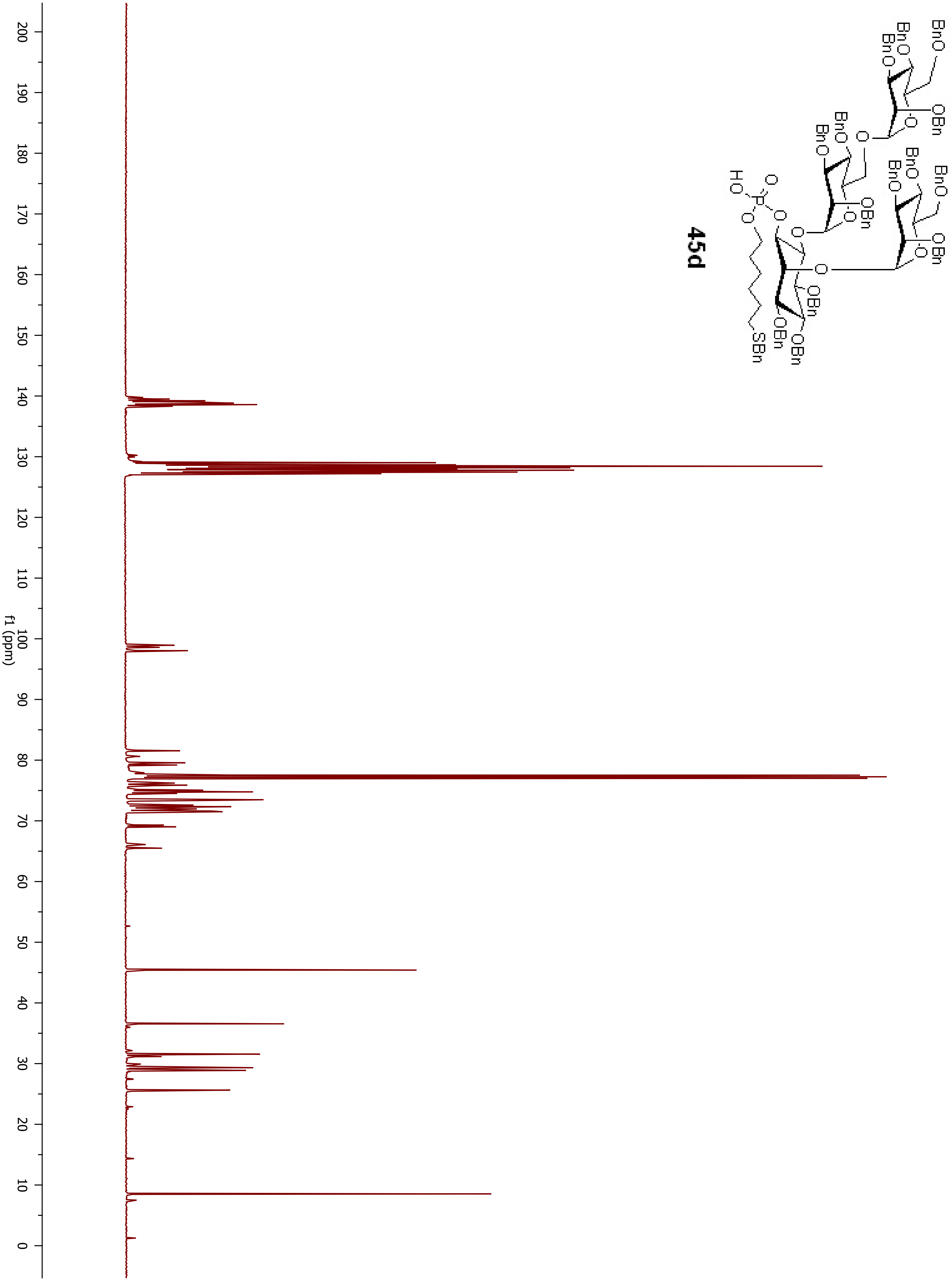

f1 (ppm)
200
190
180
170
160
150
140
130
120
110
100
90
80
70
60
50
40
30
20
10
0

45d

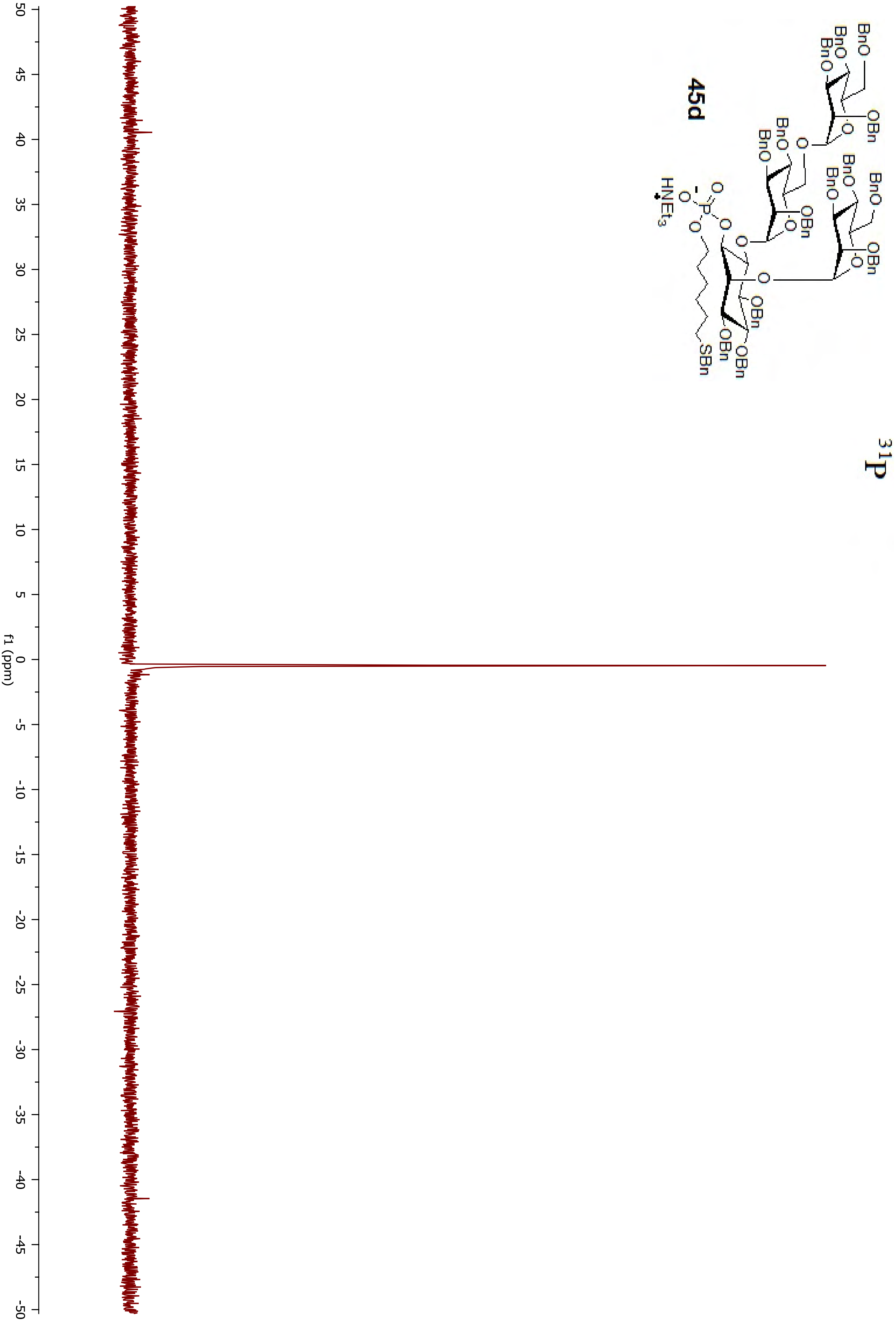

31P
45d
f1 (ppm)
50 45 40 35 30 25 20 15 10 5 0 -5 -10 -15 -20 -25 -30 -35 -40 -45 -50

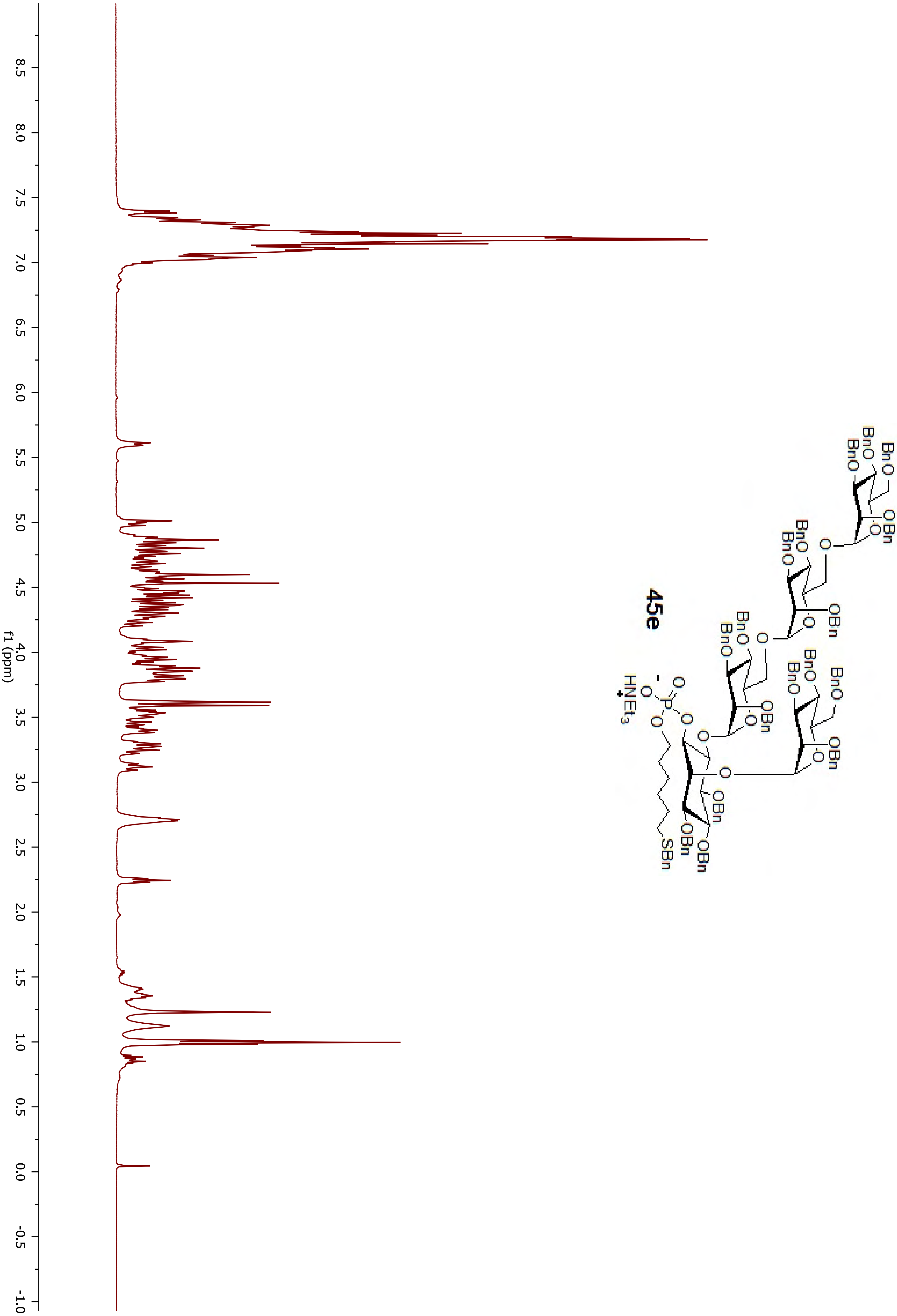
8.5
8.0
7.5
7.0
6.5
6.0
5.5
5.0
4.5
4.0
3.5
3.0
2.5
2.0
1.5
1.0
0.5
0.0
-0.5
-1.0
f1 (ppm)
45e
BnO
OBn
O
SBn
HNEt$_3$
P

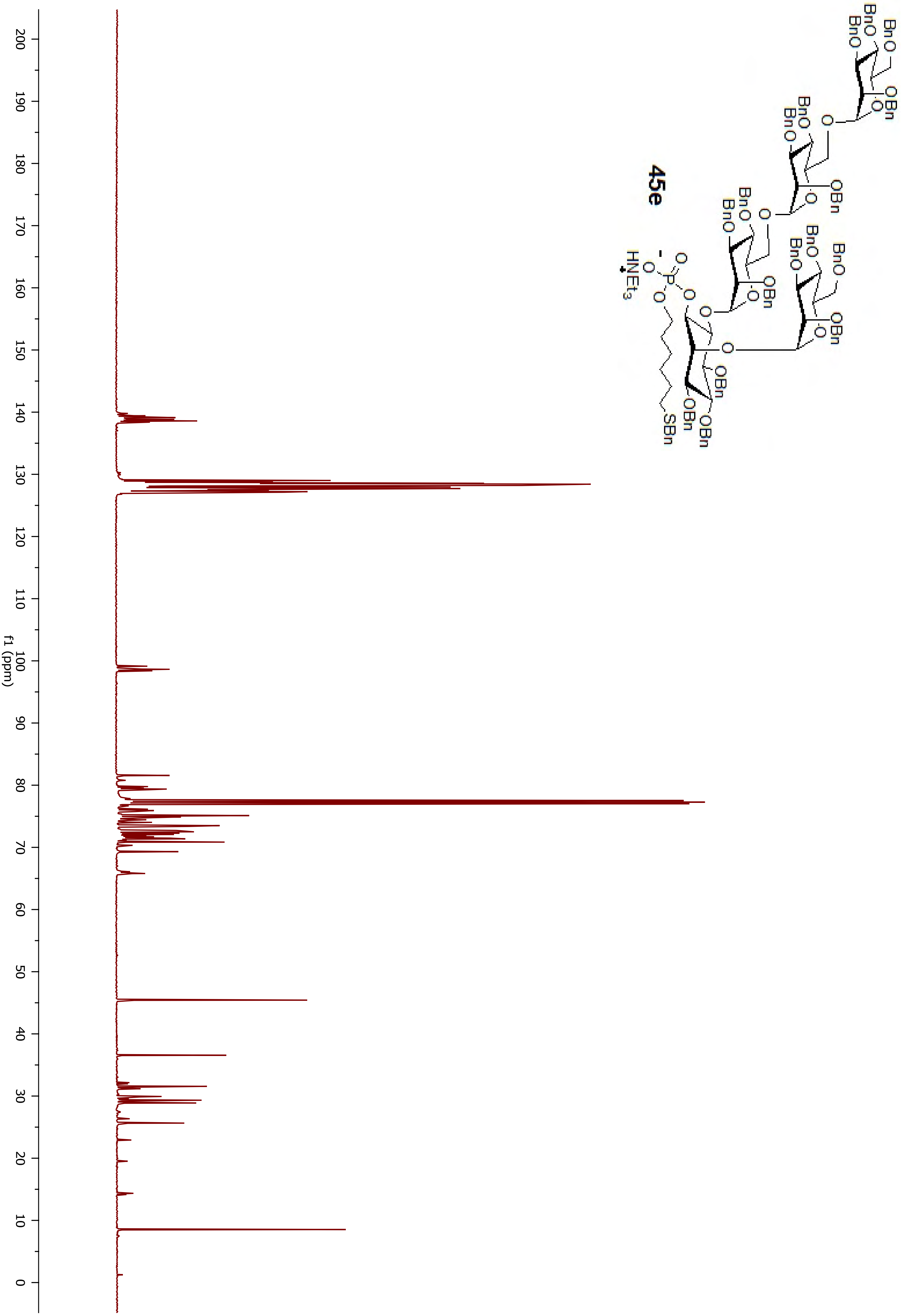
45e
f1 (ppm)

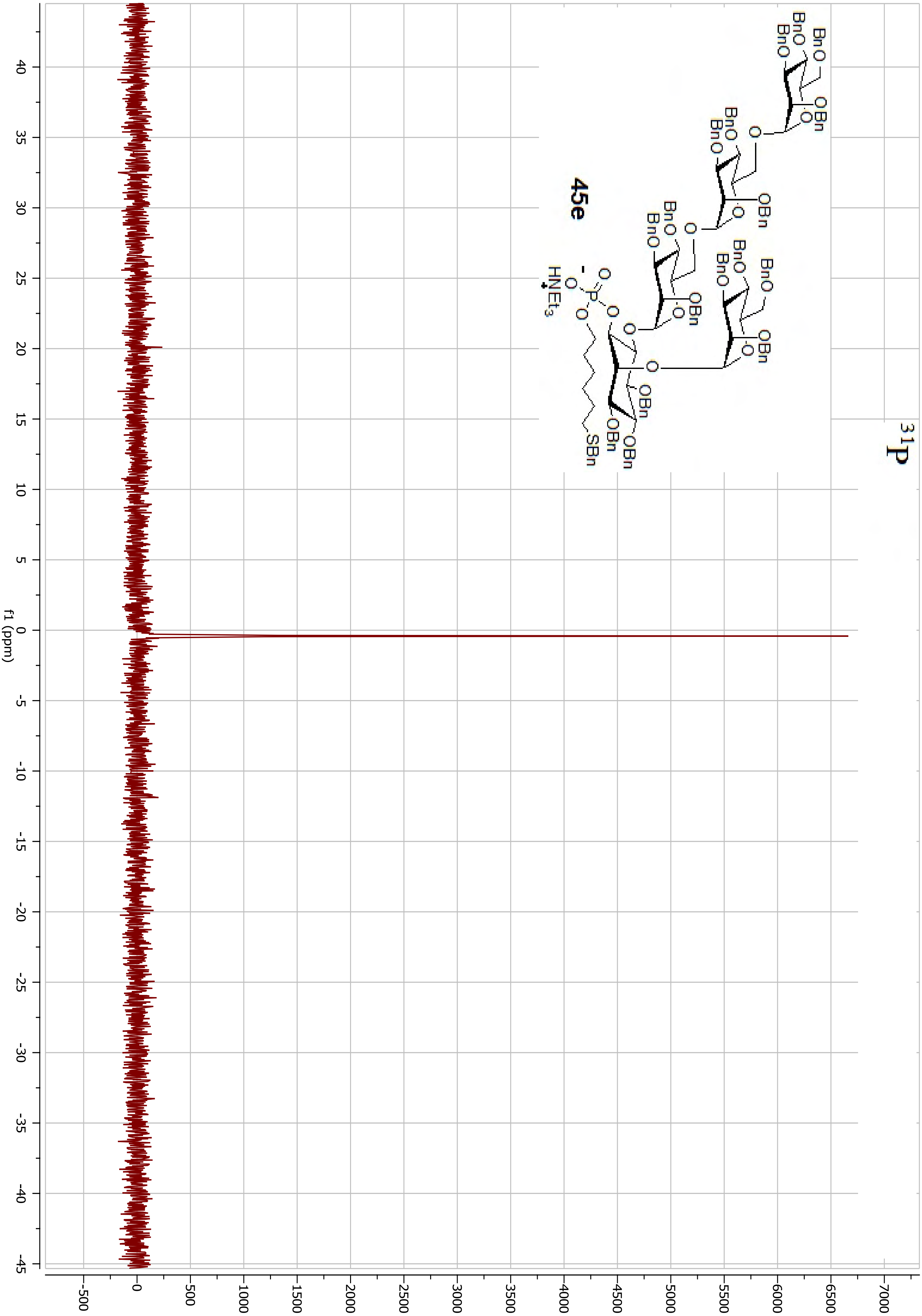

^{31}P
45e
f1 (ppm)

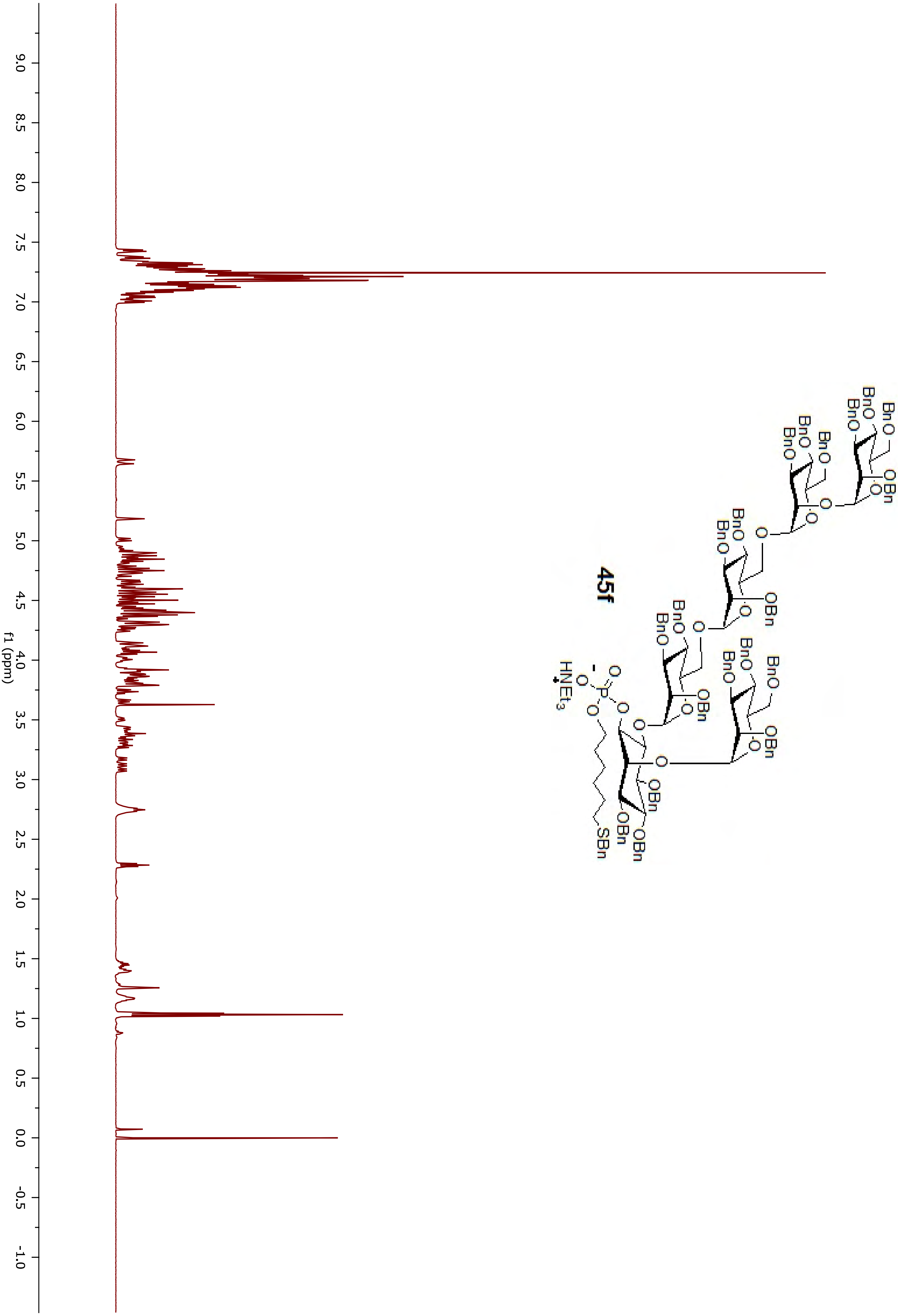
f1 (ppm)
45f

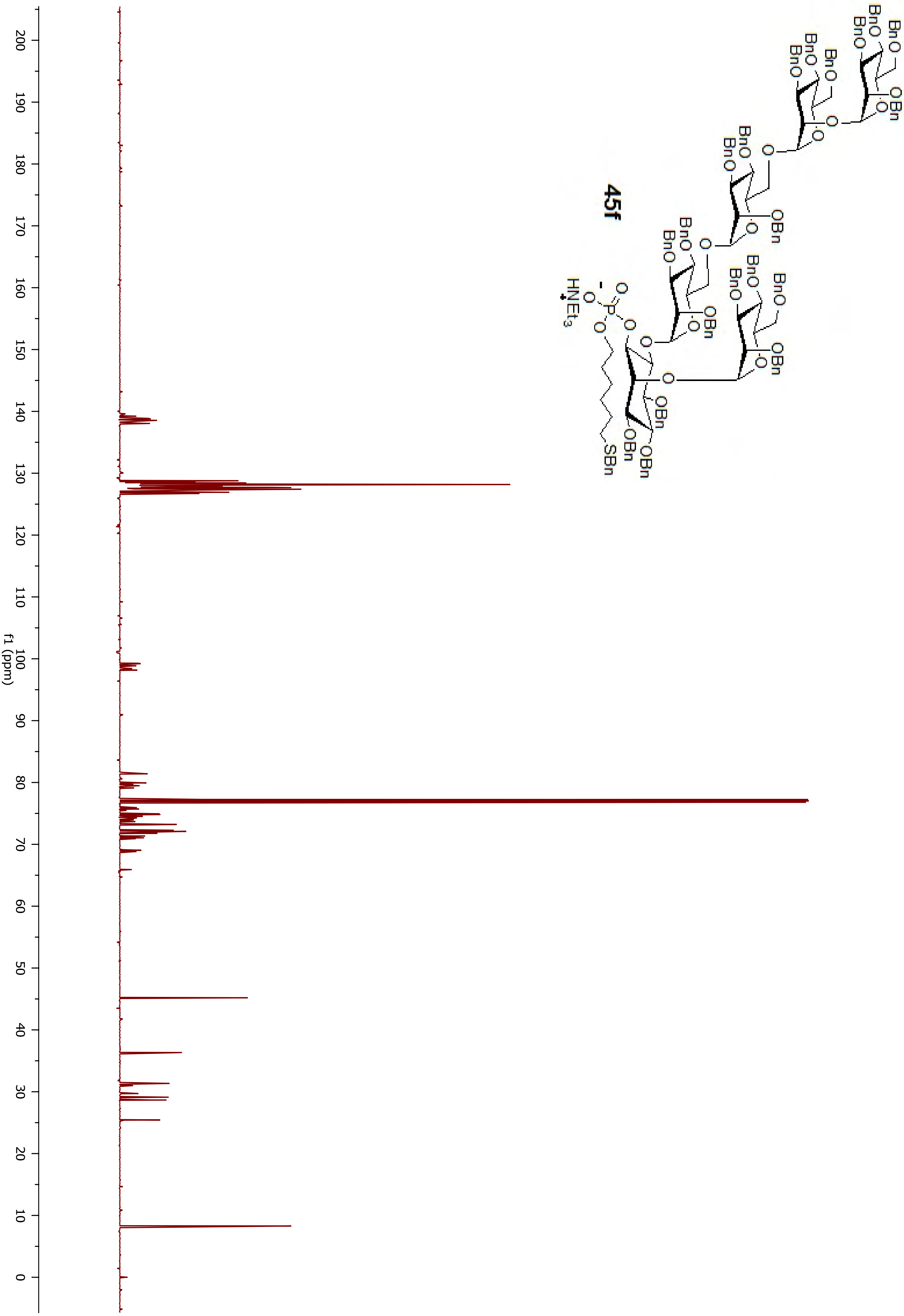
f1 (ppm)
200
190
180
170
160
150
140
130
120
110
100
90
80
70
60
50
40
30
20
10
0
BnO
OBn
SBn
HNEt3
P
O

45f

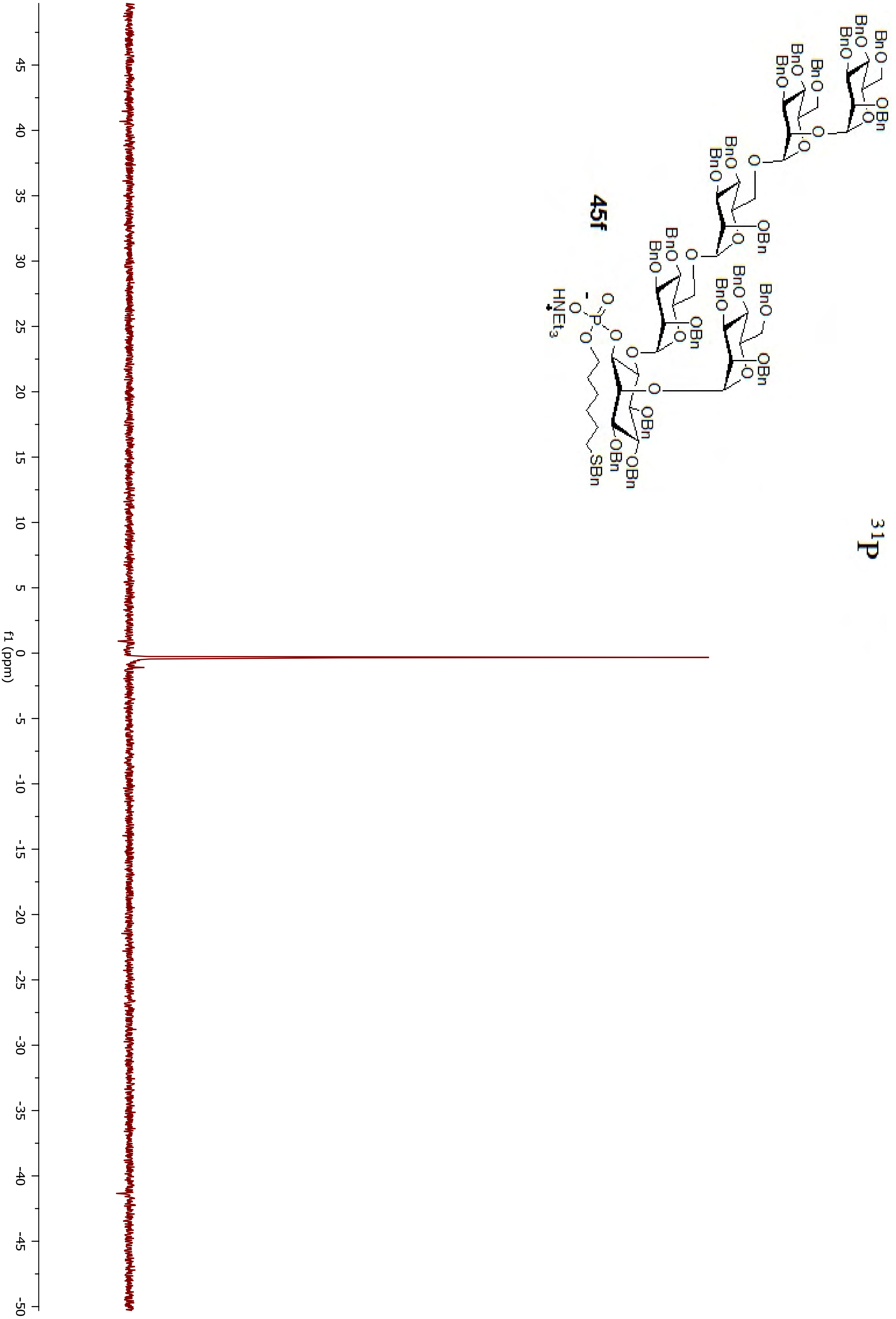

31P
45f
f1 (ppm)

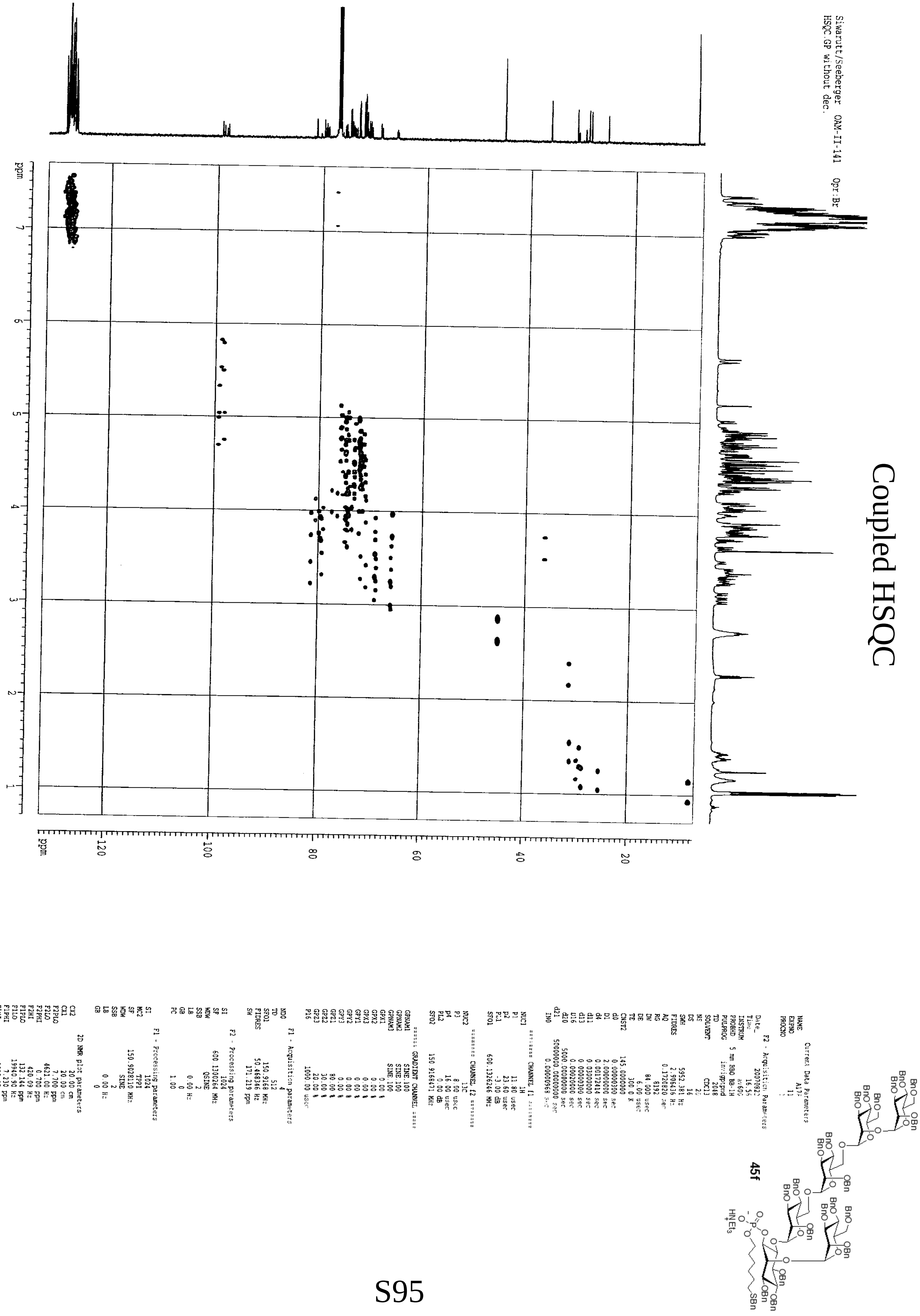
Coupled HSQC
45f

Coupled HSQC

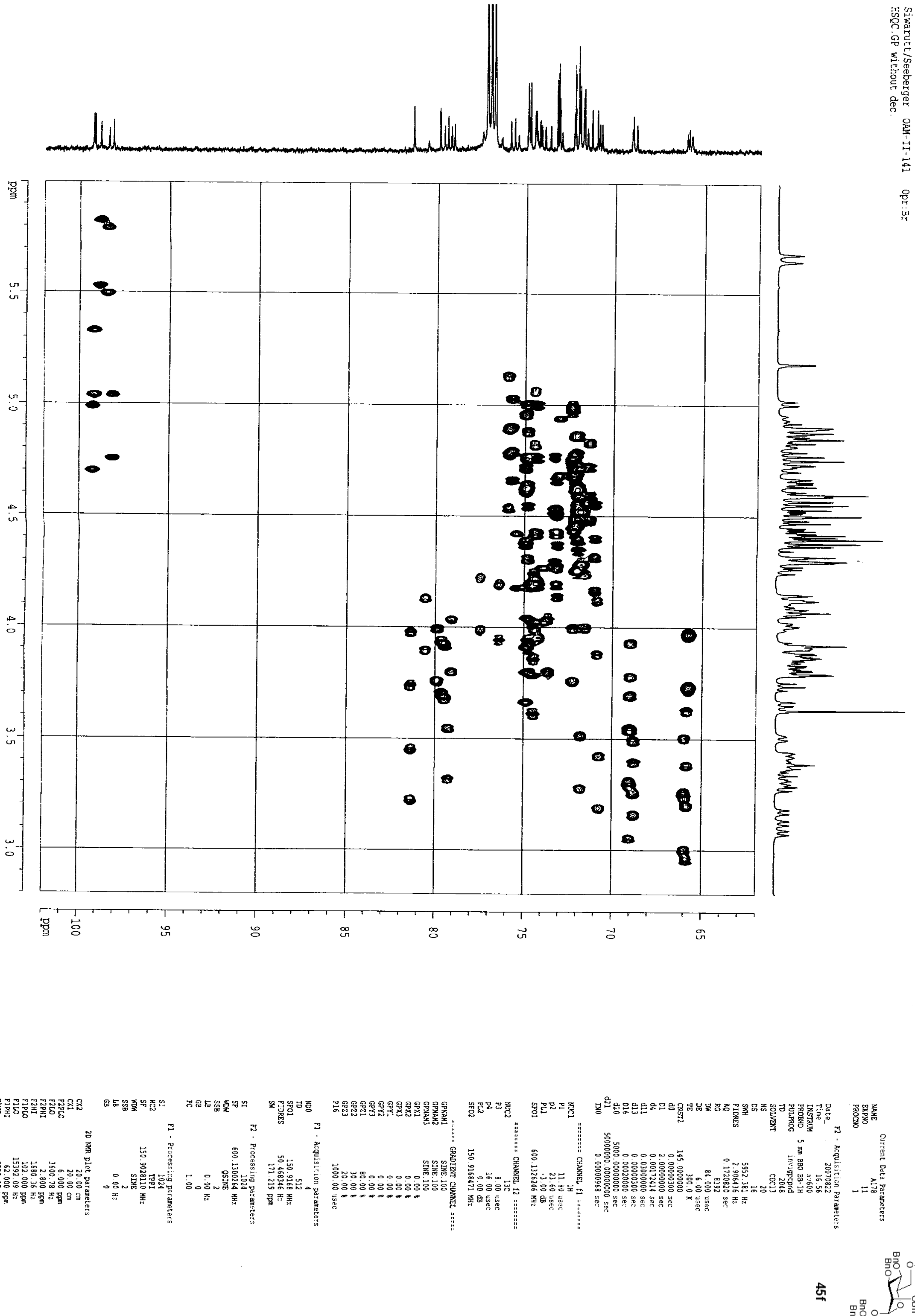

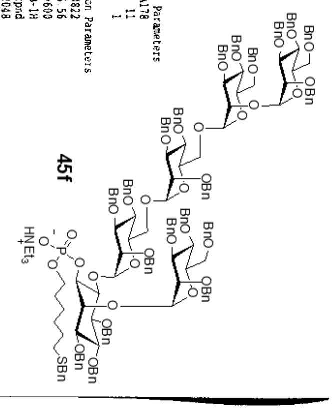

45f

COSY

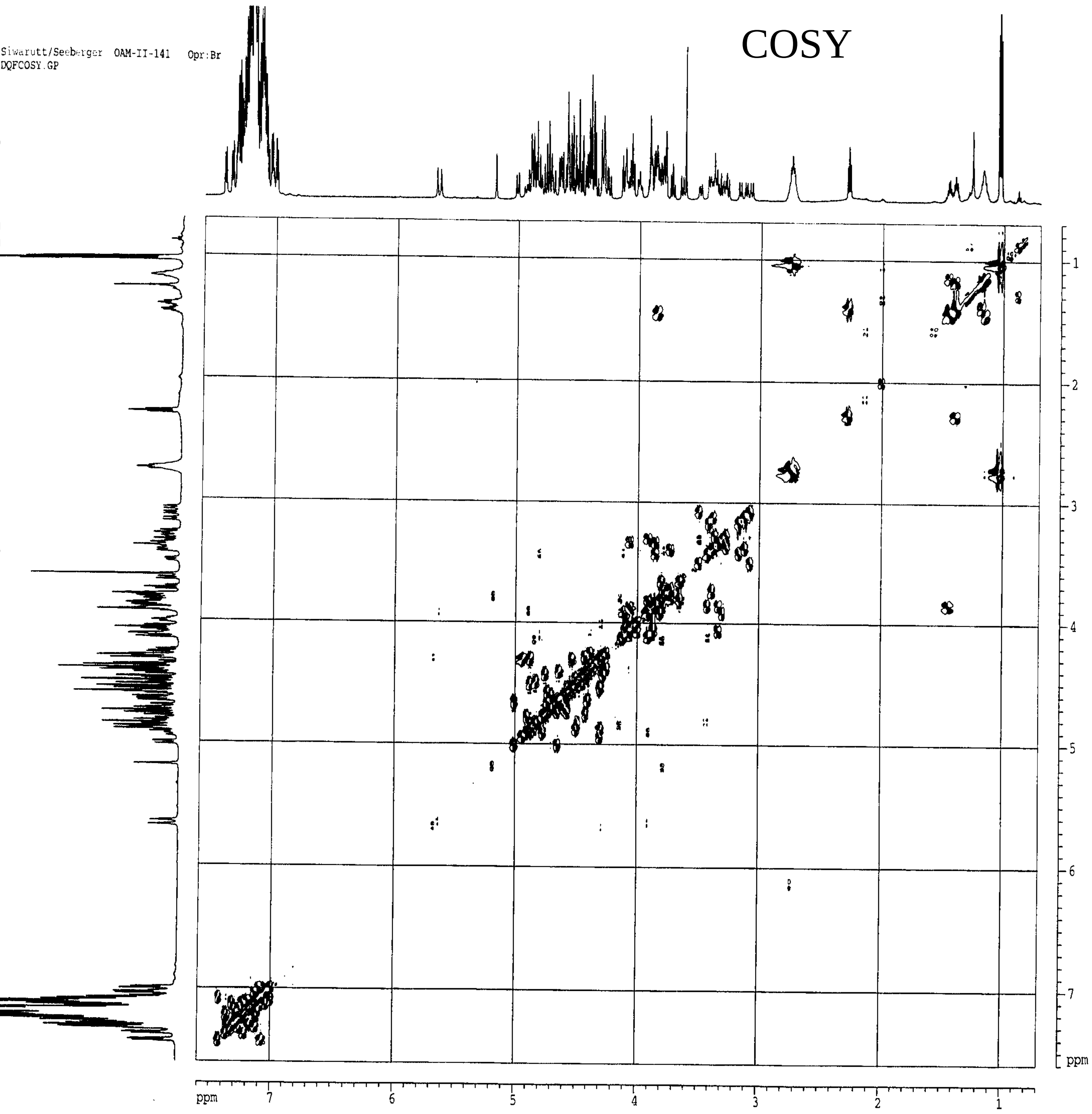

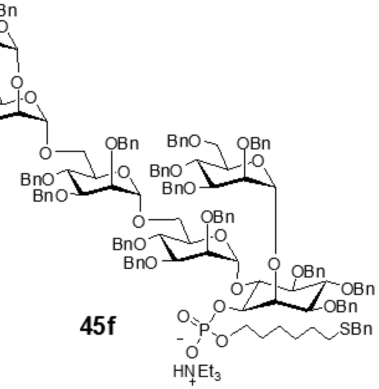

45f

Current Data Parameters

NAME	A178
EXPNO	10
PROCNO	1

F2 - Acquisition Parameters

Date_	20070822
Time	13.48
INSTRUM	av600
PROBHD	5 mm BBO BB-1H
PULPROG	cosydfgptp
TD	2048
SOLVENT	CDCl3
NS	8
DS	16
SWH	5952.381 Hz
FIDRES	2.906436 Hz
AQ	0.1720820 sec
RG	4096
DW	84.000 usec
DE	6.00 usec
TE	300.0 K
d0	0.00000300 sec
D1	2.50000000 sec
d11	0.03000000 sec
d12	0.00002000 sec
d13	0.00000300 sec
D16	0.00020000 sec
d20	5000.00000000 sec
IN0	0.00008400 sec

======== CHANNEL f1 ========

NUC1	1H
P1	11.60 usec
p2	23.20 usec
PL1	-3.00 dB
PL12	120.00 dB
SFO1	600.1326246 MHz

====== GRADIENT CHANNEL =====

GPNAM1	SINE.100
GPNAM2	SINE.100
GPX1	0.00 %
GPX2	0.00 %
GPY1	0.00 %
GPY2	0.00 %
GPZ1	10.00 %
GPZ2	20.00 %
P16	1000.00 usec

F1 - Acquisition parameters

ND0	2
TD	512
SFO1	600.1326 MHz
FIDRES	11.625744 Hz
SW	9.918 ppm

F2 - Processing parameters

SI	1024
SF	600.1300264 MHz
WDW	QSINE
SSB	3
LB	0.00 Hz
GB	0
PC	1.00

F1 - Processing parameters

SI	1024
MC2	TPPI
SF	600.1300264 MHz
WDW	QSINE
SSB	2
LB	0.00 Hz
GB	0

2D NMR plot parameters

CX2	20.00 cm
CX1	20.00 cm
F2PLO	7.603 ppm
F2LO	4562.95 Hz
F2PHI	0.697 ppm
F2HI	418.37 Hz
F1PLO	7.603 ppm
F1LO	4562.95 Hz
F1PHI	0.697 ppm
F1HI	418.37 Hz
F2PPMCM	0.34531 ppm/cm
F2HZCM	207.22887 Hz/cm
F1PPMCM	0.34531 ppm/cm

COSY

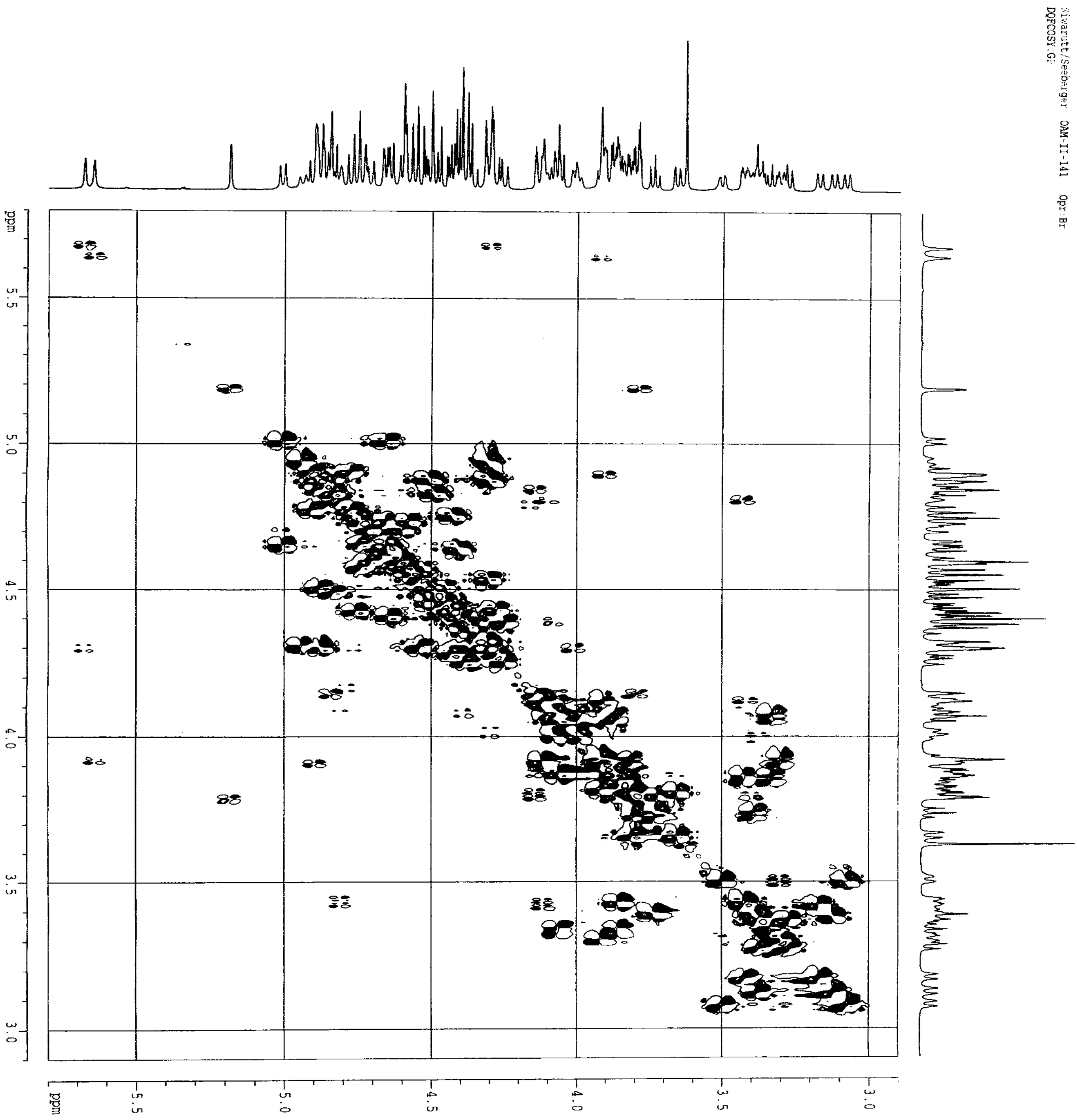

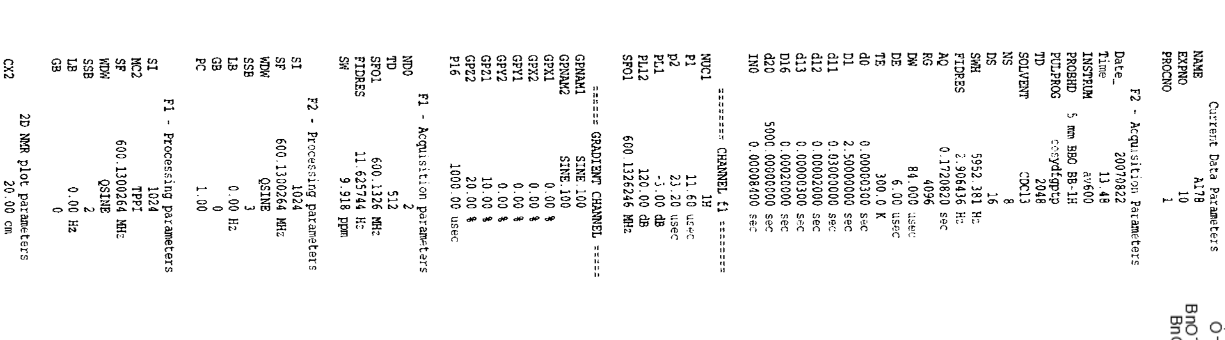

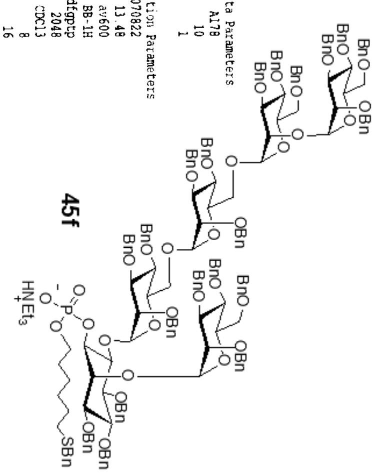

45f

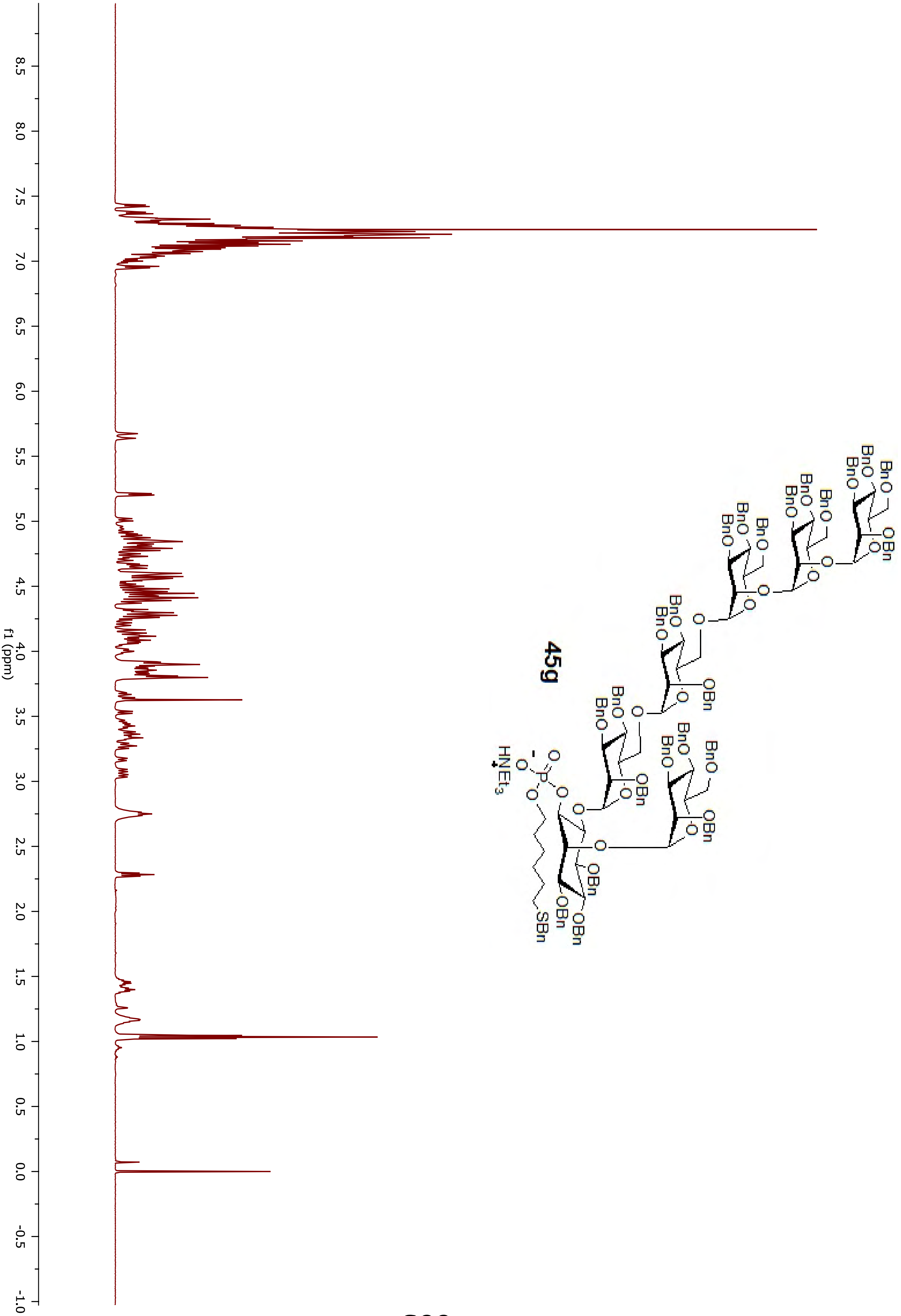
45g
f1 (ppm)

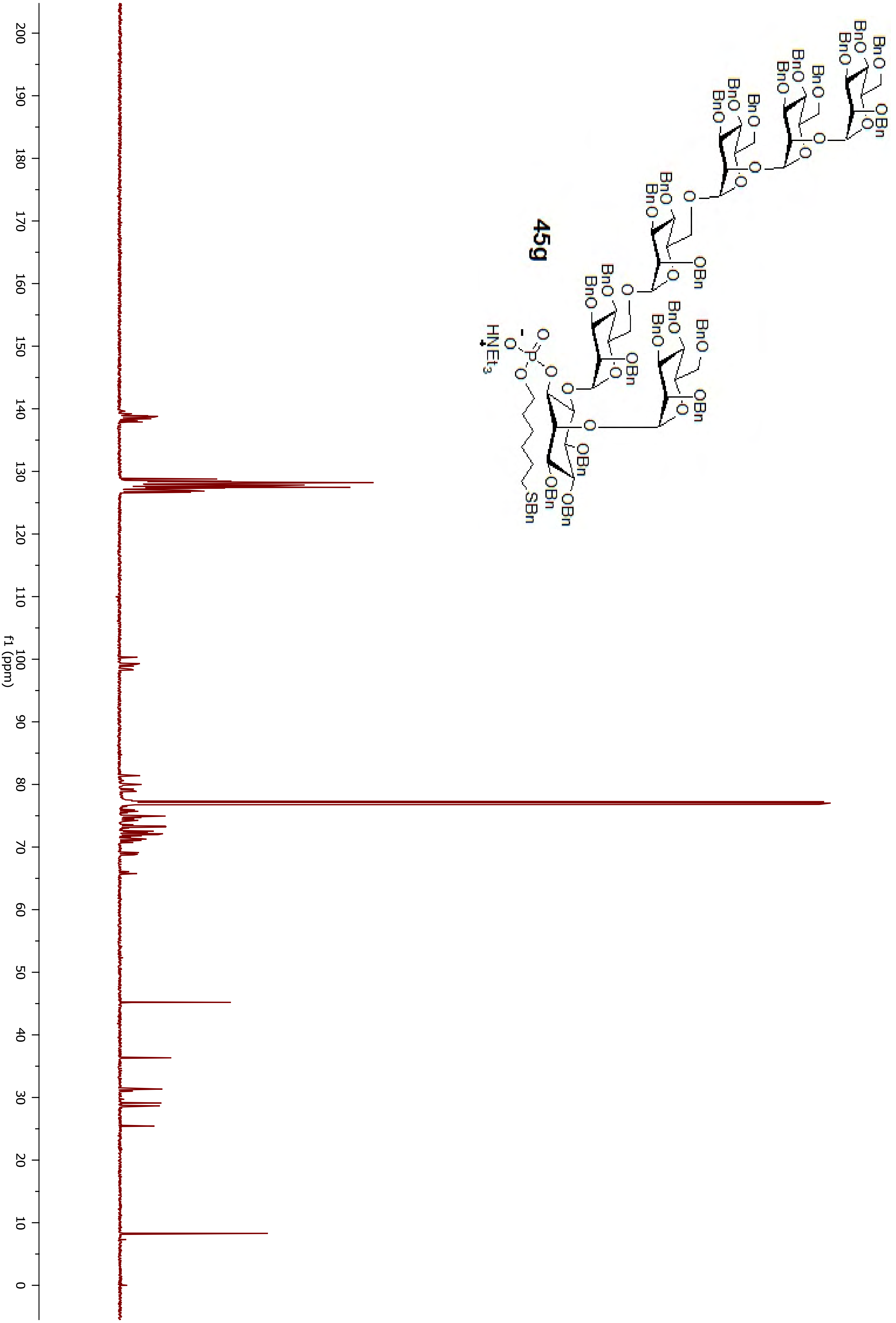
45g
f1 (ppm)

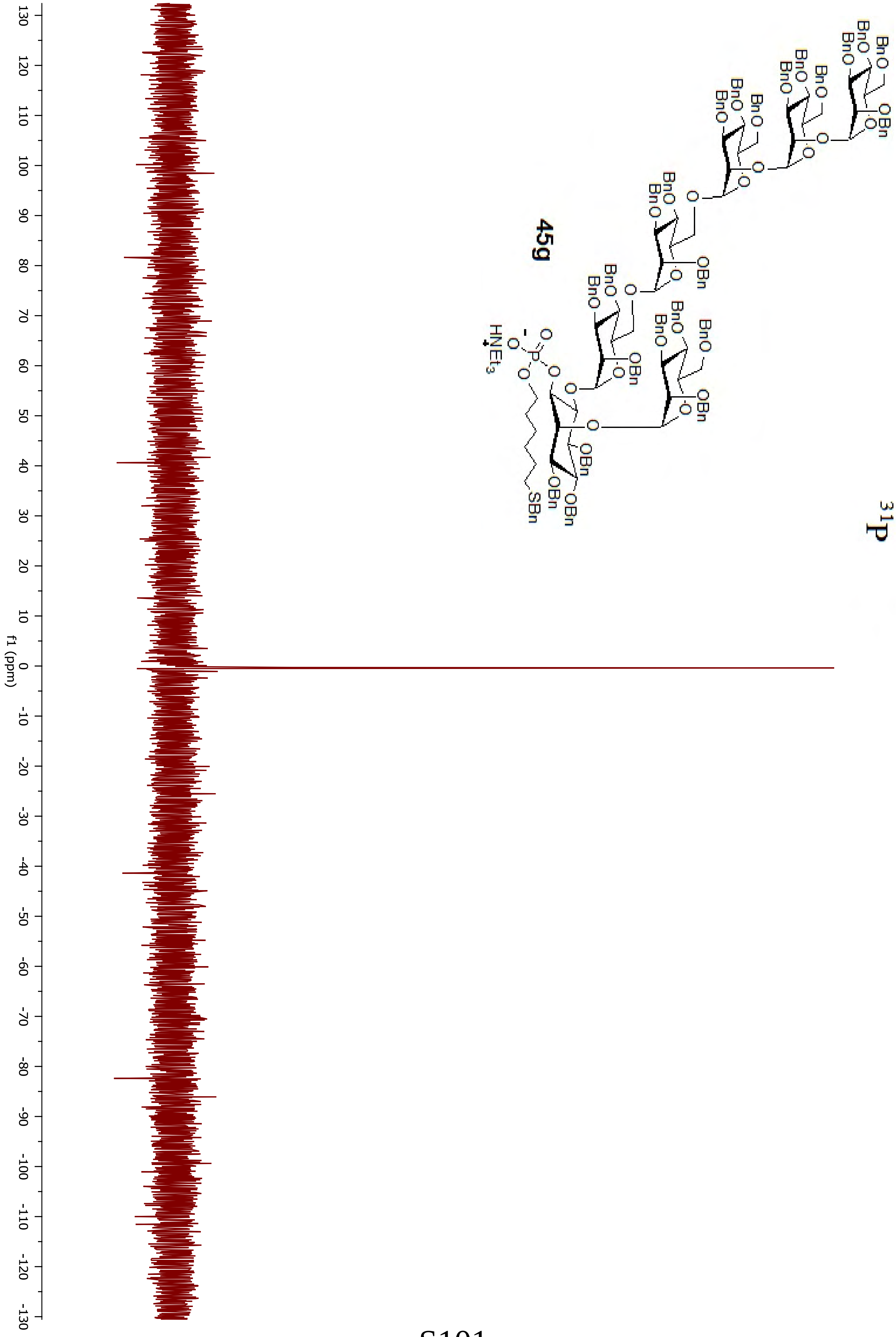
31P
45g
f1 (ppm)

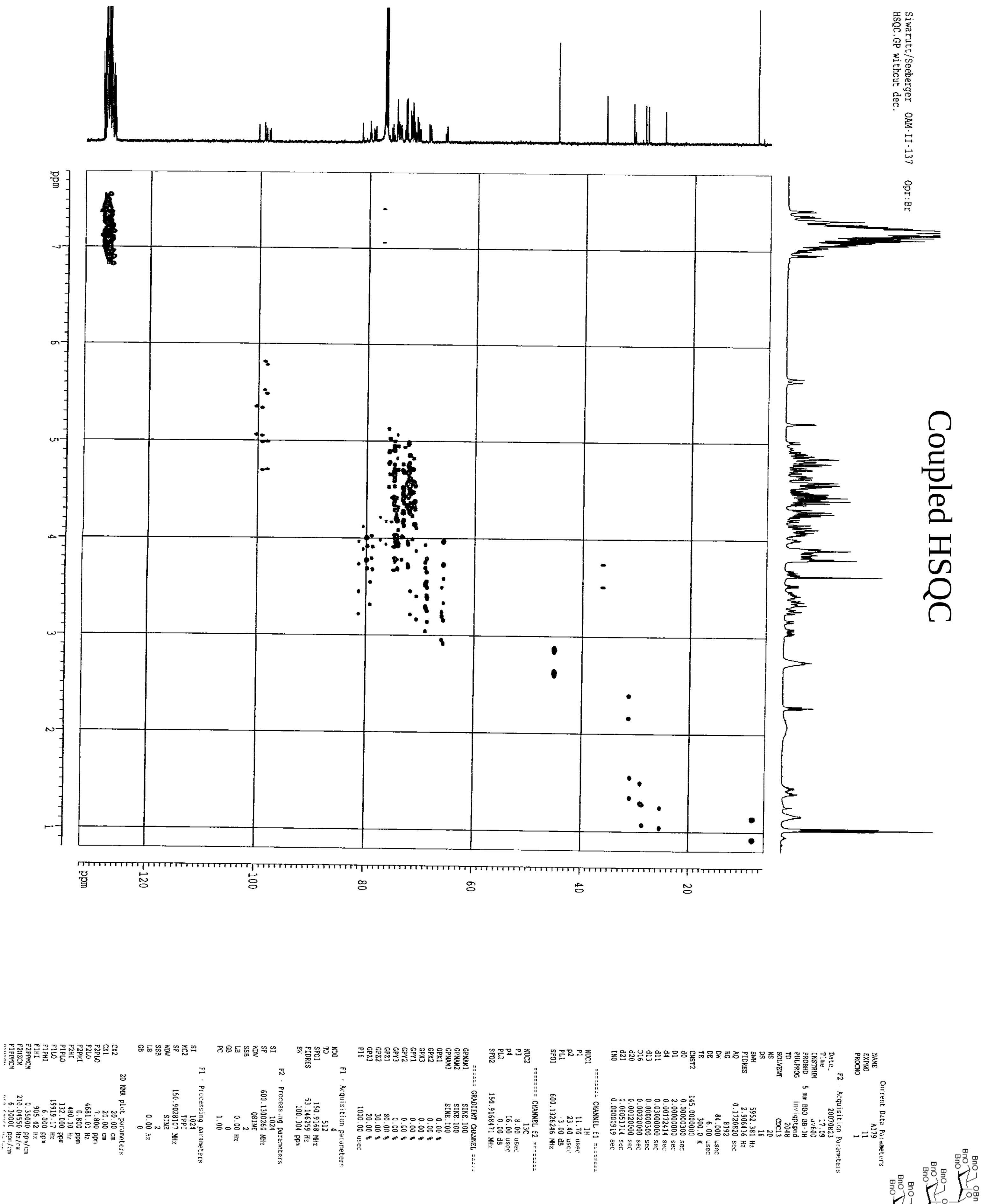
Coupled HSQC
Siwarut/Seeberger OAM-II-137 Opr:Br
HSQC.GP without dec.

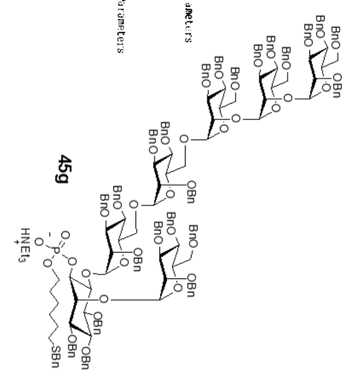

45g

Coupled HSQC

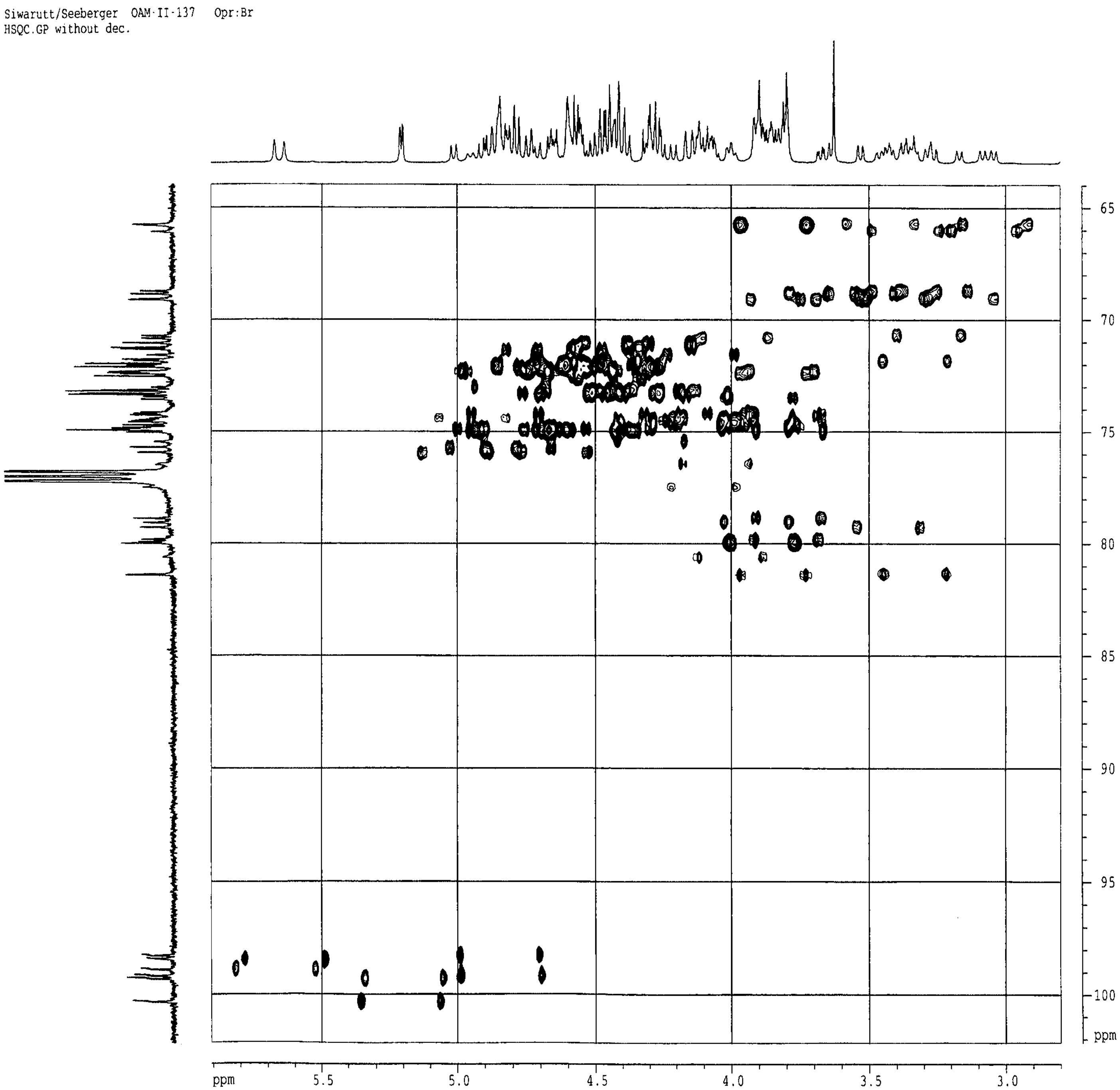

Current Data Parameters

NAME	A179
EXPNO	11
PROCNO	1

F2 - Acquisition Parameters

Date_	20070823
Time	17.09
INSTRUM	av600
PROBHD	5 mm BBO BB-1H
PULPROG	invigptpnd
TD	2048
SOLVENT	CDCl3
NS	20
DS	16
SWH	5952.381 Hz
FIDRES	2.906436 Hz
AQ	0.1720820 sec
RG	8192
DW	84.000 usec
DE	6.00 usec
TE	300.0 K
CNST2	145.0000000
d0	0.00000300 sec
D1	2.00000000 sec
d4	0.00172414 sec
d11	0.03000000 sec
d13	0.00000300 sec
D16	0.00020000 sec
d20	0.00120000 sec
d21	0.00051714 sec
IN0	0.00000919 sec

======== CHANNEL f1 ========

NUC1	1H
P1	11.70 usec
p2	23.40 usec
PL1	-3.00 dB
SFO1	600.1326246 MHz

======== CHANNEL f2 ========

NUC2	13C
P3	8.00 usec
p4	16.00 usec
PL2	0.00 dB
SFO2	150.9168471 MHz

====== GRADIENT CHANNEL =====

GPNAM1	SINE.100
GPNAM2	SINE.100
GPNAM3	SINE.100
GPX1	0.00 %
GPX2	0.00 %
GPX3	0.00 %
GPY1	0.00 %
GPY2	0.00 %
GPY3	0.00 %
GPZ1	80.00 %
GPZ2	30.00 %
GPZ3	20.00 %
P16	1000.00 usec

F1 - Acquisition parameters

ND0	4
TD	512
SFO1	150.9168 MHz
FIDRES	53.146259 Hz
SW	180.304 ppm

F2 - Processing parameters

SI	1024
SF	600.1300260 MHz
WDW	QSINE
SSB	2
LB	0.00 Hz
GB	0
PC	1.00

F1 - Processing parameters

SI	1024
MC2	TPPI
SF	150.9028107 MHz
WDW	SINE
SSB	2
LB	0.00 Hz
GB	0

2D NMR plot parameters

CX2	20.00 cm
CX1	20.00 cm
F2PLO	5.909 ppm
F2LO	3546.10 Hz
F2PHI	2.800 ppm
F2HI	1680.36 Hz
F1PLO	102.173 ppm
F1LO	15418.21 Hz
F1PHI	63.961 ppm
F1HI	9651.84 Hz
F2PPMCM	0.15544 ppm/cm
F2HZCM	93.28671 Hz/cm
F1PPMCM	1.91062 ppm/cm

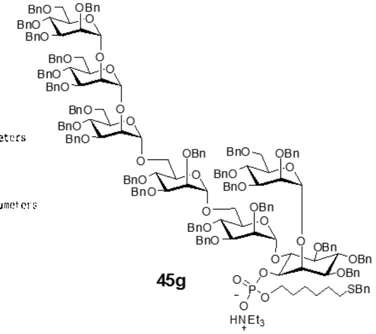

45g

COSY

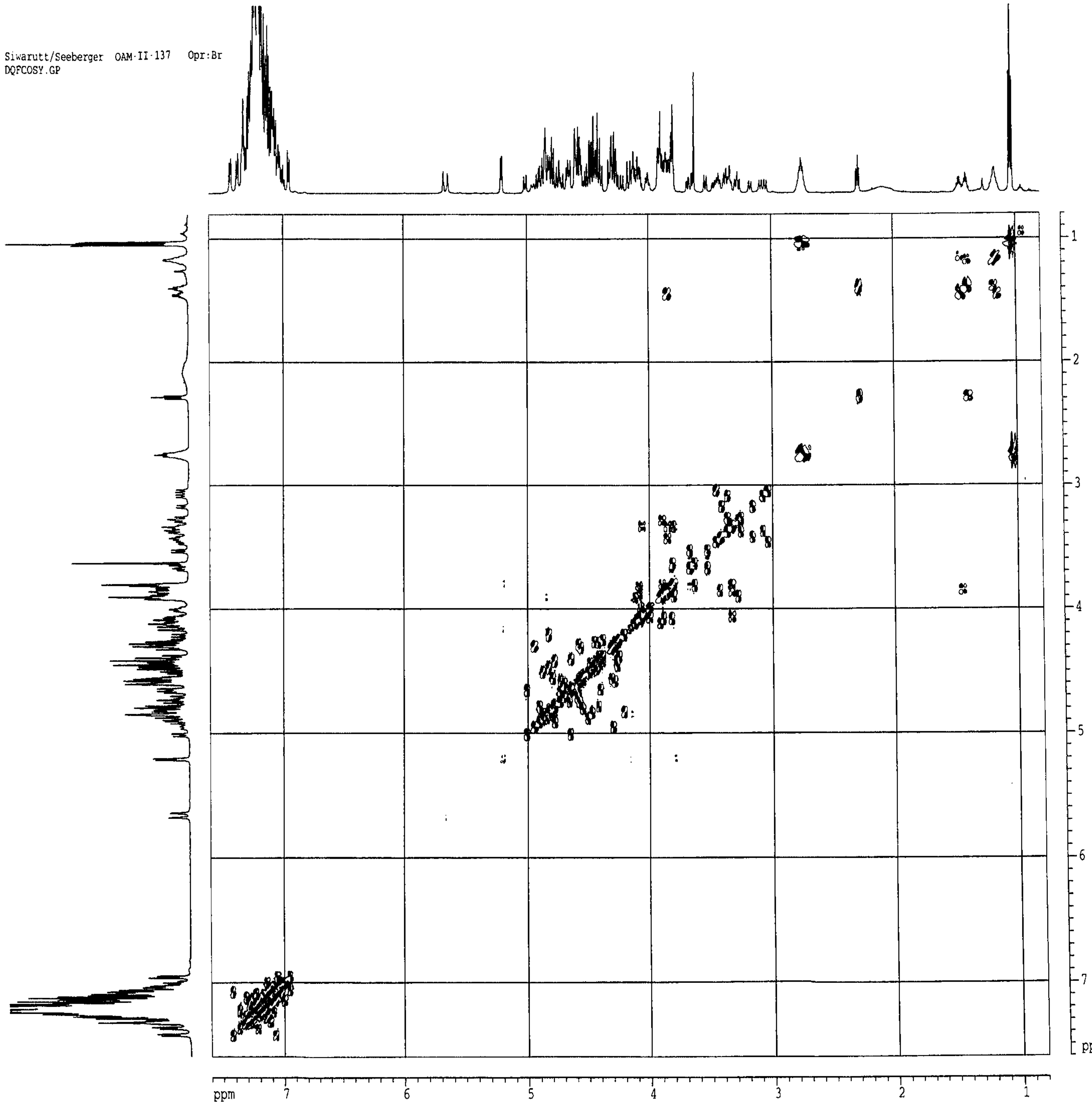

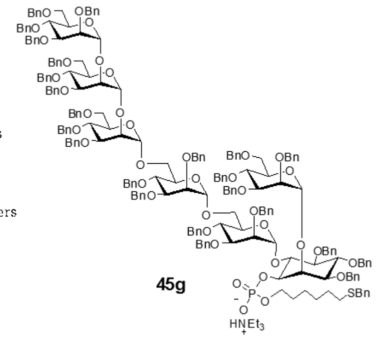

45g

Current Data Parameters

NAME	A179
EXPNO	10
PROCNO	1

F2 - Acquisition Parameters

Date_	20070823
Time	14.01
INSTRUM	av600
PROBHD	5 mm BBO BB-1H
PULPROG	cosydfqptp
TD	2048
SOLVENT	CDCl3
NS	8
DS	16
SWH	5952.381 Hz
FIDRES	2.906436 Hz
AQ	0.1720820 sec
RG	4096
DW	84.000 usec
DE	6.00 usec
TE	300.0 K
d0	0.00000300 sec
D1	2.50000000 sec
d11	0.03000000 sec
d12	0.00002000 sec
d13	0.00000300 sec
D16	0.00020000 sec
d20	0.00120300 sec
IN0	0.00008400 sec

======== CHANNEL f1 ========

NUC1	1H
P1	11.70 usec
p2	23.40 usec
PL1	-3.00 dB
PL12	120.00 dB
SFO1	600.1326246 MHz

====== GRADIENT CHANNEL =====

GPNAM1	SINE.100
GPNAM2	SINE.100
GPX1	0.00 %
GPX2	0.00 %
GPY1	0.00 %
GPY2	0.00 %
GPZ1	10.00 %
GPZ2	20.00 %
P16	1000.00 usec

F1 - Acquisition parameters

ND0	2
TD	512
SFO1	600.1326 MHz
FIDRES	11.625744 Hz
SW	9.918 ppm

F2 - Processing parameters

SI	1024
SF	600.1300260 MHz
WDW	QSINE
SSB	3
LB	0.00 Hz
GB	0
PC	1.00

F1 - Processing parameters

SI	1024
MC2	TPPI
SF	600.1300260 MHz
WDW	QSINE
SSB	2
LB	0.00 Hz
GB	0

2D NMR plot parameters

CX2	20.00 cm
CX1	20.00 cm
F2PLO	7.604 ppm
F2LO	4563.35 Hz
F2PHI	0.800 ppm
F2HI	480.10 Hz
F1PLO	7.604 ppm
F1LO	4563.35 Hz
F1PHI	0.800 ppm
F1HI	480.10 Hz
F2PPMCM	0.34020 ppm/cm
F2HZCM	204.16234 Hz/cm
F1PPMCM	0.34020 ppm/cm

COSY

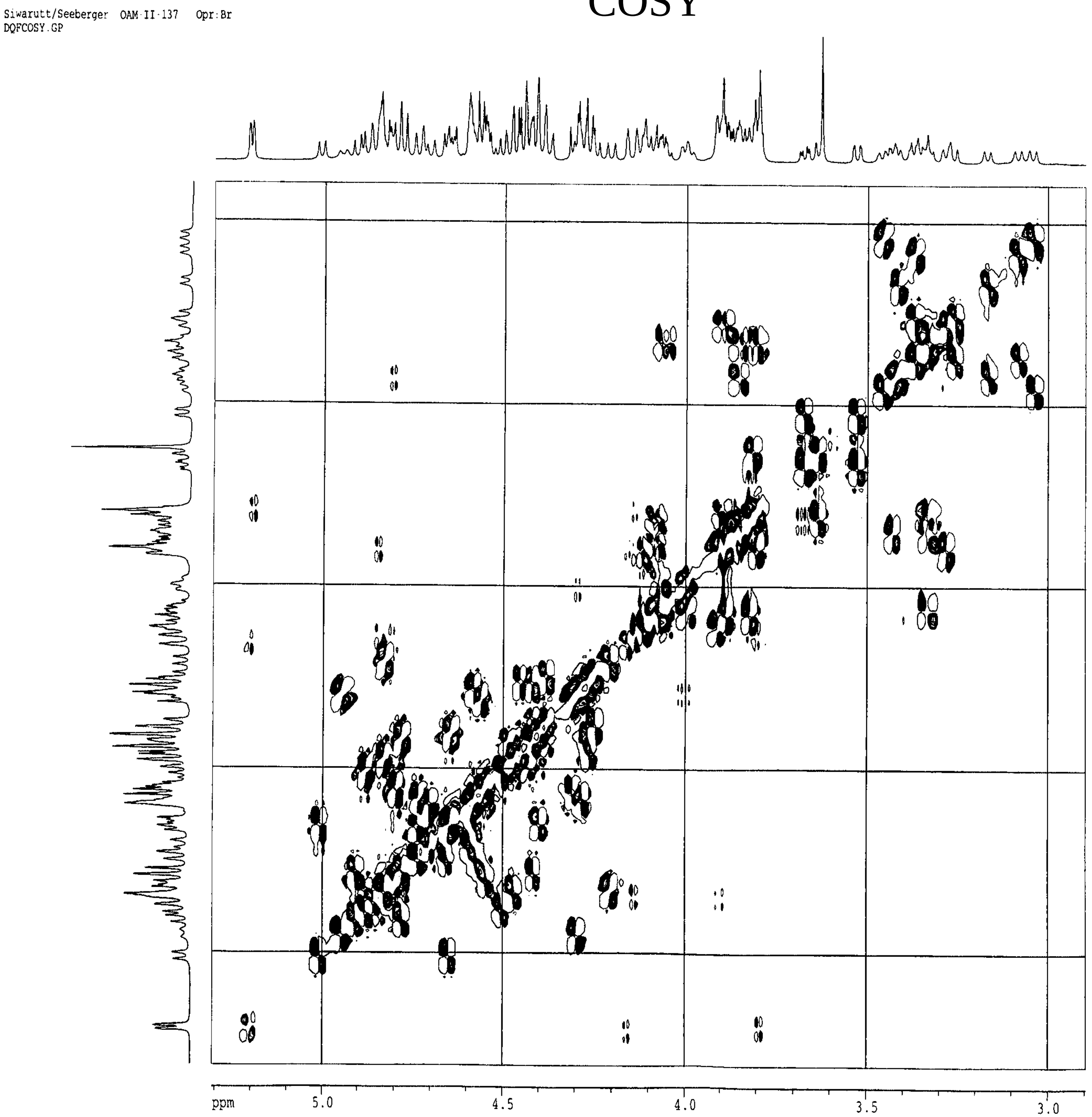

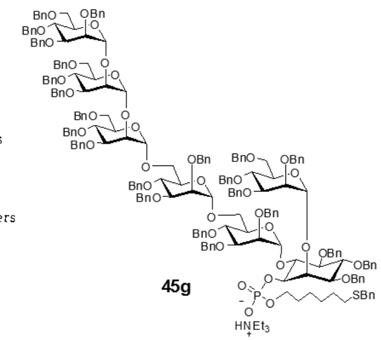

45g

Current Data Parameters

NAME	A179
EXPNO	10
PROCNO	1
F2 - Acquisition Parameters	
Date_	20070823
Time	14.01
INSTRUM	av600
PROBHD	5 mm BBO BB-1H
PULPROG	cosydfgptp
TD	2048
SOLVENT	CDCl3
NS	8
DS	16
SWH	5952.381 Hz
FIDRES	2.906436 Hz
AQ	0.1720820 sec
RG	4096
DW	84.000 usec
DE	6.00 usec
TE	300.0 K
d0	0.00000300 sec
D1	2.50000000 sec
d11	0.03000000 sec
d12	0.00002000 sec
d13	0.00000300 sec
D16	0.00020000 sec
d20	0.00120300 sec
IN0	0.00008400 sec
======== CHANNEL f1 ========	
NUC1	1H
P1	11.70 usec
p2	23.40 usec
PL1	-3.00 dB
PL12	120.00 dB
SFO1	600.1326246 MHz
====== GRADIENT CHANNEL =====	
GPNAM1	SINE.100
GPNAM2	SINE.100
GPX1	0.00 %
GPX2	0.00 %
GPY1	0.00 %
GPY2	0.00 %
GPZ1	10.00 %
GPZ2	20.00 %
P16	1000.00 usec
F1 - Acquisition parameters	
ND0	2
TD	512
SFO1	600.1326 MHz
FIDRES	11.625744 Hz
SW	9.918 ppm
F2 - Processing parameters	
SI	1024
SF	600.1300260 MHz
WDW	QSINE
SSB	3
LB	0.00 Hz
GB	0
PC	1.00
F1 - Processing parameters	
SI	1024
MC2	TPPI
SF	600.1300260 MHz
WDW	QSINE
SSB	2
LB	0.00 Hz
GB	0
2D NMR plot parameters	
CX2	20.00 cm
CX1	20.00 cm
F2PLO	5.308 ppm
F2LO	3185.70 Hz
F2PHI	2.897 ppm
F2HI	1738.30 Hz
F1PLO	5.308 ppm
F1LO	3185.70 Hz
F1PHI	2.897 ppm
F1HI	1738.30 Hz
F2PPMCM	0.12059 ppm/cm
F2HZCM	72.37025 Hz/cm
F1PPMCM	0.12059 ppm/cm

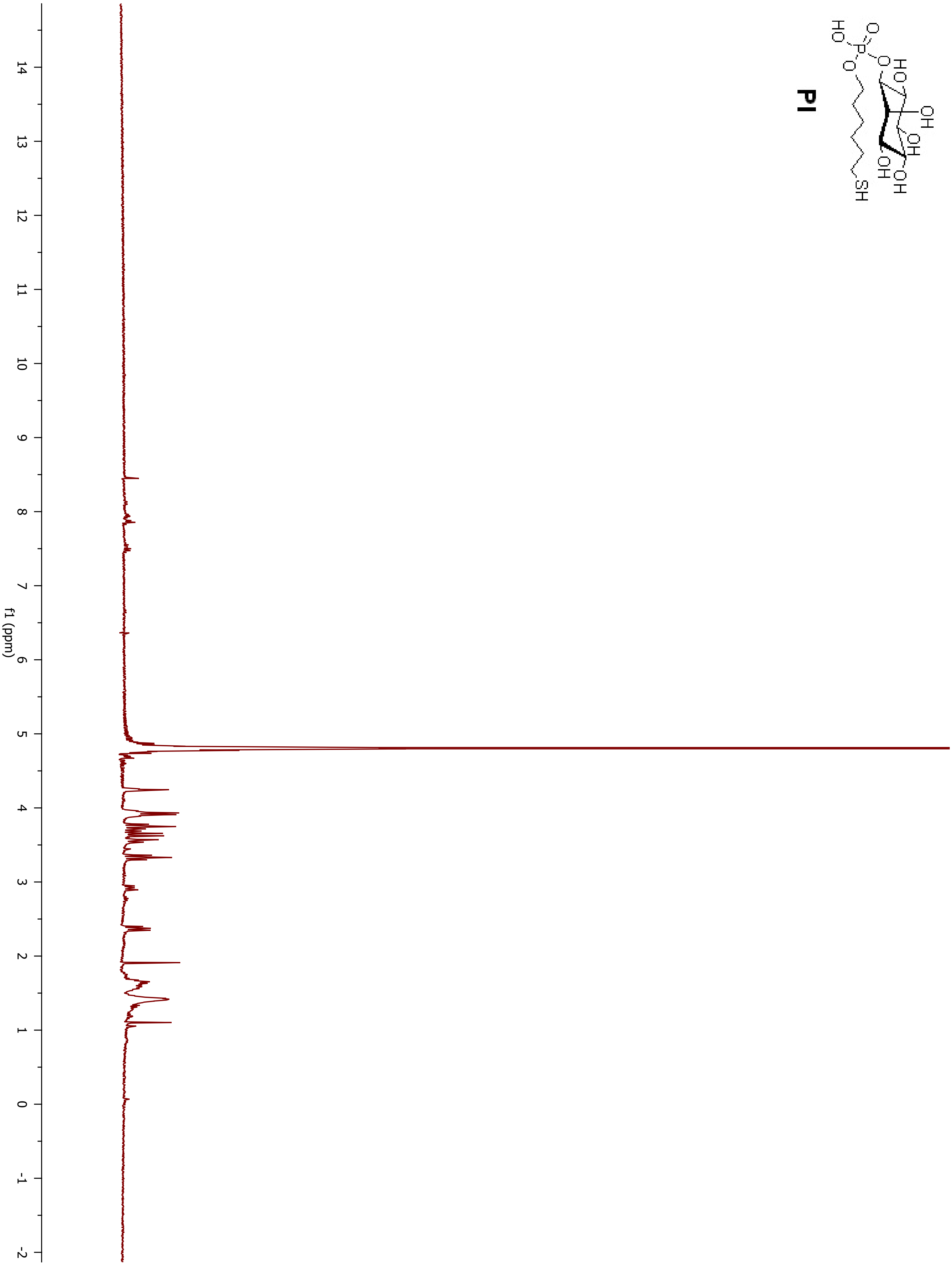
PI
f1 (ppm)
14
13
12
11
10
9
8
7
6
5
4
3
2
1
0
-1
-2

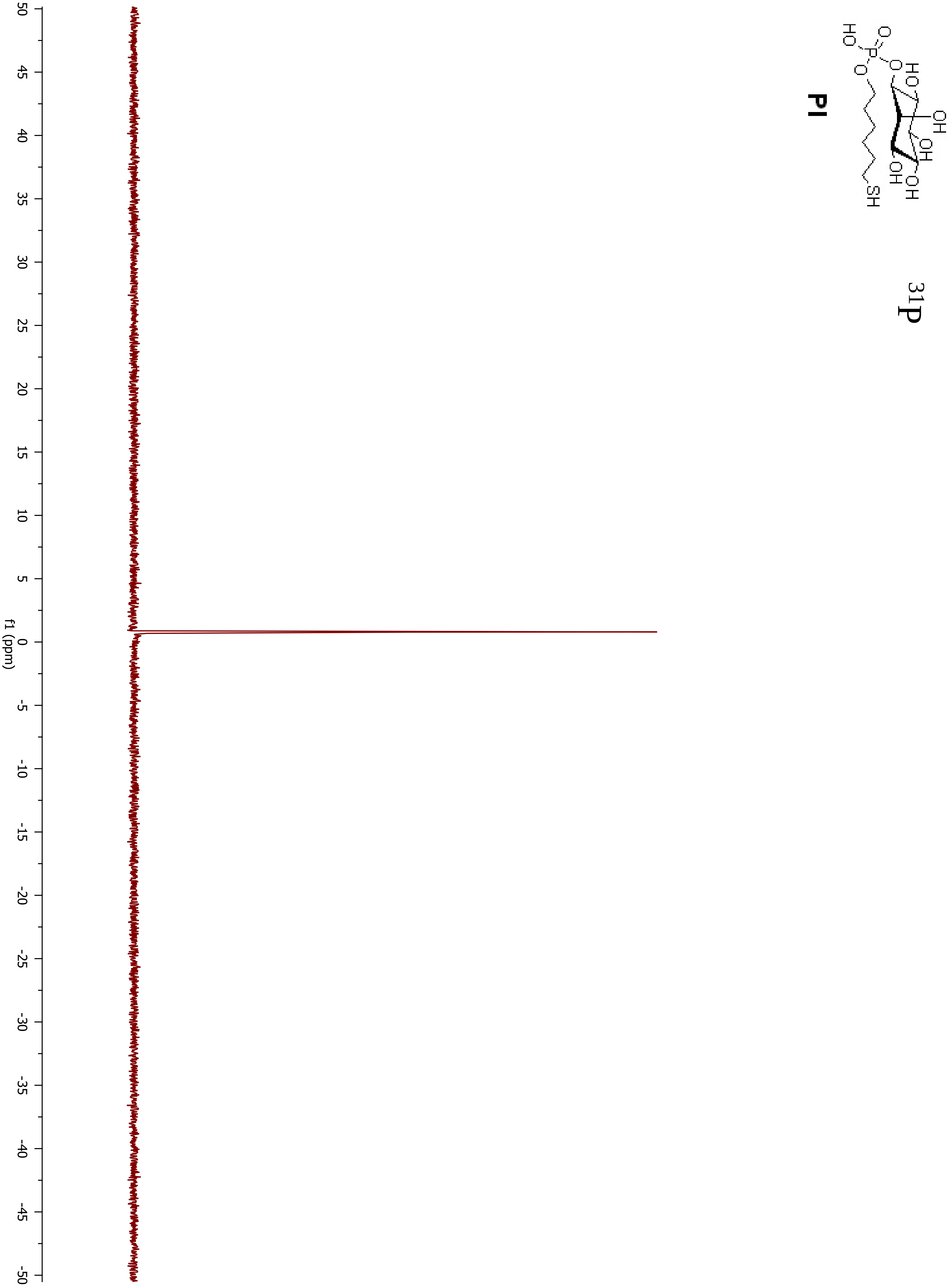

31P
PI
f1 (ppm)
50
45
40
35
30
25
20
15
10
5
0
-5
-10
-15
-20
-25
-30
-35
-40
-45
-50

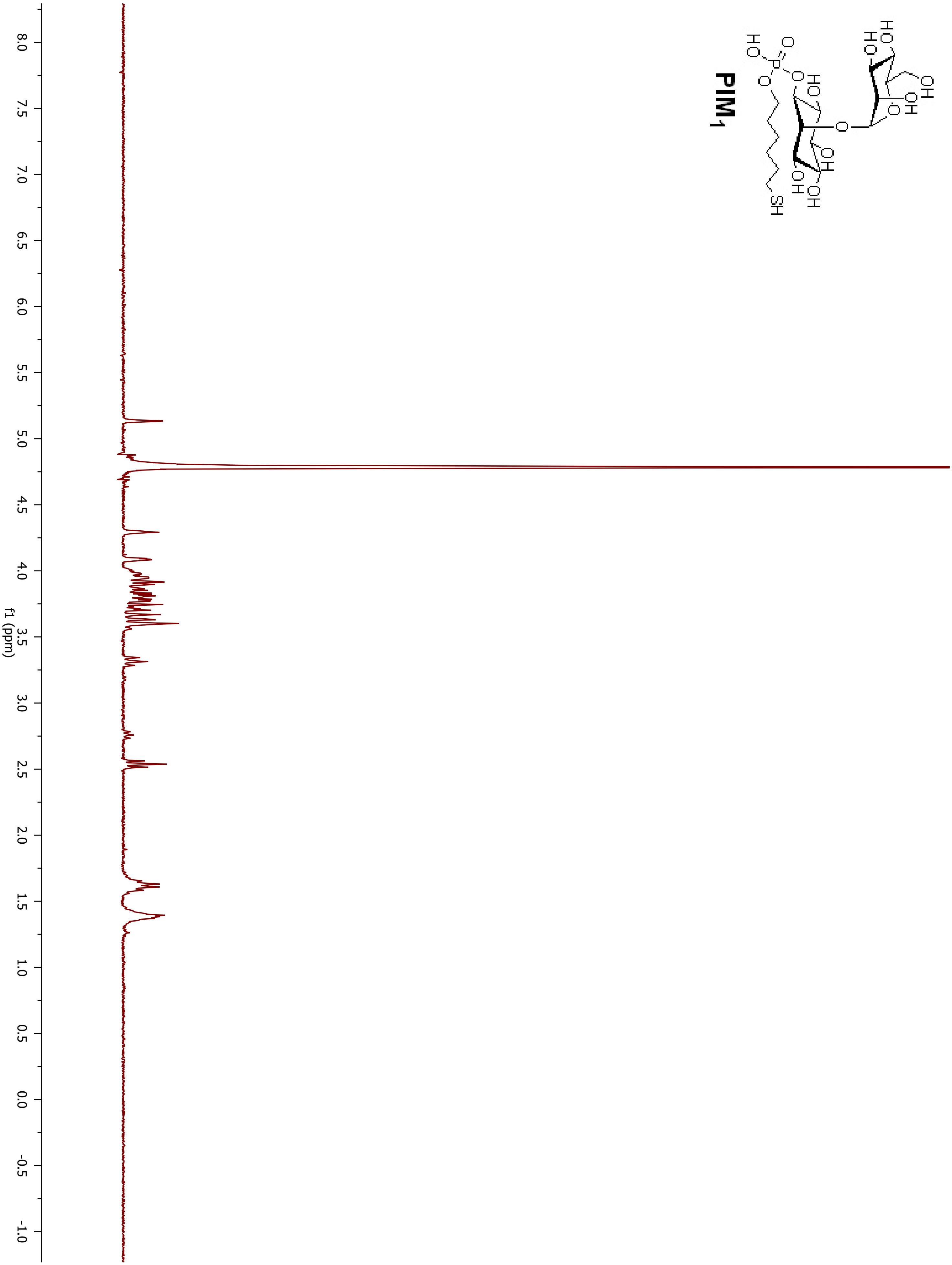
PIM1
f1 (ppm)

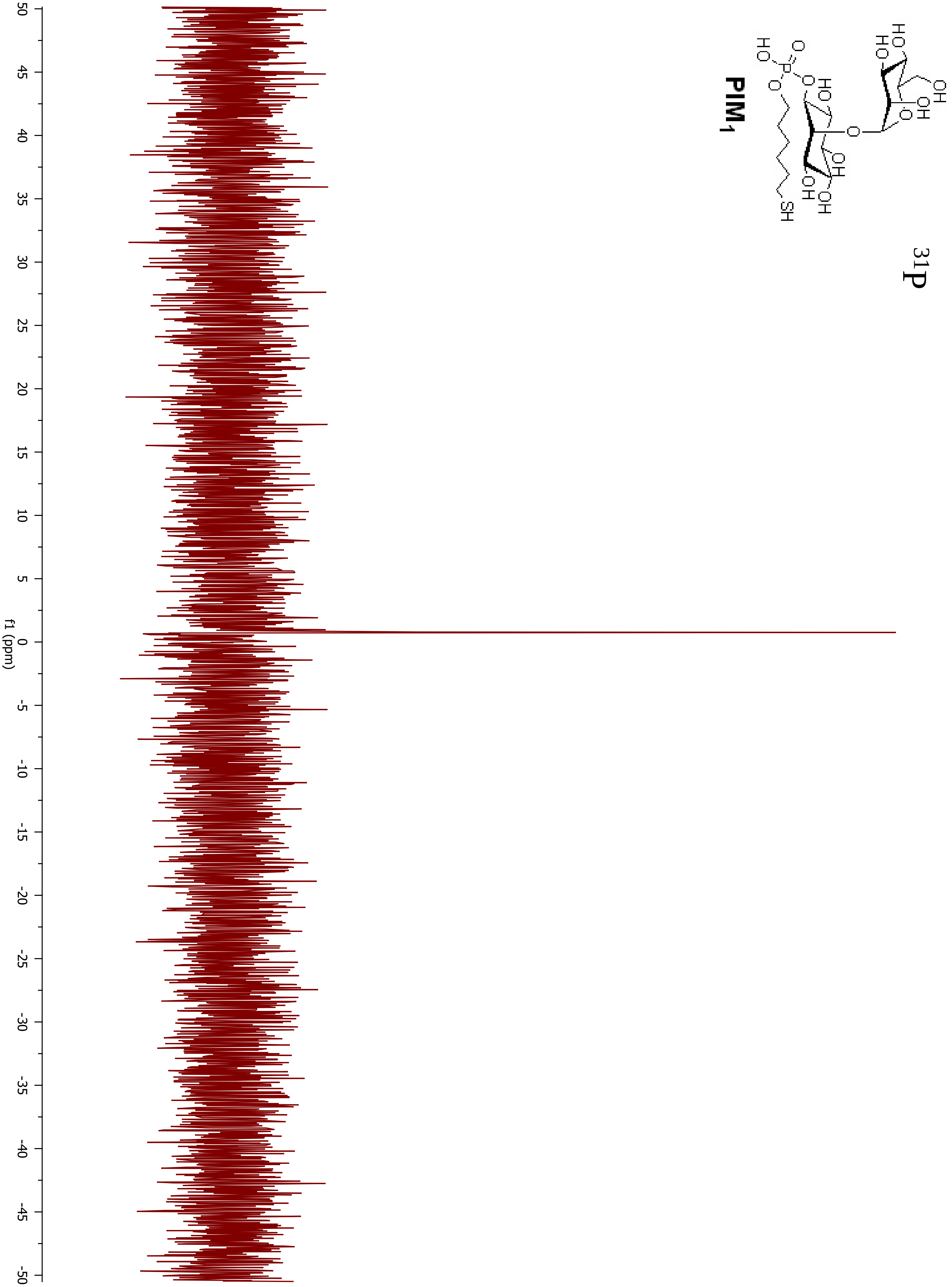
31P
PIM1
f1 (ppm)

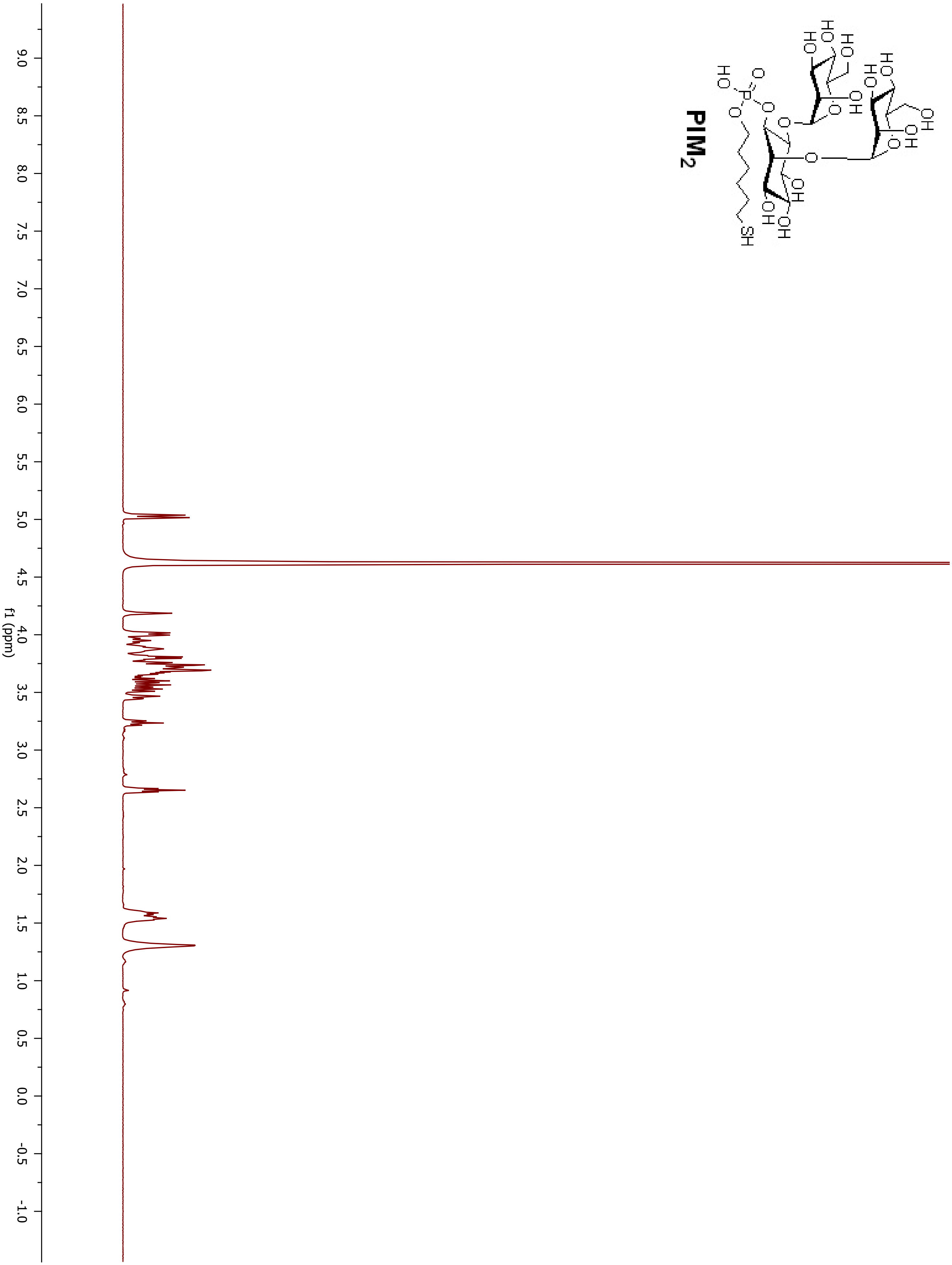
PIM2
f1 (ppm)

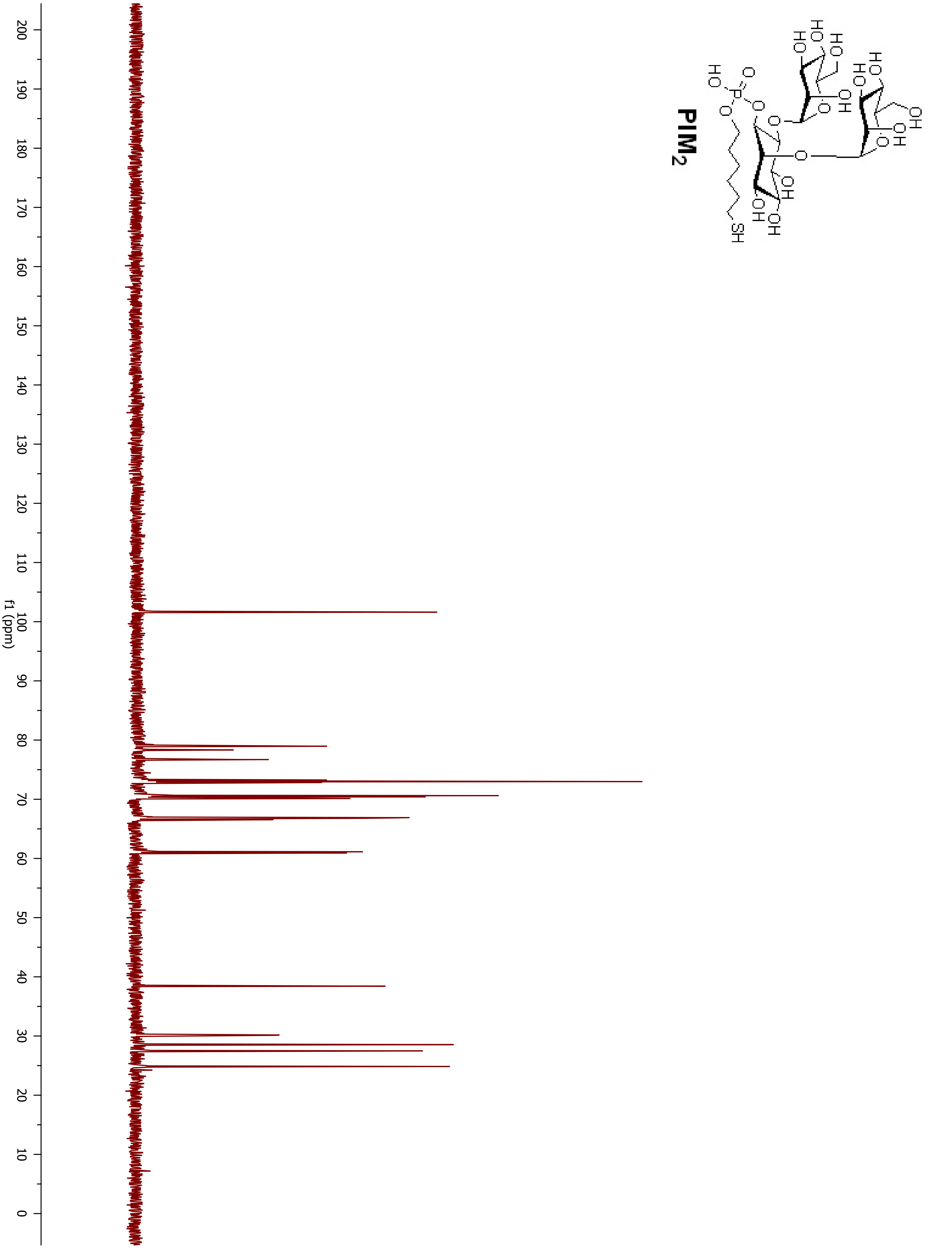
PIM2
f1 (ppm)

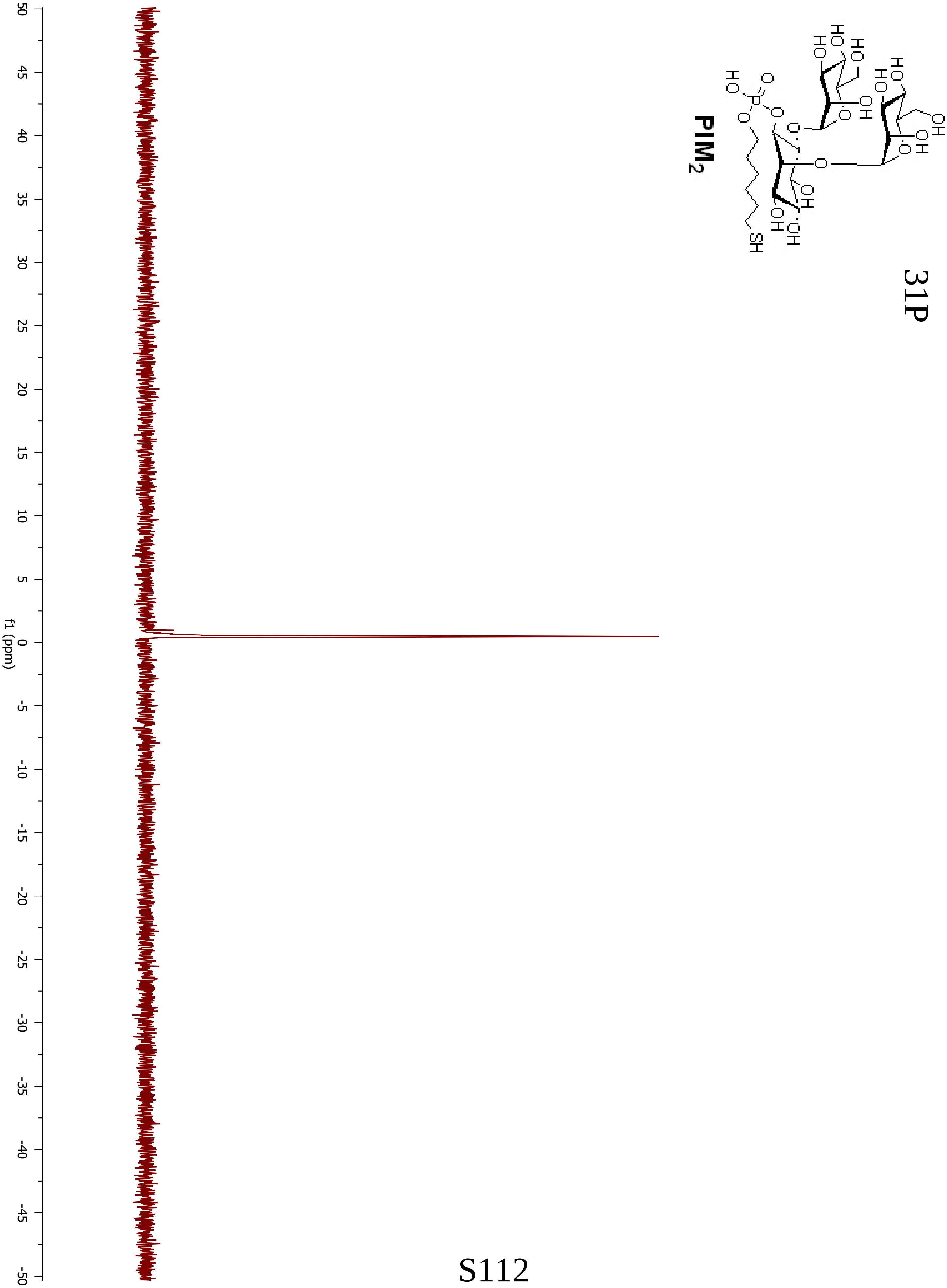
31P
PIM2
f1 (ppm)

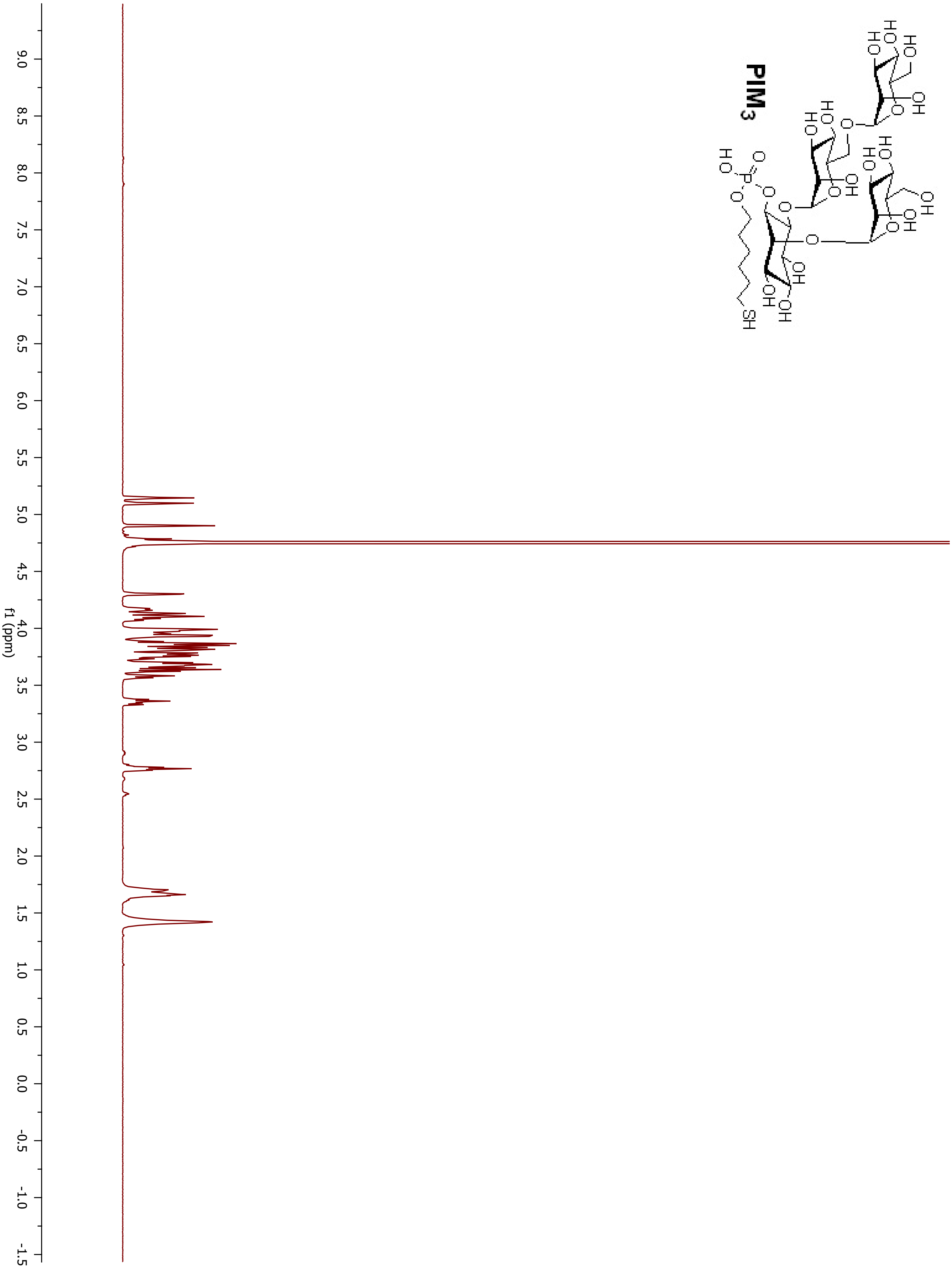
PIM$_3$
f1 (ppm)

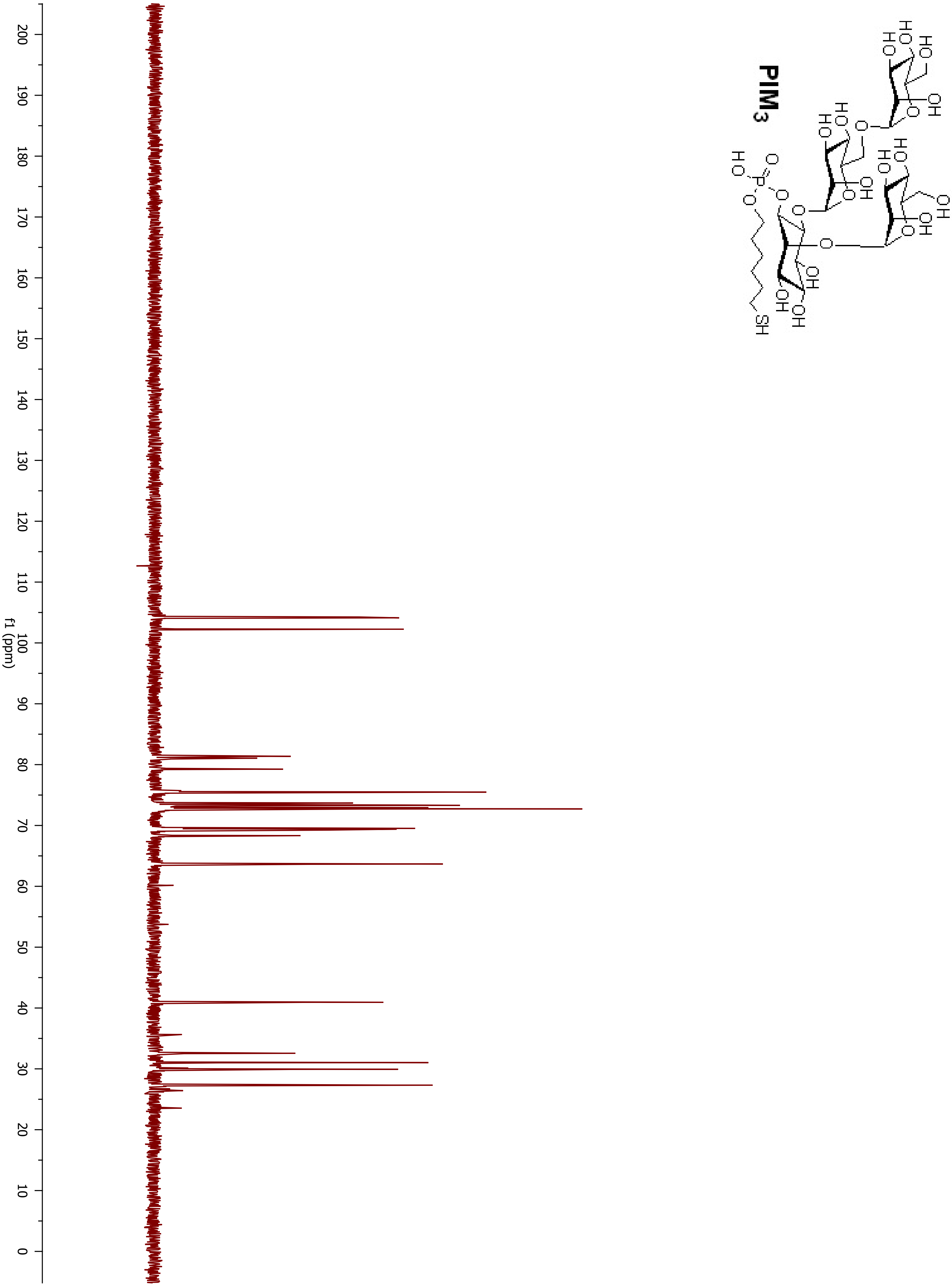
PIM3
f1 (ppm)
200
190
180
170
160
150
140
130
120
110
100
90
80
70
60
50
40
30
20
10
0

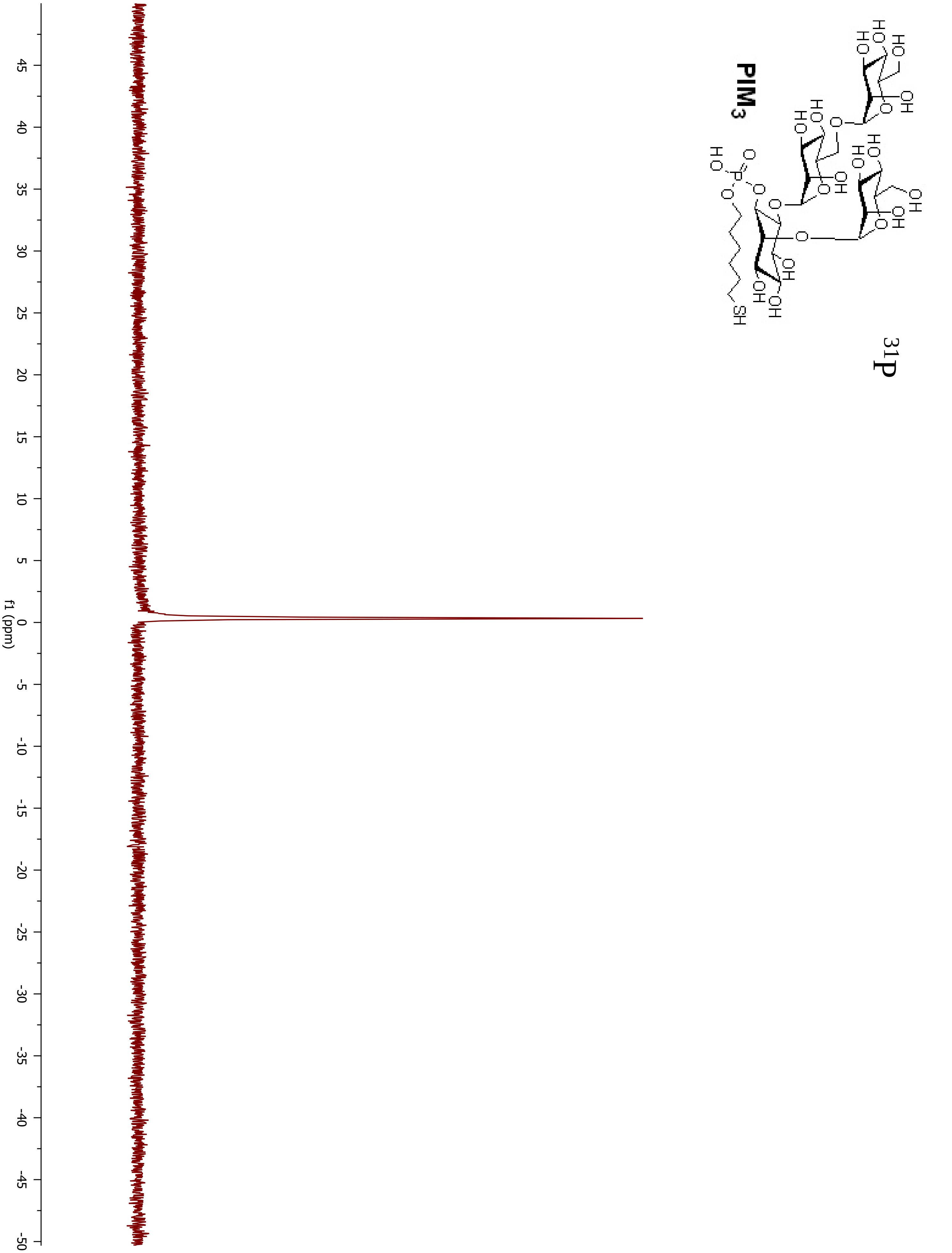
31P
PIM3
f1 (ppm)

COSY

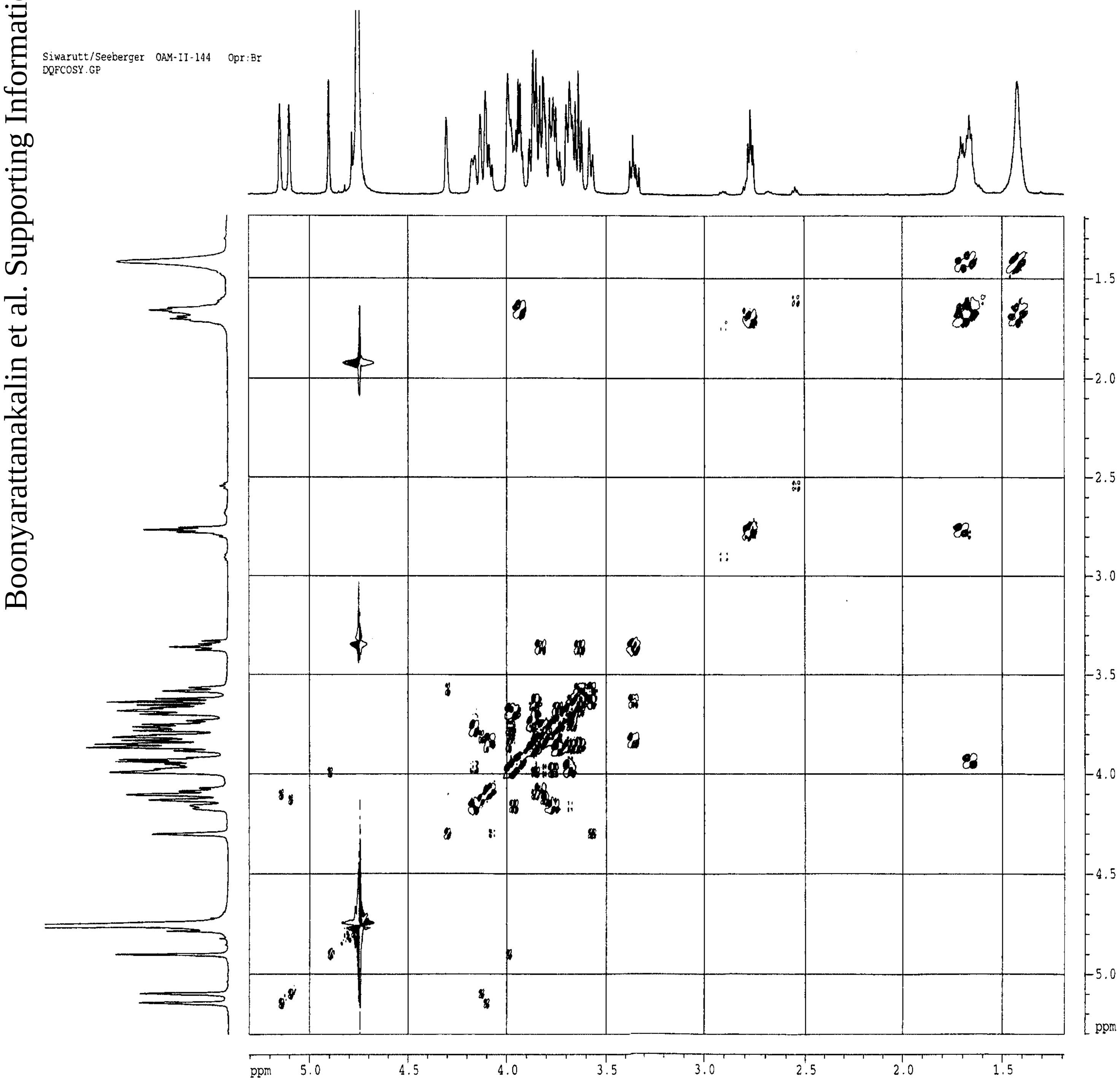

Current Data Parameters

NAME	A183
EXPNO	10
PROCNO	1

F2 - Acquisition Parameters

Date_	20070927
Time	7.43
INSTRUM	av600
PROBHD	5 mm BBO BB-1H
PULPROG	cosydfgptp
TD	2048
SOLVENT	D2O
NS	12
DS	16
SWH	3687.316 Hz
FIDRES	1.800447 Hz
AQ	0.2777588 sec
RG	4096
DW	135.600 usec
DE	6.00 usec
TE	300.0 K
d0	0.00000300 sec
D1	2.50000000 sec
d11	0.03000000 sec
d12	0.00002000 sec
d13	0.00000300 sec
D16	0.00020000 sec
d20	5000.00000000 sec
IN0	0.00013560 sec

======== CHANNEL f1 ========

NUC1	1H
P1	12.00 usec
p2	24.00 usec
PL1	-3.00 dB
PL12	120.00 dB
SFO1	600.1318310 MHz

====== GRADIENT CHANNEL =====

GPNAM1	SINE.100
GPNAM2	SINE.100
GPX1	0.00 %
GPX2	0.00 %
GPY1	0.00 %
GPY2	0.00 %
GPZ1	10.00 %
GPZ2	20.00 %
P16	1000.00 usec

F1 - Acquisition parameters

ND0	2
TD	512
SFO1	600.1318 MHz
FIDRES	7.201788 Hz
SW	6.144 ppm

F2 - Processing parameters

SI	1024
SF	600.1299727 MHz
WDW	QSINE
SSB	3
LB	0.00 Hz
GB	0
PC	1.00

F1 - Processing parameters

SI	1024
MC2	TPPI
SF	600.1299727 MHz
WDW	QSINE
SSB	2
LB	0.00 Hz
GB	0

2D NMR plot parameters

CX2	20.00 cm
CX1	20.00 cm
F2PLO	5.305 ppm
F2LO	3183.43 Hz
F2PHI	1.188 ppm
F2HI	713.22 Hz
F1PLO	5.305 ppm
F1LO	3183.43 Hz
F1PHI	1.188 ppm
F1HI	713.22 Hz
F2PPMCM	0.20581 ppm/cm
F2HZCM	123.51067 Hz/cm
F1PPMCM	0.20581 ppm/cm

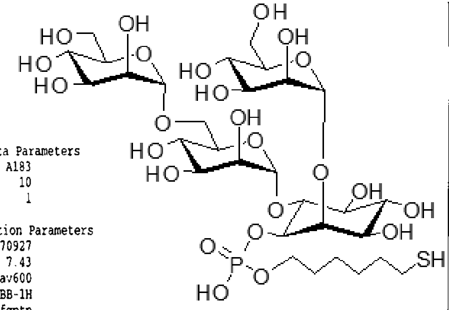

PIM$_3$

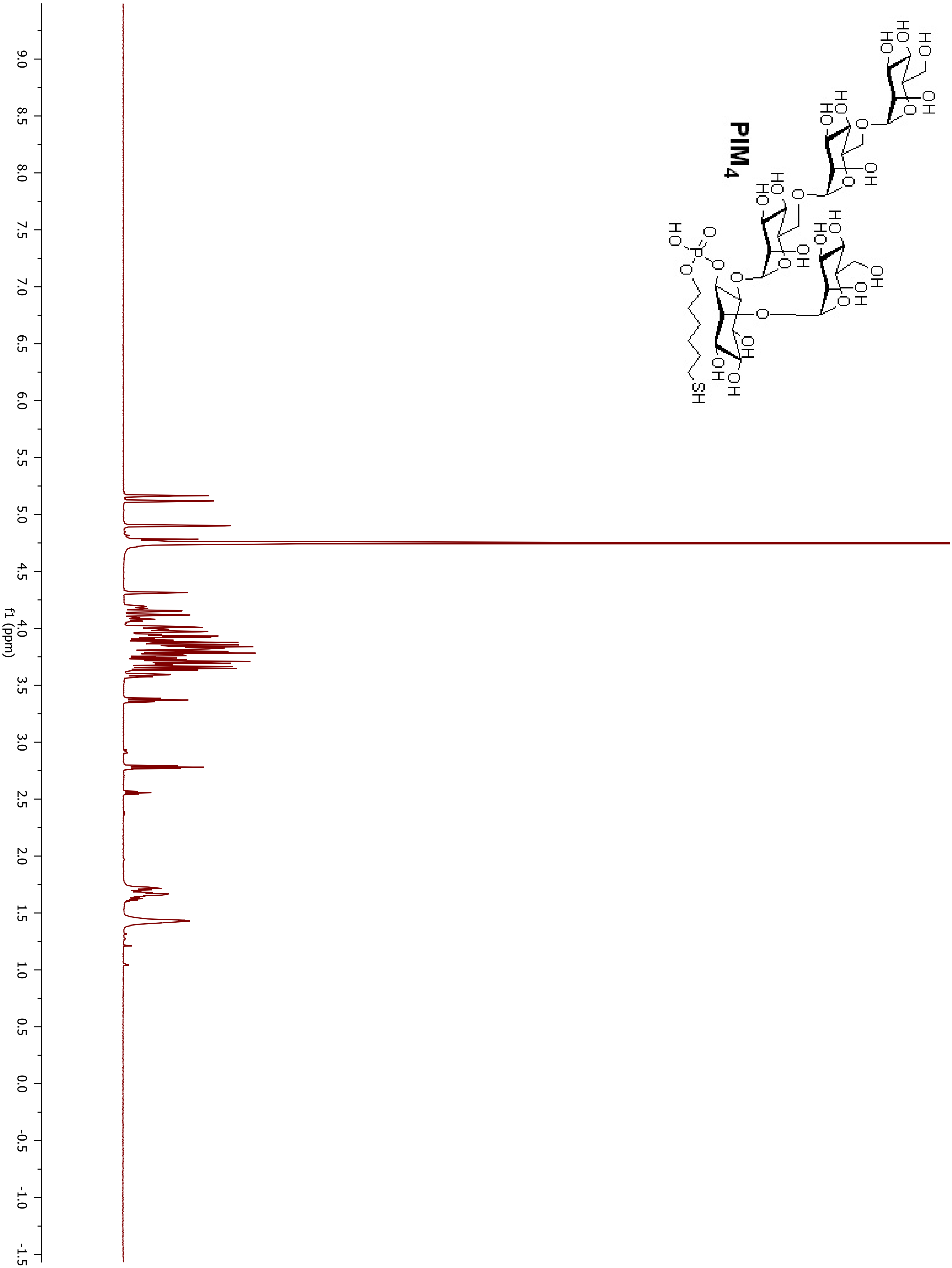
PIM4
f1 (ppm)

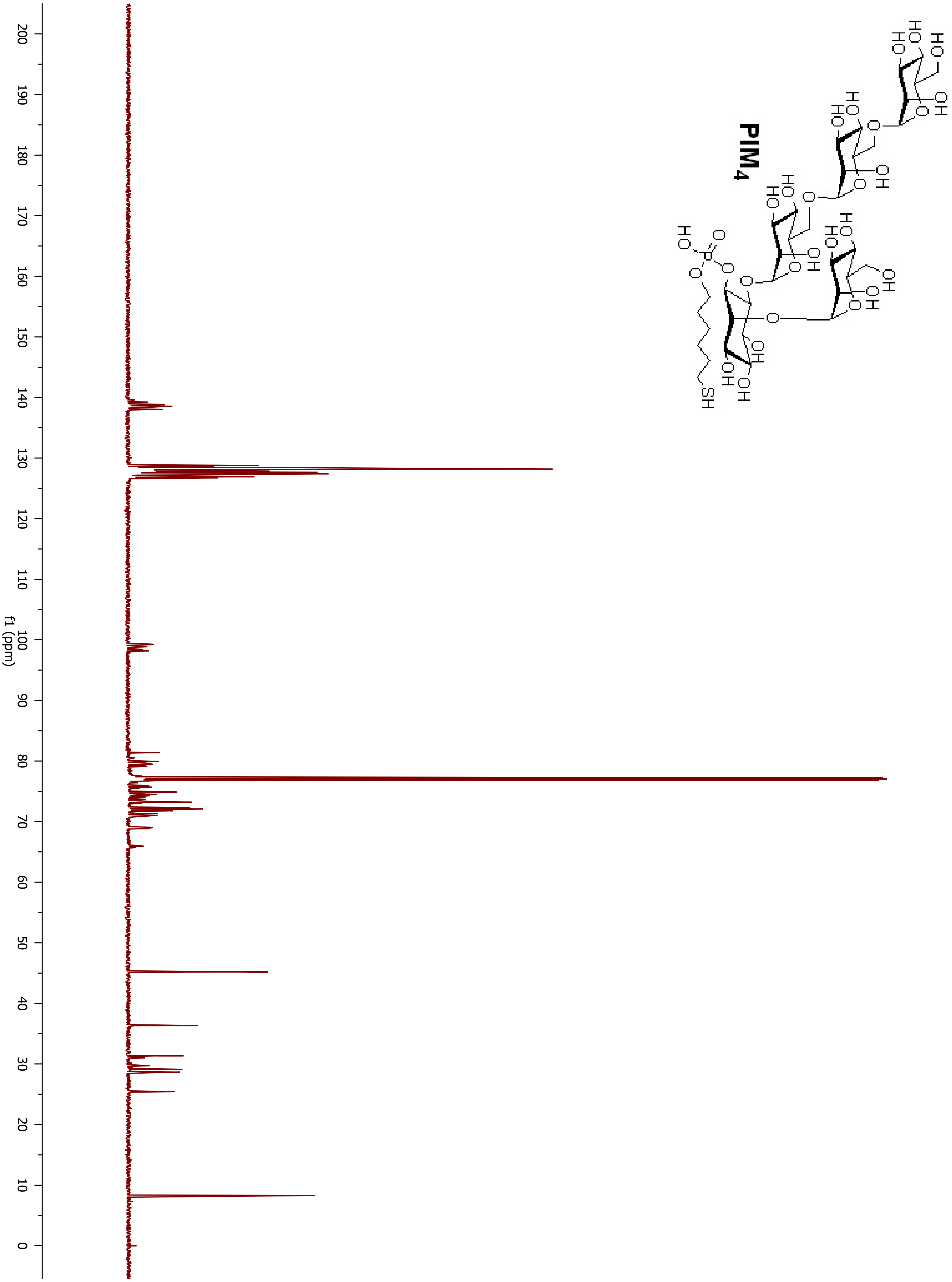
PIM4
f1 (ppm)
200
190
180
170
160
150
140
130
120
110
100
90
80
70
60
50
40
30
20
10
0

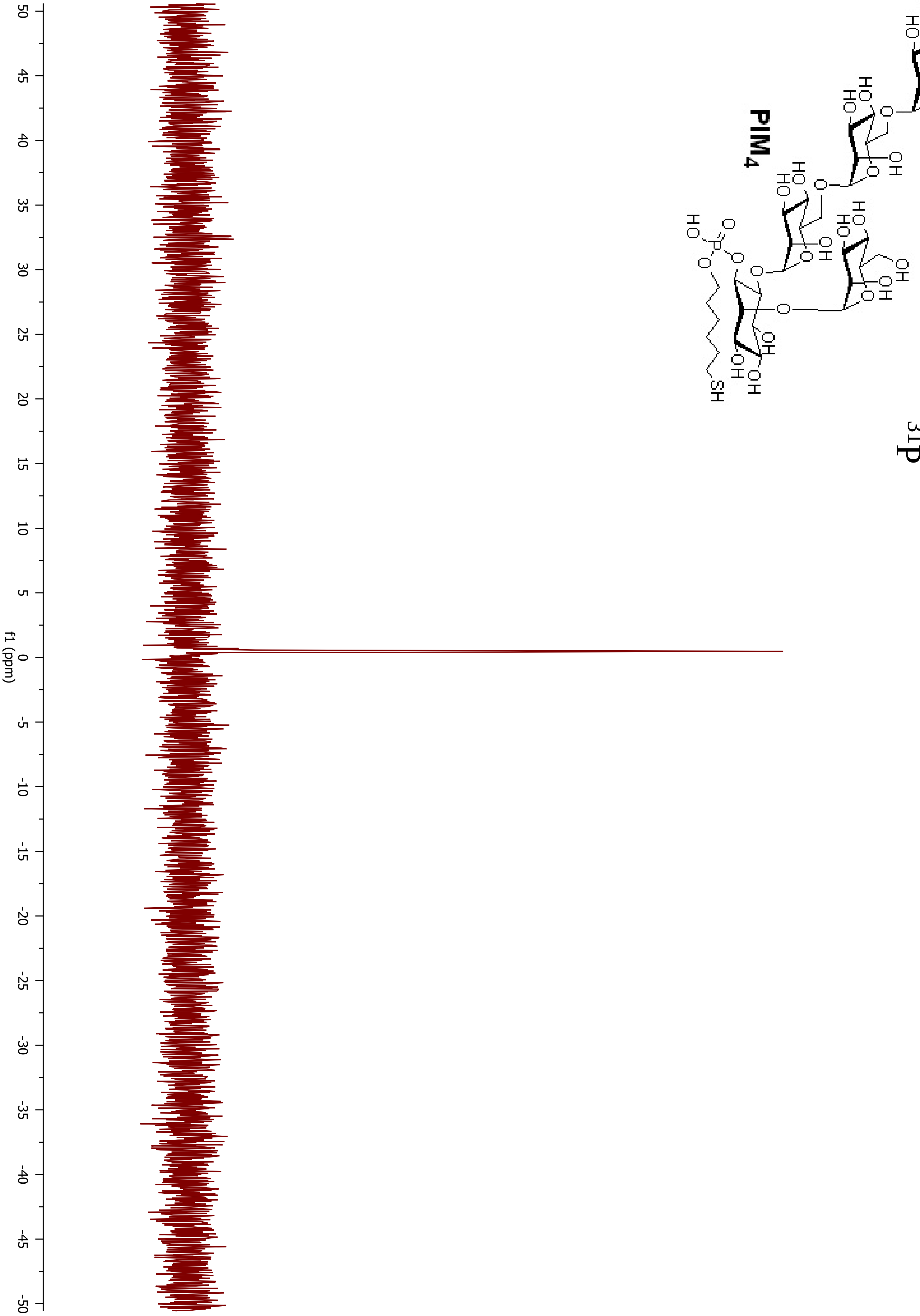

^{31}P
PIM$_4$
f1 (ppm)

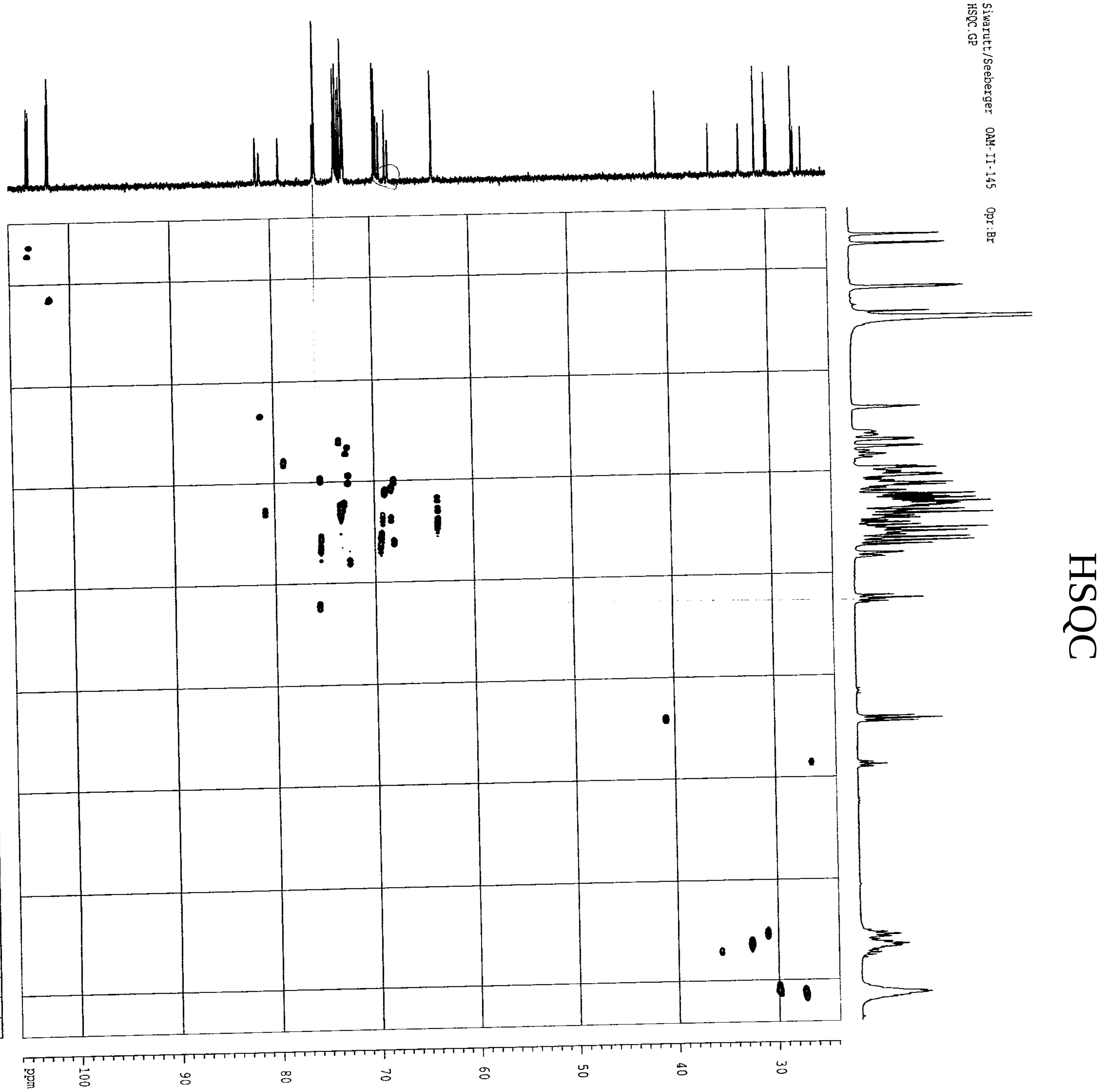
HSQC
Siwarut/Seeberger OAM-II-145 Opr:Br
HSQC.GP
ppm

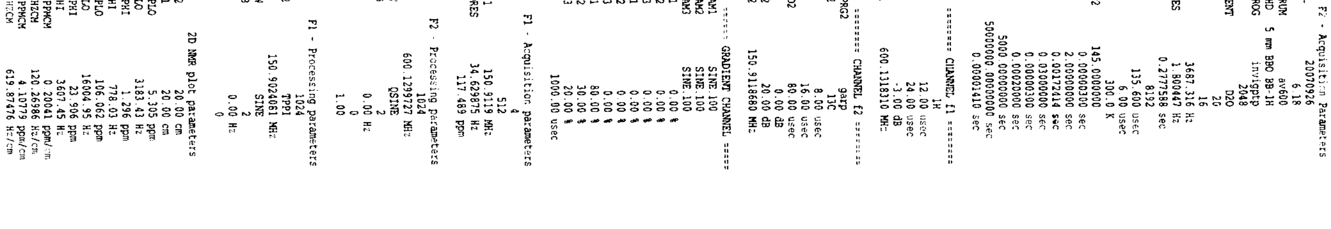

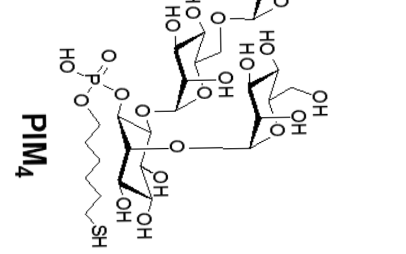
PIM4

HSQC

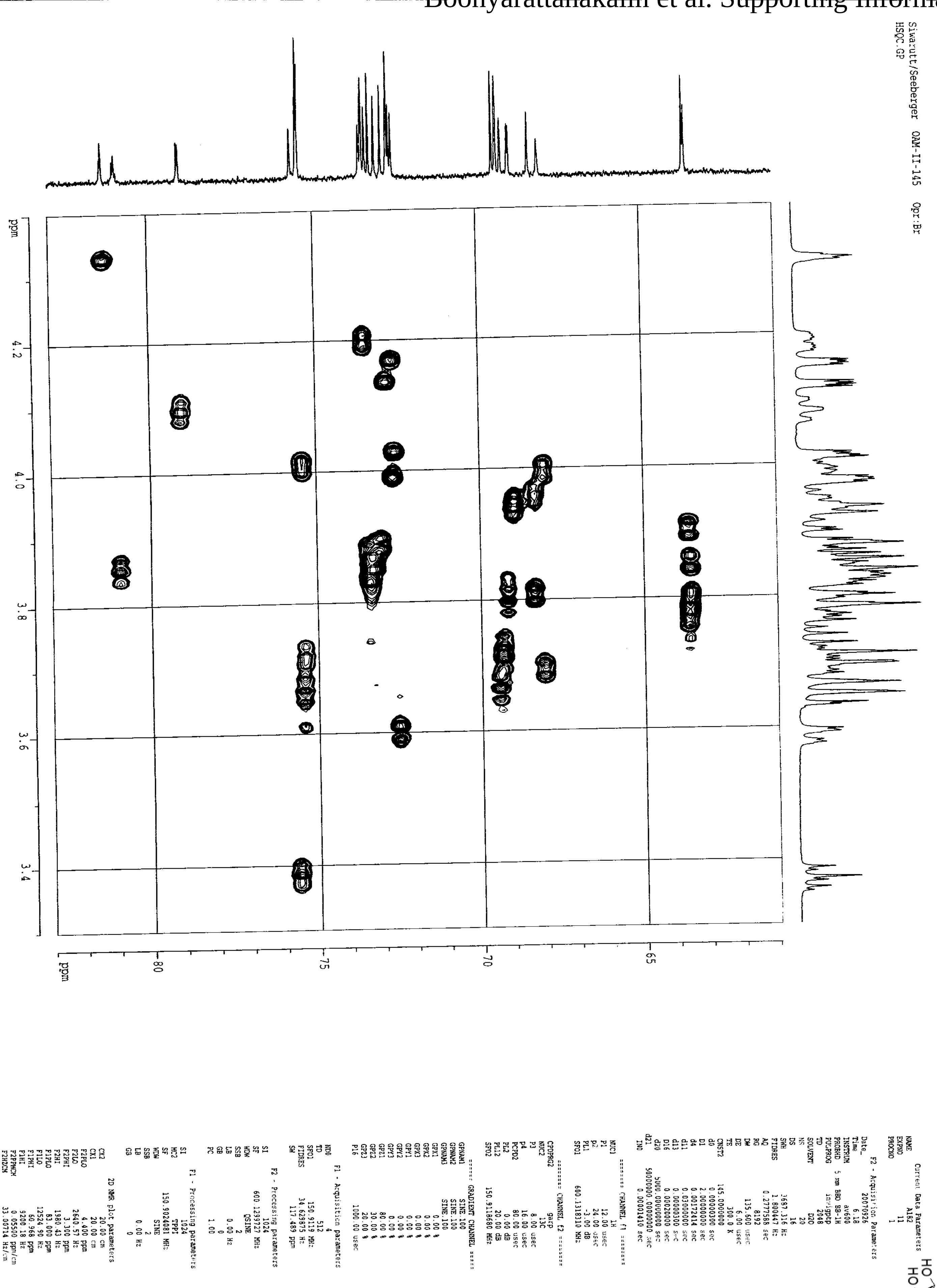
Siwarutt/Seeberger OAM-II-145 Opr:Br
HSQC.GP
ppm
4.2
4.0
3.8
3.6
3.4
80
75
70
65

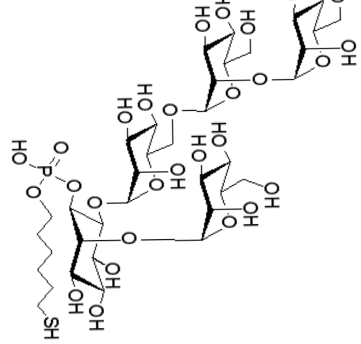

PIM$_4$

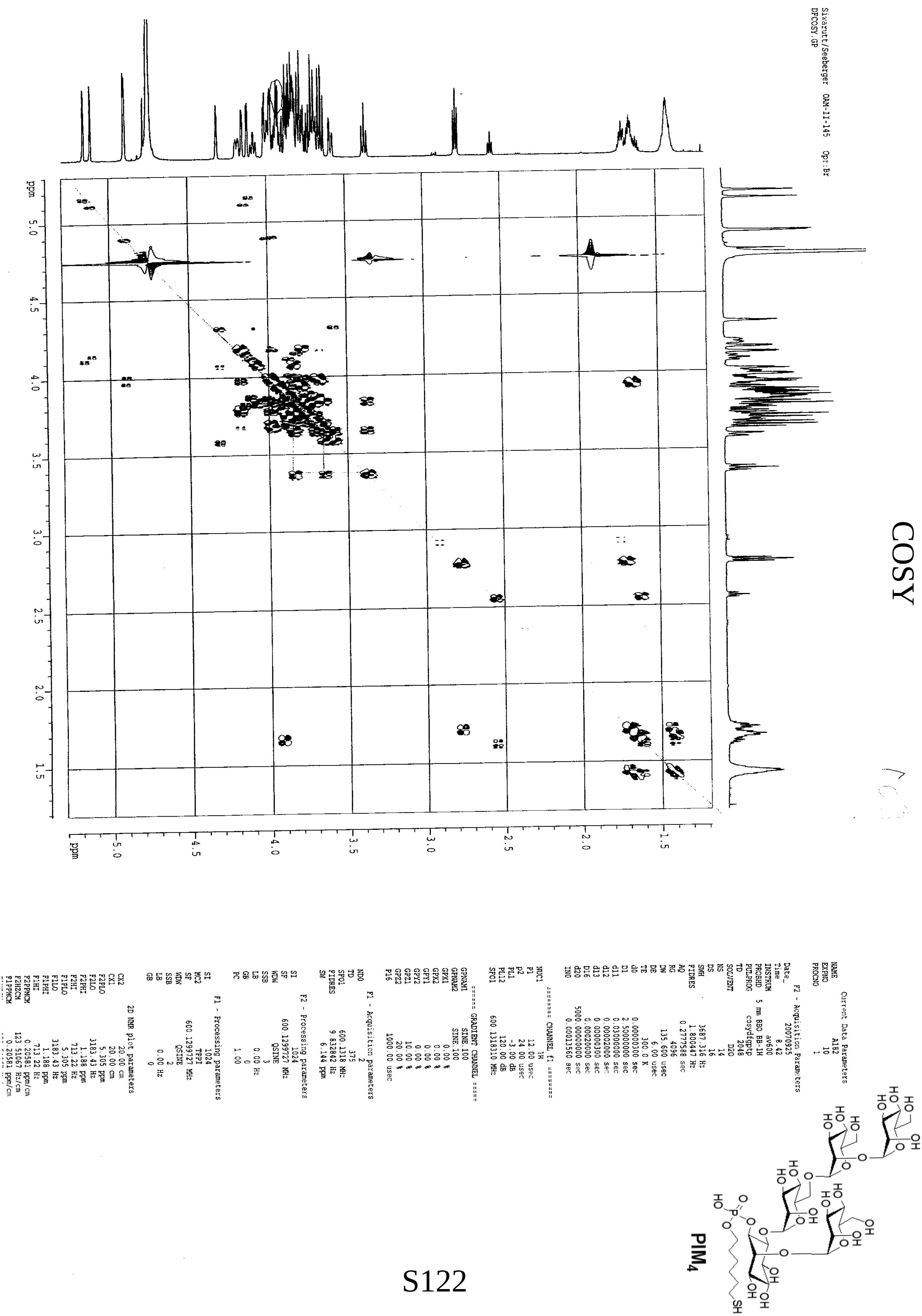
COSY
PIM4
Sivarut/Seeberger OAM-II-145
ppm

COSY

Siwarutt/Seeberger OAM-II-145 Opr:Br
DFCOSY.GP

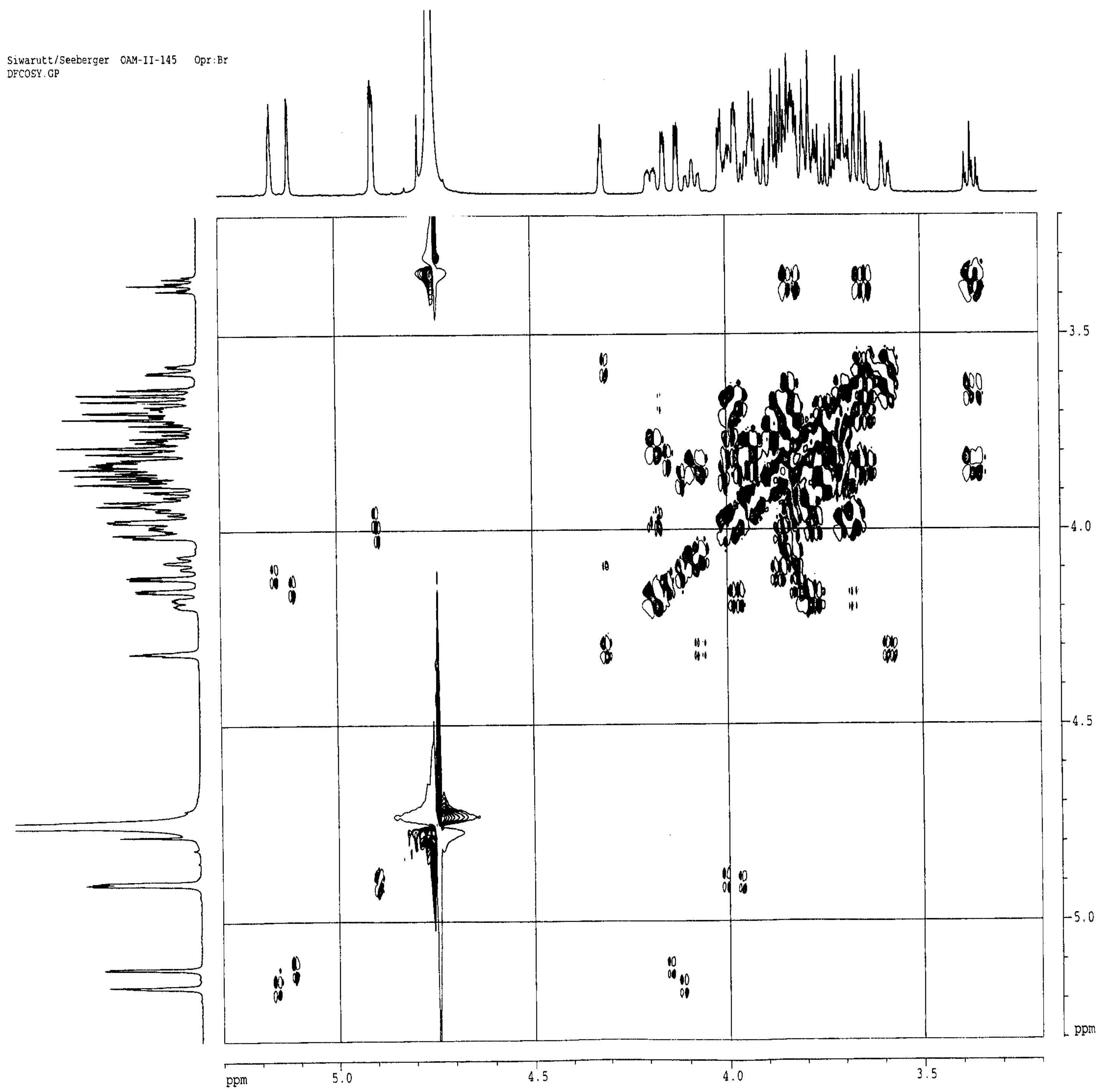

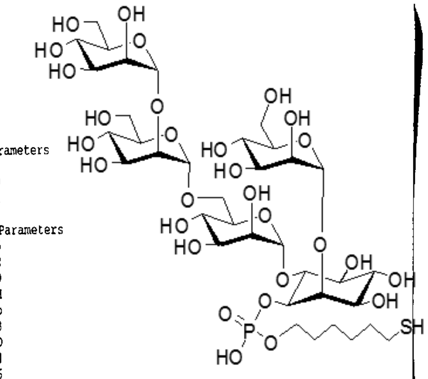

PIM$_4$

Current Data Parameters

NAME	A182
EXPNO	10
PROCNO	1

F2 - Acquisition Parameters

Date_	20070925
Time	8.42
INSTRUM	av600
PROBHD	5 mm BBO BB-1H
PULPROG	cosydfgptp
TD	2048
SOLVENT	D2O
NS	14
DS	16
SWH	3687.316 Hz
FIDRES	1.800447 Hz
AQ	0.2777588 sec
RG	4096
DW	135.600 usec
DE	6.00 usec
TE	300.0 K
d0	0.00000300 sec
D1	2.50000000 sec
d11	0.03000000 sec
d12	0.00002000 sec
d13	0.00000300 sec
D16	0.00020000 sec
d20	5000.00000000 sec
IN0	0.00013560 sec

======== CHANNEL f1 ========

NUC1	1H
P1	12.00 usec
p2	24.00 usec
PL1	-3.00 dB
PL12	120.00 dB
SFO1	600.1318310 MHz

====== GRADIENT CHANNEL =====

GPNAM1	SINE.100
GPNAM2	SINE.100
GPX1	0.00 %
GPX2	0.00 %
GPY1	0.00 %
GPY2	0.00 %
GPZ1	10.00 %
GPZ2	20.00 %
P16	1000.00 usec

F1 - Acquisition parameters

ND0	2
TD	375
SFO1	600.1318 MHz
FIDRES	9.832842 Hz
SW	6.144 ppm

F2 - Processing parameters

SI	1024
SF	600.1299727 MHz
WDW	QSINE
SSB	3
LB	0.00 Hz
GB	0
PC	1.00

F1 - Processing parameters

SI	1024
MC2	TPPI
SF	600.1299727 MHz
WDW	QSINE
SSB	2
LB	0.00 Hz
GB	0

2D NMR plot parameters

CX2	20.00 cm
CX1	20.00 cm
F2PLO	5.300 ppm
F2LO	3180.69 Hz
F2PHI	3.198 ppm
F2HI	1919.51 Hz
F1PLO	5.305 ppm
F1LO	3183.43 Hz
F1PHI	3.198 ppm
F1HI	1919.51 Hz
F2PPMCM	0.10508 ppm/cm
F2HZCM	63.05870 Hz/cm
F1PPMCM	0.10530 ppm/cm

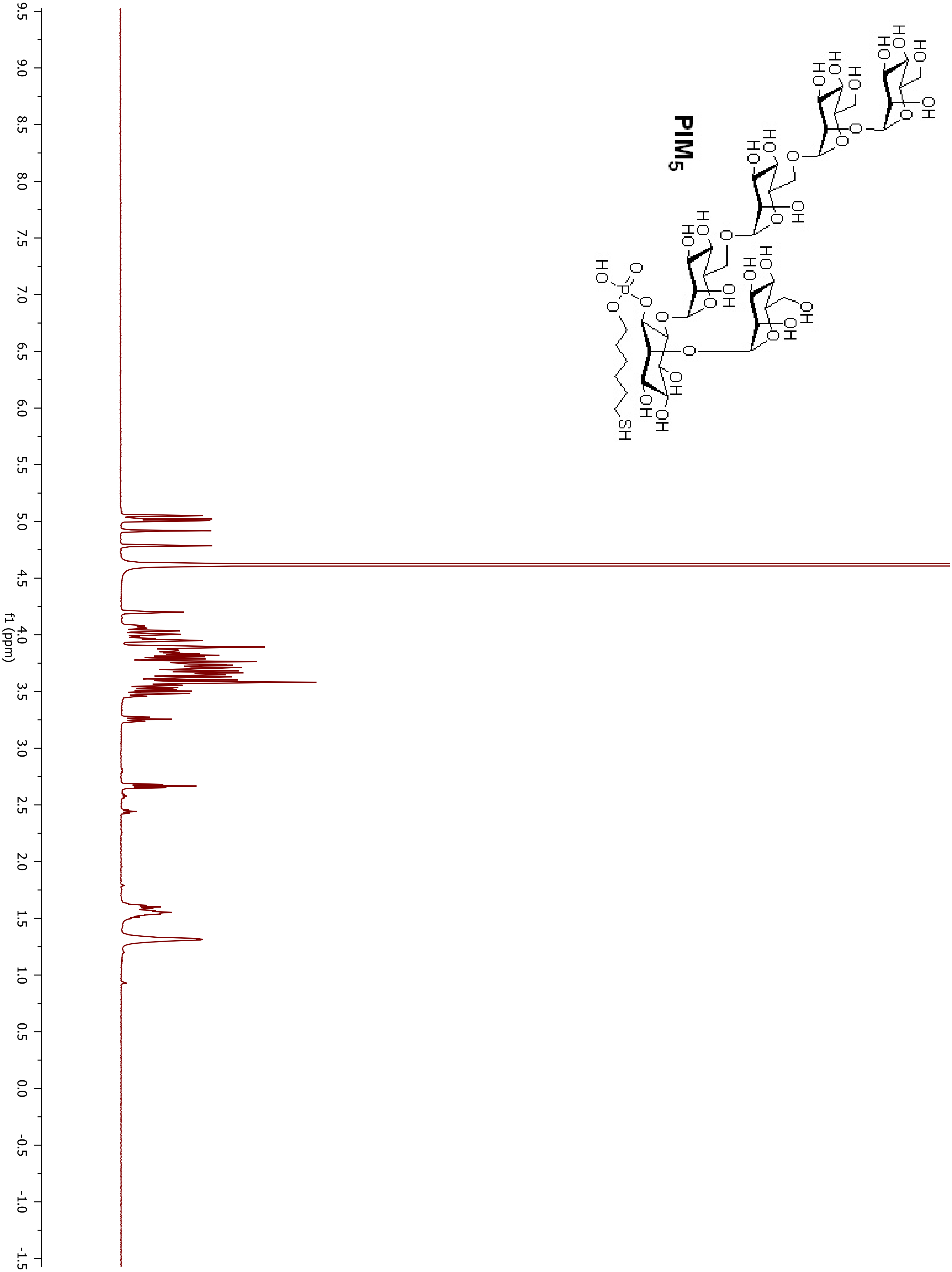
PIM$_5$
f1 (ppm)
9.5
9.0
8.5
8.0
7.5
7.0
6.5
6.0
5.5
5.0
4.5
4.0
3.5
3.0
2.5
2.0
1.5
1.0
0.5
0.0
-0.5
-1.0
-1.5

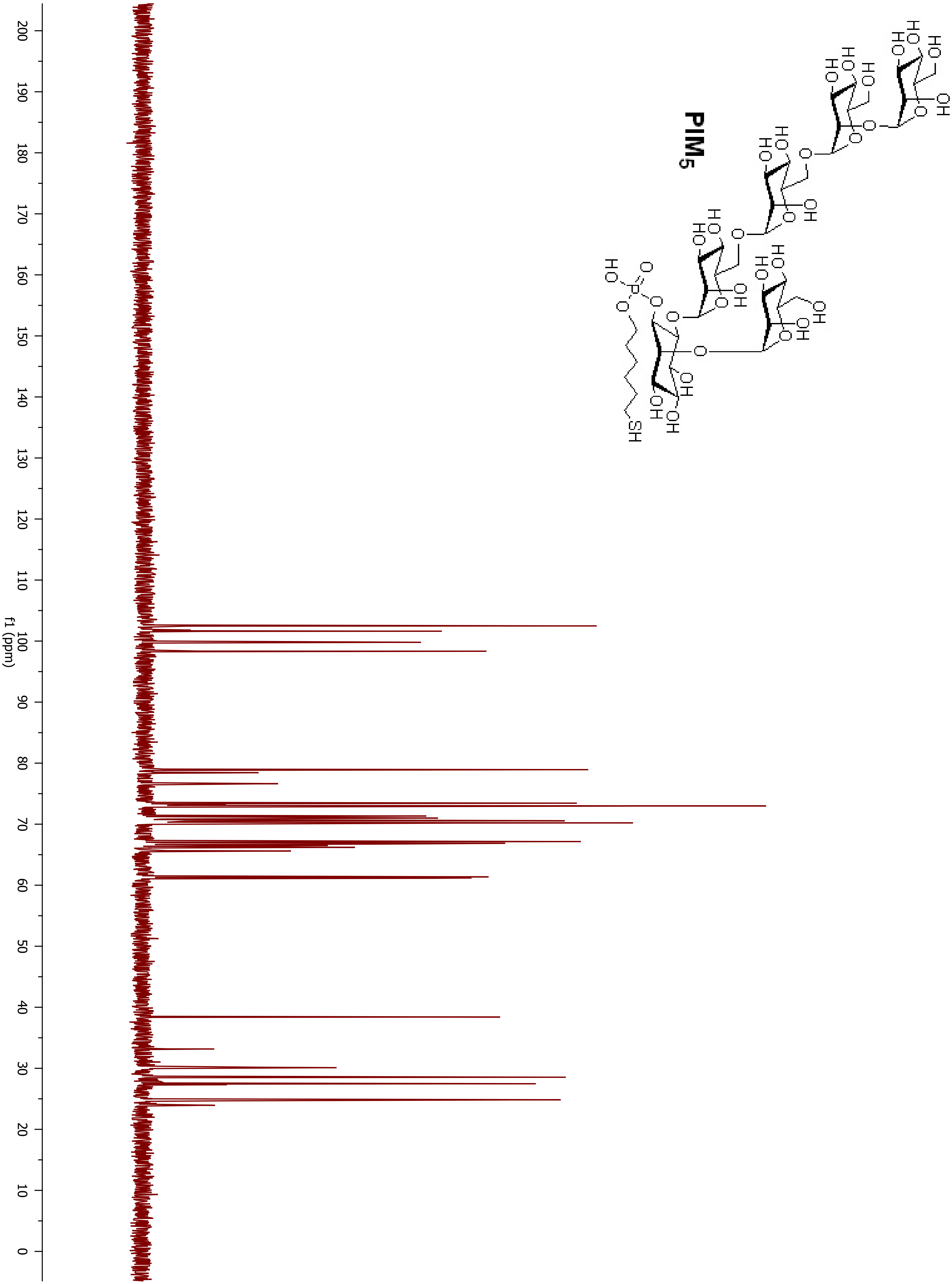
PIM$_5$
f1 (ppm)

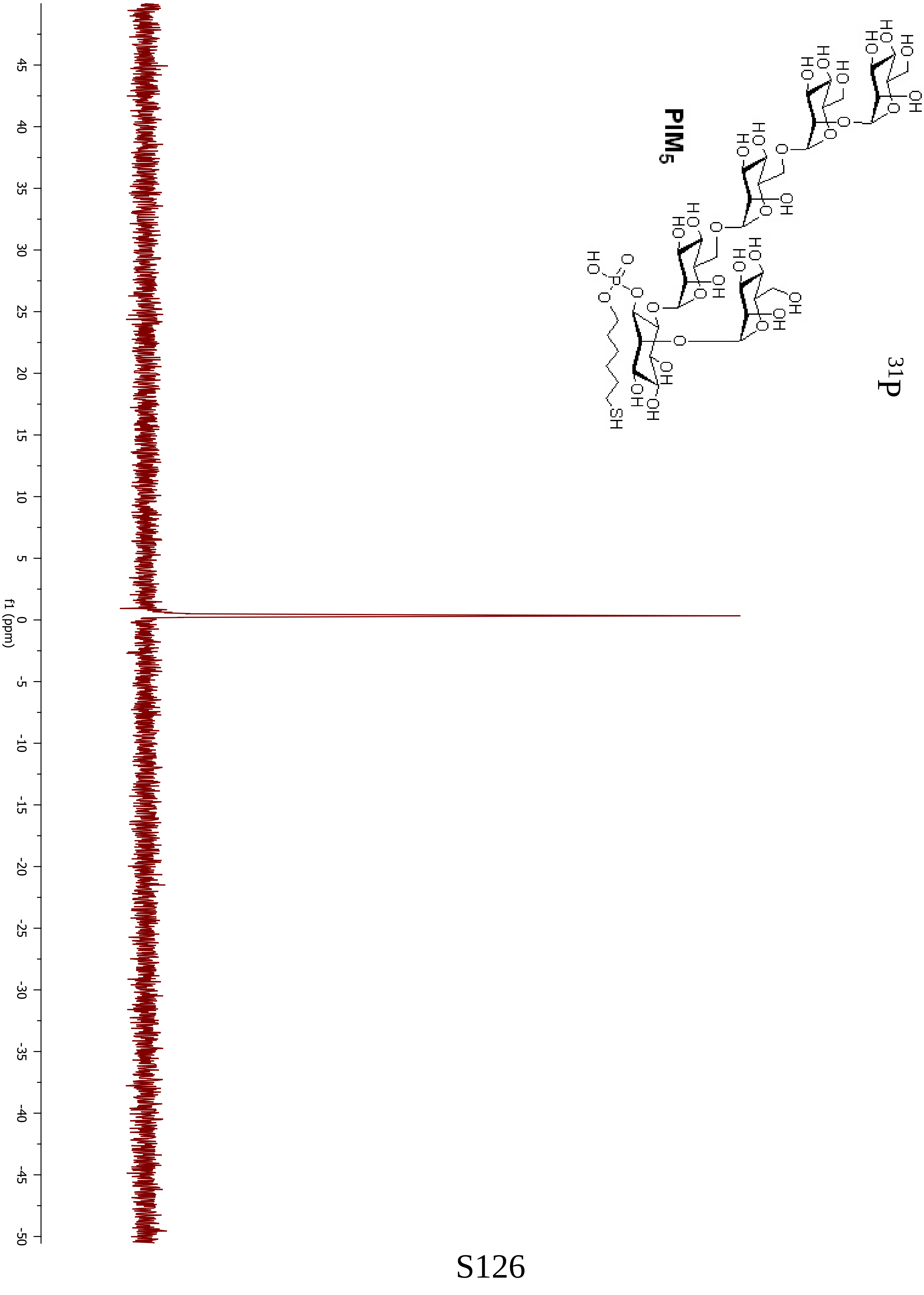
31P
PIM5
f1 (ppm)

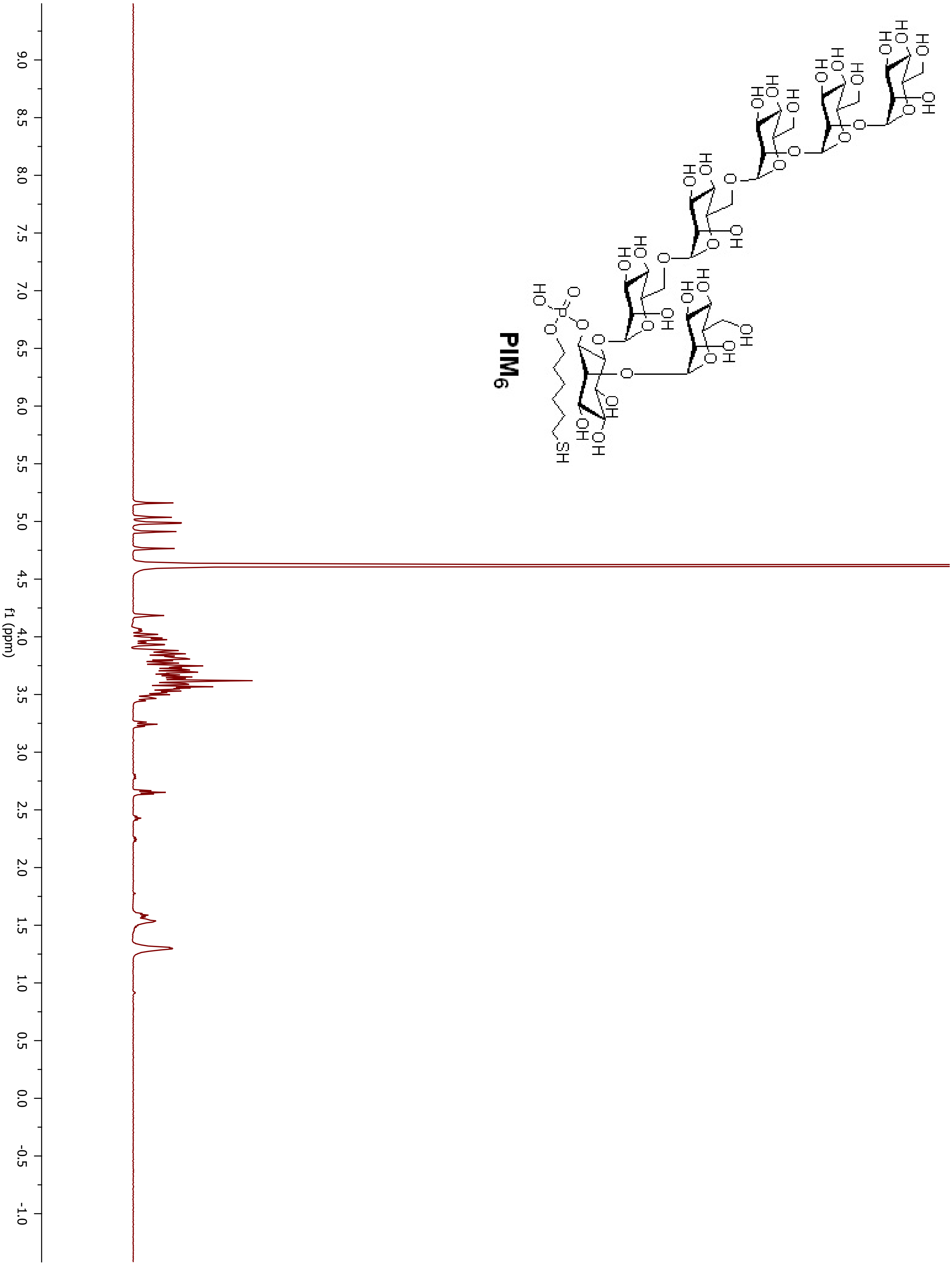
PIM6
f1 (ppm)

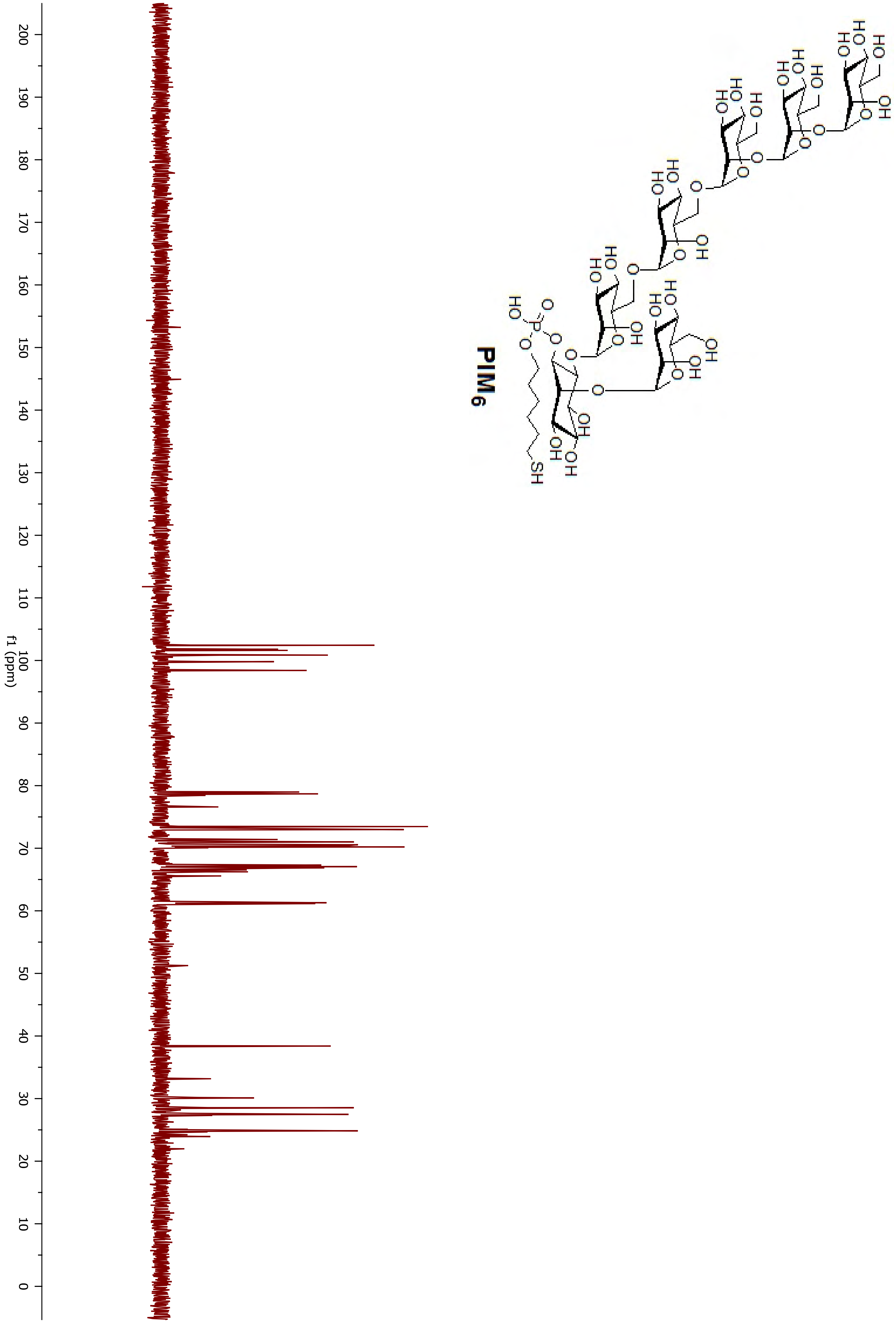
PIM6
f1 (ppm)

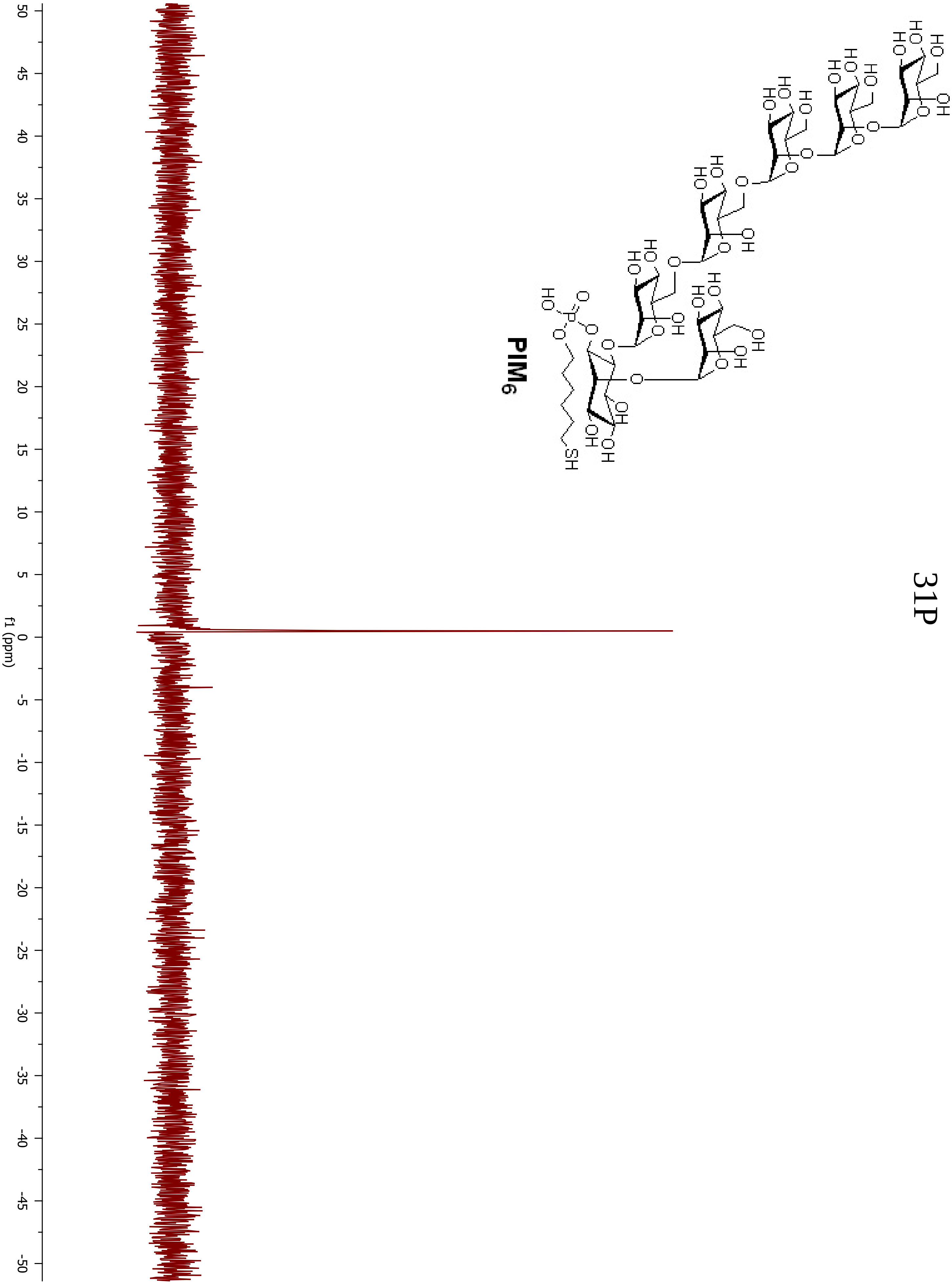
31P
PIM$_6$
f1 (ppm)

CONVERGENT SYNTHESIS OF PHOSPHATIDYLINOSITOL HEXAMANNOSIDE GLYCAN OF *Mycobacterium tuberculosis*

S. Boonyarattanakalin[1] and P. H. Seeberger[2*]

[1] School of Biochemical Engineering and Technology, Sirindhorn International Institute of Technology, Thammasat University, P.O.Box 22 Thammasat-Rangsit Post Office, Pathumthani 12121, Thailand
[2] Laboratory for Organic Chemistry, Swiss Federal Institute of Technology (ETH) Zürich, Zürich, Switzerland

[*]Corresponding author, for contact person: siwarutt@siit.tu.ac.th

Abstract: *Mycobacterium tuberculosis* (*Mtb*) is the causative agent of tuberculosis (TB). *Mtb* has infected approximately one third of the world population.[1] Among these infected population, seven million cases develop into TB every year resulting in two million deaths annually.[2] *Mtb* has evolved sophisticated mechanisms to survive and persist in humans host cells via the interactions of its cell wall components with host cells as well as relying on its unusually complex cell wall as a protective barrier.[1,3,4] Phosphatidylinositol mannosides (PIMs) are one of the major components of mycobacterial cell wall.[5] PIMs play crucial roles in compromising host immune responses and increasing number of PIMs biological functions were recently revealed.[6-10] Among the natural occurring series of PIMs, phosphatidylinositol hexamannoside is the largest in size, composed of six mannose units. A highly convergent and efficient synthesis of phosphatidylinositol hexamannoside glycan (1) is described here. The utilizations of bicyclic and tricyclic orthoesters as well as mannosyl phosphates as glycosylating agents constitute a more robust and practical synthetic protocol. The key intermediate orthoesters were prepared rapidly in scalable syntheses of mannoside building blocks. Glycosylations of mannosyl phosphates reliably resulted in excellent yields and selectivity. 1 is equipped with a thiol-linker for convenient immobilizations on surfaces and proteins to generate tools that can be further employed in biological and immunological studies.

Introduction

Among pathogenic organisms, *Mycobacterium tuberculosis (Mtb)* is the most disastrous human killer. This infectious pathogenic organism causes more deaths in human than any other single organism.[2,11,12] *Mtb* is a facultative intracellular pathogen which has sophisticatedly evolved to survive efficiently in human macrophages host cells.[1,3,4] The distinctive compositions of cell envelope of this bacteria is paramount important for its survival because they are the first to contact host cellular constituents during initial steps of infections. The bacterial cell envelope plays crucial roles in modulating immune responses from mammalian host cells, and later serves as a protective barrier to prevent anti-tuberculosis agents from permeating inside. The disclosed biological significance of different constituents in mycobacterial cell envelope has further heightened research interest in this area. However, many of these studies are hindered by the limited amount of naturally occurring components that are also often difficult to isolate in their pure entities. Therefore, successful chemical constructions of such compounds will facilitate and accelerate immunological studies of *Mtb*. Here, we report a highly convergent and efficient synthesis of the glycan in phosphatidylinositol hexamannoside that is one of the important components in mycobacterial cell wall.

Phosphatidylinositol mannosides (PIMs) displayed on the surface of *Mtb* play a critical part in interactions with host cells and host cell immune response modulation.[6-10,13-15] The functional importance of PIMs was emphasized by surprising finding that despite relatively less abundance of PIMs in the mycobacterium envelope comparing with other components, PIMs have been identified as the important ligands that bind receptors on both phagocytic[6,16,17] and nonphagocytic[4] mammalian cell surface.

Among the natural occurring series of PIMs, phosphatidylinositol hexamannoside is the largest in size. This glycan is composed of six mannose units and a *myo*-inositol moiety assembled in the sequence – $Man\alpha \rightarrow 2Man\alpha \rightarrow 2Man\alpha \rightarrow 6Man\alpha \rightarrow 6Man\alpha \rightarrow 6myo\text{-}Ins2 \leftarrow \alpha Man$. Several synthetic PIMs containing lower numbers of mannoside units have been synthesized employing various chemical methodologies.[18-26] The largest PIM which contain distinctive α1,2 mannoside linkages may exhibit different biological activities from smaller PIMs. Most reported synthetic PIMs were not designed to contain linkers for immobilization on supports commonly used as biochemical tools such as carrier proteins, microarray, beads, quantum dots, and surface plasma resonance sensor surface. To serve these purposes, the synthetic glycan **1** (Figure 1) is designed to have a thiol linker appended on the phosphorus atom by a phosphate diester linkage. The thiol linker is served as a handle to conveniently immobilize this well-defined synthetic molecule for biochemical and biological experiments.

Materials and Methods

All chemicals used were reagent grade and used as supplied except where noted. All reactions were performed in oven-dried glassware under an inert atmosphere unless noted otherwise. Reagent grade *N*,*N*-dimethylformamide (DMF) was dried over activated molecular sieves prior to use. Pyridine, triethylamine (NEt_3) and acetonitrile (MeCN) were distilled over CaH_2 prior to use. Dichloromethane (CH_2Cl_2), toluene and tetrahydrofuran (THF) were purified by a Cycle-Tainer Solvent Delivery System unless noted otherwise. Analytical thin layer chromatography (TLC) was performed on Merck silica gel 60 F254 plates (0.25mm). Compounds were visualized by UV irradiation or dipping the plate in a cerium sulfate-ammonium molybdate (CAM) solution. Flash column chromatography was carried out using forced flow of the indicated solvent on Fluka Kieselgel 60 (230-400 mesh). Gel filtration chromatography was carried out using Sephadex LH-20 from Amersham Biosciences.

All new compounds were characterized by NMR spectroscopy (^{1}H, ^{13}C, ^{31}P NMR and 2D NMR for some key intermediates), high resolution mass spectroscopy (HRMS), optical rotation activity, and melting point. NMR spectra were recorded on a Varian Mercury 300 (300 MHz), Bruker DRX500 (500 MHz), or Bruker DRX600 (600 MHz) spectrometer in $CDCl_3$ with chemical shifts referenced to internal standards $CDCl_3$ (7.26 ppm ^{1}H, 77.0 ppm ^{13}C). ^{31}P spectra are reported in δ value relative to H_3PO_4 (0.0 ppm) as an external reference.

General procedures for glycosylations: Glycosylating agent and nucleophile were co-evaporated with anhydrous toluene (3x) *in vacuo* and placed under high vacuum for at least 4 h. Glycosylations were performed without molecular sieves. Under argon atmosphere, the glycosylating agent and nucleophile mixtures were dissolved in a solvent at room temperature (rt) before being cooled to a desired temperature (0 °C by ice-water bath, -10 °C by ice-acetone bath, and -40 °C by dry ice-acetonitrile bath). A promoter (TMSOTf or TBDMSOTf) was added to this reaction solution in one portion via syringe. After the reaction had finished, excess triethylamine (NEt_3) was added to quench the reaction at the reaction temperature. The reaction mixture was concentrated *in vacuo* and purified by flash silica column chromatography or directly used as a starting material in the next reaction.

Results and Discussion

The glycan synthetic target **1** (Figure 1) can be assembled in a highly convergent fashion from three major fragments including 1) tetramannoside, 2) pseudotrisaccharide, and 3) thiol linker. The key glycosylations was [4+3] coupling between the tetramannoside donor and the *myo*-inositol containing pseudotrisaccharide acceptor. After this glycosylation unites the two main carbohydrate moieties, the ester protecting groups on this oligosaccharide was converted to the benzyl protecting group to ensure smooth installations of thiol terminated phosphate diester linker. This protecting group manipulations were also done to avoid the peersistence of the benzoyl protecting groups in the final deprotection reaction. The linker was installed via H-phosphonation and immediately followed by oxidation of the phosphorus atom. Because the target molecules contain a sulfur atom which is known to deactivate the Pd/C catalyst, the final removal of the permanent benzyl protecting groups must rely on dissolved sodium metal Birch reduction.

The stereoselectivity of each glycosylic bond is controlled by neighbouring C-2 acyl participating group. We decided to employ dibutyl phosphate ester as a leaving group for all of the monosaccharide mannose donors because of its known in excellent yields and desired selectivity outcomes of glycosylations. The choice of phosphate donors in this synthesis was proved to be one of the advantages over the previous reports on syntheses of PIMs. Moreover, the utilizations of monosaccharide mannosyl phosphate donors allow rapid preparations of the building blocks.[27] In addition, molecular sieves were not neccessary when setting up the glycosylation reactions with the phosphate donors. In addition to the inositol building block **5**,[26,28] we had to prepare only three mannose building blocks[27,29] (**2**-**4**)

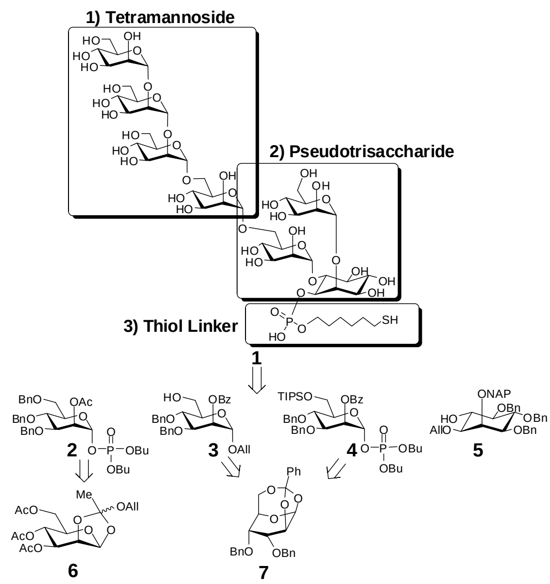

Figure 1. Structure and retrosynthetic analysis of phosphatidylinositol hexamannoside glycan equipped with thiol terminated phosphate linker (**1**).

The tetramannoside imidate donor **11** was assembled in a linear fashion (Figure 2). The phosphate donor **2** and the TMSOTf activator were employed in three consecutive glycosylation steps. The 1,6 α glycosylic bond was readily formed at 0 ºC with quantitative isolated yield but the 1,2 α glycosylations must be carried out at lower temperature of - 40 ºC. After the allyl group at the reducing end was removed, the conversion to the trichloroacetimidate donor **11** was done in the presence of NaH as a base.

In a gram scale preparation of pseudotrisaccharide acceptor **13** (Figure 3)**,** the glycosylation between the mannosyl phosphate donor **4** and the inositol acceptor **5** was achieved at -40 °C, in toluene, with stoichiome-

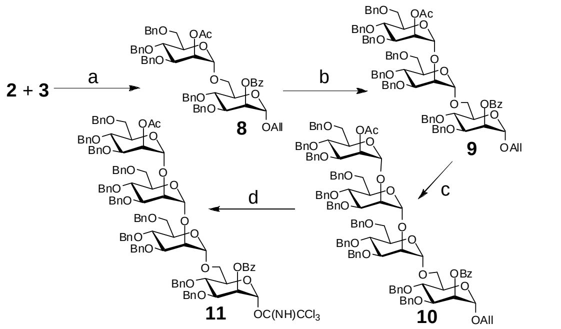

Figure 2. Linear assembly of tetramannoside imidate donor **11**. Reagents and conditions: (a) TMSOTf, CH_2Cl_2, -10 °C, quant.; (b) i) AcCl, MeOH, CH_2Cl_2, 0 °C, 91%, ii) **2**, TMSOTf, -40 °C, Toluene, 95%; (c) i) AcCl, MeOH, CH_2Cl_2, 0 °C, 84%, ii) **2**, TMSOTf, Toluene, -40 °C, 96%; (d) i) $Pd(OAc)_2$, MeOH, PPh_3, Et_2NH, 83%, ii) Cl_3CCN, NaH, rt, 89%.

tric amount TMSOTf as a promoter. The TIPS protecting group was replaced by the more acid stable levulinoyl protecting group in order to sustain further glycosylation conditions. DDQ unmasked the C2 hydroxyl of the inositol to function as nucleophile for the next glycosylation to install another mannose unit at this position. In the glycosylation between **2** and **12**, the difference in reactivities between the highly activated donor **2** and the less active acceptor **12** was evidenced by poor yield and selectivity. To obtain the desired glycosylation product, the reactivity of donor **4** was subsided by using the milder activator TBDMSOTf and the reactivity of the acceptor **12** was enhanced by elevating reaction temperature. Then, the acceptor **13** was obtained after the Lev protecting group was removed by careful treatment with hydrazine acetate and MeOH for 4-5 h.

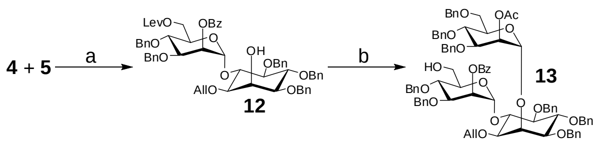

Figure 3. Synthesis of pseudotrisaccharide acceptor **13**. Reagents and conditions: (a) i) TMSOTf , Toluene, -40 °C, 90%, ii) AcCl, MeOH, CH_2Cl_2, 0 °C, quant., iii) LevOH, DIPC, DMAP, quant., iv) DDQ, CH_2Cl_2, MeOH, 0 °C, 95%; (b) i) **2**, TBDMSOTf, Toluene, -40 °C, 95%, ii); (f) H_2NNH_3OAc, MeOH, rt, 89%.

The key [4+3] glycosylation between the tetramannoside donor **11** and pseudotrisaccharide acceptor **13** was found to give better yield and selectivity when the reaction was carried out at -10 °C rather than at a lower temperatures (Figure 4). The heptasaccharide **14** was thoroughly characterized by 1D and 2D NMR spectroscopy including C-H coupled HSQC[30] to confirm its structural identity. C-H coupled HSQC revealed six anomeric proton signals having $J_{C1,H1}$ within the typical[30] α-manno range as the followings (chemical shift in ppm, $J_{C1,H1}$ in Hz): (1) 5.54, 177.9; (2) 5.26, 172.1; (3) 5.16, 175.9; (4) 5.10, 173.2; (5) 4.92, 172.5; (6) 4.80, 172.1.

All of the ester protecting groups on the heptasaccharide **14** were removed by treatments with NaOMe in MeOH at an elevated temperature (50 °C) before the resulting free hydroxyl groups were masked by benzyl groups. The early removals of ester protecting groups would eliminate an expected difficulty arising from the persistence of these groups under Birch conditions in the final step.[31]

The hydrogen activated iridium complex, $Ir\{(COD)[PCH_3(C_6H_5)_2]_2\}PF_6$ was found to be the most efficient reagent to isomerize the allyl group of **15** to its corresponding enol ether. In the same pot, excess amount of *p*-toluenesulfonic acid (*p*-TsOH) was needed to efficiently cleave the enol ether and furnish compound **16**. The thiol terminated phosphate moiety was installed on the inositol C1 hydroxyl of oligosaccharide **16** by treatment with pivaloyl chloride in the presence of the linker **17**[32] and pyridine.[31] Subsequently, in the same pot, the H phosphonated intermediate was oxidized by wet iodine to provide the fully benzylated phosphodiester **18** as a triethylamine salt in excellent yields. The fully protected oligosaccharide **18** was treated with sodium dissolved in ammonia to globally remove all of the benzyl protecting groups. The final product **1** was achieved as a mixture along with its disulfide dimeric form.

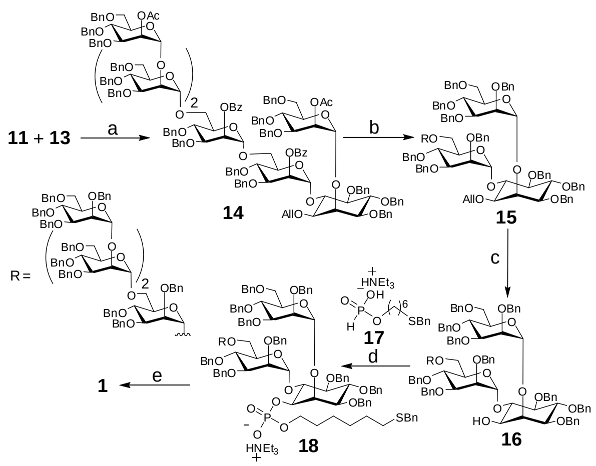

Figure 4. Synthesis of phosphatidylinositol hexamannosides glycan **1**. Reagents and conditions: (a) i) TMSOTf , CH_2Cl_2, -10 °C, 48%; (b) i) NaOMe/MeOH, 50 °C, 24 h, ii) BnBr, NaH, 0 °C to rt, 12, 97%, 2 steps. (c) i) $[Ir(COD)(PCH_3Ph_2)_2]PF_6$ (cat.), H_2, THF, 1 h, ii) *p*-TsOH (10 eq.), CH_2Cl_2/MeOH (1:3), rt, 89%, 2 steps; (d) i) **17**, PivCl, pyridine, ii) I_2, H_2O, pyridine, 95%, 2 steps; (e) Na/NH_3 (l) /*t*-BuOH, -78 °C, 1 h, then MeOH, 84%.

Conclusions

The efficient synthesis of the phosphatidylinositol hexamannoside glycan **1** is demonstrated here. The synthesis was designed to be both practical and scalable based on the careful selections of building blocks. The bicyclic and tricyclic orthoesters as well as mannosyl phosphates were prepared rapidly in multi-gram scale. Glycosylations of mannosyl phosphates reliably resulted in excellent yields and selectivity. The synthetic glycan **1** equipped with a thiol-linker would be suitable to attach on appropriate surfaces for further studies in biological and immunological experiments.

Acknowledgements

This research was supported by ETH Zürich, the Swiss National Science Foundation (SNF Grant 200121-101593), Thailand Research Fund (TRF Grant MRG5180240) and Roche Research Foundation.

References

[1] D. G. Russell, *Nat Rev Microbiol* **5** (2007), pp. 39-47.
[2] C. Martin, *Eur Respir J* **26** (2005), pp. 162-167.
[3] D. G. Russell, *Nat Rev Mol Cell Biol* **2** (2001), pp. 569-577.
[4] H. C. Hoppe, B. J. de Wet, C. Cywes, M. Daffe, M. R. Ehlers, *Infect Immun* **65** (1997), pp. 3896-3905.
[5] S. Berg, D. Kaur, M. Jackson, P. J. Brennan, *Glycobiology* **17** (2007), pp. 35-56R.
[6] C. Villeneuve, M. Gilleron, I. Maridonneau-Parini, M. Daffe, C. Astarie-Dequeker, G. Etienne, *J Lipid Res* **46** (2005), pp. 475-483.
[7] V. Sundaramurthy, J. Pieters, *Microbes Infect* **9** (2007), pp. 1671-1679.
[8] I. Apostolou, Y. Takahama, C. Belmant, T. Kawano, M. Huerre, G. Marchal, J. Cui, M. Taniguchi, H. Nakauchi, J. J. Fournie, P. Kourilsky, G. Gachelin, *Proc Natl Acad Sci U S A* **96** (1999), pp. 5141-5146.
[9] J. Nigou, M. Gilleron, M. Rojas, L. F. Garcia, M. Thurnher, G. Puzo, *Microbes Infect* **4** (2002), pp. 945-953.
[10] R. E. Rojas, J. J. Thomas, A. J. Gehring, P. J. Hill, J. T. Belisle, C. V. Harding, W. H. Boom, *J Immunol* **177** (2006), pp. 2959-2968.
[11] A. S. Malin, D. B. Young, *BMJ* **312** (1996), pp. 1495.
[12] S. K. Sharma, A. Mohan, *Indian J Med Res* **120** (2004), pp. 354-376.
[13] D. Chatterjee, K. H. Khoo, *Glycobiology* **8** (1998), pp. 113-120.
[14] H. de la Salle, S. Mariotti, C. Angenieux, M. Gilleron, L. F. Garcia-Alles, D. Malm, T. Berg, S. Paoletti, B. Maitre, L. Mourey, J. Salamero, J. P. Cazenave, D. Hanau, L. Mori, G. Puzo, G. De Libero, *Science* **310** (2005), pp. 1321-1324.
[15] J. F. Vliegenthart, *FEBS Lett* **580** (2006), pp. 2945-2950.
[16] L. M. Thorson, D. Doxsee, M. G. Scott, P. Wheeler, R. W. Stokes, *Infect Immun* **69** (2001), pp. 2172-2179.
[17] J. B. Torrelles, A. K. Azad, L. S. Schlesinger, *J Immunol* **177** (2006), pp. 1805-1816.
[18] C. J. J. Elie, C. E. Dreef, R. Verduyn, G. A. Van der Marel, J. H. Van Boom, *Tetrahedron* **45** (1989), pp. 3477-3486.
[19] C. J. J. Elie, R. Verduyn, C. E. Dreef, D. M. Brounts, G. A. Van der Marel, J. H. Van Boom, *Tetrahedron* **46** (1990), pp. 8243-8254.
[20] C. J. J. Elie, R. Verduyn, C. E. Dreef, G. A. Van der Marel, J. H. Van Boom, *Journal of Carbohydrate Chemistry* **11** (1992), pp. 715-739.
[21] K. N. Jayaprakash, J. Lu, B. Fraser-Reid, *Bioorg Med Chem Lett* **14** (2004), pp. 3815-3819.
[22] A. Stadelmaier, M. B. Biskup, R. R. Schmidt, *European Journal of Organic Chemistry* (2004), pp. 3292-3303.
[23] A. Stadelmaier, R. R. Schmidt, *Carbohydr Res* **338** (2003), pp. 2557-2569.
[24] Y. Watanabe, T. Yamamoto, T. Okazaki, *Tetrahedron* **53** (1997), pp. 903-918.
[25] Y. Watanabe, T. Yamamoto, S. Ozaki, *Journal of Organic Chemistry* **61** (1996), pp. 14-15.
[26] X. Liu, B. L. Stocker, P. H. Seeberger, *J Am Chem Soc* **128** (2006), pp. 3638-3648.
[27] X. Liu, R. Wada, S. Boonyarattanakalin, B. Castagner, P. H. Seeberger, *Chemical Communications* (2008), pp. 3510-3512.
[28] Z. J. Jia, L. Olsson, B. Fraser-Reid, *J. Chem. Soc., Perkin Trans. 1* (1998), pp. 631.
[29] A. Ravida, X. Liu, L. Kovacs, P. H. Seeberger, *Org Lett* **8** (2006), pp. 1815-1818.
[30] C. A. Podlasek, J. Wu, W. A. Stripe, P. B. Bondo, A. S. Serianni, *J. Am. Chem. Soc* **117** (1995), pp. 8635-8644.
[31] Y. U. Kwon, R. L. Soucy, D. A. Snyder, P. H. Seeberger, *Chemistry* **11** (2005), pp. 2493-2504.
[32] I. Lindh, J. Stawinski, *Nucleic Acids Symp Ser* (1987), pp. 189-192.

SYNTHESIS OF TRICYCLIC ORTHOESTERS OF MANNOSE FOR RING-OPENING OLIGOMERIZATION TOWARD D-MANNOPYRANAN

Moragot Sungsilp[1], Chanokpon Yongyat[1], Somsak Ruchirawat[2] and Siwarutt Boonyarattanakalin[1]*

[1]Department of Bio-Chemical Engineering, Sirindhorn International Institute of Technology, Thammasat University, Pathum Thani, Thailand, 12121
[2]Laboratory of Medicinal Chemistry, Chulabhorn Research Institute, and Program in Chemical Biology, Chulabhorn Graduate Institute, Vipavadee-Rangsit Highway, Bangkok 10210 Thailand.

* Corresponding Author: siwarutt@siit.ac.th, Tel: +66-2-986-9009 ext 2305

Abstract: Oligo- and polysaccharides have recently been recognized for their various significant biological activities other than being the main energy sources. Polysaccharides found on bacterial surface have significant roles in immune response.[1-3] The intricate cell wall structure contributes to bacterial virulence, causing severe diseases in humans, such as tuberculosis and leprosy.[4] Although poly- and oligomannoses are available in nature, there are many limitations to access the homogeneous substances because of the difficulty in isolation, purification, and identification.[5] Therefore, chemical synthesis is employed as an reliable approach to obtain structurally defined oligosaccharides.[5,6] A more favorable method for the synthesis of oligosaccharide is controlled oligomerization rather than traditional stepwise synthetic method. Oligomerizations of monosaccharide building blocks create several glycosidic bonds in a single chemical reaction. Oligomerizations require much shorter time for chemical processing when comparing with the step by step synthesis. Furthermore, oligomerization can provide desired compounds in substantial quantity.

For rapid synthesis of oligomannosides, tricyclic orthoester building blocks of mannose provide suitable structural features for ring-opening oligomerizations. The building blocks 3,4-*O*-benzyl-β-D-mannopyranose 1,2,6-orthobenzoate (1) and 3,4-*O*-benzyl-β-D-mannopyranose 1,2,6-orthopivalate (2) were synthesized and for utilization as monomer in ring opening oligomerizations. The synthetic protocols for both building blocks were developed based on previous reports.[2,7] Orthoesters 1 and 2 were successfully prepared in six multiple-gram scale and high yielding chemical reactions. The whole synthesis requires only two purification steps. The transformation conditions were adjusted to fit the high humidity climate for versatility in possible industrial scale-up. Preliminary results from oligomerization of building block 1 and 2 proved that the substituent on the orthoester carbon of the building block 1 and 2 determine the diversity and size of oligomannoside products.

Introduction

In addition to macromolecules including proteins, DNA, and RNA, oligo- and polysaccharides play essential roles in biological systems other than being the main energy source. The oligo- and polysaccharides play crucial activities in various significant biological functions, such as, cell recognitions, cell differentiation, cell-cell adhesion, viral replication, parasitic infection, host-pathogen interactions, and immune responses.[8-10] Nowadays, the biological activities of these polysaccharides draw more attention from researchers in biochemical and medical fields due to their immunomodulatory and antitumor effects.[11]

Oligo- and polysaccharides have significant structural roles in immune response.[1-3] They are found on the envelope of pathogenic bacteria including *Mycobacterium tuberculosis* (*Mtb*), which has unique and complicated features.[4] This intricate cell wall structure contributes to bacterial virulence, causing severe diseases in humans.[4] The cell wall structure of *Mtb* consists of arabinogalactan (AG), lipoarabinomannan (LAM), mannose capped lipoarabinomannan (ManLAM) and lipomannan (LM).[4] AG, LAM, and also phosphatidylinositol mannosides (PIMs) play a critical role in interacting with host cells and moderating immune response.[4,12]

In spite of the availability of poly- and oligomannoses in nature, there are many limitations to access the homogeneous compounds because it requires multiple steps in order to isolate and purify them.[5] Therefore, chemical synthesis is considered to be a reliable approach to synthesize structurally-defined oligosaccharides.[5,6] Apart from traditional stepwise synthetic methods, automation and oligomerization are employed to be more favorable methods for the synthesis of oligosaccharide because they take much shorter time for chemical processing. Oligomerization of monosaccharide building blocks creates several glycosidic bonds in a single chemical reaction and gives desired products in a significant amount.

There are several reports on the synthesis of polysaccharide by ring-opening polymerizations of various building blocks, e.g. 3-*O*-benzyl-β-L-arabinofuranose 1,2,5-orthopivalate[13], 3,6-di-*O*-benzyl-α-D-glucopyranose 1,2,4-orthopivalate[14,15], 3-*O*-benzyl-6-*O*-pivaloyl-α-D-glucopyranose 1,2,4-orthopivalate[15], 3-*O*-benzyl-6-deoxy-α-D-glucopyranose 1,2,4-orthopivalate[16], and 3-*O*-benzyl-α-D-xylopyranose 1,2,4-orthopivalate[17]. Hori *et al.*

(2000) reported that the ring-opening polymerization of 3-*O*-benzyl-β-L-arabinofuranose 1,2,5-orthopivalate by using $BF_3{\cdot}Et_2O$ as a catalyst gave the stereoregular polysaccharide (1→5)-α-L-arabinofuranan with DPn = 91.[13] The benzyl group at 3-*O* position and the pivaloyl group at 2-*O* position are necessary for stereoregularity and regioregularity in the synthesis of arabinofuranan.[13] Moreover, stereoregular polysaccharide of glucose was synthesized by ring-opening polymerization of 3,6-di-*O*-benzyl-α-D-glucopyranose 1,2,4-orthopivalate or 3-*O*-benzyl-6-*O*-pivaloyl-α-D-glucopyranose 1,2,4-orthopivalate. Similar to the synthesis of arabinofuranan, the 3-*O*-benzyl group and 2-*O*-pivaloyl group of glucopyranose play a significant role in the stereospecificity and regiospecificity of the resulting polymer.[18,19] The resulting polymer contained only (1→4)-glycosidic bond, but not (1→2)-bond.[19]

Apart from the substituents at 2-*O* and 3-*O* position, the protecting group (R) of $-CH_2OR$ at *C6*-position affected the stereo- and regioregularity of the resulting polymer due to electronic effect of the protecting group.[16] Therefore, the alkyl group at the orthoester carbon should be an electron-donating or a slightly withdrawing group such as benzoyl or pivaloyl group. Moreover, types of initiators and temperatures also affected the regioregularity of resulting polymers.[13-15] In brief, the previous studies of cationic ring opening polymerizations of glycosyl tricyclic orthoesters suggested that the regio and stereo selectivity of the resulting polymer could be achieved. The pattern of protecting groups on the hydroxyls of building blocks heavily influenced both the polymerization efficiency and the selectivity of the resulting polymer. The regio selectivity was created by the preferential attacks of a Lewis acid at different oxygen atoms bonding with orthoester carbon.

In spite of many biological roles of oligomannosides, rarely there are accounts for one-step synthesis of poly- or oligomannose. The synthesis of mannopyranan will be useful contributions for biological studies. To serve this purpose, we have designed and synthesized tricyclic orthoester of mannose for the ring-opening oligomerization toward D-mannopyranan.

Materials and Methods

All chemicals used were reagent grade and used as supplied except where noted. All reactions were performed in oven-dried glassware under an inert atmosphere unless noted otherwise. Dichloromethane (CH_2Cl_2) was dried over calcium hydride (CaH_2) prior to use. Lutidine was treated by potassium hydroxide (KOH) and allyl alcohol was treated with potassium carbonate (K_2CO_3) prior to use. 4Å Molecular sieves were activated by a heat gun under high vacuum. Analytical thin layer chromatography (TLC) was performed on Merck silica gel 60 F254 plates (0.25 mm). Compounds were visualized by dipping the plate in a cerium sulfate-ammonium molybdate (CAM) solution and phosphomolybdic acid (PMA) solution. Flash column chromatography was carried out using forced flow of the indicated solvent on Fluka Kieselgel 60 (230-400 mesh).

All new compounds were characterized by NMR chromatography (^1H, ^{13}C NMR and 2D NMR for some key intermediates), high resolution mass spectroscopy (HRMS), optical rotation activity, and melting point. NMR spectra were recorded on a Varian Gemini 2000 (200 MHz) and Bruker AVANCE 400 (400 MHz) in $CDCl_3$ with chemical shift reference to internal standards $CDCl_3$ (7.26 ppm for ^1H NMR and 77.0 ppm for ^{13}C NMR).

Results and discussion

The design of mannoside monomer: For a rapid synthesis of oligo- and polymannosides, tricyclic orthoester building blocks of mannose are suitable structural features for ring-opening oligomerizations. The building blocks 3,4-*O*-benzyl-β-D-mannopyranose 1,2,6-orthobenzoate (**1**) and 3,4-*O*-benzyl-β-D-mannopyranose 1,2,6-orthopivalate (**2**) were synthesized and utilized as monomer in ring opening oligomerizations. The monomers **1** and **2** contain a highly strained tricyclic structure which is readily susceptible for ring opening oligomerization upon activation with Lewis acids.

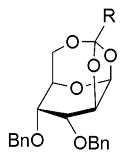

1: R = C_6H_5
2: R = $C(CH_3)_3$

Figure 1. The structures of tricyclic orthoester mannoside building blocks

The C-3 and C-4 hydroxyl groups of both building block monomers 1 and 2 were protected with an electron donating group, *O*-benzyl ether. The 1-, 2- and 6-*O* positions are masked in a form of tricyclic orthobenzoate and orthopivaloate in building blocks **1** and **2**, respectively. During the ring-opening oligomerization, the 3-*O* benzyl group has a considerable effect on chemical activity because the benzyl group is an electron-donating group, which is responsible for stabilizing the dioxalenium intermediate, resulting in the formation of glycosidic bond via S_N2 attack of the next monomer, after the activation by Lewis acid initiators.

Furthermore, the 4-*O* benzyl group will play an important role in the regioregularity of the resulting polymer because it has a high electron-donating property. The electron donating group contributes to the high electron density of *C6*-oxygen of the monomers. It has been shown that when treated with BF_3Et_2O and allyl alcohol in CH_2Cl_2, the C-O bond between the orthoester carbon and the *C6*-oxygen atom was cleaved.[2] Therefore, we envisioned that during the oligomerization of monomer **1** and **2**, the C-O orthoester carbon - oxygen bonds will be selectively cleaved at the *C6*-oxygen atom and the resulting glycosidic bond formation will favor 1,6 linkage.

In addition to the benzyl groups at 3-*O* and 4-*O* positions, the alkyl substituent on the orthoester carbon of the building blocks **1** and **2** is essential for stabilization of cation intermediate on the orthoester carbon and thus promotes the growth of oligomer chains. During propagation step of oligomerization, the next monomer will favorably attack at the bottom face of anomeric carbon due to the steric effect from the acyl protected *C2* hydroxyl group that oriented out of the top face. Consequently, the incoming nucleophilic oxygen is likely to form an α glycosidic bond with the anomeric carbon. Therefore, the stereospecificity in the oligomannoside product will be achieved by the acyl protecting group of the *C2*-hydroxyl.

The synthesis of mannoside building blocks: With ultimate goal of being able to prepare the building blocks in large scales and a rapid fashion, we set to develop a synthetic route that is robust and scalable. The synthesis of monomer **1** and **2** was developed based on the previously published report.[2,7] We found that the some chemical reagents used in the previous report were not suitable for high humidity climate in a country like Thailand. We successfully develop a new synthesis route that would not be affected by humid atmosphere. The overall redesigned synthesis of monomers **1** and **2** was illustrated in Scheme 1. We have developed a short synthetic route that requires only six chemical transformations, of which only two column purifications were necessary. We have developed short synthetic route that requires only six chemical transformations of which only two column purifications were necessary. Moreover, the same chemical conditions can be applied to produce both building blocks **1** and **2** in multiple-gram scale.

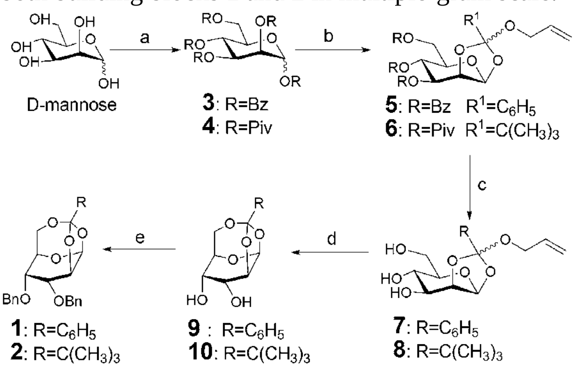

Scheme 1. Synthesis of building blocks **1** and **2**. Reagents and conditions: (a) BzCl, pyridine, 0 °C, 12 h or PivCl, pyridine, reflux, 24 h; (b) HBr/HOAc (33%), acetic anhydride, 24 h c) AllOH, lutidine, 83% (3 steps) for **3**, 42% (3 steps) for **4** ; (d) KOH, H_2O, MeOH, THF, rt, 24 h; (e) 0.05 equivalence CSA, CH_2Cl_2, 1 h; (f) BnBr, NaH, DMF, 0 °C to rt, 12 h, 37% (3 steps) for **1** and 56% (3 steps) for **2**.

The synthesis routes for building blocks **1** and **2** are different in the first step of global protection of hydroxyl groups in the native mannose. First, the native mannose sugar was globally protected with benzoate esters (Bz) and pivalate esters (Piv) for the synthesis of building blocks **1** and **2**, respectively. More than twice of stoichiometric amount of the acid chlorides (BzCl and PivCl) and high temperatures were required to drive the reaction to completion. The benzyl chloride (12 eq.) and pivaloyl chloride (12 eq.) were added dropwise to the sugar starting material suspended in pyridine (45 eq.) at 4 °C. The reaction mixture was allowed to stir for 24 h at room temperature (rt) to give **4**. In case of the more bulky PivCl, the reaction mixture needed to be refluxed for 16 h to yield **4**. Compound **4** was obtained as anomeric mixtures having the same molecular weight characterized by hi-resolution ESI mass spectrometry. The 1H NMR of the major product showed the anomeric peak as a doublet at 5.82 ppm (J = 1.0 Hz). The crude products from both reactions mostly contained the desired products **3** and **4**. Only filtration and extraction were necessary to treat the crude products before using in the next step. Without further purifications, compounds **3** and **4** were treated with acetic anhydride (8 equiv.), and a solution of 33%.

Without further purifications, the mannosyl bromides **3** and **4** were transformed to the bicyclic orthoester **5** and **6** by treatment with 2,6-lutidine (6 equiv.) and allyl alcohol (30 equiv.). Under the basic conditions, the carbonyl oxygen of the acetate protecting group on the C-2 oxygen attacked the anomeric carbon and replaced the bromine atom from the top face. A carbocation temporarily generated on the orthoester carbon was relieved by the attack of incoming hydroxyl group of the allyl alcohol. The side products obtained from this reaction were 2,3,4,6-O-tetra acyl D-mannopyranose which can be recovered by treatment with reaction condition b (Scheme 1) to give **5** and **6**. The anomeric doublet resonance of **6** was at 5.51 ppm (J = 3.0 Hz).

To globally remove the acyl protecting groups, which are benzoyl and pivaloyl groups, we initially performed the typical transesterification reactions which relied on the basic sodium methoxide generated *in situ* from the reaction between solid sodium and methanol. Under the transesterification conditions, benzoyl groups were partially removed only at elevated temperatures. The amounts of NaOMe used, from catalytic (5%) to stoichiometric at reflux temperature (THF/MeOH ratio of 1:1) failed to remove the acyl protecting groups. The starting material was gradually decomposed by basic and heated conditions. Even though, we attempted to perform the reactions under inert atmosphere, we suspected that NaOMe was degraded under highly humid conditions in Thailand. NaOMe reacted with moisture (H_2O) to form NaOH which is too weakly basic to catalyze the transesterification reactions. We then turned to hydrolysis reaction to remove the acyl protecting groups. Moisture in the laboratory atmosphere was irrelevant during hydrolysis setup because water is one of the reagents used in this reaction. First, different equivalences of hydrate lithium hydroxide ($LiOH{\cdot}H_2O$) were applied to compounds **5** and **6** in MeOH and THF, but the desired products were not obtained and the starting material was decomposed. The hydrolysis took place much better when applying potassium hydroxide as a base in hydrolysis reactions. The acyl groups of the bicyclic orthoesters **5** and **6** were successfully removed after treatment with KOH (4 equiv.)/H_2O at rt. Compounds **7** and **8** were obtained in almost quantitative yield. After organic solvent/aqueous extraction, compounds **7** and **8** were used in the next step without further purifications. Due to the high polarity of compounds **7** and **8**, some amounts of compounds **7** and **8** were lost during the extractions.

To obtain tricyclic orthoesters **9** and **10**, the cyclizations of compounds **7** and **8** were induced by catalytic amount of acids. We found that CH_2Cl_2 was a better solvent for tricycic formations than CH_3CN. We omitted the use of 4Å molecular sieves as done in the previous report. 4Å molecular sieves suppressed the activity of acid cayalyst resulting in long reaction time (more than 24 hr) and consequently more lactol side product. By applying only 5 mol% of camphor-10-sulfonic acid, the reactions were completed within one or two hr with quantitative conversions. The products **9** and **10** were used in the next step without further purifications. The isolated compound **10** was also characterized for its structural identity. The anomeric doublet of 10 was at 5.77 ppm (J = 5.8 Hz). The final benzylation protections on compounds **9** and **10** were done by the treatments with benzyl bromide (BnBr) and sodium hydride (NaH) as a base at 0 ^{o}C. The crude products were purified by silica gel flash column chromatography (hexanes / EtOAc) to obtain the monomer **1** and **2** as white solids. The overall synthesis yields of building blocks **1** and **2** from D-mannose were 31% and 24%, respectively. The ^{1}H and ^{13}C NMR spectra of compound **1** synthesized by the developed route are similar to the previously published data. The monomer **2** was characterized extensively by 1D and 2D NMR and the anomeric doublet resonance of **2** was at 5.67 ppm (J = 5.8 Hz).

Conclusion

The building blocks 3,4-*O*-benzyl-β-D-mannopyranose 1,2,6-orthobenzoate (**1**) and 3,4-*O*-benzyl-β-D-mannopyranose 1,2,6-orthopivalate (**2**) were synthesized for utilization as monomers in ring opening oligomerizations for rapid synthesis of oligomannosides. The synthetic protocols of both building blocks were developed based on previous reports.[2,7] Orthoesters **1** and **2** were successfully prepared in six steps in multiple-gram scale and high yielding chemical reactions. The whole synthesis requires only two column purification steps. To be suitable for high humidity climate in Thailand, the removal of acyl protecting groups was done by hydrolysis reactions. The synthetic protocols were designed to be robust and scalable. Preliminary results from oligomerization of building block **1** and **2** proved that the building blocks monomers can form multiple glycosidic bonds upon single activation by Lewis acids. The more detailed studies on the oligomerization are under investigations.

Acknowledgement

This research was supported by Thailand Research Fund (TRF Grant # MRG5180240) and Thammasat University Research Fund. C. Yongyat and M. Sungsilp thank the National Science and Technology Development Agency (NSTDA) for the undergraduate scholarships from the Young Scientist and Technologist Program (YSTP). We thank CRI for chemical reagents and equipments.

References

[1] Ni, J.; Song, H.; Wang, Y.; Stamatos, N. M.; Wang, L.-X. *Bioconjugate Chemistry* **2006**, *17*, 493-500.

[2] Boonyarattanakalin, S.; Liu, X.; Michieletti, M.; Lepenies, B.; Seeberger, P. H. *Journal of the American Chemical Society* **2008**, *130*, 16791-16799.

[3] Wang, H.; Obenauer-Kutner, L.; Lin, M.; Huang, Y.; Grace, M. J.; Lindsay, S. M. *Journal of the American Chemical Society* **2008**, *130*, 8154-8155.

[4] Brown, J. R.; Field, R. A.; Barker, A.; Guy, M.; Grewal, R.; Khoo, K.-H.; Brennan, P. J.; Besra, G. S.; Chatterjee, D. *Bioorganic & Medicinal Chemistry* **2001**, *9*, 815-824.

[5] Wang, Z.-G.; Warren, J. D.; Dudkin, V. Y.; Zhang, X.; Iserloh, U.; Visser, M.; Eckhardt, M.; Seeberger, P. H.; Danishefsky, S. J. *Tetrahedron* **2006**, *62*, 4954-4978.

[6] Hattori, K.; Yoshida, T.; Uryu, T. *Carbohydrate Polymers* **1998**, *36*, 129-135.

[7] Liu, X.; Wada, R.; Boonyarattanakalin, S.; Castagner, B.; Seeberger, P. H. *Chem Commun (Camb)* **2008**, 3510-2.

[8] Li, B.-G.; Zhang, L.-M. *Carbohydrate Polymers* **2008**, *74*, 390-395.

[9] Singh, S.; Ni, J.; Wang, L. X. *Bioorg Med Chem Lett* **2003**, *13*, 327-30.

[10] Dwek, R. A. *Chemical Reviews* **1996**, *96*, 683-720.

[11] Gan, L.; Zhang, S.-H.; Liu, Q.; Xu, H.-B. *European Journal of Pharmacology* **2003**, *471*, 217-222.

[12] Nigou, J. m.; Gilleron, M.; Rojas, M.; Garča, L. F.; Thurnher, M.; Puzo, G. *Microbes and Infection* **2002**, *4*, 945-953.

[13] Hori, M.; Nakatsubo, F. *Macromolecules* **2000**, *33*, 1148-1151.

[14] Nakatsubo, F.; Kamitakahara, H.; Hori, M. *Journal of the American Chemical Society* **1996**, *118*, 1677-1681.
[15] Kamitakahara, H.; Hori, M.; Nakatsubo, F. *Macromolecules* **1996**, *29*, 6126-6131.
[16] Hori, M.; Nakatsubo, F. *Macromolecules* **2001**, *34*, 2476-2481.
[17] Hori, M.; Nakatsubo, F. *Carbohydrate Research* **2001**, *332*, 405-414.
[18] Hori, M.; Kamitakahara, H.; Nakatsubo, F. *Macromolecules* **1997**, *30*, 2891-2896.
[19] Kamitakahara, H.; Nakatsubo, F. *Macromolecules* **1996**, *29*, 1119-1122.

Langmuir Letter

pubs.acs.org/Langmuir

Ru(II) Glycodendrimers as Probes to Study Lectin−Carbohydrate Interactions and Electrochemically Measure Monosaccharide and Oligosaccharide Concentrations

Raghavendra Kikkeri,[†,⊥] Faustin Kamena,[†,⊥] Tarkeshwar Gupta,[‡] Laila H. Hossain,[†] Siwarutt Boonyarattanakalin,[§] Ganna Gorodyska,[||] Eva Beurer,[||] Géraldine Coullerez,[||] Marcus Textor,[||] and Peter H. Seeberger*[,†,⊥]

[†]*Laboratory for Organic Chemistry, ETH Zurich, Switzerland,* [‡]*Department of Chemistry, University of California, Berkeley, California 94720-1460,* [§]*Sirindhorn International Institute of Technology, Thammasat University, P.O. Box 22 Thammasat-rangsit Post Office, Pathumthani 12121, Thailand, and* [||]*Laboratory for Organic Chemistry, Swiss Federal Institute of Technology (ETH), Zurich, Wolfgang-Pauli-Str. 10, 8093 Zurich, Switzerland.* [⊥]*Current address: Max-Planck-Institute of Colloids and Interfaces, Department of Biomolecular Systems, Am Mühlenberg 1, 14476 Potsdam, Germany.*

Received October 17, 2009. Revised Manuscript Received November 13, 2009

We describe a novel platform on which to study carbohydrate−protein interactions based on ruthenium(II) glycodendrimers as optical and electrochemical probes. Using the prototypical concanavalin A (ConA)−mannose lectin−carbohydrate interaction as an example, oligosaccharide concentrations were electrochemically monitored. The displacement of the Ru(II) complex from lectin-functionalized gold surfaces was repeatedly regenerated. This new platform presents a method to monitor many different complex sugars in parallel.

The interaction of carbohydrates and carbohydrate-binding proteins, so-called lectins, is key to diverse processes such as cell growth, inflammatory responses, and viral infections.[1] Glycan patterns on the surface of different organisms but also between healthy and cancerous cells differ significantly. Cell-surface carbohydrates are potential diagnostic markers as well as targets for the design of carbohydrate-based vaccines.[2] Therefore, it is desirable to quantitatively analyze glycans of interest as well as their interactions with the lectins that bind them.[3] Microarrays,[4a,4b] electrochemical methods,[4c] surface plasmon resonance, and quartz crystal microbalance biosensors[4d] have been employed to analyze lectin−sugar interactions and cell−surface carbohydrates. These methods rely on multivalent carbohydrate ligand presentation because the monosaccharide−lectin binding affinity is often weak. Carbohydrate clusters on molecular templates including cyclodextrins,[5] calixarenes,[5d] dendrimers,[6] and gold nanoparticles[7] create a multivalent sugar display. Glycodendrimers have been synthesized on organic fluorescent probes, CdSe, CdS, and gold nanoparticles to monitor recognition events by electronic, optical, or microgravimetric means.[4c,7,8] However, nanoparticle−sugar conjugation requires special polymer coats to avoid nonspecific interactions.[8b] Fluorescent metallo-glycodendrimers provide an alternative to nanoparticles. Lanthanide, Ru(II), Re(II), and Ir(II) metal complexes[6b,6c] are tunable, stable, nonbleaching fluorescent probes with microsecond lifetimes.

Among these metals, the Ru(II) core is most attractive for its octahedral core symmetry and robustness. Ru(II) complexes exhibit a low excited triplet metal-to-ligand charge-transfer (^{3}MLCT) state and room-temperature ^{3}MLCT lifetimes up to 1 μs. High-emission quantum yields[9] and strong oxidizing and reducing capabilities[10] are further key characteristics. Ru(II) dendrimers have been explored as chromophoric components in light-emitting devices,[11] artificial photosynthesis,[12a] and

*Corresponding author. E-mail: peter.seeberger@mpikg.mpg.de.

(1) (a) Rudd, P. M.; Elliott, T.; Cresswell, P.; Wilson, I. A.; Dwek, R. A. *Science* **2001**, *291*, 2370. (b) Varki, A. *Glycobiology* **1993**, *3*, 97–130. (c) Bertozzi, C. R.; Kiessling, L. L. *Science* **2001**, *291*, 2357. (d) Pilobello, K. T.; Slawek, D. E.; Mahal, L. K. *Proc. Natl. Acad. Sci. U.S.A.* **2007**, *104*, 11534.
(2) (a) Seeberger, P. H.; Werz, D. B. *Nat. Rev. Drug. Discovery* **2005**, *4*, 751. (b) Boonyarattanakalin, S.; Liu, X.; Michieletti, M.; Lepenies, B.; Seeberger, P. H. *J. Am. Chem. Soc.* **2008**, *130*, 16791. (c) Keding, S. J; Danishefsky, S. J. *Proc. Natl. Acad. Sci. U.S.A.* **2004**, *101*, 11937.
(3) (a) Chen, S.; LaRoche, T.; Hamelinck, D.; Bergsma, D.; Brenner, D.; Simeone, D.; Brand, R. E.; Haab, B. B. *Nat. Methods* **2007**, *4*, 437. (b) Chen, S.; Haab, B. B. *Clin. Proteomics* **2008**, 101. (c) Lekka, M.; Laidler, P.; Labedz, M.; Kulik, A. J.; Lekki, J.; Zajac, W.; Stachura, Z. *Chem. Biol.* **2006**, *13*, 505.
(4) (a) Hsu, K.-L.; Mahal, L. K. *Nat. Protoc.* **2006**, *1*, 543. (b) Horlacher, T.; Seeberger, P. H. *Chem. Soc. Rev.* **2008**, *37*, 1414. (c) Dai, Z.; Kawde, A.-N.; Xiang, Y.; La Belle, J. T.; Gerlach, J.; Bhavanandan, V. P.; Joshi, L.; Wang, J. *J. Am. Chem. Soc.* **2006**, *128*, 10018. (d) Pei, Y.; Yu, H.; Pei, Z.; Theurer, M.; Ammer, C.; Andre, S; Gabius, H.-J.; Yan, M.; Ramstrom, O. *Anal. Chem.* **2007**, *79*, 6897.
(5) (a) Gomez-Garcia, M.; Benito, J. M.; Rodriguez-Lucena, D.; Yu, J.-X.; Chmurski, K.; Mellet, C. O.; Gallego, R. G.; Maestre, A.; Defaye, J.; Fernandez, J. M. G. *J. Am. Chem. Soc.* **2005**, *127*, 7970. (b) Benito, J. M.; Gomez-Garcia, M.; Ortiz Mellet, C.; Baussanne, I.; Dafaye, J.; Fernandez, J. M.G. *J. Am. Chem. Soc.* **2004**, *126*, 10355. (c) Mellet, C. O.; Defaye, J.; Fernandez, J. M. G. *Chem.−Eur. J.* **2002**, *8*, 1982. (d) Fulton, D. A.; Stoddart, J. F. *Bioconjugate Chem.* **2001**, *12*, 655.
(6) (a) De Paz, J. L.; Noti, C.; Boehm, F.; Werner, S.; Seeberger, P. H. *Chem. Biol.* **2007**, *14*, 879. (b) Kikeri, R.; Hossain, L. H.; Seeberger, P. H. *Chem. Commun.* **2008**, 2127. (c) Kikkeri, R.; Garcia-Rubio, I.; Seeberger, P. H. *Chem. Commun.* **2009**, 235.
(7) (a) Huang, C.-C.; Chen, C.-T.; Shiang, Y.-C.; Lin, Z.-H.; Chang, H.-T. *Anal. Chem.* **2009**, *81*, 875. (b) Gao, J.; Liu, D.; Wang, Z. *Anal. Chem.* **2008**, *80*, 8822. (c) Lyu, Y.-K.; Lim, K.-R.; Lee, B. Y.; Kim, K. S.; Lee, W.-Y. *Chem. Commun.* **2008**, *39*, 4771. (d) Lin, C.-C.; Yeh, Y.-C.; Yang, C.-Y.; Chen, C.-L.; Chen, G.-F.; Chen, C.-C.; Wu, Y.-C. *J. Am. Chem. Soc.* **2002**, *124*, 3508.
(8) (a) Otsuka, H.; Akiyama, Y.; Nagasaki, Y.; Kataoka, K. *J. Am. Chem. Soc.* **2001**, *123*, 8226. (b) Kikeri, R.; Lepenies, B.; Adibekian, A.; Laurino, P.; Seeberger, P. H., *J. Am. Chem. Soc.* 2009, **2009**, *131*, 2110.
(9) (a) Voegtle, F.; Plevoets, M.; Nieger, M.; Azzellini, G. C.; Credi, A.; De Cola, L.; De Marchis, V.; Venturi, M.; Balzani, V. *J. Am. Chem. Soc.* **1999**, *121*, 6290. (b) Takashima, H.; Shinkai, S.; Hamachi, I. *Chem. Commun.* **1999**, *23*, 2345.
(10) Wang, J.; Fang, Y.-Q.; Bourget-Merle, L.; Polson, M. I.; Garry, S.; Juris, A.; Loiseau, F.; Campagna, S. *Chem.−Eur. J.* **2006**, *12*, 8539.
(11) Rusak, D. A.; James, W. H., III; Ferzola, M. J.; Stefanski, M. J. *J. Chem. Educ.* **2006**, *83*, 1857.
(12) (a) Hu, Y.-Z.; Tsukiji, S.; Shinkai, S.; Oishi, S.; Hamachi, I. *J. Am. Chem. Soc.* **2000**, *122*, 241. (b) Weh, J.; Duerkop, A.; Wolfbeis, O. S. *ChemBioChem* **2007**, *8*, 122.

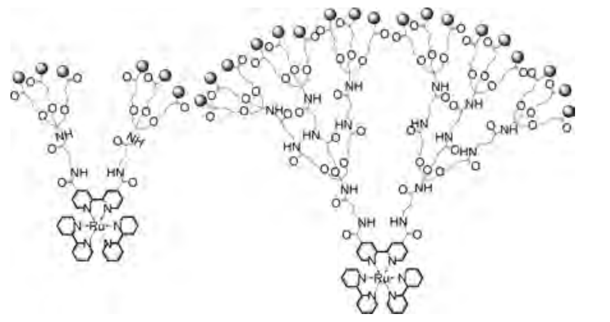

Figure 1. Mannose- and galactose-capped Ru(II)-based glycodendrimers.

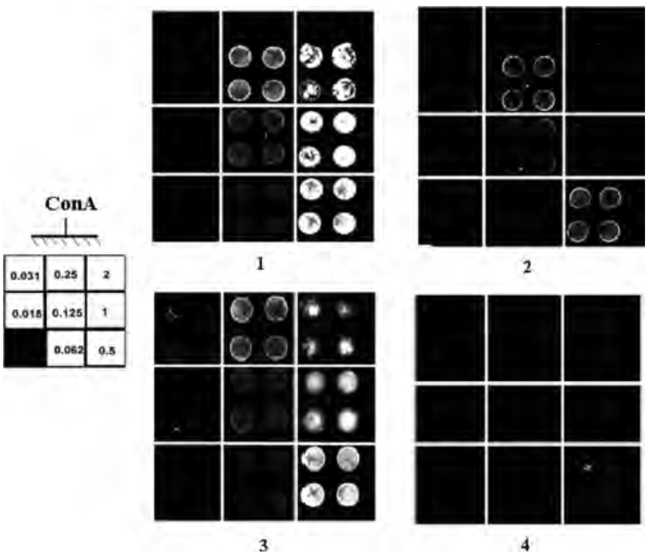

Figure 2. Incubation of Ru(II) dendrimers **1**−**4** with protein microarrays that contain different concentrations (mg/mL) of lectin ConA (excitation at 480 nm).

immunoassay[12b] and as chemosensors for phosphate,[13] oxygen,[14] and glucose.[15] Monolayers of Ru(II)-confined complexes may serve as components for memory devices and molecular switches and sensors[16] as well as electrochemical sensors for oxygen and DNA damage.[17]

Here, we report the use of robust ruthenium(II) bipyridine glycodendrimers as stable fluorescent and electrochemical probes to detect lectin−carbohydrate interactions on microarrays and gold substrates. The prototypical concanavalin A (ConA)−mannose interaction serves as a model to illustrate the new approach.

Displacement of the redox-active Ru(II) complex by mannose, dimannose, trimannose, and phosphatidylinositol mannosides (PIMs) from surface-immobilized lectin quenches the electrochemical signal. Simplicity and sensor regeneration render this method attractive for monitoring even complex sugars at the micromolar level.

(13) Aoki, S.; Zulkefeli, M.; Shiro, M.; Kohsako, M.; Takeda, K.; Kimura, E. *J. Am. Chem. Soc.* **2005**, *127*, 9129.
(14) Lei, B.; Li, B.; Zhang, H.; Lu, S.; Zheng, Z.; Li, W.; Wang, Y. *Adv. Funct. Mater.* **2006**, *16*, 1883.
(15) Murtaza, Z.; Tolosa, L.; Harms, P.; Lakowicz, J. R. *J. Fluoresc.* **2002**, *12*, 187.
(16) (a) Shukla, A. D.; Das, A.; Van der Boom, M. E. *Angew. Chem., Int. Ed.* **2005**, *44*, 3237. (b) Gupta, T.; van der Boom, M. E. *Angew. Chem., Int. Ed.* **2008**, *120*, 2292. (c) Gulino, A.; Gupta, T.; Mineo, P. G.; Van der Boom, M. E. *Chem. Commun.* **2007**, 4878.
(17) (a) Mugweru, A.; Wang, B.; Rusling, J. *Anal. Chem.* **2004**, *76*, 5557. (b) Janata, J.; Josowicz, M. *Nat. Mater.* **2003**, *2*, 19. (c) Drummond, T. G.; Hill, M. G.; Barton, J. K. *Nat. Biotechnol.* **2003**, *21*, 1192. (d) Lei, B.; Li, B.; Zhang, H.; Zhang, L.; Li, W. *J. Phys. Chem. C* **2007**, *111*, 11291. (e) Aoki, S.; Zulkefeli, M.; Shiro, M.; Kohsako, M.; Takeda, L.; Kimura, E. *J. Am. Chem. Soc.* **2005**, *127*, 9129.

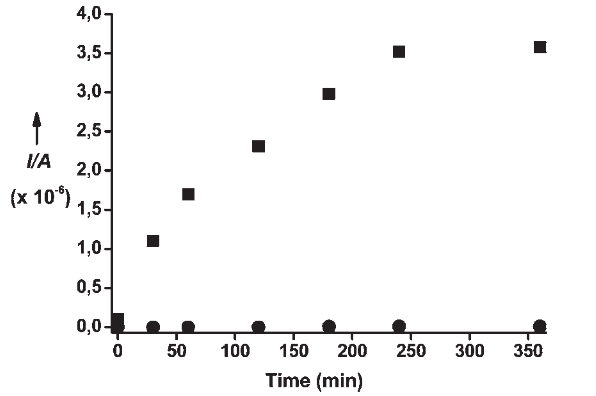

Figure 3. Square-wave voltammetry at 1.14 V following the incubation of complexes **1** (■) and **2** (•) with ConA-functionalized surfaces for 6 h.

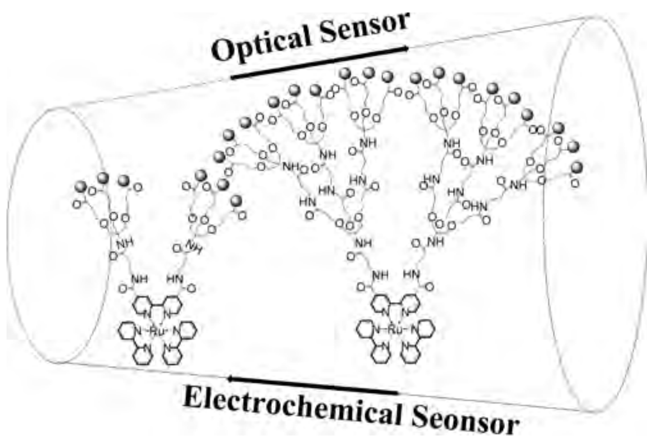

Figure 4. Schematic representation of the optical and electrochemical behavior of complexes **1** and **3**.

Carbohydrate Ru(II) dendrimers **1**−**4** (Figure 1) were prepared using methods that we reported previously.[6c] The photophysical properties of dendrimers **1**−**4** were compared to the reference compound $[Ru(bipy)_3]^{2+}$. The UV−visible spectra of metal dendrimers **1**−**4** in methanol show the characteristic metal-to-ligand charge-transfer band (MLCT) at around 450−500 nm and the intense ligand center (LC) absorption at around 300 nm. The MLCT absorptions of **1**−**4** show a bathochromic shift when compared to $[Ru(bipy)_3]^{2+}$ because of the presence of the electron-withdrawing amide groups on the bipyridines (Figure S2). The emission properties of all compounds exhibit the characteristic luminescence of the triplet metal-to-ligand charge-transfer (MLCT) excited state of the $[Ru(bipy)_3]^{2+}$ core. Minor differences related to different chemical compositions can be noted. Complexes **1**−**4** show a bathochromic shift of 30 nm compared to the reference complex due to an electron-withdrawing group on the bipyridine moiety (Figure S3). Quantum yields of all compounds were calculated by using a standard formula with $[Ru(bipy)_3]Cl_2$ as a reference. Quantum yields of complexes **1** and **2** are nearly half the value of that for **3** and **4**. This alteration in photophysical properties may be due to differences in sugar density around the ruthenium(II) core. The cyclic voltammetric (CV) response in acetonitrile using a glassy carbon (GC) electrode for **1**−**4** showed a single, metal-centered, one-electron redox process. The electrochemical behavior was similar to that of $[Ru(bipy)_3]Cl_2$ and related complexes. The redox process is

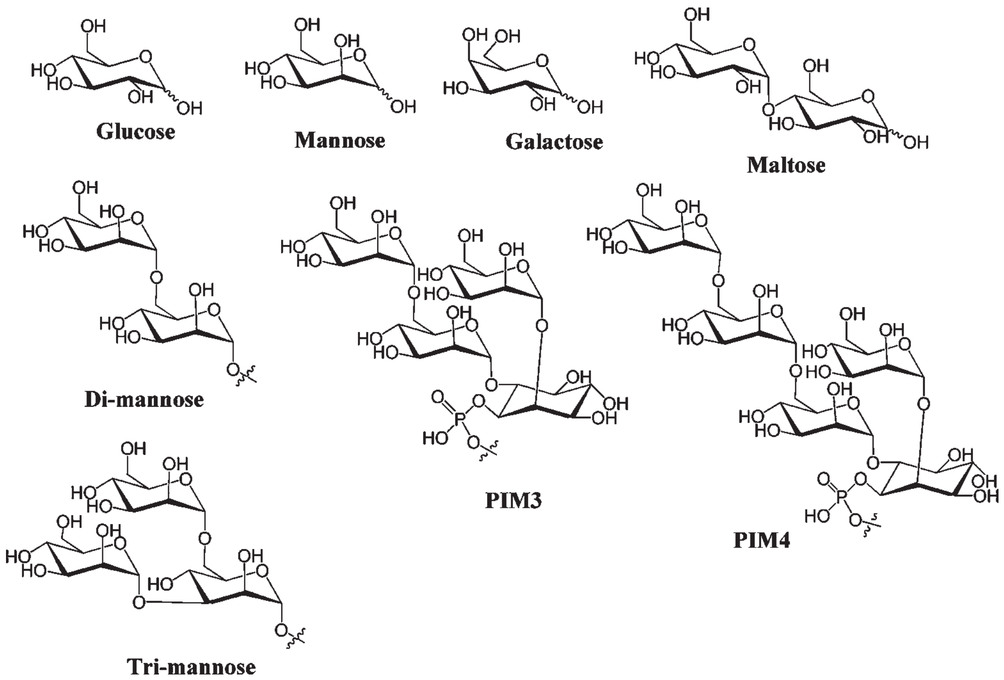

Figure 5. Structures of carbohydrates used for sensing.

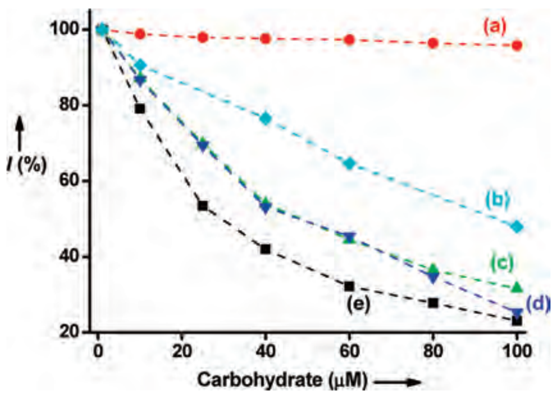

Figure 6. Response of square-wave voltammetric signals to increasing concentrations of (i) (a) D-galactose (red ●), (b) D-glucose (blue ♦), (c) D-maltose (green ▲), (d) D-mannose (blue ▲), and (e) α-D-man-(1→6)man (■).

electrochemically reversible with an $i_p^a/i_p^c \approx 1$ and $E_p^c - E_p^a \approx 80$ mV. In the case of **1**, $E_{1/2}(+2/+3) = +1.32$ V versus Ag/AgCl and 0.47 V versus Fc/Fc^+. The oxidation of $[Ru(bipy)_3]^{2+}$ occurs at a lower potential [$E_{1/2}(+2/+3) = 0.881$ V versus Fc/Fc^+ in acetonitrile], indicating that sugar substitution increases the electron-withdrawing nature of the bipyridyl groups.

Mannose-binding lectin ConA was immobilized on a microarray prior to incubation with complexes **1**−**4** (100 μM solution for 30 min), and $[Ru(bipy)_3](NO_3)_2$ served as a control. Upon fluorescence scanning of rinsed slides, strong fluorescence signals were observed on slides that were incubated with mannose complexes **1** and **3**. At high ConA concentrations (e.g., 2 mg/mL), the microarray spots appeared to be heterogeneous on the array surfaces. Protein aggregation may result in poor fluorescence. Using dendrimers **1** and **3** that contain 6 and 18 mannoses, respectively, ConA was detected at 0.125 mg/mL (620 nM). ConA does not bind galactose. Therefore, as expected, dendrimers **2** adorned with galactose showed weak nonspecific binding at high concentrations, but **4** did not show any fluorescence (Figure 2). These initial experiments demonstrated that mannose complex **3** is a more selective optical probe for lectins than **1** (Table S2).

After establishing that Ru(II) glycodendrimers can be detected visually, we wanted to establish that this detection system can also be utilized for the electrochemical detection of protein−carbohydrate interactions. ConA was immobilized on a self-assembled monolayer on a gold surface[18] prior to incubating these surfaces with Ru(II) complexes **1**−**4** or the control $[Ru(bipy)_3](Cl)_2$ for 30 min. Following incubation, the chip was transferred to a electrochemical cell containing phosphate buffer. The scanning potential of 100 mV/s in the region of 1.0−1.4 V shows a peak at 1.62 μA (Figures S7a and S8a). Repeated measurements revealed that maximal ConA/Ru(II)−complex interactions were reached after 240 min of incubation (Figure 3). Neither galactose-bearing dendrimers **2** and **4** nor $[Ru(bipy)_3](Cl)_2$ bound ConA. Interestingly, the incubation of complex **3** carrying 18 mannoses with ConA monolayers showed a very weak signal in the region of 1.0−1.4 V. An optimum current at 4.1 nA was obtained after 180 min of incubation (Figures S7b and S8b). On the basis of these findings, complex **1** is better suited for electrochemical sensing than the more complex dendrimer **3** (Figure 4).

After establishing that the lectin−glycodendrimer interactions can be measured electrochemically, we determined the detection limit when using dendrimer **1**. Different concentrations of ConA were immobilized on gold substrates and treated with 0.5 mM **1** prior to recording square-wave voltammetric (SWV) signals (Figures S9 and S10). At 2.5 nM, the detection limit for **1** is comparable to other sensors.[6c,7a,19]

Replacement of the glycodendrimer from the lectin-functionalized gold chips should allow for the detection of any sugar that is bound by the lectin. ConA-functionalized gold chips containing **1** were immersed in solutions containing varying concentrations of D-glucose, D-mannose, α-D-man-(1→6)man, D-galactose, D-maltose, or PIM glycans (Figure 5) before SWV signals for Ru(II)

(18) Ahamed, T.; Barbara, H.; Andrea, V.; Frederic, A. D.; Yves, F. D. *Langmuir* **2003**, *19*, 1745.
(19) Guo, C.; Boullanger, P.; Jiang, L.; Liu, T. *Biosens. Bioelectron.* **2007**, *22*, 1830.

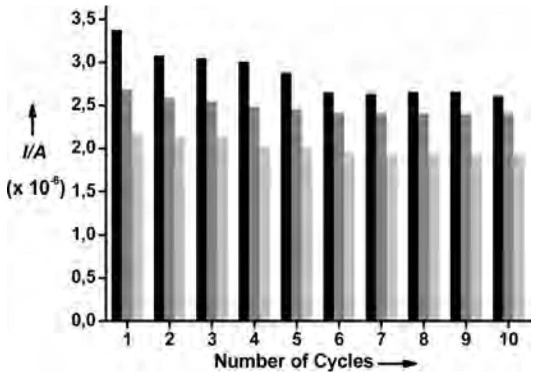

Figure 7. Maximum current signal upon regeneration of the ConA/**1** glucose detector: complex **1** on a gold substrate (black), addition of 40 μM D-glucose (gray), and addition of 80 μM D-glucose (light gray).

Scheme 1. Schematic Representation of the Ru(II)−Sugar Complex Interaction with the Lectin ConA that is Immobilized on a Gold Surface/Microarray for Use as a Sugar Sensor[a]

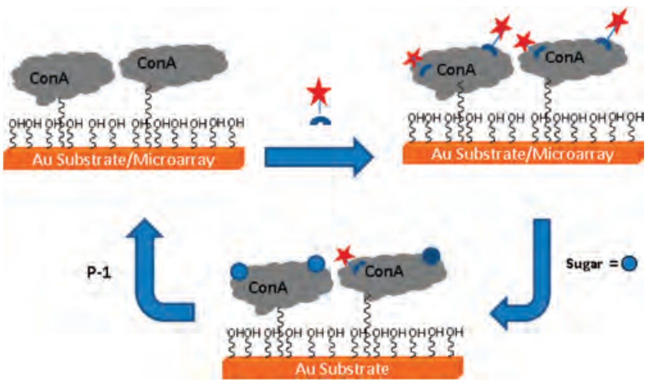

[a] P-1 represents the boronic acid-substituted polymer.

were recorded (Figures 6 and S11). The current decreased in a concentration-dependent manner, indicating that redox-active complex **1** is replaced in a competitive manner by the preferentially binding carbohydrate. The detection limit for glucose of 7 μM[20] compares favorably with the detection limits for other methods that are in the micromolar range.[21]

Increasing concentrations of D-mannose and disaccharide D-maltose resulted in a rapid concentration-dependent decrease in the current. The detection limit for these two sugars was in the range of 3 μM. Disaccharide α-D-man-(1→6)man was displaced most rapidly with a detection limit of 1.4 μM (Figure 6). More complex oligosaccharides trimannose, PIM3, and PIM4 rapidly quenched the electrochemical signal up to 25 μM, followed by a slowing decrease at higher concentrations. Detection limits of 0.61, 1.4, and 0.63 μM for these three mannose-containing structures were calculated (Figures S11, S12, and S13). Rapid

Table 1. Photophysical Properties of Complexes 1−4

compound	λ_{max} (nm)	τ (μs)	Φ	$E_{1/2}$ (V)
1	643	0.61	0.072	+1.32
2	643	0.63	0.071	+1.32
3	645	1.26	0.062	+1.35
4	645	1.27	0.112	+1.34
$[Ru(bipy)_3]Cl_2$	613	0.54	0.115	+0.88

quenching can be interpreted as the simultaneous displacement of weakly bound complex **1** from immobilized ConA and a high affinity of the sugar for lectin. The trend in sensitivity, PIM4 > Triman > PIM3 > α-D-man-(1→6)man > Man ≥ Mal > Glu, is consistent with the binding affinity of these glycans to ConA.[22]

Ideally, sensors can be regenerated for repeated use. Glucose served to demonstrate the regeneration of the lectin−glycodendrimer sensing platform. A gold chip exposed to 100 μM D-glucose solution was incubated with boronic acid-substituted Merrifield resin (P-1, Supporting Information)[23] for 5 min to displace any sugar attached to the immobilized ConA. Incubation with complex **1** regenerated the surface for the next measurement. To verify the quality of the readings after regenerating the electrochemical detector, the chip was exposed to solutions containing 40 and 80 μM D-glucose. The platform was regenerated 10 times using this reiterative process (Figure 7). The SWV signal decreases over the first six cycles and then remains constant for the last four regeneration cycles. Deactivation or effective hosting of glucose by ConA may be responsible for the observed decrease in the electrochemical signal after each cycle.

In conclusion, we have demonstrated that tris-bipyridyl ruthenium glycodendrimers containing defined numbers of carbohydrates enable the direct optical and electrochemical detection of carbohydrate-binding proteins at the nanomolar level. Using surface-immobilized lectin−glycodendrimer complexes, we have developed a sensitive, continuous, and inexpensive electrochemical biosensor. The sensitivity of the sensor depends on the lectin that is employed. Using ConA, we detected D-mannose, D-glucose, D-maltose, α-D-Man-(1→6)Man, PIM3, and PIM4 even at low levels. The sensitive detection of PIMs illustrates the new approach that couples the specificity of lectin−carbohydrate interactions with the sensitivity and convenience of an electrochemical readout. Regeneration of the gold substrate for continuous sugar sensing renders this detection method potentially useful for detecting bacteria and eukaryotic cells as well as any glycoconjugate. Microarrays containing multiple lectin−glycodendrimer complexes for the high-throughput detection of different sugars on a single platform are currently under investigation.

Acknowledgment. We thank the ETH Zurich, CCMX, TRF Grant MRG5180240 (fund to S.B.) and EMBO (fellowship to F.K.) for financial support.

Supporting Information Available: NMR spectral copies of all new compounds and additional related experimental procedures. This material is available free of charge via the Internet at http://pubs.acs.org.

(20) (a) Miller, J. N. *Analyst* **1991**, *116*, 3. (b) Ingle, J. D.; Wilson, A. L. *Anal. Chem.* **1976**, *48*, 1641.
(21) (a) Takahashi, S.; Anzai, J. *Sens. Lett.* **2005**, *3*, 244. (b) Sato, K.; Kodama, D.; Anzai, J.-I. *Anal. Bioanal. Chem.* **2006**, *386*, 1899. (c) Sato, K.; Imoto, Y.; Sugama, J.; Seki, S.; Inoue, H.; Odagiri, T.; Hoshi, T.; Anazai, J.-I. *Langmuir* **2005**, *21*, 797. (d) Xiao, Y.; Patolsky, F.; Katz, E.; Hainfeld, J. F.; Willner, I. *Science* **2003**, *299*, 1877. (e) Zayats, M.; Katz, E.; Baron, R. *J. Am. Chem. Soc.* **2005**, *127*, 12400. (f) Bahshi, L.; Frasconi, M.; Telvered, R.; Yehezkeli, O.; Willner, I. *Anal. Chem.* **2008**, *80*, 8253. (g) Malitesta, C.; Losito, L.; Zambonin, P. G. *Anal. Chem.* **1999**, *71*, 1366. (h) Jazkumar, d. R. S.; Narayanan, S. S. *Carbon* **2009**, *47*, 957.
(22) (a) Schwarz, F. P.; Puri, K. D.; Bhat, R. G.; Surolia, A. *J. Biol. Chem.* **1993**, *268*, 7668. (b) Hasegawa, T.; Yonemara, T.; Matasuura, K.; Kobayashi, K. *Bioconjugate Chem.* **2003**, *14*, 728.
(23) (a) Abed, O.; Wanunu, M.; Vaskevich, A.; Arad-Yellin, R.; Shanzer, A.; Rubinstein, I. *Chem. Mater.* **2006**, *18*, 1247. (b) Abed, O.; Vaskevich, A.; Arad-Yellin, R.; Shanzer, A.; Rubinstein, I. *Chem.−Eur. J.* **2005**, *11*, 2836.

Ru(II)-Glycodendrimers as Probes to Study Lectin-Carbohydrate Interactions and Electrochemically Measure Mono- and Oligosaccharide Concentrations

Raghavendra Kikkeri,[†,¶] *Faustin Kamena,* [†,¶] *Tarkeshwar Gupta,*[±] *Laila H. Hossain,*[†] *Siwarutt Boonyarattanakalin,* [Φ] *Ganna Gorodyska,*[£] *Eva Beurer,* [£] *Géraldine Coullerez,* [£] *Marcus Textor* [£] *and Peter H. Seeberger*[†,¶ *]

[†]Laboratory for Surface Science and Technology, Dept. of Organic Chemistry, ETH Zurich, Wolfgang-Pauli-Str. 10, 8093, Zurich, Switzerland.

[¶]Current Address: Max-Planck-Institute of Colloids and Interfaces, Department of Biomolecular Systems, Research Campus Golm, Am Mühlenberg 1, 14476 Potsdam, Germany.

[£]Laboratory for Surface Science and Technology, Dept. of Materials, ETH Zurich, Wolfgang-Pauli-Str. 10, 8093, Zurich, Switzerland.

[±]Department of Chemistry, University of California, Berkeley, CA 94720-1460, USA.

[Φ]Sirindhorn International Institute of Technology, Thammasat University, P. O. Box 22 Thammasat-rangsit Post Office, Pathumthani 12121, Thailand.

Supporting Information

Table of Contents:

7. **References**

1. General Information

All chemicals used were reagent grade and used as supplied except where noted. Dichloromethane (CH_2Cl_2) was purified by a Cycle-Tainer Solvent Delivery System. Triethylamine was distilled over CaH_2 prior to use. Analytical thin layer chromatography (TLC) was performed on Merck silica gel 60 F_{254} plates (0.25 mm). Compounds were visualized by UV irradiation or dipping the plate in CAN solution followed by heating. Flash column chromatography was carried out using force flow of the indicated solvent on Fluka Kieselgel 60 (230-400 mesh).

^{1}H and ^{13}C NMR spectra were recorded on a Varian VXR-300 (300 MHz) or Bruker DRX500 (500 MHz) spectrometer. High-resolution mass spectra (HR MALDI MS) were performed by the Mass Spectrometry-service at the Laboratory for Organic Chemistry (ETH Zurich). ESI-MS were run on an Agilent 1100 Series LC/MSD instrument. IR spectra were recorded on a Perkin-Elmer 1600 FTIR spectrometer. Optical rotation measurements were conducted using a Perkin-Elmer 241 polarimeter.

$RuCl_3 \cdot x\ H_2O$ and 2,3,4,5,6-pentafluorophenol were purchased from Fluka. Acrylonitrile was purchased from Alfa Aesar and used directly in the reaction. ConcanavalinA was purchased from Appli Chem (Axon Lab AG). Slides were scanned using a LS400 scanner from Tecan and quantified using Scan Array Express Software. Absorption spectra were recorded using a Varian CARY 50 spectrophotometer fitted with Hellma optical fibers (Hellma, 041.002-UV) and an immersion probe made of quartz suprazil (Hellma, 661.500-QX). Fluorescence emission spectra were recorded on a Perkin-Elmer LS-50B spectrofluorometer. Confocal microscopy was performed on a SP1 Leica confocal microscope (Leica Germany). Synthesis of 2,2'-bipyridine-4,4'-dicarboxylic acid and *cis*-$Ru(bipy)_2Cl_2$ was carried out as described previously.[1]

2. Synthesis of Complexes 2 and 4

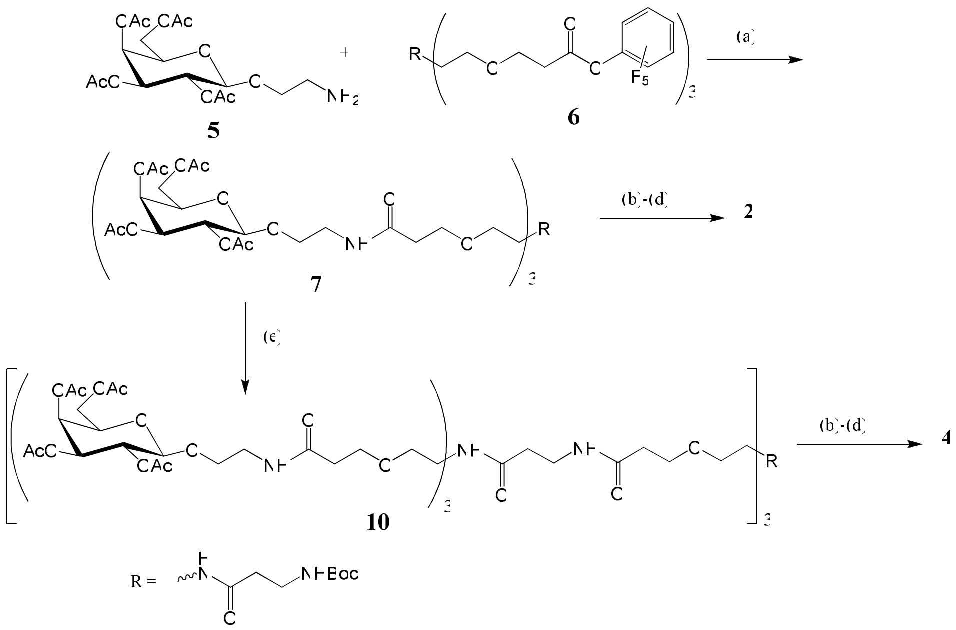

Fig S1. Synthesis of Ru(II)-bispyridyl dendrimers **2** and **4**. (a) TEA/DCM, 12 h, 52% (b) TFA, 2,2'-bipyridine 4,4'-dicarboxylic acyl chloride, DCM, TEA, 12 h, 35% (c) *cis*-Ru(bipy)$_2$Cl$_2$, EtOH, 6 h, 52% (d) NaOMe, MeOH, 2 h, 65% (e) **6**, TEA, DCM, 12 h, 52%

General Procedure A: Synthesis of Sugar-tripods: The Boc-protected amino-sugar (4.0 eq) was dissolved in 10 mL dichloromethane/trifluoroacetic acid (3:1) and stirred at room temperature for 1 h. The solvent was evaporated under reduced pressure and the resulting oil was dissolved in anhydrous dichloromethane (20 mL). To this mixture, was added *tert*-butoxycarbonyl-3-{*N*-{tris[3-[pentafluoro-phenyl-carboxyl-ethoxy)methyl]} methyl amine}-3-*β*-alanine (1.0 eq), the pH was adjusted to 8 with triethylamine (TEA) and the mixture was stirred at room temperature for 12 h. The solvent was evaporated *in vacuo* and purified by flash silica column chromatography.

General Procedure B: Synthesis of Bipyridine Derivatives: 2,2'Bipyridine-4,4'-dicarboxylic acid (1.0 eq) was dissolved in SOCl$_2$ (1 mL) and refluxed under nitrogen for 12 h. Excess SOCl$_2$ was removed in *vacuo* and the crude 2,2'bipyridine-4,4'-dicarboxylic acyl chloride was used directly in the next step. Boc-protected amino-sugar-tripod (3.0 eq) was dissolved dichloromethane/trifluoroacetic acid (10 mL, 3:1 resp.) and stirred at room temperature for 1 h. The mixture was concentrated *in vacuo* and then redissolved in dichloromethane (20 mL). To this mixture was added 2,2'bipyridine-4,4'-dicarboxylic acyl chloride (1 eq) and the pH adjusted using TEA to pH 8. The reaction mixture was stirred for 12 h, the solvent removed *in vacuo* and the mixture purified by silica column flash chromatography.

General Procedure C: Synthesis of Ruthenium(II)-Complexes: The bipyridine-sugar derivative (1.0 eq) and *cis*-ruthenium(II)bis(bipyridine)dichloride (1.1 eq) were dissolved in de-oxygenated ethanol (30 mL) and the mixture was refluxed for 6-8 h. The compound was then purified by silica column flash chromatography.

General Procedure D: Synthesis of Ruthenium(II)-sugar Complexes: Ruthenium(II) complex (1.0 eq) and sodium methoxide (0.2 eq) were dissolved in methanol (10 mL) and stirred at room temperature for 2 h. The solvent was then evaporated *in vacuo*, the residue was redissolved in water and dialyzed against water using 500 molecular weight cut-off resin. After two days of dialysis, the sample was lyophilized.

***tert*-Butoxycarbonyl-3-{tris[3-[2-ethoxy-2,3,4,6-tetra-*O*-acetyl-*β*-D-galactopyranoside-ethoxy]methyl]methylamide}-3-*β*-alanine (7).** General procedure A with 2-(*tert*-butoxycarbonylamino)ethoxy-2,3,4,6-tetra-*O*-acetyl-*β*-D-galactopyranoside **5** (0.85 g, 1.73 mmol), *tert*-butoxycarbonyl-3-{*N*-{tris[3-[pentafluoro-phenyl-carboxyl-ethoxy)methyl]}methyl amine}-3-*β*-alanine **6** (0.43 g, 0.43 mmol) and flash silica column chromatography yielded *tert*-butoxycarbonyl-3-{tris[3-[2-ethoxy-2,3,4,6-tetra-*O*-acetyl-*β*-D-galactopyranoside-ethoxy]methyl]methylamide}-3-*β*-alanine (0.26 g, 52%). R_f = 0.45 (CH_2Cl_2/MeOH, 93:7); $[\alpha]_D^{r.t}$ = +10.2 (c =1.0, $CHCl_3$); ^{1}H NMR (300 MHz, $CDCl_3$): δ 6.90 (br.s, 1H), 6.47 (br.s, 3H), 5.37 (d, J = 3.3 Hz, 4H), 5.14 (t, J = 7.8 Hz, 3H), 4.99 (dd, J = 3.3, 4.2 Hz, 3H), 4.49 (d, J = 7.8 Hz, 3H), 4.12-4.10 (m, 6H), 3.92 (t, J = 6.2 Hz, 3H), 3.84-3.83 (m, 3H), 3.70 (t, J = 5.4 Hz, 8H), 3.65 (s, 9H), 3.42 (t, J = 5.7 Hz, 6H), 3.33 (q, J =

5.7 Hz, 2H), 2.39 (t, *J* = 5.4 Hz, 6H), 2.14 (s, 9H), 2.04 (s, 9H), 2.02 (s, 9H), 1.96 (s, 9H), 1.40 (s, 9H), ^{13}C NMR (75 MHz, $CDCl_3$): *δ* 171.1, 170.0, 169.8, 169.7, 155.7, 101.1, 70.6, 69.1, 68.7, 67.2, 67.0, 66.9, 61.2, 59.7, 45.65, 41.67, 39.1, 37.0, 36.4, 28.3, 20.6; FTIR($CHCl_3$): 3343, 2945, 1751, 1560, 1458, 1350 cm^{-1}; HRMS (MALDI-ToF) (*m/z*): $[M+Na]^+$ calcd. for $C_{69}H_{105}N_5O_{39}Na$ 1650.6284; found: 1650.6252.

(v) 1,1'-(2,2'-Bipyridine-4,4'-diyl)bis-3-*β*-propane-{-3-{tris[3-[2-ethoxy-2,3,4,6-tetra-*O*-acetyl-*β*-D-galactopyranoside-ethoxy]methyl]methylamide (8). General procedure B with *tert*-butoxycarbonyl-3-{tris[3-[2-ethoxy-2,3,4,6-tetra-*O*-acetyl-*α*-D-galactopyranoside-ethoxy]methyl]methylamide}-3-*β*-alanine **7** (0.25 g, 0.15 mmol), 2,2'bipyridine-4,4'-dicarboxylic acid (12.5 mg, 0.52 mmol) and flash silica column chromatography yielded 1,1'-(2,2'-bipyridine-4,4'-diyl)bis-3-beta-propane-{-3-{tris[3-[2-ethoxy-2,3,4,6-tetra-*O*-acetyl-*β*-D-galactopyranoside-ethoxy] methyl]methylamide (96 mg, 35%). R_f = 0.5 (CH_2Cl_2/MeOH, 92:8); $[\alpha]_D^{r.t}$ = +12.8 (c = 1.0, $CHCl_3$); ^{1}H NMR (300 MHz, $CDCl_3$): *δ* 8.85 (d, *J* = 4.5 Hz, 2H), 8.85 (br.s, 2H), 7.83 (d, *J* = 4.5 Hz, 2H), 5.24 (d, *J* = 3.6 Hz, 6H), 5.13-5.10 (m, 14H), 4.68 (d, *J* = 7.2 Hz, 6H), 4.13 (br.s, 24H), 3.85-3.83 (m, 6H), 3.68 (br.s, 29H), 3.42-3.39 (m, 18H), 2.60 (t, *J* = 6.6 Hz, 4H), 2.42 (t, *J* = 5.4 Hz, 12H), 2.13 (s, 18H), 2.05 (s, 18H), 2.01 (s, 18H), 1.94 (s, 18H), ^{13}C NMR (75 MHz, $CDCl_3$): *δ* 173.7, 171.8, 171.0, 170.9, 167.3, 163.3, 162.9, 162.4, 161.9, 155.4, 149.1, 143.5, 125.7, 115.7, 101.8, 71.9, 71.5, 69.9, 69.7, 68.9, 68.4, 68.2, 62.2, 54.4, 40.2, 36.9, 20.2; FTIR($CHCl_3$): 3684, 3489, 1752, 1675, 1454, 1442, 1065 cm^{-1}; HRMS-MALDI: Calcd for $C_{140}H_{197}N_{12}O_{76}Na$ 3286.189; Found : 3286.199.

(vii) *Cis*-Ruthenium(II)bis(bipyridine){1,1'-(2,2'-bipyridine-4,4'-diyl)bis-3-*β*-propane-{tris-[3-4-ethoxy-2,3,4,6-tetra-*O*-acetyl-*β*-D-galactopyranoside-ethoxy}methyl]methylamide (9). General procedure C with 1,1'-(2,2'-bipyridine-4,4'-diyl)bis-3-beta-propane-{tris-[3-4-ethoxy-2,3,4,6-tetra-O-acetyl-β-D-galactopyranoside-ethoxy}methyl]methylamide (90 mg, 0.027 mmol), *cis*-ruthenium(II)bis(bipyridine)dichloride (16 mg, 0.03 mmol) purification by flash silica column chromatography by using acetronitrile/water/saturated KNO_3 (7.5:1:1.5-7:3) as eluent yielded *cis*-ruthenium(II)bis(bipyridine){1,1'-(2,2'-bipyridine-4,4'-diyl)bis-3-beta-propane-{tris-[3-4-ethoxy-2,3,4,6-tetra-*O*-acetyl-*β*-D-galactopyranoside-ethoxy}methyl] methyl amide (48 mg, 52%). R_f = 0.5 (acetonitrile/Sat KNO_3, 80:20); $[\alpha]_D^{r.t}$ = +8.9 (c = 1.0, H_2O); ^1H NMR (300 MHz, CD_3OD): δ 9.16 (s, 2H), 8.72 (d, *J* = 7.1 Hz, 4H), 8.14 (t, *J* = 4.8 Hz, 6H), 8.01 (d, *J* = 5.7 Hz, 4H), 7.92 (t, *J* = 5.4 Hz, 4H), 7.85 (dd, *J* = 5.7, 4.8 Hz, 6H), 7.53 (t, *J* = 4.5 Hz, 4H), 7.30 (br.s, 1H), 5.37 (d, *J* = 3.0 Hz, 6H), 5.13-5.08 (m, 14H), 4.71 (d, *J* = 4.5 Hz, 6H), 4.13 (br.s, 18H), 3.88-3.85 (m, 6H), 3.65 (br.s, 36H), 3.37 (t, *J* = 4.2 Hz, 9H), 2.62 (t, *J* = 6.3 Hz, 4H), 2.41 (t, *J* = 5.1 Hz, 12H), 2.12 (s, 18H), 2.05 (s, 18H), 2.00 (s, 18H), 1.95 (s, 18H), ^{13}C NMR (75 MHz, CD_3OD): δ 173.5, 173.1, 171.6, 171.4, 170.8, 165.2, 162.8, 158.5, 157.7, 153.0, 151.7, 143.4, 139.1, 132.8, 128.7, 128.4, 125.3, 101.8, 72.0. 71.5, 70.0, 69.6, 69.0, 68.5, 68.3, 62.3, 61.3, 59.5,54.5, 40.3, 38.2, 36.7, 20.4; HRMS-MALDI (*m/z*): Calcd for $C_{160}H_{215}N_{16}O_{76}Ru$ 3677.242; Found: 3678.244.

(viii) *Cis*-Ruthenium(II)bis(bipyridine){1,1'-(2,2'-bipyridine-4,4'-diyl)bis-3-*β*-propane-{tris-[3-4-ethoxy-*β*-D-galactopyranosyl-ethoxy}methyl] methyl amide (2). General procedure D with *cis*-ruthenium(II)bis(bipyridine){1,1'-(2,2'-bipyridine-4,4'-diyl)bis-3-β-propane-{tris-[3-4-ethoxy-2,3,4,6-tetra-*O*-acetyl-*β*-D-galactopyranoside-ethoxy}methyl]methylamide (42 mg, 11.3 μmol) sodium methoxide (10 mg, 2.2 μmol) yielded 17 mg, (65%) of *cis*-ruthenium(II)bis(bipyridine){1,1'-(2,2'-bipyridine-4,4'-diyl)bis-3-*β*-beta-propane-{tris-[3-4-ethoxy-*β*-D-galactopyranosyl-ethoxy}methyl] methylamide. $[\alpha]_D^{r.t}$ = +1.8 (c = 1.0, H_2O); ^1H NMR (300 MHz, D_2O/MeOD): δ 8.95 (br.s, 2H), 8.56 (d, *J* = 7.8 Hz, 4H), 8.04 (dd, *J* = 7.8, 6.0 Hz, 6H), 7.70 (t, *J* = 5.4 Hz, 4H), 7.65 (d, *J* = 6.0 Hz, 2H), 7.39 (t, *J* = 6.0 Hz, 4H), 4.36 (d, *J* = 7.8 Hz, 6H), 3.96-3.94 (m, 4H), 3.90 (d, *J* = 2.7 Hz, 12H), 3.75-3.65 (m, 34H), 3.61 (br.s, 24H), 3.49-3.46 (m, 12H), 3.43-3.41 (m, 2H), 2.57 (t, *J* = 6.0 Hz, 4H), 2.35 (t, *J* = 5.7 Hz, 12H), ^{13}C NMR (125 MHz, CD_3OD): δ 181.7. 174.9, 173.2, 172.6, 158.6. 157.9, 152.1, 138.6, 131.6, 129.2, 126.7, 122.4, 110.8, 104.3, 77.8, 73.5, 71.8, 71.8, 68.5, 67.6, 66.6, 62.4, 61.4, 40.0, 37.3, MALDI-ToF (*m/z*): [M-1]$^+$ Calcd for $C_{112}H1_{166}N_{16}O_{52}Ru$ 2668.988; Found: 2667.978.

(i) *tert*-Butoxycarbonyl-3-{tris[3-carboxyl ethoxy]methyl] 3'-{tris[2'-ethoxy-2,3,4,6-tetra-*O*-acetyl-β-D-galactopyranoside-ethoxy]methyl]methylamide}-3-β-alanine (10). General procedure A with *tert*-butoxycarbonyl-3-{tris[3-[2-ethoxy-2,3,4,6-tetra-*O*-acetyl-β-D-galactopyranoside-ethoxy]methyl]methylamide}-3-β-alanine (0.45 g, 0.27 mmol), *tert*-butoxycarbonyl-3-{*N*-{tris[3-[pentafluoro phenyl carboxyl-ethoxy)methyl]}methylamine}-3-β-alanine (92 mg, 0.091 mmol) and flash silica column chromatography by CH_2Cl_2/CH_3OH (12-13%) as eluent yielded 0.26 g (52%) of *tert*-butoxycarbonyl-3-{tris[3-carboxylethoxy]methyl]3'-{tris[2'-ethoxy-2,3,4,6-tetra-*O*-acetyl-β-D-galactopyranoside-ethoxy]methyl]methylamide}-3-β-alanine. R_f 0.55 (CH_2Cl_2:MeOH = 90:10); $[\alpha]_D^{r.t}$ = +2.7 (c =1.0, $CHCl_3$); ^1H NMR (300 MHz, $CDCl_3$): δ 6.84 (br.s, 1H), 6.63 (br.s, 1H), 5.37 (d, *J* = 3.3 Hz, 9H), 5.12 (t, *J* = 7.8 Hz, 9H), 4.99 (dd, *J* = 3.3, 4.2 Hz, 9H), 4.51-4.45 (m, 9H), 4.14-4.08 (m, 18H), 3.95-3.92 (m, 9H), 3.84-3.78 (m, 9H), 3.66-3.56 (m, 64H), 3.41-3.36 (m, 34H), 2.41 (t, *J* = 5.4 Hz, 32H), 2.14 (s, 27H), 2.04 (s, 27H), 2.02 (s, 27H), 1.96 (s, 27H), 1.41 (s, 9H); ^{13}C NMR (75 MHz, $CDCl_3$): δ171.3, 170.2, 170.0, 169.8, 169.6, 101.2, 70.7, 69.0, 68.9, 68.7, 67.4, 67.3, 67.0, 39.3, 36.4, 28.9, 20.9,FTIR($CHCl_3$): 3385, 3019, 1749, 1658, 1522, 1232, 1205 cm^{-1}; HRMS-MALDI (m/z): [M+ Na]$^+$ Calcd for $C_{215}H_{321}N_{17}O_{120}$ 5036.9538; Found : 5060.9534.

(iii) 1,1'-(2,2'-Bipyridine-4,4'-diyl)bis-3-beta-propane-{*tris*-[3-carboxylethoxy]methyl]3'-{*tris*[2'-ethoxy-2,3,4,6-tetra-*O*-acetyl-β-D-galactopyranoside-ethoxy]methyl]methylamide (11). General procedure B with *tert*-butoxycarbonyl-3-{tris[3-carboxyl ethoxy]methyl]3'-{tris[2'-ethoxy-2,3,4,6-tetra-*O*-acetyl-α-D-galactopyranoside-ethoxy]methyl]methylamide}-3-β-alanine (0.15 g, 0.029 mmol), 2,2'bipyridine-4,4'-dicarboxylic acid (2.4 mg, 0.0098 mmol) and flash silica column chromatography by CH_2Cl_2/CH_3OH (15-16%) as eluent gave 36 mg (14 %) of 1,1'-(2,2'-bipyridine-4,4'-diyl)bis-3-beta-propane-{tris-[3-carboxylethoxy]methyl]3'-{tris[2'-ethoxy-2,3,4,6-tetra-*O*-acetyl-β-D-galactopyranoside-ethoxy]methyl]methylamide. R_f 0.35 (CH_2Cl_2:MeOH =

86:14); $[\alpha]_D^{r.t}$ = +5.8 (c =1.0, $CHCl_3$); ^{1}H NMR (300 MHz, $CDCl_3$): δ 8.85 (d, *J* = 4.5 Hz, 4H), 7.86 (br.s, 2H), 7.24 (br.s, 2H), 5.39 (d, *J* = 3.6 Hz,18H), 5.12-5.07 (m, 48H), 4.68 (d, *J* = 7.2 Hz, 18H), 4.14-4.06 (m, 48H), 3.86-3.81 (m, 18H), 3.68-3.52 (m, 118H), 3.40-3.31(m, 56H), 3.12-3.07 (m, 14H), 2.73 (t, *J* = 5.2 Hz. 2H), 2.45-2.38 (m, 64H), 2.13 (s, 54H), 2.05 (s, 54H), 2.01 (s, 54H), 1.94 (s, 54H); ^{13}C NMR (125MHz, $CDCl_3$): δ 173.5, 171.5, 171.4, 170.9, 163.2, 162.8, 162.3, 161.8, 153.1, 147.6, 144.2, 123.4, 111.8, 101.8, 71.9, 71.6, 70.1, 69.0, 68.5, 68.3, 62.3, 54.6, 39.0, 34.5, 20.5; FTIR($CHCl_3$): 3404, 2944, 2478, 1752, 1680, 1543, 1455, 1405, 1333, 1264, 1232 cm^{-1}; MALDI-HRMS (m/z): $[M+1]^+$ Calcd for $C_{428}H_{630}N_{36}O_{238}$ 10081.8301; Found : 10082.831.

(iv) *Cis*-Ruthenium(II)bis(bipyridine)1,1'-(2,2'-bipyridine-4,4'-diyl)bis-3-beta-propane-{tris-[3-carboxylethoxy]methyl]3'-{tris[2'-ethoxy2,3,4,6-tetra-*O*-acetyl-β-D-galactopyranoside-ethoxy]methyl]methylamide (12). General procedure C with 1,1'-(2,2'-bipyridine-4,4'-diyl)bis-3-beta-propane-{tris-[3-carboxyl-ethoxy]methyl]3'-{tris[2'-ethoxy-2,3,4,6-tetra-*O*-acetyl-β-D-galactopyranoside-ethoxy] methyl]methyl amide (35 mg, 3.47 µmol), ***cis***-ruthenium(II)bis(bipyridine)dichloride (3.4 mg, 6.8 µmol) and flash silica column chromatography by acetronitrile/saturated KNO_3 (7:3) as eluent gave 21 mg (58%) of *cis*-ruthenium(II) bis(bipyridine)1,1'-(2,2'-bipyridine-4,4'-diyl)bis-3-beta-propane-{tris-[3-carboxyl ethoxy]methyl]3'-{tris[2'-ethoxy2,3,4,6-tetra-*O*-acetyl-β-D-galactopyranoside-ethoxy]methyl] methylamide. R_f 0.3 (acetonitrile:Sat KNO_3 = 7.5:2.5); $[\alpha]_D^{r.t}$ = +1.9 (c =1.0, H_2O); ^{1}H NMR (300MHz, CD_3OD): δ = 9.1 (s, 2H), 8.75 (d, *J* = 7.1 Hz, 4H), 8.14 (br.s, 6H), 8.01 (d, *J* = 5.7 Hz, 6H), 7.95-7.92 (m, 6H), 7.85 (br.s, 4H), 7.5 (t, *J* = 4.5 Hz, 4H), 7.30 (br.s, 1H), 5.39 (d, *J* = 3.6 Hz, 18H), 5.12-5.07 (m, 36H), 4.68 (d, *J* = 7.2 Hz, 18H), 4.14 (br.s, 58H), 3.85-3.81 (m, 18H), 3.67-3.57(br, 130H), 3.41-3.36 (m, 51H), 2.43-2.38 (m, 68H), 2.12 (s, 54H), 2.06 (s, 54H), 2.03 (s, 54H), 1.95 (s, 54H); ^{13}C NMR (125MHz, CD_3OD): δ 174.1; 172.0, 171.8, 171.4, 171.3, 165.1, 162.8, 158.5, 157.7, 153.0, 151.7, 143.4, 139.1, 132.8, 128.7, 128.4, 125.3, 103.0, 72.2. 71.7, 70.1, 69.8, 69.1, 68.7, 68.6, 68.5, 62.4,

61.5, 54.7, 40.4, 36.2, 20.5; MALDI-HRMS (m/z): $[M+1]^+$ Calcd for $C_{448}H_{646}N_{40}O_{238}Ru$ 10495.871; Found: 10495.8731.

(v) ***Cis*-Ruthenium(II)bis(bipyridine)1,1'-(2,2'-bipyridine-4,4'-diyl)bis-3-beta-propane-{tris-[3-carboxyl-ethoxy]methyl]3'-{tris[2'-ethoxy-β-D-galactopyranosyl-ethoxy]methyl]methyl amide (4).** General procedure D with *cis*-ruthenium(II) bis(bipyridine)1,1'-(2,2'-bipyridine-4,4'-diyl)bis-3-beta-propane-{tris-[3-carboxylethoxy]methyl]3'-{tris[2'-ethoxy-2,3,4,6-tetra-*O*-acetyl-β-D-galactopyranoside-ethoxy]methyl]methylamide (16 mg, 1.54 µmol) and sodium methoxide (3 mg, 20%) gave 9 mg (65%) of *cis*-ruthenium(II) bis(bipyridine) 1,1'-(2,2'-bipyridine-4,4'-diyl)bis-3-beta-propane-{tris-[3-carboxyl-ethoxy]methyl]3'-{tris[2'-ethoxy-β-D-galactopyranosyl-ethoxy]methyl]methylamide. $[\alpha]_D^{r.t}$ = -5.3 (c =1.0, H_2O); ^{1}H NMR (300MHz, MeOD): δ 9.05 (s, 2H), 8.65 (d, *J* = 7.8 Hz, 4H), 8.45 (s, 6H), 8.03 (br.s, 6H), 7.8 (d, *J* = 6.0 Hz, 6H), 7.39 (d, *J* = 6.0 Hz, 2H), 4.39 (d, *J* = 7.8 Hz, 18H), 3.95 (q, *J* =4.8 Hz, 8H), 3.91-3.85 (m, 36H), 3.76-3.60 (m, 186H), 3.47-3.45 (m, 4H), 3.41-3.35 (m, 58H), 2.47-2.42 (m, 64H); ^{13}C NMR (125MHz, CD_3OD): δ 181.1, 174.4, 173.3, 172.7, 158.8. 157.0, 152.1, 138.6, 131.6, 129.2, 126.7, 122.3, 110.8, 104.3, 77.8, 73.5, 71.8, 71.8, 68.5, 67.6, 66.6, 62.4, 61.4, 40.1, 37.3. MALDI-HRMS (m/z): $[M-1]^+$ Calcd for $C_{304}H_{502}N_{40}O_{166}Ru$ 7471.1113; Found: 7471.112.

3. Photophysical and electrochemical properties

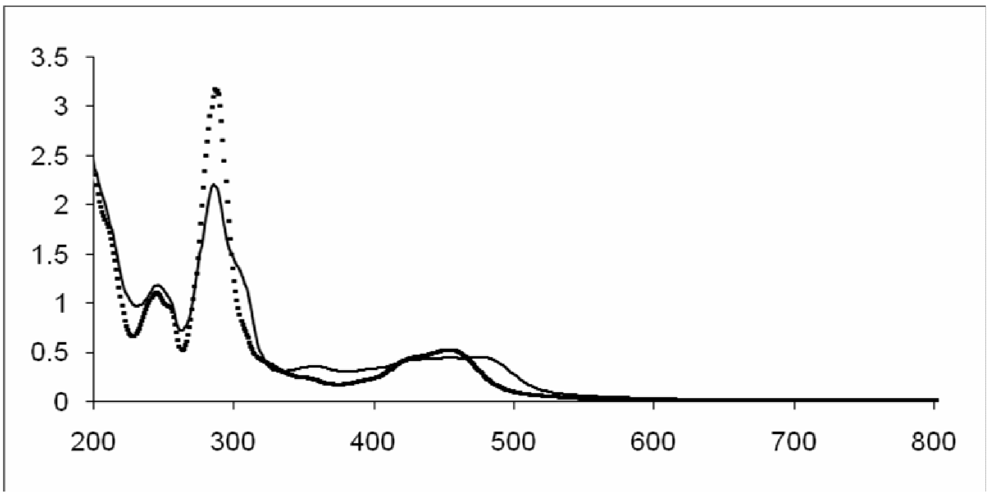

Fig S2. UV-Visible spectra of **1** (solid line) and $\mathbf{Ru(bipy)_3(NO_3)_2}$ (dotted line)

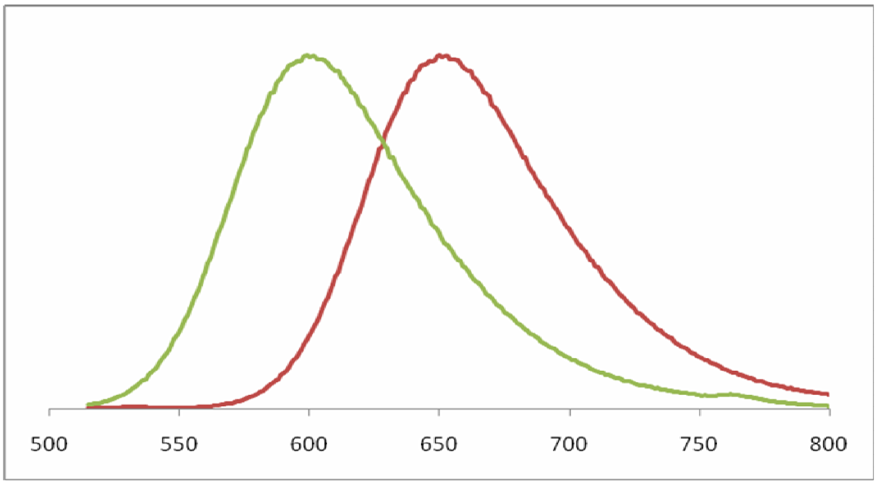

Fig S3. Normalized fluorescence spectra of **1** (red line) and Ru(bipy)$_3$(NO$_3$)$_2$ (green line)

Electrochemical Measurements. Cyclic voltammetry experiments were carried out using a CHI-660A potentiostat. A three electrode setup was used for measurements consisting of a glassy carbon working electrode, a platinum wire counter electrode and an Ag/AgCl, KCl(sat'd) reference electrode. The measurements were performed using methanol solutions of compounds (2 × 10^{-3} M) under nitrogen bubbling with N_2 layer of blanket over the sample at room temperature (22°C). $^tBu_4NPF_6$ (0.1 M) was used as supporting electrolyte. The setup was calibrated with ferrocenium/ferrocene couple for which the $E_{1/2}$ was observed at 0.45 V. Square-wave voltammetry (SWV) was carried out using modified gold surface as working electrode, platinum wire as a counter and Ag/AgCl as a reference electrode. All measurements were performed at room temperature (22°C).

Cyclic Voltametry of Ru-complexes in Solution. The cyclic voltammetry measurements for the Ru-complex were carried out in methanol using $^tBu_4NPF_6$ as supporting electrolyte. The Ru-complex exhibits reversible redox processes in positive potential ($E_{1/2}$ = 1.32 V *vs* Ag/AgCl and 0.87 V *vs* fc/fc$^+$) (Fig S4). The analysis of the redox waves at the scan rates 100-900 mVs^{-1} provides clear evidence that an oxidation process occurs for the Ru(II) to Ru(III) couple. Each couple is diffusion controlled as evidenced by the constant current function (i_p *vs* $v^{-1/2}$) over the scan rates for 100-900 mVs^{-1}. The ΔE value (80 mV) for the redox process was in the range expected for one-electron couples. The i_c/i_a is found to be unity indicating this process is reversible.

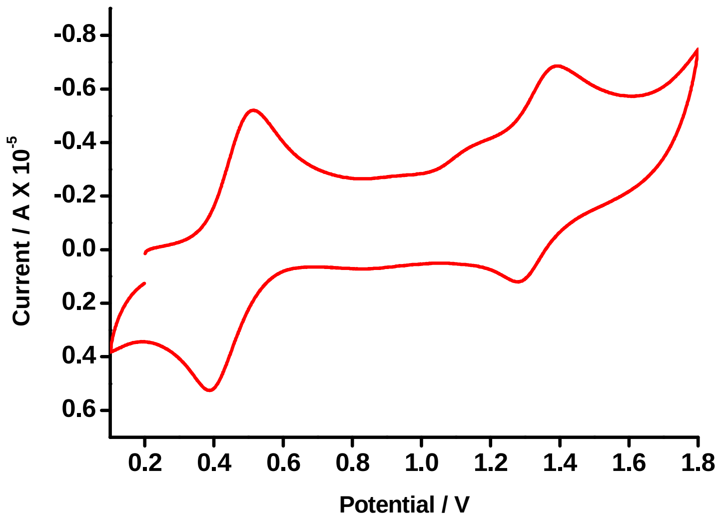

Fig S4. Cyclic voltammeter of the complex **1** in acetonitrile solution (2 mM) using glassy carbon as working, Pt as counter and Ag/AgCl as reference electrode. The measurement was also calibrated with fc/fc+.

4. Optical Lectin Sensor.

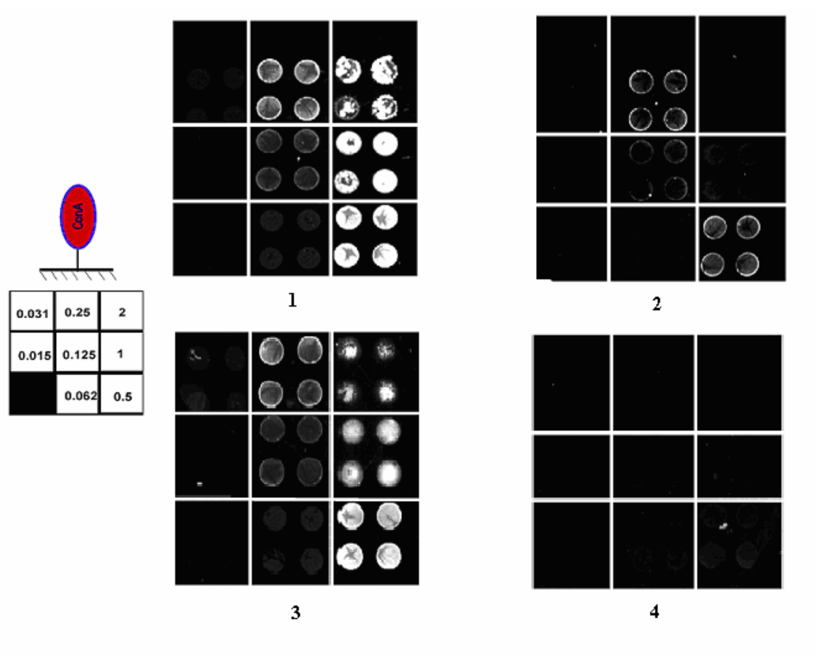

Fig. S5. Incubation of Ru(II) dendrimers **1-4** with protein microarrays that contain different concentrations (mg/mL) of the lectin ConA (excitation at 480 nm).

Lectin Microarray Construction. Concanavalin A was diluted to 2, 1, 0.5, 0.25, 0.125, 0.062, 0.031 and 0.015 mg/mL in PBS buffer. Each sample was printed in quadruplicate on the surface of aldehyde-derivatized glass slides. The printed slides were incubated for 24 h in a humid chamber then quenched with 1% BSA in PBS for 24h at room temperature. The slides were washed three times with PBS before use.

Microarray Binding Assay. Microarray slides were incubated with 10 µM solution of Ru-sugar complexes dissolved in lectin binding buffer (10 mM Hepes pH 6.5, 1mM $MgCl_2$, 1mM $CaCl_2$, 1% BSA) for 1h at room temperature. The slides were subsequently washed three times with PBS and three times with water, then visualised with Perking Elmer scanner. Excitation was done at 488 nM and the detection at 633 nM.

5. Electrochemical Lectin Sensor

Preparation of Mixed SAM Monolayers and Immobilization of ConA Lectin and Ru(II) Complex.

Materials. Gold coated glass slides modified with coupling layer, lectin, ethanol amine, *N*-hydroxysuccinimide (NHS), 1-ethyl-3-(3-dimethyl aminopropyl)carbodiimide (EDAC), phosphate buffer (20 mM, pH: 8.6), Trsi-HCl (pH: 7.4, 50 mM), D(+)glucose. D(+)mannose, D(+)galactose, D(+)maltose, D(+)manα(1-6)man, PIM3, PIM4, Tri-mannose. Coupling buffer: 20 mM phosphate buffer (pH: 8.6) containing 100 mM NaCl. Washing buffer: 50 mM Tris-HCl (pH: 7.4) containing 0.1 M NaCl.

Atomic Force Microscopy (AFM) Measurement

Topography of the modified surfaces were investigated in the dry state with a multimode instrument (Digital Instruments, Santa Barbara, CA) operating in the tapping mode. Silicon tips (OMCL-AC160TS from Olympus Corporation, Japan) with a radius less then 7 nm, spring constant of 42 N/m, and resonance frequency of 300 kHz were used.

The gold substrate appears on AFM images as stack of relatively small (up to 700 nm long) atomically flat platelets (plates/scales/flakes) with a root-mean-square (rms) roughtness of about 0.2 nm. Modification with thiol self assembled monolayer was not changing the morphology of the surface noticeably (See SI, Fig S4). Overall rms roughness of the 2x2 μm image of the gold surface modified by SAM is 0.67 nm mostly due to the gaps between the plates. In contrast to SAM, ConA immobilization changes surface morphology significantly revealing well-defined, globular features with a mean height of about 2.2 nm that can be attributed to the presence of ConA. One can notice only a slight increase in rms roughness (0.82 nm for 2x2 μm image) that is mostly due to the ConA globules since gaps in the surface are almost closed and not contributing to the surface roughness.

Gold Samples Used for CV

Glass slides (approx. 1x4 cm) were washed with EtOH. The glass slides used for SAM films were prepared by evaporating gold (purity >99.99%, Umicore, Balzers, Liechtenstein). The silicon wafers were coated with a 10 nm chromium adhesion layer, followed by an 50-nm gold film in an evaporation chamber (MED 020 coating system, BALTEC, Balzers, Liechtenstein) at a pressure of about $2x10^{-5}$ mbar. Samples were then immediately immersed into a solution of 6-mercaptohexan-1-ol and 11-mercaptoundecanoic acid (9:1 by volume, of 0.1M solution of both compounds, all solutions were made up using 4:1 EtOH/H_2O) for 16 h.[1] If not functionalized immediately, samples were washed in Pirhana solution (7:3 conc. H_2SO_4, 30 % H_2O_2, respectively) for 15 min, rinsed exhaustively with water, then with EtOH (absolute). Samples were then immersed into a mixture of solutions of 6-mercaptohexan-1-ol and 11-mercaptoundecanoic acid (as described above). The samples were then rinsed with EtOH and dried under a stream of nitrogen.

Gold Samples Used for AFM

The freshly cleaned (Pirhana solution, 10 min) silicon wafers were coated with a 170 nm gold film in an evaporation chamber (MED 020 coating system, BALTEC, Balzers, Liechtenstein) at a pressure of about $2x10^{-5}$ mbar. Onto these surfaces, was deposited a small drop of Norland Optical adhesive 61 (NOA 61) and these were then covered with pre-cleaned glass. The samples were cured using a UV lamp (Radium Sanolux, HRC 300-280, 300W, 230V AC) and then the gold layer was transferred onto the glass, by means of mechanical separation of the silicon wafer and glass slides.

Ellipsometry. Single-sided polished silicon wafers (approx 1x1 cm) for VASE measurements were prepared like the samples for CV. However, polished silicon wafers were used instead of glass pieces.

VASE. The monolayer thickness was measured using a VASE ellipsometer (M-2000FTM, J.A. Wollam, Inc., Lincoln, NE). Data were evaluated using the software WVASE32 (WexTech Systems Inc., New York). The measurement was conducted in the spectral range of 370-995 nm at angle of incidence of 65°C, 70°C and 75°C under ambient conditions (in air), immediately after monolayer formation (average thickness of 10.4 Å). The changes observed on the SAM after immobilization of ConA were monitored by VASE ellipsometry measurements (average value of approx. 20.6 Å).

Lectin Immobilization. The gold substrate (modified with a mixed monolayer) was washed twice with EtOH. The substrate was then placed in PBS (10 mL) containing NHS (1 mg) and EDAC (1 mg). After approximately 30 min mixing the supernatant was removed. Lectin solution (1 mL of 10 mg/100 mL) was added to PBS (20 mM, 100 mL, pH 8.6); then 10 mL of this solution was distributed to each of the six different vials, containing SAM-coated gold substrates. After 6 h mixing, the solution was removed and the substrate was placed in aqueous solution of ethanolamine (0.1 mL in 10 mL H_2O) for 10 min. After removing the solution, the gold substrates were washed with 10 mL of 50 mM Tris-HCl buffer (3 x containing 100 mM NaCl, pH 7.4).

Immobilization of Ru-Complex. The ConA functionalized gold substrates were placed in a solution of Ru-complex (**1-4**) (0.5 mM in Tris-HCl containing 10 mm NaCl) at room temperature. After 30 min immersion, the substrate was removed and washed three times with Tris-HCl buffer and square wave voltammetry reading were recorded in Tris-HCl (containing 10 mM NaCl). The substrate was placed again in the same Ru-complex solution. The square-wave voltammetry reading was recorded on the same substrate after 30 min, 1h, 2h, 3h, and 4h immersion time in the same solution and washing.

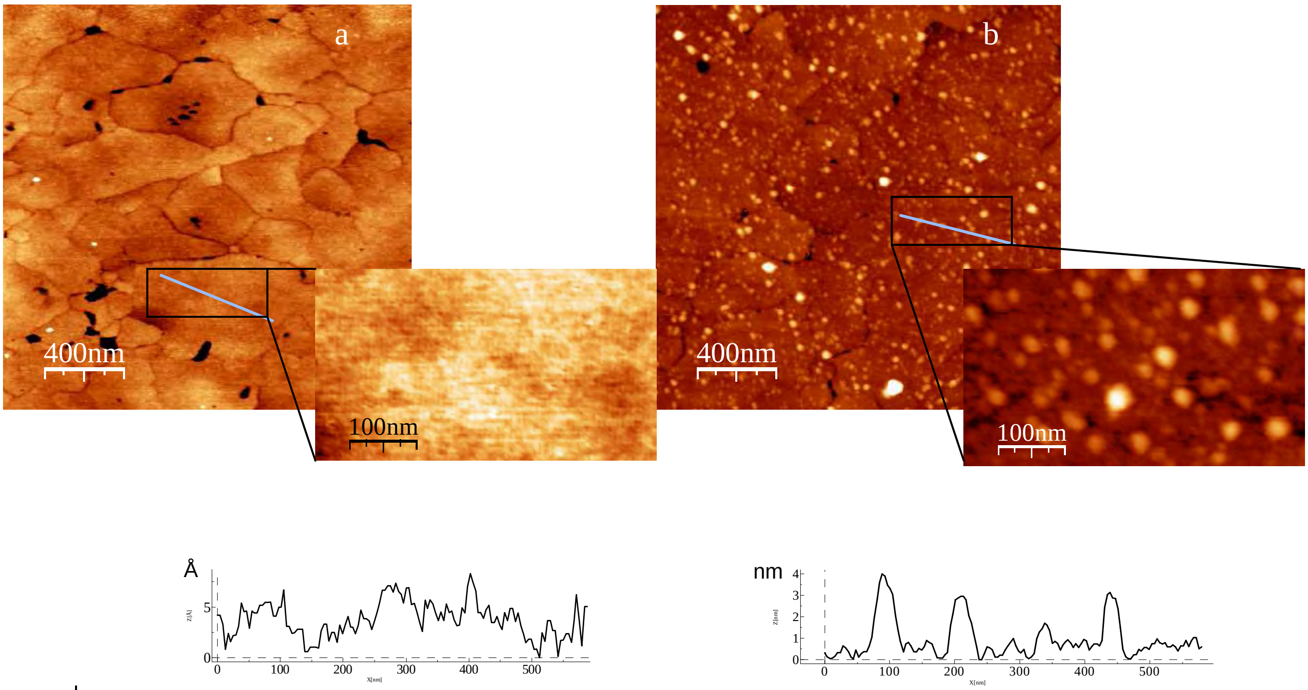

Fig S6. AFM topographical images (2 µm × 2 µm) of (a) mixed SAM (z – range 4 nm), (b) immobilized ConA (z – range 10 nm) with corresponding cross-sections.

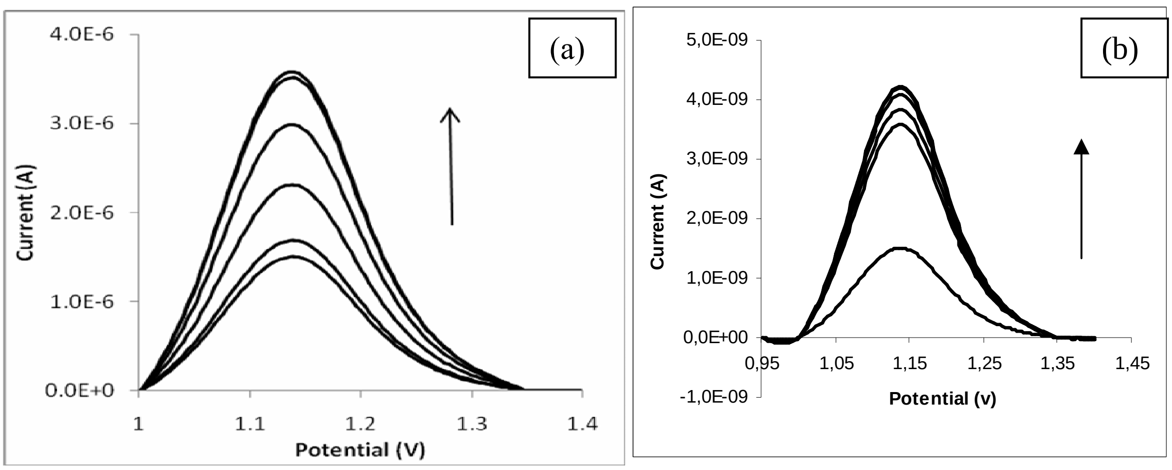

Fig S7. **(a)** Square-wave voltammetric signals of the complex **1**-based monolayer formation after 30 min, 60 min, 120 min, 180 min, 240 min and 360 min immersion time in 0.5 mM ; **(b)** SWV signals of complex 3-based monolayer formation.

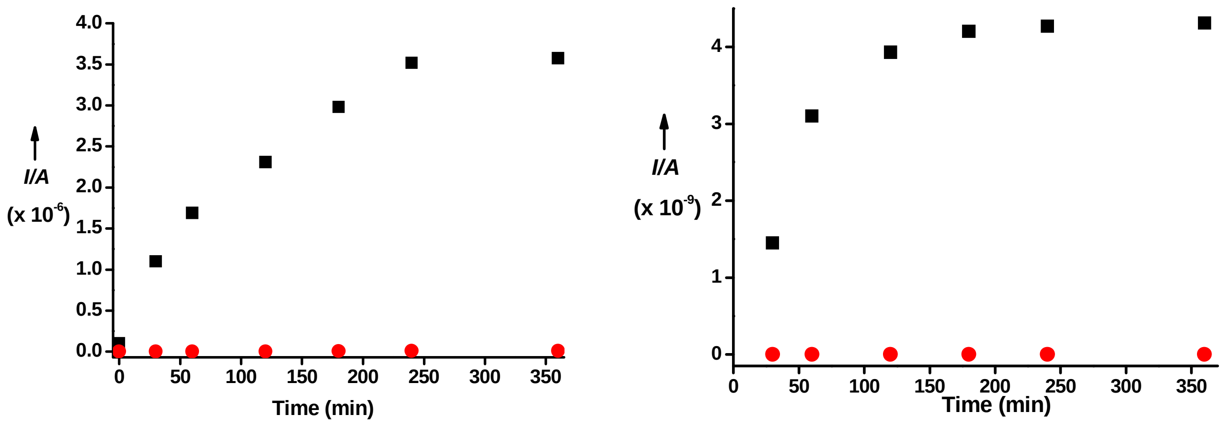

Fig. S8. Square-wave voltammetric measurements at 1.14 V following incubation of (a) complexes **1** **(■)** and **2** **(●)** with ConA-functionalized surfaces for six hours; (b) complex **3** **(■)** and **2** **(●)** with ConA-functionalized surfaces for six hours.

Different concentrations of ConA were immobilized on gold substrates and treated with 0.5 mM of complex **1** and **3** and SWV single was recorded. Complex **1** showed a steady and linear decrease in current single at 10^{-6} to 10^{-10} M of ConA lectin. In contrast, complex **3** showed a modest and relatively variable current response (Fig S9). The detection limits for the complex **1** calculated by this results showed comparable sensitivity than other sensors described in the literature (Table 2). These results indicate that a high degree of carbohydrate density around the ruthenium core allows for efficient encapsulation of the Ru(II) core and alter the rates of electron transfer between complex **3**[20,8c] and Au-surface results less sensitive biosensors.

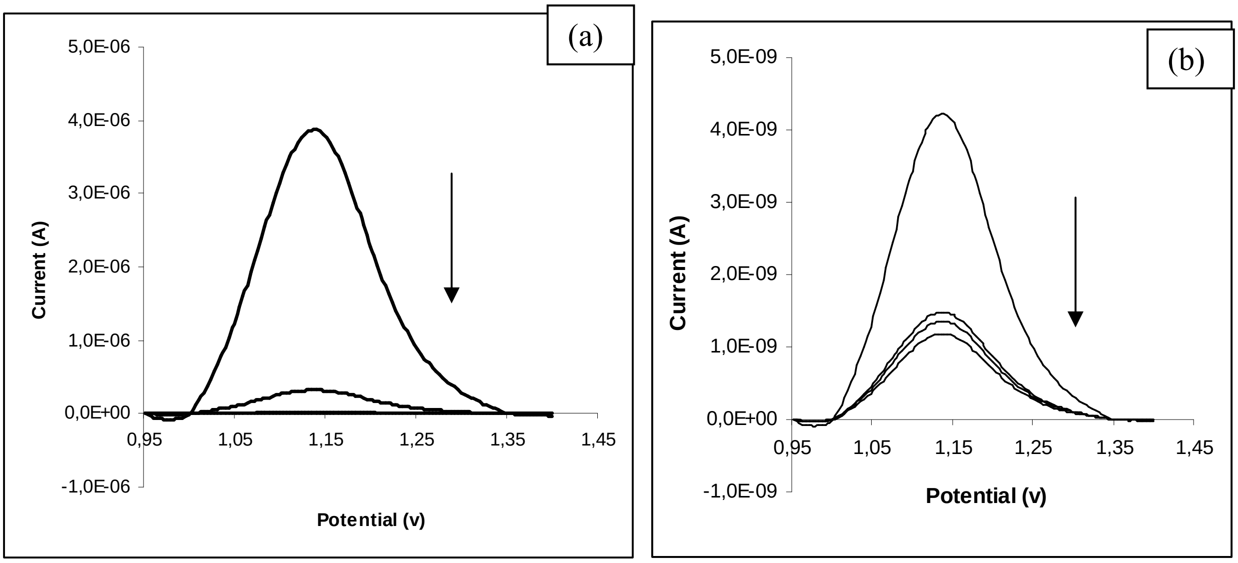

Fig. S9. (a) Current signal with complex **1;** (b) Current response with complex **3** at 10^{-6}, 10^{-7}, 10^{-8}, 10^{-10} M concentration of ConA immobilized on the gold substrate;

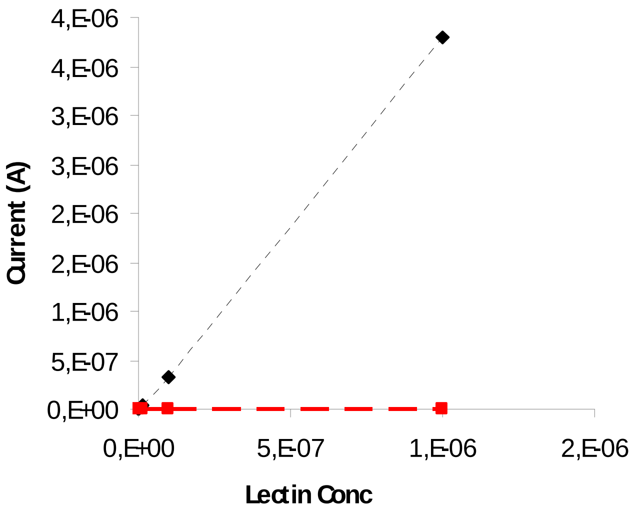

Fig. S10. Current signal with complex **1** (black line) **3** (red line) at different concentrations of ConA immobilized on a gold substrate.

Methods	Detection limits	Ref
Optical detection by Ru(II)-carbohydrate coated dendrimers and BBV by photoinduced electron transfer process	28 ± 3 nM	2a
Optical detection by fluorescent carbohydrate protected Au nanodots and ConA interactions	0.7 nM	2b
Optical detection by gold nanoparticles chips with a self-assembled sugar bilayer	0.1 nM	2c
Optical detection by ConA microarray with Ru(II)-carbohydrate dendrimers	620 nM	Current method
Electrochemical detection by immobilizing ConA-Ru(II) dendrimers	2.5 ± 0.12 nM	Current method

Table S2. Detection limits of ConA by different sensor systems.

6. Sugar Detection

1 mM stock solution of sugars were made in millipore water and diluted to desired concentrations using millipore water. The Con A-functionalized gold substrate was treated with a series of aqueous solutions of glucose (1×10^{-6} - 1×10^{-4} M). The substitution of the Ru-mannose complex by the sugar was monitored using square-wave voltammetry. In a set of experiments, gold substrate modified wit Ru-complex was immersed in aqueous solutions containing 1×10^{-6} M of sugar for 5 min. The sample was rinsed with water, then with Tris-HCl buffer and dried under N_2 before recording SWV.

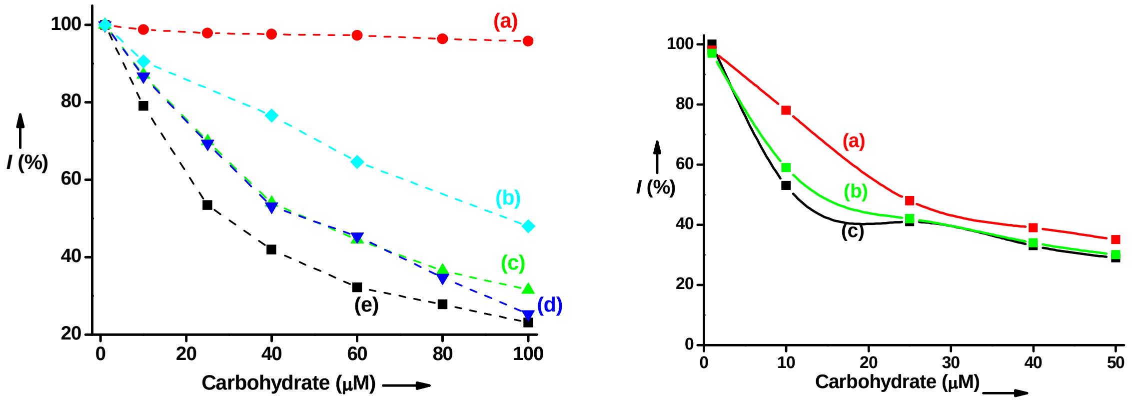

Fig. S11: Response of square-wave voltammetric signals to increasing concentrations of **(i)** (a) D-galactose (●) (b) D-glucose (♦)(c) D-maltose(▲) (d) D-mannose(▲) and (e) D-manα(1-6)man (■); **(ii)** (a) PIM3 (■); (b)Tri-mannose(■); (c) PIM4 (■).

Methods	Detection limits (μM)
D-glucose	7 ± 0.12
D-mannose	3 ± 0.11
D-maltose	3 ± 0.06
D-galactose	-
D-manα(1-6)man	1.4 ± 0.12
PIM3	1.4 ± 0.11
Tri-mannose	0.61 ± 0.07
PIM4	0.61 ± 0.11

TableS 3. Detection limits of differents free sugars by electrochemical ConA/Ru(II)-glycodendrimer method.

Methods	Detection limits (M)	Ref
Multilayer Displacement method (ConA/ferrocene)	10^{-3}	3a, 3b
AuNPs/Glucose oxidase (direct wiring)	10^{-4}	3c
PtNPs/Glucose oxidase(analysis of H_2O_2)	10^{-2}	3d
Molecular Imprinting method	10^{-3}	3e
Quantum dots/lectin interactions method to detect of GalNH, Gal, *β*-D-Gal-[1-3]-D-GalNAc	2.7 x10^{-6}, 10^{-6}, 10^{-7}	3f
Carbon nanotubes/Glucose oxidase (direct wiring)	3.0 x 10^{-9}	3g

Table S4. Detection limits of glucose and different free sugars by electrochemical methods.

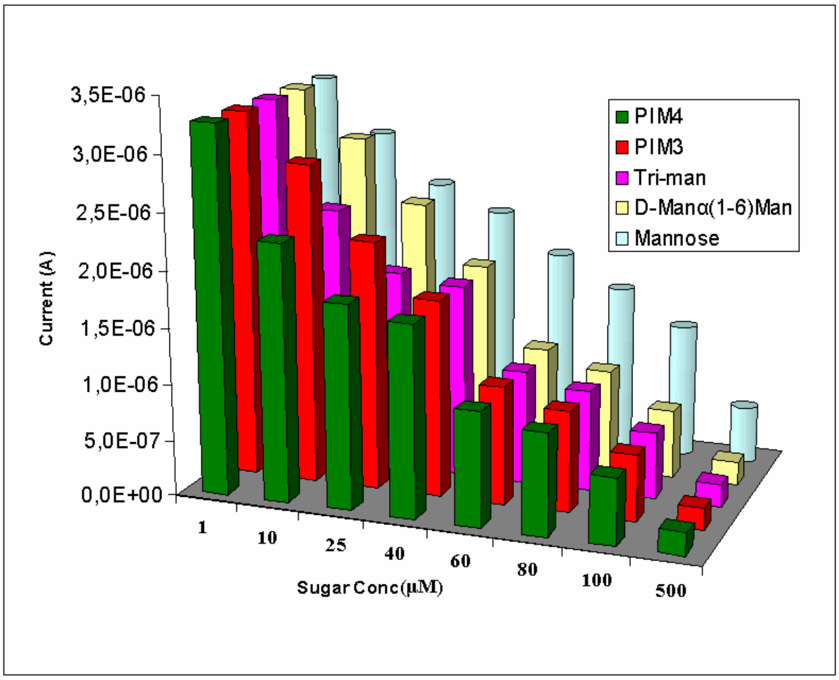

Fig S12. Square wave voltammetric signals in the presence of 1- 500 µM concentration of different mannose structures.

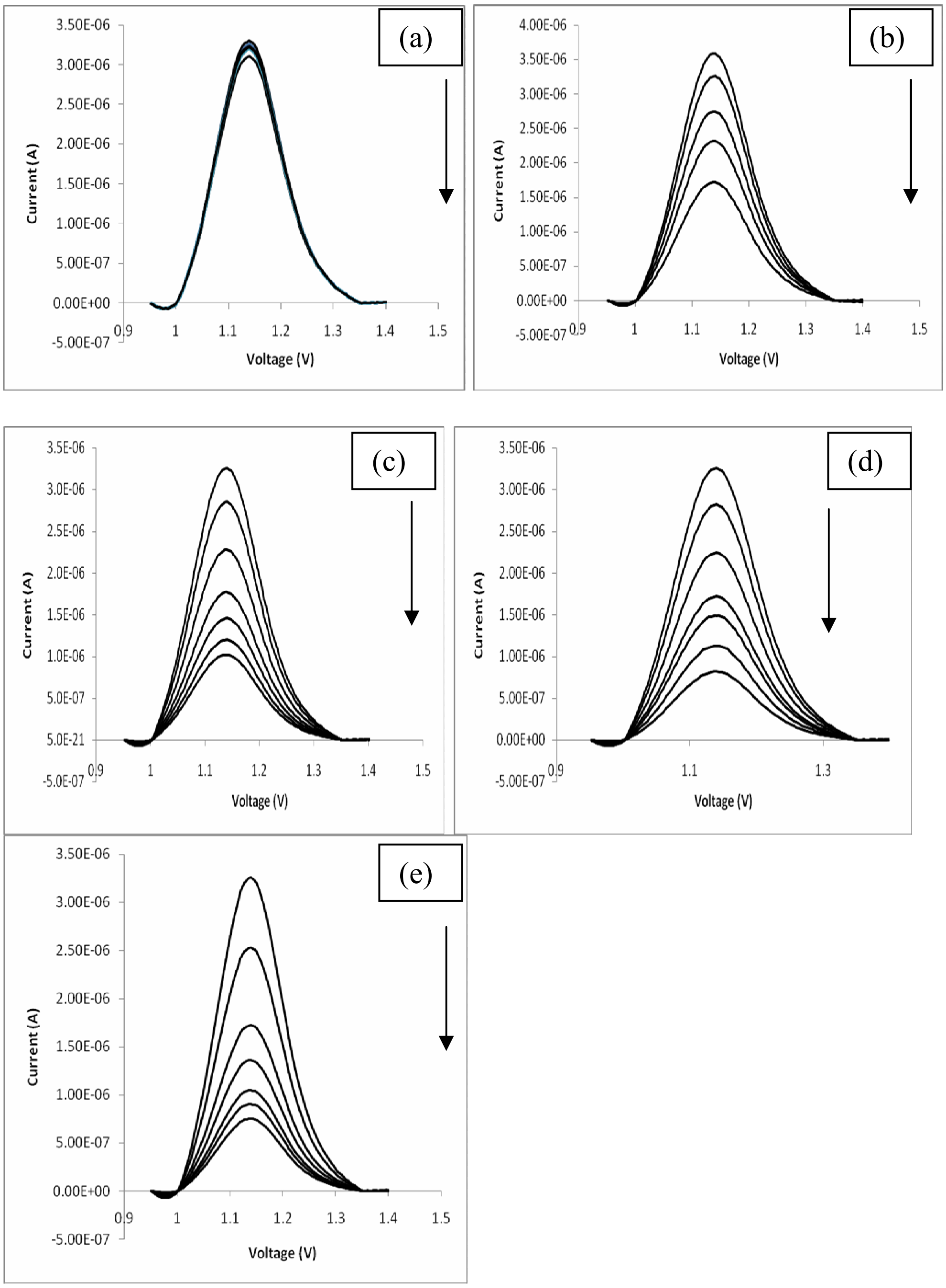

Fig S13. Square wave voltammetric signals in the presence of 1- 100 µM concentration of (a) D-Galactose (b) D-Glucose (c) D-Mannose (d) D-Maltose (e) D-Manα(1-6)Man.

Procedure for Regeneration of ConA-Au Substrate. A stock solution of 50 mg boronic acid confined Merrifield resin[26] was swelled in a 6:4 mixture of DMF and 0.1M of phosphate buffer at pH 9.8 (3 mL). The gold substrate was immersed into the aqueous solution for 2-3 min. The sample was rinsed with phosphate buffer (0.1 M, pH 7.5), deionized water and then dried under a stream of

N_2. This substrate was once again incubated in a solution of complex **1** (0.5 mM) for 4 h, to obtain the regenerated substrate used for sugar sensing.

7. References.

1. Yavin, E.; Weiner, L.; Arad-Yellin, R.; Shanzer, A., *J. Phy. Chem A*, **2001**, 34, 8018

2. (a) Kikkeri, R.; Garcia-Rubio, I.; Seeberger, P. H., *Chem Comm.* **2009**, 235; (b) Huang, C-C.; Chen, C-T.; Shiang, Y-C.; Lin, Z-H.; Chang, H-T, *Anal. Chem*. **2009**, 81, 875. (c) Guo, C.; Boullanger, P.; Jiang, L.; Liu, T, *Biosens. Bioelectron*. **2007**, 22, 1830

3. (a) Xiao, Y.; Patolsky, F.; Katz, E.; Hainfeld, J. F.; Willner, I. *Science*. **2003**, 299, 1877. (b) Zayats, M.; Katz, E.; Baron, R.; *J. Am. Chem. Soc*. **2005**, 127,12400. (c) Bahshi, L.; Frasconi, M.; Telvered, R.; Yehezkeli, O.; Willner, I. *Anal. Chem*. **2008**, 80, 8253. (d) Sato, K.; Kodama, D.; Anzai, J. -I., *Anal. Bioanal. Chem.* **2006**, 386, 1899. (e) Malitesta, c.; Losito, L.; Zambonin, P. G. *Anal. Chem*. **1999**, 71, 1366. (f) Dai, Z.; Kawde, A.-N.; Xiang, Y.; La Belle, J. T.; Gerlach, J.; Bhavanandan, V. P.; Joshi. L.; Wang, J., *J. Am. Chem. Soc* **2006,** 128, 10018. (g) Jazkumar, d. R. S.; Narayanan, S. S. *Carbon*, **2009**, 47, 957.